TOWARDS IMPROVED PARAMETER ESTIMATION IN STREAMFLOW PREDICTIONS USING THE *ACRU* MODEL

M Royappen

BSc Honours (Hydrology)

Submitted in partial fulfilment of the requirements for

the degree of

MASTER OF SCIENCE IN HYDROLOGY

School of Bioresources Engineering and Environmental Hydrology

University of Natal

Pietermaritzburg

June 2002

ABSTRACT

An unresolved problem in hydrology has been to establish relationships between catchment attributes and the flow characteristics of the stream. Such information is commonly sought to improve streamflow predictions, often in a process of extrapolating research results obtained from relatively few, but intensively studied catchments, to a broader region. This study has attempted to clarify terminology related to streamflow generation processes and mechanisms, and to investigate relevant physiographic and climatic characteristics which critically influence the hydrological responses of catchments. Fourteen catchments were selected for this study. They comprised both operational and research catchments. These catchments were selected to be representative of variations in climate, topography, vegetation and geology occurring throughout the Republic of South Africa (RSA). The selection of catchments was also restricted to areas less than 100 km^2, and to the higher rainfall regions of the country, where runoff is significant and any land use changes may lead to marked changes in evapotranspiration and streamflow. A catchment was also selected from an arid zone in the USA, to capture the flow characteristics that are typical of such areas. A frequently applied simulation model on RSA catchments is the *ACRU* model. While physical-conceptual in structure it contains some parameters which, while not determining total streamflow magnitudes, governs the time distribution of the streamflows generated. Two such parameters from the *ACRU* model selected were the coefficient of baseflow response (COFRU) and the quickflow response fraction of the catchment (QFRESP). These parameters are not explicitly physically based, and therefore improved guidelines of initial parameter values are required. Relationships between catchment characteristics and these two parameters were sought to provide guidelines for effective parameterisation of these parameters in future studies. Trends between QFRESP and COFRU, and catchment physical and climatic attributes such as catchment area, average depth of the soil profile, maximum basin relief, MAP and profile plant available water were identified, and could prove useful to future users of the *ACRU* model and guide experimentation in estimating initial parameter values. However, only a single significant multiple regression model was obtained for the baseflow release fraction COFRU from a catchment using MAP, catchment area and profile plant available water.

DECLARATION

The work described in this dissertation was carried out for post-graduate degree purposes within the School of Bioresources Engineering and Environmental Hydrology, University of Natal, Pietermaritzburg under the supervision of Prof. R.E. Schulze. It also contributed towards an externally funded contract research project which was undertaken by a larger project team.

I wish to certify that the work reported in this dissertation is my own original and unaided work except where specific acknowledgment is made.

Signed: _____

Marilyn Royappen

ACKNOWLEDGEMENTS

"I can do all things through Christ who strengthens me."
Phil. 4:13

TABLE OF CONTENTS

LIST OF FIGURES

LIST OF TABLES

1. INTRODUCTION

A fundamental, but largely unresolved, problem in hydrology has been to establish relationships between the physical attributes of a catchment and the flow characteristics of the stream draining the catchment. These relationships are commonly sought to improve model-based predictions of streamflows, often by the procedure of regionalising research findings obtained from relatively few, intensively studied catchments. Flow characteristics such as total stormflow and baseflow volumes, baseflow recession rates and peak stormflow rates have major implications for downstream assurance of water supply, risk of flood damage, water quality or catchment erosion potential, and need to be predicted with useful accuracy if water resources are to be managed effectively. Predicting flow characteristics is especially important where changes in land use are anticipated and where alterations to the flow regime need to be assessed.

Acreman and Sinclair (1986) comment on the necessary links between the physical characteristics of a catchment and the hydrological processes that occur therein, and express the opinion that it must be possible to predict the dominant features of flow without recourse to detailed research data. There has been acknowledgement over the various soil/subsoil processes potentially affecting the conversion of rainfall to streamflow since the early 1970's (Freeze, 1974), but prediction of dominant streamflow generation mechanisms (and therefore flow characteristics) from catchment physical characteristics (e.g. area, morphology and relief, shape, drainage density, vegetation, geology, soils and climate) has, to date, remained a difficult and partially elusive goal.

In the southern African context, accurate streamflow simulations are especially vital for the management and allocation of the scarce water resources. Allocation of water rights is already a contentious issue, and will become even more so as demand for water grows and as the country moves towards a more participatory system of water management, in which all major interest groups are represented in the decision-making process. Added complexity derives from the wide temporal fluctuations in river flows caused by highly variable rainfall regimes.

The complexities of predicting catchment flow regimes are great. Therefore, it is common to make use of computer models to simulate the major hydrological processes occurring in catchments. The *ACRU* hydrological model (Schulze, 1995) is widely used in southern Africa, and is particularly well suited to scenario analyses of the hydrological impacts of various land use options. Many past *ACRU* simulations have highlighted a general problem of correctly simulating flows from small catchments. Over larger catchments, spatial variations in geology and soil are averaged out, allowing easier simulations of the combined flows from the many smaller sub-catchments to mimic observations more closely. At the smaller scale, however, individual catchment characteristics express themselves strongly through the hydrograph, and highlight our incomplete understanding in the link between rainfall and streamflow.

The objectives of this research were to firstly characterise streamflow generation patterns from a wide range of small catchments (<100 km^2) in order to improve our understanding of streamflow generation processes. Secondly, to seek relationships between dominant streamflow generation patterns and catchment physical and climatic attributes, and the *ACRU* model parameters which govern the time distribution of streamflow simulated by the model.

A comprehensive, literature review of streamflow generation mechanisms (SGMs) and the relevant physiographic and climatic characteristics which are believed to critically influence the hydrological responses of catchments was completed. These are summarised in Chapter 2. Methodologies employed are described in Chapter 3, and include an outline of the general structure and streamflow generation routines of the *ACRU* model. Catchment descriptions, and procedures adopted in parameterisng the *ACRU* input menus are also included. The results which followed from the *ACRU* model simulations together with the investigation of relationships between catchment descriptors and *ACRU* input parameter values are provided in Chapter 4. A discussion of the results from this research study is presented in Chapter 5, together with recommendations for future research.

2. LITERATURE REVIEW

Streamflow generation is a complex process which has been conceptualised differently by distinguished researchers over the years. The sections which follow include illustrations of the differences in the conceptualisations of SGMs, descriptions of the various components of streamflow, and the physiographic and climatic factors which influence the hydrological response of catchments.

2.1 Differences in the Conceptualisations of Streamflow Generation Mechanisms

In the 1970s, during the International Hydrological Decade, there was much research activity aimed at improving insights into SGMs. In more recent years, tracer methods combined with hydrometric measurements (i.e. discharge at different sites, groundwater levels and soil water distributions) have proved to be effective for identifying SGMs at the small catchment scale (Uhlenbrook et al., 2001). The mechanisms by which streamflow is generated have caused considerable debate in the past and to this day. Different SGMs may occur within the same catchment depending on climatically related conditions (e.g. antecedent soil moisture conditions and rainfall intensity) and the physical characteristics of the landscape such as the soil properties and underlying bedrock topography. From field observations, Pearce and Mckerchar (1979) concluded that the three mechanisms that satisfactorily explain streamflow production in combination with the above controlling factors are Hortonian overland flow, saturation overland flow and subsurface stormflow, to which has to be added baseflow.

Smith and Hebbert (1983) believed that Hortonian and saturation overland flow, and subsurface stormflow can be three parts of a continuum in the hydrological response of a single catchment where layered soils exist. These SGMs are not mutually exclusive in their spatial distribution, and can occur at different times on certain sections of a slope. This would depend upon changes in rainfall intensities in relation to either the saturated hydraulic conductivity of the soil, differences in conductivities between contrasting soils, land use changes that modify the soil surface hydraulic

properties, and the position and shape of the slope in a landscape (convex, concave or straight). This already illustrates the complexity of SGMs.

This complexity has resulted, *inter alia*, in different conceptualisations of SGMs and, consequently, a plethora of terms describing catchment processes and flow components, for the actual route that a drop of rainwater follows from the time it falls until it enters the stream, is not a simple one. Water may start out as surface runoff, infiltrate the soil and continue as interflow. However, interflow may follow two paths. It may encounter an impermeable layer, exfiltrate because of slope concavity and become surface runoff again, or it may accrete to the groundwater store.

Over the years distinguished researchers have used differing, and often confusing, terminology to represent common elements of SGMs. The following diagrams provide examples of differences in the conceptualisations of SGMs. The processes which affect streamflow generation and their sequence in the terrestrial phase of the hydrological cycle, as conceptualised by Becker *et al.* (2002), are shown in Figure 1.
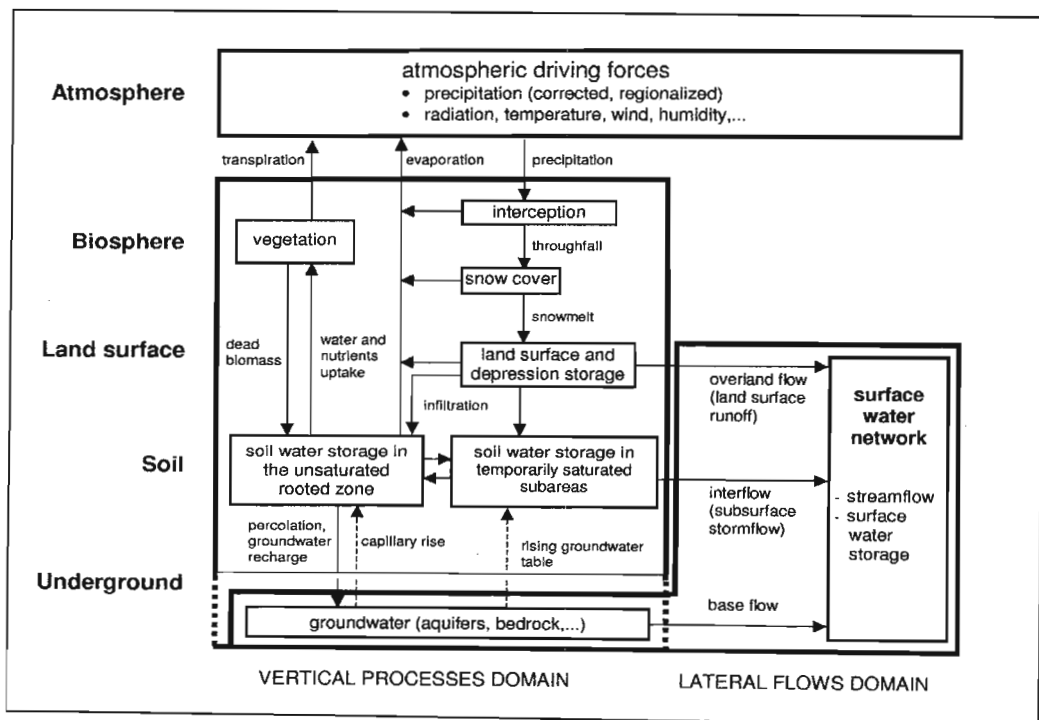
Figure 1: Schematic representation of sequences of terrestrial hydrological processes, with an indication of vertical processes and lateral flows (Becker *et al.*, 2002). Open water surfaces have been excluded.

This figure illustrates the vertical processes, i.e. precipitation and evaporation, and their influence on the lateral flow processes such as overland flow and baseflow, with the variable responses of streamflow to precipitation, both spatially and with time, reflecting the contrasting flow paths towards the stream or river channels. The three components of the total streamflow, as described by Becker *et* al. (2002) in Figure 1, are overland flow (or land surface runoff), subsurface stormflow (or interflow), and baseflow generated through groundwater recharge.

Becker *et al.* (2002) also illustrated preferred streamflow generation areas of different flow components, as shown in Figure 2. It may be seen from Figure 2 that most water which reaches a stream has cascaded down at least part of a hillslope and may have been subject to a number of processes depending on the hillslope characteristics. Brief descriptions of the various abbreviated components and their associated landscape characteristics are given in Table 1.
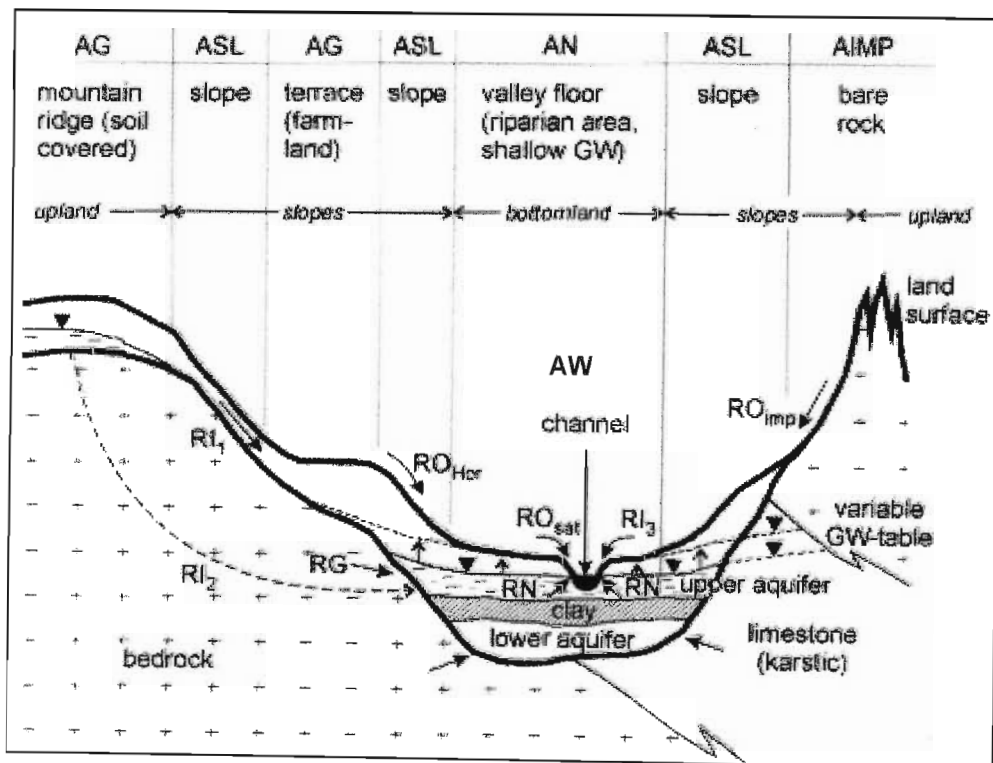
Figure 2: Representation of a valley cross-section indicating (i) typical landscape sub-units similar in their streamflow generation and evaporation behavior and (ii) preferred streamflow generation areas of the different flow components (Becker *et al.*, 2002). Abbreviations are explained in Table 1.

Table 1: Streamflow components and associated essential landscape characteristics, as conceptualized by Becker *et al.* (2002).

Overland flow	
RO_{HOR}	Infiltration excess overland flow from soils when rainfall or snowmelt intensity exceeds infiltration capacity ("Hortonian" flow, high spatial variability). Preferred conditions: bare soil and cropland, arid and semi-arid regions and high intensity rainstorm events.
RO_{imp}	Runoff from impervious areas such as bare rock, sealed areas (e.g. paved, built-up) in all climate zones (nearly constant areal extent during rainfall). After an initial loss of about 2 mm, RO_{imp} amounts to 100 % of rainfall or snowmelt in each event.
RO_{sat}	Saturation excess overland flow ("Dunne" flow) from dynamically varying saturated areas due to rising groundwater tables intersecting the land surface, with RO_{sat} amounts also nearly equal to rainfall or snowmelt. Preferred conditions: riparian areas, flat valleys with gentle concave slopes, shallow groundwater areas, mainly in humid and semi-humid regions, even with low intensity long lasting rain or snowmelt.
Subsurface flow (interflow) occurring as short-term exfiltration of subsurface water to the land surface in depressions, or at lower slopes, or directly into channels	
RI_1	Subsurface flow through preferential flow pathways such as macropores, pipes, highly permeable layers, e.g. at the soil bedrock interface, often included by transmissivity feedback.
RI_2	Piston flow as subsurface pressure wave transmission, especially in mountainous terrain.
RI_3	Groundwater ridging as subsurface pressure wave transmission in lowland and riparian zone aquifers.
RN	Direct subsurface flow or quick return baseflow into the channel system from the riparian zone.
RG	Baseflow which flows first into the valley floor aquifers and then passes through them into the river system.
Typical landscape sub-units	
AG	Areas with the groundwater table deep below the surface so that plant roots cannot reach it.
AN	Areas with shallow groundwater tables, e.g. wetlands near stream riparian areas.
AW	Open water surfaces.
ASL	Slope areas with increased potential for infiltration excess overland flow generation.
AIMP	Impervious or less permeable areas, e.g. uncovered rocks, clay and gleyic soils, sealed areas.

Ward and Robinson (1999), in contrast to the terminology used by Becker *et al.* (2002), define surface flow as that part of the total flow that reaches the drainage basin outlet via overland flow and channel precipitation. In some instances their

surface flow includes throughflow that has discharged to the ground surface at some distance from the stream channel. Subsurface flow is defined by them as the sum of throughflow and groundwater flow and is normally equal to the total flow of water arriving at the stream as saturated flow through the channel bed and banks. They use the term quickflow as the sum of the channel precipitation, surface flow and quick throughflow which together, dominate the streamflow contribution during storms or floods. Baseflow is the sum of groundwater flows and delayed throughflow, and typically recedes very much slower than the stormflow. Some hydrologists include total throughflow when defining baseflow.

Another detailed representation of the flow route of the different hillslope processes, as depicted by Anderson and Burt (1990), is illustrated in Figure 3. Figure 3 focusses on the detailed processes at the hillslope scale which contribute to the generation of flow towards the stream channel.
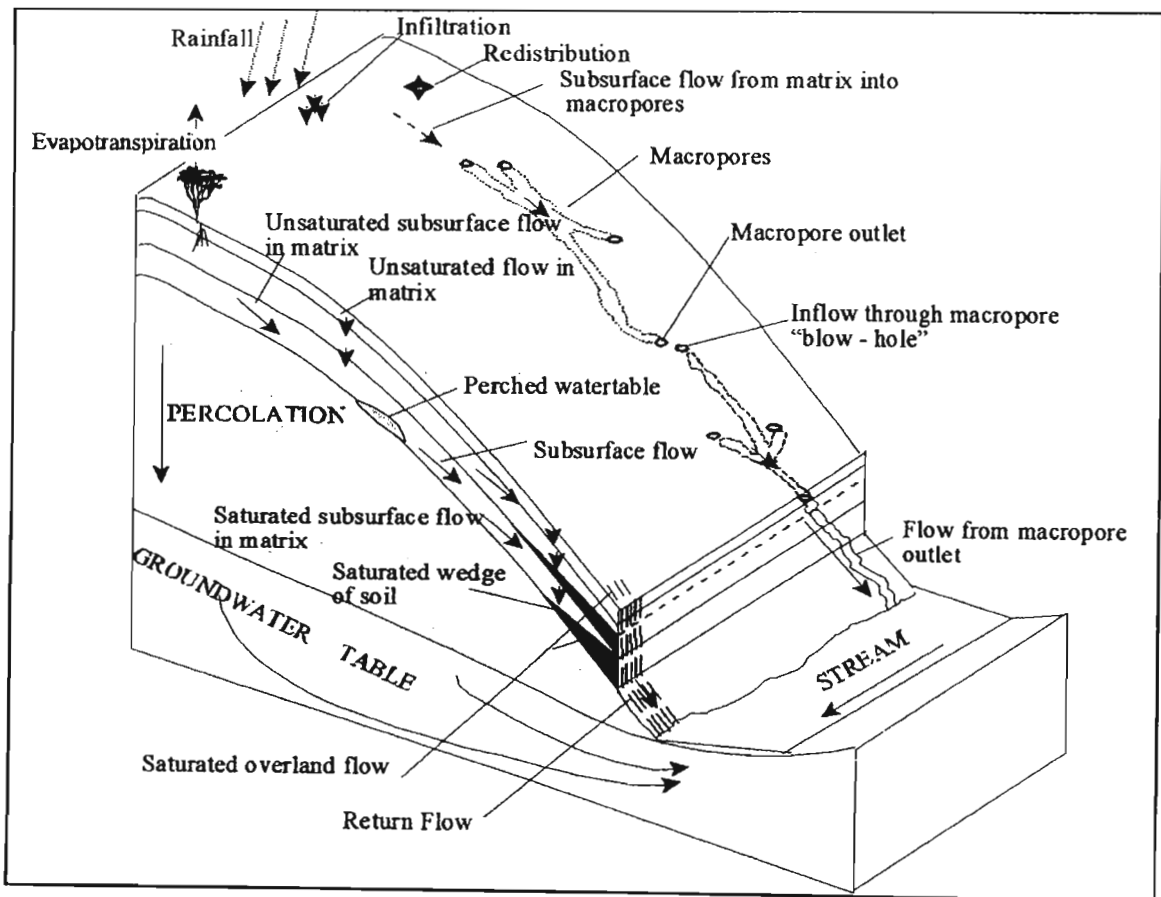
Figure 3: Flow routes of different hillslope processes (after Anderson and Burt, 1990).

It is worth remembering that the relative importance of the numerous sources of streamflow depicted in Figures 1-3 may vary spatially, depending upon many catchment characteristics, such as soil type, the nature and density of the vegetation cover, and the type of rainfall experienced. Figure 4 illustrates the major controls and the different characteristics of the SGMs.
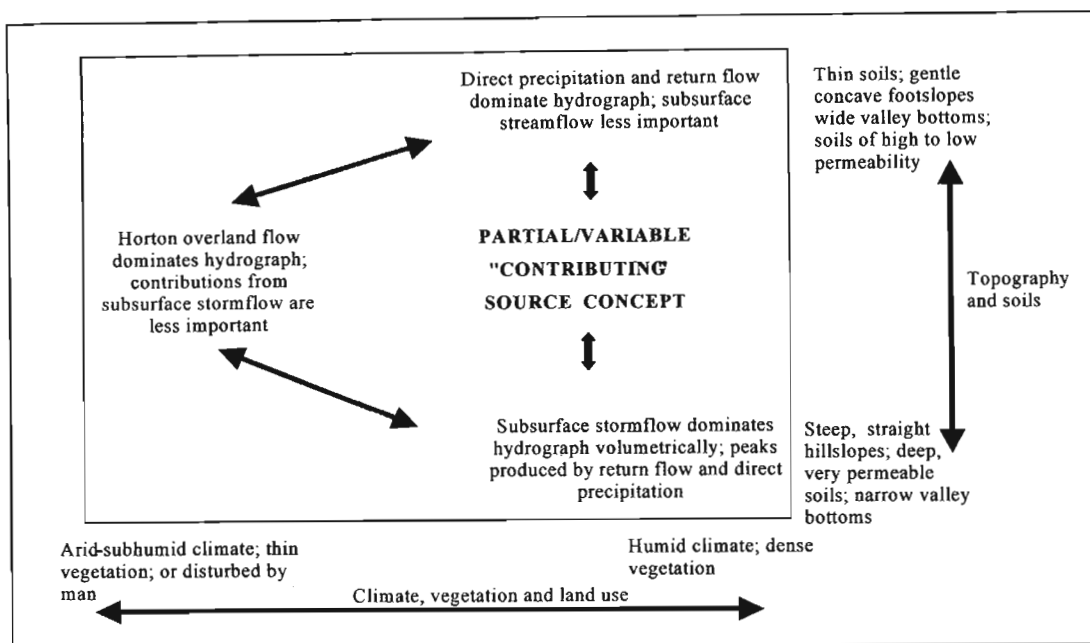
Figure 4: The major controls on streamflow generating mechanisms as conceptualised by Dunne (1978).

Figure 4 illustrates the controls which climate and landuse, topography and soils have on streamflow generation. However, the importance of individual streamflow sources may also vary over time or even seasonally, and may change quite markedly during an storm or sequence of rainfall events in response to variations of infiltration capacity, water table levels and surface water area (Ward and Robinson, 1999).

It is evident from the conceptualisations of SGMs illustrated by Figures 1-4 that various terms have been used by different researchers to explain similar concepts or processes. Therefore, it is necessary to draw commonalities from various studies and to present a terminology to describe elements of SGMs in order to avoid further confusion. From the above conceptualisations of SGMs the common factors identified are elements of direct stormflow, subsurface and lateral flows and groundwater flow. Section 2.2 will discuss these common elements in further detail.

2.2 Processes and Components of Streamflow Generation Mechanisms

In this section, the common processes which are identified, *viz.* the elements of direct stormflows, subsurface and lateral flows and groundwater flow, will be discussed in further detail with reference to illustrations found in the previous section of Chapter 2.

2.2.1 Direct stormflows

In explaining the differences in the hydrological behaviour of catchments, it is necessary to make clear distinctions about the processes by which rainfall is partitioned into different components of streamflow (e.g. stormflow, baseflow) under different climatic and physiographic regimes. Processes contributing to direct stormflows from catchments that will be discussed include channel and open water precipitation and overland flow.

2.2.1.1 Channel and open water precipitation

The percentage of rain-intercepting water surfaces in natural catchments is generally small since the area of the channel system only occupies a small proportion (typically 1-2 %) of most catchments, as illustrated in Figure 2. Exceptions occur where lakes and wetlands increase the surface area of a channel system. Prolonged rainfall events in flat riparian zones may also cause the channel network to expand and therefore increase channel precipitation (Ward and Robinson, 1999).

2.2.1.2 Overland flow

Overland flow is the process by which water flows over the land surface, above the ground, toward the stream channel (Anderson and Burt, 1990). Hills (1971) defines overland flow as any water flowing over the surface of the soil, which constitutes an excess of water that does not infiltrate the soil. In areas where overland flow occurs, the interception, storage and evaporation of rainfall must be estimated to accurately predict the quantity of excess water available for soil infiltration and overland flow (Hills, 1971). Estimates of the minimum amount of rainfall that must fall on various

surfaces before overland flow occurs have been investigated in various studies. An example from Hills (1971) is presented in Table 2.

Table 2: Estimates of interception and surface depression storage before overland flow can occur (after Hills, 1971).

Surface	Interception (mm)	Depression storage (mm)	Total (mm)
Bare ground	0.00	0.27	0.27
Heavy grazing, cultivation	0.13	2.50	2.63
Light grazing	0.25	2.50	2.79
Shrub and woodland	2.50	2.50	5.00

Hillslope characteristics such as the slope gradient, land use and soil types, micro-topography and gullies in the landscape have a direct influence on overland flow thresholds and rates. For example, Schulze (1975) computed the dependence of depression storage (DS) on slope (y) for light grazed land from information contained in Chow (1964) as follows:

$$DS = 3.81 - 0.225y \text{ for slopes} \leq 2° \qquad \text{(in mm)}$$
$$DS = 6.60 - 2.032y \text{ for slopes} \geq 2° \qquad \text{(in mm)}$$

Conditions which favour overland flow include high rainfall intensity and low soil infiltrability. These conditions are commonly met on moderate to steep slopes in arid or semi-arid catchments, where vegetation cover is either sparse or non-existent, exposing the surface to raindrop impact which promotes surface crusting. Overland flow is also commonly associated with poorly permeable soil horizons, such as sodic soils and old lands with plough pans. In catchments where the vegetation cover is dense, overland flow is rarely observed, even in tropical rain forests.

Past research has identified three main types of overland flow, *viz.* Hortonian overland flow, saturated overland flow and return flow (Burt, 1989; Gerits *et al.*, 1990; Kirkby, 1988). Hortonian and saturated overland flow mechanisms will be discussed further.

2.2.1.2.1   Hortonian overland flow

Hortonian overland flow is produced when rainfall rates exceed the infiltrability of the soil and the surface of the soil becomes saturated (Horton, 1933). The excess rainfall becomes available for surface detention and overland flow. Water accumulates on the soil surface and in small depressions. This is referred to as depression storage. Depression storage does not contribute to storm runoff and either evaporates or infiltrates later. When the depression storage is exceeded, water spills over to run downslope as a thin film or as an irregular sheet or series of tiny rivulets of overland flow. The amount of water stored on the hillside in the process of flowing downslope is termed surface detention (Dunne and Leopold, 1978).

Once the rainfall intensity exceeds the infiltration rate, runoff arises rapidly to a sharp peak at the end of the rainfall event, followed by a rapid decline as soon as the rainfall intensity decreases. Water stored as surface detention during the storm drains away to provide the steep recession limb of the hydrograph. It is common for only certain soils or certain areas in a catchment to generate overland flow in this manner, which can occur as immediate or delayed Hortonian flow (Scherrer and Naef, 2001).

Immediate Hortonian flow occurs on soils, or under surface conditions, with infiltration hindrances. Alternatively, it takes place when soils have a high clay content, or have been compacted by agricultural machines and cattle, or the bedrock surfaces have a low permeability. Delayed Hortonian flow results in areas where the soils have a very dense root network near the surface, or are compacted and display low macropore density, are sealed or crusted, and on macroporous soils with low water exchange between macropores and soil matrix (Mosley, 1979; Scherrer and Naef, 2001; Becker *et al.*, 2002). Rates of Hortonian overland flow may vary with storm size and intensity, and with factors that affect infiltration. Marked differences can occur between regions and between storms.

2.2.1.2.2   *Saturation overland flow*

Saturation overland flow is generated by rainfall on saturated areas near stream channels and in valleys. In many areas where the effects of topography, or the nature of the soil profile, facilitate the rise of shallow water tables to the ground surface during rainfall (or throughflow) events, the infiltrability at the surface drops to near zero, leading to saturation overland flow as illustrated in Figures 2 and 3. Such saturated areas expand and contract during each storm, and also seasonally.

In more humid climates, saturation excess overland flow can dominate SGMs. Saturation overland flow will occur predominantly in riparian zones and on thin or shallow soils due to the rising groundwater tables, as well as on gentle topography with concave lower slopes and wide valley bottoms (Dunne, 1978; Becker *et al.*, 2002), where there is an absence of lateral flow structures (Scherrer and Naef, 2001). In Figure 2 this is illustrated by the dashed line in the valley floor aquifer which temporarily intersects the soil surface and thus produces growing saturated areas in the riparian zone during long lasting rainfall and snowmelt. These areas also generate an increase in subsurface stormflow into the channel (Becker *et al.*, 2002).

McDonnell *et al.* (1999) states that these saturated areas scale directly with catchment area, since topographic gradient generally decreases as catchment scale increases. Therefore, saturation excess overland flow has been identified as a major streamflow producing mechanism across scales, but playing an increasing role with increasing spatial scale. The variable source area concept introduced by Hewlett and Hibbert (1967), which was based on research in the Coweeta catchments of the eastern USA, can be considered as an appropriate formulation of this kind of catchment-scale runoff generation. By the variable source area concept surface saturation can occur due to two quite distinct mechanisms (Dunne, 1978). These mechanisms can be represented by the "partial area model", which models saturation from the upper slopes towards the channel, and the "variable source area model", which models saturation from the stream outwards into the catchment. Rising water tables fed partly by rainfall that has entered the soil upslope of the runoff source area reaches the soil surface during a rainfall event. Further precipitation generates

overland flow, resulting in saturated areas which expand and contract during each storm, and also seasonally.

Infiltration of rainfall into the soil is one of the most important factors in determining the amount of excess rainfall available for runoff and is affected by a number of factors, including the soil's antecedent moisture content (AMC) as well as the rainfall's duration and intensity. Particularly under extreme precipitation, the infiltration conditions control the partitioning of water that is transferred to the river system, either directly by generating infiltration excess overland flow, or indirectly by influencing the development of subsurface stormflow as well as the extent of saturated surface areas, thus causing saturation-excess overland flows (Bronstert and Katzenmaier, 2001).

Recent research (Dingman, 1995; cited in Howe, 1999; Becker *et al.*, 2002) has shown that there is a continuum of surface and subsurface processes by which a hillslope responds to rainfall. The mechanisms and processes described in the preceeding sections may operate simultaneously in a given catchment, and their relative importance may fluctuate seasonally or even during a single event.

2.2.2 Subsurface and lateral stormflows

Subsurface stormflow is a generic term for different below-ground SGMs which respond rapidly enough to a rainfall or snowmelt event to contribute to the flood hydrograph (Anderson and Burt, 1990). Chorley (1978) defines it as "the flow of water in soil zones above water-impeding layers, especially in basal hillslope soils, which discharge water directly into the stream channel without entering into the groundwater zone". Its contribution to streamflow, however, is dependent on the type and duration of the event and topographic characteristics of the catchment (Hewlett and Hibbert, 1967; Bonell, 1998). Over the past three decades, research in many catchments has confirmed the importance of subsurface flow processes (Freeze, 1972; Freeze, 1974; Mosley, 1979; Pearce and Mckerchar, 1979; Kirkby, 1988; Burt, 1989; Weiler *et* al., 1998; Schultz, 1999).

Subsurface flow is generated by rapid infiltration of rainfall into the soil, and the consequent increase in hydraulic conductivity of the soil as moisture content rises. The infiltrated water moves laterally through permeable horizons, or in perched saturated zones, and empties directly into the stream network, which then expands both upstream and laterally as rainfall continues. Hewlett and Hibbert (1967) observed that infiltration into the soil is seldom restricted in forested catchments and that subsurface stormflow is the predominant quickflow mechanism in such catchments. Since this observation was first made, subsurface stormflow has come to be viewed as the major SGM in most undisturbed humid environments, because of its influence on saturated overland flow and as an important contributor to stormflow in its own right (Bonell, 1993).

Subsurface and lateral flow processes may occur either at different levels below the surface which correspond with textural changes between horizons, or at the junction between weathered mantle and bedrock. There is also much evidence that water may travel downslope through macropores and macrofissures, and in some circumstances, soil biological activity may play an important role in streamflow generation (Bonell et al., 1984).

Alternative terms also found for subsurface stormflows in the literature include throughflow, storm seepage and secondary baseflow. Throughflow may occur when the lateral hydraulic conductivity of the surface soil horizons exceeds the overall vertical hydraulic conductivity through the soil profile. During prolonged or heavy rainfall events, water enters the upper part of the profile more rapidly than it can drain vertically through the lower horizons, therefore accumulating and forming a perched saturated layer which encourages movement of water in the direction of greater hydraulic conductivity (Ward and Robinson, 1999). Conditions which favour throughflow generation include thin permeable soils which overlie impermeable bedrock, a markedly stratified soil profile, or a subsurface iron pan or plough pan (Ward and Robinson, 1999).

In areas with steep slopes, incised channels, narrow valley bottoms and deep, permeable soils, subsurface flow dominates the storm hydrograph (Dunne, 1978). This source of streamflow is generated in the form of transmissivity feedback, lateral

preferential flow through macropores or pipes and highly impermeable layers, or by pressure wave translatory flow, which includes piston flow and groundwater ridging. These processes are illustrated in Figures 2 and 3 and will be briefly addressed below.

2.2.2.1   Transmissivity feedbacks

Transmissivity feedback results from rapid subsurface flow where water tables rise vertically into more transmissive layers and result in rapid lateral flux of water. In glaciated till-mantled terrain, or in more temperate or sub-tropical areas where saprolite is found, the process known as transmissivity feedback (Rodhe, 1987) may dominate the generation of rapid subsurface stormflow. In such cases vertical recharge of saprolite takes place first before the water tables rise into the more transmissive mineral soil zone, resulting in lateral flow, and has been observed by many to coincide with rapid streamflow response (e.g. Kendall *et al.*, 1999).

2.2.2.2   Rapid lateral flow through pipes and macropores

The perception of rapid subsurface flowpaths has evolved greatly over the past two decades (McGlynn *et al.*, 2002). Schultz (1999) showed that there has been a significant improvement into research efforts concerning subsurface / runoff relationships on hillslopes, resulting in a better understanding of these processes.

Several studies in different parts of the world have documented rapid lateral flow through pipes, or openings at the soil bedrock interface. These enable water to move rapidly downslope. This flow is referred to as lateral pipe flow (McDonnell, 1990). Macropore flow has been subject to considerable debate amongst researchers regarding definitions and the mechanisms of macropore flow. Germann (1990) defines macropores as "large" pores or animal burrows, such as worm tunnels or channels formed by roots, as well as cracks in a soil structure. Pipes, like macropores, also speed up the soil's drainage rates. The distribution and storage of the infiltrated water in the soil is thus influenced by the water exchange / interaction between the macropores and the surrounding soil matrix.

Defining the boundary between pipes and macropores is very difficult (Anderson and Burt, 1990). Pipes may be considered as having larger diameters and are usually formed by erosion. Hence they show a greater connectivity network than macropores. Edwards *et al.* (1988) has estimated that holes wider than 5 mm can carry as much as 10 % of the volume of an afternoon thunderstorm's water in Ohio, USA. The delivery mechanism illustrates that these flow types are a major driving force in linking subsurface flow to streamflow.

Studies by Becker and McDonnell (1998) emphasise the often dominant role of macropore and pipe flow in temporarily saturated areas above less permeable layers, particularly on bedrock (Figure 3). Such direct subsurface lateral flow is also known as interflow, and is considered to move relatively rapidly in approximately horizontal directions without reaching the zone of saturation (Ineson and Downing, 1964). It is considered to arrive at the stream promptly, but later than surface runoff. In the literature there appears to be no clear criterion for defining where interflow ceases and where baseflow begins.

2.2.2.3   Thatched roof effect

A less widely cited example of rapid subsurface flow is rapid lateral flow through the litter layer, also termed shallow interflow, or the "thatched roof effect" (Ward and Robinson, 1999), or psuedo-overland flow as reported by McDonnell *et al.* (1991). It has been shown by Brown *et al.* (1999) and Buttle and Turcotte (1999), using techniques of chemical end member mixing and isotopic tracers, that rapid lateral litter layer flow perched on the soil surface may be a dominant mechanism in upland forested catchments during summer rainstorms. This is a combination of the high short-duration rainfall intensities and water repellency that may develop at these sites during dry periods (Becker *et al.*, 2002).

2.2.2.4   Pressure wave translatory flow

The process of pressure wave translatory flow was first proposed in the early 1960s by Hewlett and colleagues (e.g. Hewlett and Hibbert, 1967), as part of the variable source area concept, and has recently been rejuvenated by Rassmussen *et al.*

16

(2000). In this process a pressure head signal advances through the soil profile faster than the estimated water and wetting front velocities, hence the initial pressure head response appears to be driven by the passage of a pressure wave rather than the advective arrival of new water. Much work remains to be done to fully explain these processes in different environments (Becker *et al.*, 2002).

2.2.3 Groundwater flows

Groundwater flow is normally defined as that water in the near saturated porous media below the phreatic surface, where the water pressure is zero. However, groundwater moving slowing through the soil matrix, could be unsaturated and at pressures less than zero. There can also still exist considerable saturated zones above the phreatic surface, but this water is held in tension or in a capillary fringe.

Under conditions of moist soil and subsoils, a rapid response of groundwater flow to precipitation during individual storm periods may take place via the 'piston displacement' mechanism and groundwater ridging. The piston displacement mechanism allows soil water to move through the profile with each new increment of rainfall displacing all preceeding increments, causing the oldest to exit simultaneously from the bottom end of the hillslope profile. However, an apparent weakness in this mechanism, is that for a given rainfall input it would only result in an equivalent output if the available moisture storage capacity within the soil system is already filled. Therefore under drier conditions such displacements will be used to increase the soil moisture store, rather than maintain the chain of displacements (Ward and Robinson, 1999).

When rain falls on an already saturated hillslope, percolation through less impermeable deeper layers or bedrock may occur. This water may contribute directly to the aquifer, a process commonly referred to as groundwater recharge. Groundwater aquifers are also influential in the streamflow response of hillslopes as they often "feed" streams directly from below the surface (Hickson, 2000). Results from tracer studies by Rice and Hornberger (1998), Weiler *et al.* (1998), Schultz (1999) and Uhlenbrook and Leibundgut (1999) show that the influence of

groundwater on streamflow is still underestimated, and that a high proportion of flow derived from hillslopes is, in fact, groundwater flow.

The ability of groundwater to contribute significantly to the storm hydrograph can be explained by the formation of a groundwater ridge. Esprey (1997) refers to this process as groundwater ridging. A groundwater ridge is located adjacent to the stream channel, and has been referred to as an ephemeral rise in the grounwater table near the stream which helps produce the storm hydrograph. Factors which encourage the formation of the groundwater ridge close to the channel include firstly, the favourable moisture potential gradient in the lower slope areas (Tsukamoto and Ohta, 1988) and secondly, the often concave shape of lowland valley areas which results in the convergence of subsurface flow lines with the ground surface leading to surface saturation, but also being deflected downwards leading to concentrated groundwater recharge (Ward and Robinson, 1999).

One school of thought amongst researchers adheres rigidly to the premise that baseflow is derived solely from groundwater sources. Definitions of baseflow in literature have been vague. Linsley *et al.* (1958) and Ineson and Downing (1964) define baseflow as being derived from that portion of infiltrated water that reaches the zone of saturation at the water table. This water then percolates laterally displacing water already in the saturated aquifer, to be discharged into the river channel at seepages or springs. The time lag for this type of seepage is generally greater than that for subsurface lateral flows and may be measured in days, weeks or months. Other definitions of baseflow include that portion of flow that comes from groundwater or other delayed sources, or the slowly varying flow in rainless periods.

Baseflow can result from a number of types of aquifers in the catchment, including aquifers in neighbouring catchments, depending on the location of the subsurface water divides. As shown in Figure 2, baseflow generally flows first into the valley floor aquifers and then passes through them into the river system in connection with, or as direct, subsurface flow. However, remarkable reductions in baseflow and streamflow can be observed during substantial long dry periods in the growing season when transpiration is increasing, and the transpired water may be fed by groundwater in the riparian zone or associated wetlands. The inflowing groundwater may then become

re-distributed into the unsaturated rooted soil zone and extracted by the riparian zone vegetation (Becker *et al.*, 2002). This redistribution plays an important role in catchments with large lowlands having shallow groundwater.

A baseflow recession analysis was conducted by Hughes (1997), in which master recession curves for 134 catchments were constructed to evaluate the assumption that South African river flows recede exponentially and to explain recession trends using a representative set of catchment characteristics. Catchment characteristics such as area, average catchment slope, drainage density, mean annual precipitation, rainfall concentration and seasonality, estimates of groundwater recharge and a geological index were considered. This study showed that the majority of South African rivers do not conform to an exponential model of recession and attempts to explain trends exhibited by the master recession curves in terms of catchment characteristics achieved limited success. The results suggest that either the factors selected were not representative, and that there are other factors which need to be considered, or that the actual streamflow data are highly variable and that the natural system is so complex that it requires more sophisticated methods of analysis.

Section 2.2 focussed on common processes and components of SGMs, as conceptualised by various researchers and hydrologists. However, it must be remembered that the flow components discussed are often not considered explicitly in hydrological modelling at the catchment scale and that usually only surface flow, subsurface stormflow and baseflow are described. In the next section of Chapter 2 the major physiographic and climatic characteristics which have been shown to critically influence the hydrological behavior of catchments will be discussed.

2.3   Physiographic and Climatic Characteristics which Influence Hydrological Responses

Streamflow generation is highly variable in space and time, depending on differences in topography, climate, vegetation and the edaphic / hydrogeological characteristics of the underlying soils and rocks of the catchment. Combinations of, and interrelationships between these factors determine the amounts and relative streamflow contributions of surface and subsurface flows (Becker *et al.*, 2002). These

significant differences in the partitioning of rainfall into components of evaporation and streamflow is illustrated by Table 3 for different climatic regimes and associated vegetation zones in the world.

Table 3: Typical water budgets (mm/a) in selected major climatic regimes and their associated vegetation zones (after L'vovich, 1979).

Climatic Regime	Vegetation Zone	Precipitation	Runoff			Evaporation + Transpiration	Potential Evaporation
			Total	Groundwater	Surface		
Temperate	Taiga	700	300 (43%)	140 (20%)	160(23%)	400(57%)	500
	Mixed forests	750	250 (33%)	100 (13%)	150(20%)	500(67%)	700
	Wooded steppes and prairies	650	120 (18%)	30 (5%)	90(13%)	530(82%)	900
	Steppes	500	50 (10%)	10 (2%)	40(8%)	450(90%)	1300
Subtropical	Desert savanna	300	20 (7%)	2 (1%)	18(6%)	280(93%)	1300
and	Dry savanna	1000	130 (13%)	30 (3%)	100(10%)	870(87%)	1300
Tropical	Wet savanna	1850	600 (32%)	240 (13%)	360(19%)	1200(68%)	1300
Equatorial	Wet evergreen forests	2000	1200 (60%)	600 (30%)	600(30%)	800(40%)	800

The diverse hydrological responses shown in Table 3, even in areas which experience similar rainfall patterns, confirms the significant influences of varying climatic regimes and vegetations zones on the partitioning of rainfall into streamflow. Therefore, predicting the hydrological responses of catchments is complex, due to the mosaic structure of landscapes together with varying climatic regimes contributing to many different streamflow generation patterns. For this reason, prediction of hydrological behaviour using physiographic and climatically related catchment attributes has been widely addressed in the literature (e.g. Zecharias and Brutsaert, 1988; Sefton and Howarth, 1998; Berger and Entekhabi, 2001), and is reviewed below.

2.3.1 Morphometry, topography and area

Numerous studies have been undertaken relating catchment morphology to components of streamflow. Distinct relationships are not always apparent, and such results emphasise the complexities of streamflow generation and the need to consider a number of morphological parameters in conjunction with one another, rather than individual ones in isolation. On a catchment scale the hydrograph is

influenced by morphometric parameters such as elevation, stream length and shape distributions of the catchment, as well as by parameters describing the drainage networks (Cook and Doornkamp, 1990). The SCS technique, for example, which has become an accepted and established method for hydrograph generation on small catchments, uses inputs such as catchment slope, area and channel characteristics, to describe to the physical characteristics of the catchment (Schulze *et al.*, 1992).

Catchment area is often identified as a morphological parameter of hydrological significance. Heerdegen and Reich (1974) confirmed that the peak of the unit hydrograph is proportional to the area of a catchment. Dunne (1978) investigated relationships between the components of the hydrograph responses to increasing catchment area for different hydrological processes and his findings are shown for sub-humid climatic conditions in Figure 5.
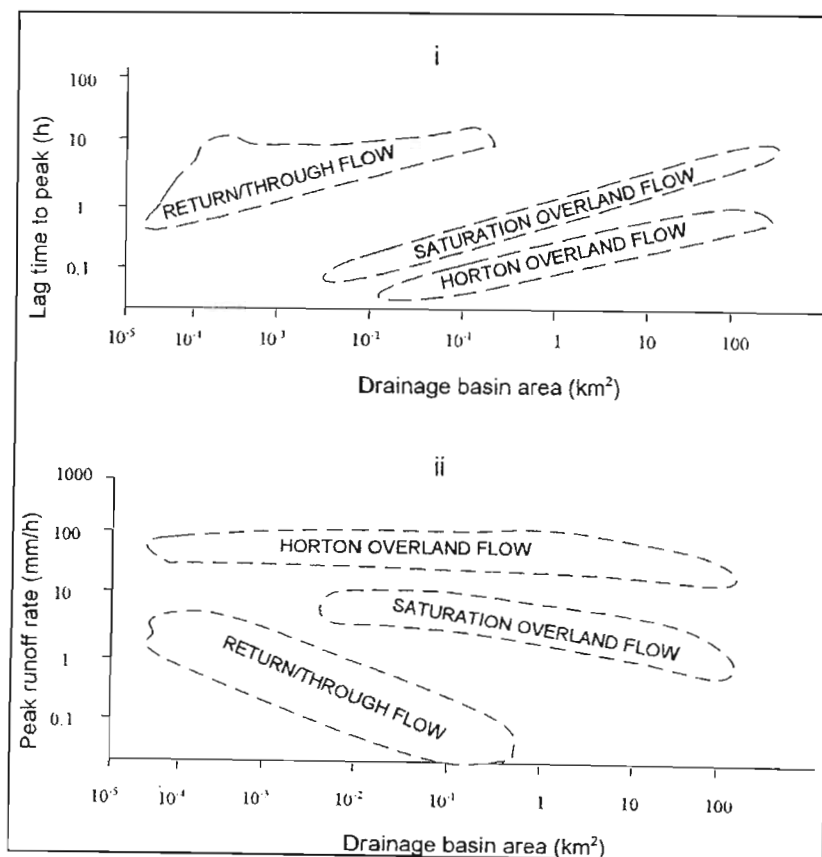
Figure 5: Generalised hydrograph responses to catchment area for a number of SGMs: (i) lag times, (ii) peak runoff rates (after Dunne, 1978).

The lag times from hydrograph commencement to the peak is shorter for overland flow than for return flows as a result of the movement through the soil media retarding the flow of water to the stream. Lag times for saturated overland flows are also shorter than for return flows due to return flow only occurring after the soil has become saturated. The peak runoff rate is, therefore, highest for Hortonian overland flow, as rain falling on the hillslope is assumed to run directly into the stream (Kirkby, 1988). Larger basin areas promote increasing length of travel of water in the channel, thus increasing the chance of loss to evapotranspiration (Ogunkoya *et al.*, 1984).

Ward and Robinson (1999) reviewed various catchment characteristics that promote quickflow and floods. Catchment area is correlated to flood severity following catchment-wide rainfall events. Where rainfall occurs only over part of a catchment, the attenuation of the resulting flood hydrograph as it moves through the channel network to the outlet, is greater in a large catchment than in a small one. Catchment shape and the pattern of drainage network, the latter expressed through the bifurcation ratio (the ratio of the number of stream segments of any order to the number of stream segments of the next order), combine to influence the size and shape of flood peaks at the catchment outlet, as shown in Figure 6.
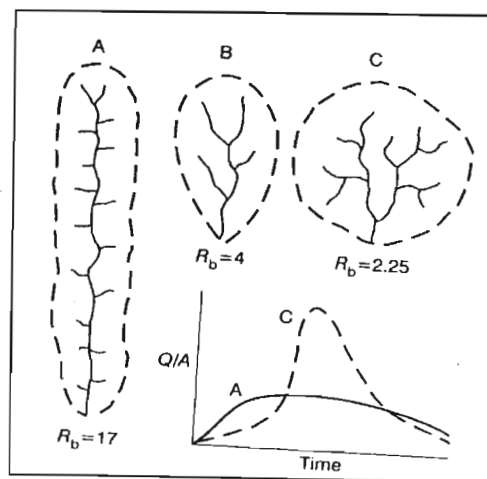
Figure 6: Relationships between catchment shape, bifurcation ratio (R_b) and the shape of the flood hydrograph (after Strahler, 1964).

The major dynamic storage component of a catchment is the soil matrix, and generally soil moisture variations need to be considered in both time and space for hydrological modelling. The storage capacity of soils and deeper subsurface layers

affect both the timing and magnitude of flood responses to precipitation, with those catchments having a low storage capacity often producing rapid and intense floods.

Ogunkoya et al. (1984) recorded annual runoff from small catchments of 2 to 18.8 km^2 in southwestern Nigeria, and found that the variability of precipitation and the geology of the basins influenced the mean annual runoff significantly. They made several investigations of the relationship between catchment size and runoff, and these showed that the characteristics of land use, soil and geology were only clearly expressed in catchments less than 5 km^2 in area. This confirms that modelling the hydrological responses of small catchments is more complex than modelling responses from large catchments. Not only can individual physiographic components influence runoff characteristics of small catchments, but partially it is also intra-daily processes (e.g. rainfall intensity) which take on significance in determining hydrograph shape. In large catchments, on the other hand, considerable spatial averaging of individual physiographic features, attenuation of flows in the channel and hence smoothing of the runoff hydrograph have taken place (Schulze, 1998). This is confirmation of the point made earlier that streamflow is more difficult to predict in small than in large catchments.

A comprehensive study conducted by Seyhan (1976) on 124 catchments ranging in area from 0.99 km^2 to 532 km^2, in which he investigated the feasibility of calculating runoff from rainfall, land use and physiographic parameters, concluded that runoff was found to be primarily a function of the physiographic parameters and rainfall characteristics. The most important physiographic parameters identified were catchment area, channel slope, length from catchment outlet to the centre of the catchment, total length of the main channel and maximum altitude difference (Seyhan, 1976; cited in Hope and Mulder, 1979).

Drainage density also influences streamflow by determining the distance water moves down catchment slopes before reaching the stream channel. A low value of drainage density corresponds to a landscape with long hillslopes, while a high drainage density indicates a dissected landscape (Berger and Entekhabi, 2001) with channels that are closer together. It is often seen as a key indicator of the hydrological response of a landscape, given the difference in velocity and residence

time of water between the hillslope and channel (Schulze, 1984). Drainage density also determines the extent of saturated areas around the channel network in the streamflow generation process since soils are more likely to be saturated close to the channels than on the upper reaches of a hillslope. Therefore, a positive relationship is expected between drainage density and the spatial extent of the riparian zone.

Schulze (1984) examined possible relationships between selected physiographic and climatic factors of a catchment and the initial abstractions, as defined for the SCS equation, that occur before stormflow begins. Abstractions are considered to consist of canopy interception, initial infiltration and surface storage. The higher the drainage density of the catchment, the more efficient the stream discharge was likely to be, and also the greater the contributing area; hence the lower the initial abstractions.

Topography is also a major controlling factor of subsurface flows (Becker and McDonnell, 1998). An early example of the recognition of topography in influencing catchment hydrological responses was the work of Hewlett and Hibbert (1967), who analysed the topography of a catchment in order to predict areas of soil water accumulation and the likely location of variable source areas.

The concavity or convexity of a slope, as well as slope length to depth ratios, all influence the rate at which subsurface flows contribute to streamflow. Bedrock topography has also been shown to influence the subsurface processes. Research conducted by Lorentz and Esprey (1998) has shown that flow along the bedrock may be different to that of the surface topography and thus needs to be taken into account when considering subsurface processes.

Hydrologists have, over the years, relied on surface topography to quantify patterns of downslope movement of water and solutes, since gravitational potential largely dominates hydraulic gradients in steep terrains. With the increased availability of digital terrain information, hydrological models that predict streamflow from surface topographical properties (e.g. TOPMODEL, TOPOG) have found increasing application (Becker and McDonnell, 1998). Howe (1999) developed new algorithms for the *ACRU* agrohydrological model to describe the spatial variability of soil water infiltration, and the respective hydrological flow pathways of water through a

catchment. This distributed grid-based component enabled the identification of areas in a catchment where surface runoff is generated and the associated potential source areas for soil erosion.

2.3.2 Climate parameters

Problems encountered when modelling hydrological systems are enhanced by the prevailing climatic conditions (Schulze, 1998). Pearce (1990) commented on the difficulties of modelling streamflows in arid catchments, where streamflow production mechanisms are often different to those in humid areas. Such regions are characterised by prolonged dry periods and ephemeral flows. Soil surface conditions (e.g. sealing, crusting) often inhibit rainfall infiltration into the soil, and promote surface runoff. Pilgrim *et al.* (1988) also reported on the difficulties of modelling hydrological processes in arid and semi-arid catchments, and made the following three comments:

- These regions are in a "delicate hydrological balance", and large changes in hydrological processes may be initiated by prolonged wet or dry weather.
- The soil type and surface properties play an important role in determining the proportion of rainfall infiltrating the soil and that lost as surface flow.
- Vegetation is generally sparse, consisting mainly of xerophytes, ephemeral grasses and small leafy plants. Large changes in cover and species composition may be evident between wet and dry periods, and such differences may cause significant spatial and temporal variation in the soil water balance.

Most hydrological research and model development has been undertaken for application in highly populated temperate zones. However, much of the developing world, in which major hydrological decisions have to be made, is hydrologically more complex and in arid / semi-arid zones unique processes such as channel transmission losses occur (Schulze, 1998). In temperate humid regions of low relief the dominant hydrological processes occurring are rainfall of low to moderate intensity, low evaporation rates, relatively rare overland flow, slow lateral drainage systems, with groundwater often rising to the surface where soils have become

saturated and hence waterlogging occurs. In arid and semi-arid regions, rainfall is usually highly variable in time and space in regard to intensity, duration, frequency, amount, location, as well as in its intra-seasonal and inter-annual distribution. A high element of uncertainty thus exists in estimating rainfall characteristics (Schulze, 1998). Many characteristics of rainfall, in association with soil properties, result in Hortonian overland flow being the dominant SGM.

In humid and semi-arid tropical areas higher rainfall intensities result in different streamflow generation processes to those observed in, for example, humid temperate forests. Bonell (1993) suggests that the link between soil hydraulic properties and topography should include synoptic climatology and, more specifically, rainfall intensity characteristics, in partly explaining the hillslope hydrological responses across the tropics (Bonell, 1993). Meyles *et al.* (2001) describe two types of rainfall-runoff responses resulting from different rainfall intensity events. During small and medium sized rainfall events the contributing area is restricted to the flat areas adjacent to the stream, and moisture patterns of the topsoil are heterogeneous. During events of larger magnitude, soil moisture patterns become more uniform and the contributing area is extended onto the hillslopes. The change from immediate adjunct source area dominated flow to entire hillslope flow generation can have important implications for risk management. Marked changes in the properties of the topsoil, or subtle changes to vegetation leading to different moisture patterns, may alter the threshold value between the two different flow mechanisms (Meyles *et al.*, 2001).

Like most hydrological processes, none of the stormflow generating processes are isolated. It is the dynamic interrelationship and interdependence of all the hydrological processes within the catchment that determine its response (Beven *et al.*, 1988). Differences in the amount and intensity of rainfall as well as in soil moisture conditions will result in different stormflow generating processes occurring at different times and areas throughout the catchment. Hortonian type flow, for example, may occur over the rocky, or soil compacted, upper slopes of a catchment during a short duration high intensity convective rainfall event. However, saturated overland flow may occur at a break of a slope or adjacent to a river channel if the rainfall event was of long duration and low intensity (Topping, 1992).

Bonell (1993) summarised the results of a series of papers describing hydrological responses from tropical rainforest catchments near Babinda in north-east Queensland. These studies supported the conclusion that storm runoff response is highly sensitive to rainfall intensity during the wet summer season, and confirmed the significance of rainfall intensity for quickflow volumes exceeding a 10 mm depth equivalent for both undisturbed and disturbed catchments.

Research has shown the marked effect that the catchment response, or lag time, has on peak discharge. Schmidt and Schulze (1987) re-evaluated the original SCS lag equation against observed hydrograph and hyetograph data using a large database of small catchments in the USA and RSA to enhance it's accuracy. This study introduced the two-year return period 30-minute rainfall intensity (I_{30}) variable into the lag equation, since it was found that an intensity-related rainfall variable affected the catchment response times significantly. Topping (1992) investigated the influence of variations in rainfall intensity on stormflow generation by the manner in which it influenced the initial abstractions which occur before stormflow commences during a rainfall event. High intensity rainfall events were shown to have lower values of initial abstraction than those from the equivalent depth of low intensity rainfall. The magnitude of initial abstractions were also found to decrease exponentially with increase in rainfall depth.

Past research studies describe the complexity which arises from modelling hydrological responses of catchments from varying climatic regimes, especially those in arid and semi-arid regions. Rainfall is an important climatic variable which influences a catchments hydrological response. Rainfall characteristics such as the intensity and duration of rainfall events have pronounced influences on the streamflow generation process, and therefore should be accounted for in hydrological models.

2.3.3 Antecedent soil moisture

Antecedent soil moisture is acknowledged as an important determinant of the conversion of rainfall to streamflow. Dunsmore (1985) cited the findings of Philip (1957), who described the effects of antecedent soil moisture on infiltrability as being

27

significant over a short period of time, with varying soil moisture levels generating different infiltration curves as time increases. These curves tend towards a common asymptote, *viz.* that of a curve for a saturated soil (Figure 7).

Hills (1971) noted that initial soil moisture is the most significant soil factor in the production of stormflow, and that changes in high antecedent moisture levels give rise to significant changes in storm runoff, maximum peak flows and, hence, total storm runoff. Many rainfall:runoff models keep a continuous balance of soil water storage in order to improve prediction of runoff (e.g. TOPMODEL, *ACRU*).
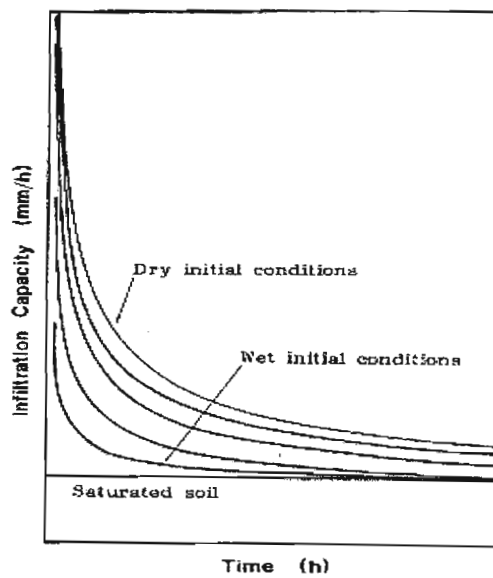
Figure 7: The influence of initial soil moisture content on infiltration rate (after Philip, 1957).

Procedures to adjust runoff response for the soil's antecedent moisture status range from simple empirical methods using, for example, an antecedent precipitation index, to complex moisture budgeting routines. Hawkins (1978) recognised some weaknesses of the 5-day rainfall accumulation antecedent moisture routines of the SCS model, and developed an alternative method which included stormflow, drainage, evapotranspiration and antecedent rainfall and expressed the relationships between curves numbers and antecedent soil moisture as a continuum rather than a discrete 3-category stepped function (Schmidt and Schulze, 1987). Schmidt and Schulze (1987) included two moisture budgeting techniques to adjust runoff response to catchment antecedent moisture status in their adaptation of the SCS technique for

28

application in RSA. These were the Median Condition Method and Joint Association Method.

Different methods and techniques have been used to represent the antecedent soil moisture conditions of a catchment. However, whichever method is used, there is agreement amongst researchers of the important role of antecedent soil moisture in the rainfall-runoff process.

2.3.4 Vegetation parameters

Changes in vegetation may occur as a result of the natural process of seasonal plant growth and die-back, or in response to a wide variety of human activities, which may have profound effects on streamflows. Alterations to the physical characteristics of the soil surface may be pronounced as a result of vegetation changes, and may significantly influence the rate of infiltration of rainfall into the soil, as well as the degree of overland flow. Catchments in the humid tropics are usually degraded agricultural landscapes, where surface infiltration rates are reduced under the influence of heavy rain. Additional disruptions to the soil structure are caused by compaction from trampling livestock, and these effects lead to enhanced overland flows and reduced subsurface flows (Bonell, 1993).

A clear example of the importance of vegetation in promoting infiltration of rainfall into the soil was reported by Scott (1993). Wild fires which swept through two Western Cape research catchments afforested with pines and eucalypts caused large and significant increases in stormflows. Quickflows in the first year following the fire increased by 201% and 92% in the pine and eucalypt covered catchments respectively. This was attributed to increased surface runoff to the stream channel.

In a comparative study of soils under grassland and *Eucalyptus* forest in RSA, Musto (1994) found that trees made significant changes to the transmission of water through the soil profile. A change from grassland to forest was associated with reductions in soil water content, increases in soil water repellency which reduced unsaturated hydraulic conductivity, and enhanced macropore conductivity.

Bonell (1993) also draws attention to the effect of forests on macropore development, especially in the surface layers. This is brought about by large root systems and enhanced soil faunal activity. Such macropores permit infiltrating water to bypass unsaturated soil horizons and reach the saturated zone more quickly than through normal soil infiltration. The importance of preferential flow paths in the rapid redistribution of surface water and solute transport was recognised as long ago as the late 19th century (Moore, 1989; cited by Bonell, 1993), but it was not until the late 1970s, when field experimentation increased, that the importance of this mechanism was widely recognised in the soil physics literature.

Marked changes in evapotranspiration (ET) losses may result from changes in land use, or in the condition of the landuse. Especially significant changes in ET have followed from the conversion of mountain grassland and fynbos to forest plantations in RSA, with annual ET rising from 700-800 mm to around 1200 mm (Bosch and von Gadow, 1990). Such figures confirm the widespread South African experience that afforestation reduces streamflow volumes (Malherbe, 1968). In RSA already 15 000 km^2 of land is under fast growing exotic forest plantations (Dye and Bosch, 2000), which pose a threat to the country's scarce water resources.

Hydrologically the characteristics of forest plantations translate to:

- reduced entry of rain water into the soil, by virtue of higher canopy cover as well as litter interception, but enhanced entry of that water which does infiltrate the soil surface, and
- enhanced evaporative losses from denser, evergreen and aerodynamically rough trees with generally deep root systems (Schulze, 2001).

These characteristics alter the streamflow generation process. Dye and Bosch (2000) have summarised results which illustrate increases in evapotranspiration from trees in different climatic regions in RSA (Figure 8).
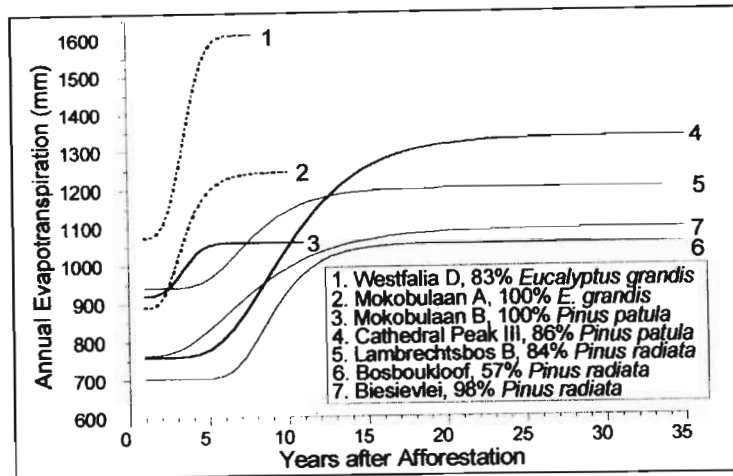
Figure 8: Increases in annual evapotranspiration in South Africa for three tree species as an index of reduction in annual runoff in afforested catchments in different climatic regions and with varying extents of forest coverage (after Dye and Bosch, 2000).

The annual increases in evapotranspiration represent equivalent reductions in runoff as the trees grow. Reductions in streamflow from forested catchments also generally take place both in stormflow generation (because of increased interception losses and infiltrability), and in baseflow generation (because of deeper rootedness), with dry season flows usually being impacted relatively more than wet season flows (Scott *et al.*, 1998; Calder, 1999; Schulze, 2001).

Federer (1973) drew attention to the influence of vegetation ET on streamflow recession rates. His study demonstrated rapid declines in recession rates in summer and slower declines in spring, and attributed these differences to higher transpiration rates in summer. Several studies of relatively large and flat catchments, where streamflow is dominated by groundwater discharge, have shown seasonal flow rates to be influenced by transpiration from plants with access to groundwater (Chow, 1964). Both Donkin *et al.* (1995; Figure 9) and Birkhead *et* al. (1996) have, in very different hydroclimatic zones within RSA, shown that in summer months evaporation from wetlands is often 1.5 to 2 times in excess of Penman open water estimates, but only approximately 0.5 times as high in winter, when dormant reeds shade the evaporating surface. Figure 9 illustrates diurnal variability through fluctuations in the water table for sedge grass in the Ntabamhlope wetland.
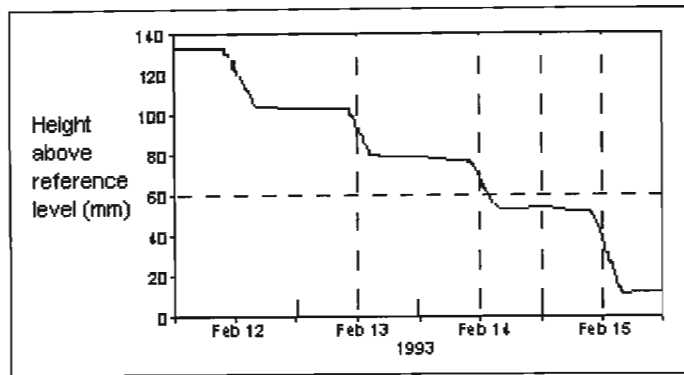
Figure 9: Diurnal water table hydrograph fluctuations in sedge grass in the Ntabamhlope wetland, South Africa, showing the influence of wetlands on evaporation (after Donkin *et al.*, 1995).

Donkin *et al.* (1995) adopted the method of using the diurnal fluctuation of the water table to estimate total evaporation from the wetland. The net fall in the water table over a 24 hour period along with the water retention characteristics of the soils were used to determine the amount of water removed from the vadose zone on a daily basis. Therefore the daily total evaporation estimated was a function of the specific yield of the soil, rate of groundwater inflow and the net rise or fall of the water table during the 24 hour period. The assumption made in this study is that the lateral flow of groundwater into the wetland is constant and that night time total evaporation is negligible. However, a disadvantage of this method is that it may only apply to the recession limb of the hydrograph and hence excludes rain days.

The proportion of a catchment covered by riparian vegetation may be an important attribute affecting streamflow patterns. Riparian vegetation has better access to soil water, and is able to maintain a potential rate of ET for longer than vegetation in non-riparian sites where soil water is less available. These attributes may be simulated by the *ACRU* model (e.g. Meier *et al.*, 1997).

Investigations by Farvolden (1963) into controls on groundwater storage and baseflow generation showed that evapotranspiration losses from the groundwater reservoir can be estimated from the recovery of the baseflow at the end of the growing season. This evapotranspiration bears an approximate relationship to the length of the channel lined with phreatophytes.

32

Changes in vegetation across a catchment due to natural processes or land management operations may have marked effects on streamflow generation. Significant differences are expected when partitioning rainfall into streamflow and evaporation components depending upon the type of vegetation and their location within the catchment.

2.3.5 Soils parameters

A vital role is played by soil in determining streamflow rates and volumes because of its capacity to absorb, retain and release water, of which all these affect the hydrological response of a catchment (Schulze, 1995). Ayers and Ding (1967) concluded that steeper cumulative frequency curves, indicative of high streamflow variability, are associated with fine textured soils. Such soils exhibit poor internal drainage, high rates of runoff during the rainy season, and low rates of groundwater recharge. By comparison, medium to coarse textured soils are more likely to exhibit greater amounts of groundwater recharge and are, therefore, more likely to sustain baseflows. Ayers and Ding (1967) also noted a definite decrease in baseflow recession constants, implying that baseflow which recede at a slower rate, as soil textures become finer. As expected, immediate saturated overland flow occurs from moist or wet soils, while on the other hand, a strongly delayed saturation overland flow occurs from thick macroporous soils with a permeable matrix (Scherrer and Naef, 2001).

Work by Hills (1971) showed that the influence of soil texture on soil infiltration capacities might be of less significance than soil disturbance. Thus:

- changes in soil moisture levels between winter and summer were much smaller for compacted sites than for other sites, and
- reduced infiltration rates were attributed to surface crusting as well as to soil compaction.

Pronounced differences in the magnitude and sequence of hydrological processes have been observed in soil "units" within a catchment. The delineation of soil groups which are relatively homogenous with respect to hydrological response is thus necessary. Schulze and Arnold (1979) identified a parameter which provides the

basis for a hydrological classification of soils in RSA as "the typical amount of infiltration for the soil at a likely moisture content to the point of maximum runoff rate". The hydrological properties considered by Schulze and Arnold (1979) when deriving the four basic hydrological soil groups for RSA were, the infiltration rate at soil surface, permeability and the water storage capacity. Further classification of soils for the application of the SCS model in RSA also considered soil texture, leaching properties, water table depth, soil crusting, soil depth, surface sealing, topographic position, parent material and the interflow potential of the soil (Schmidt and Schulze, 1987).

Soil surface conditions are of particular importance for the infiltration process and for the generation of infiltration excess overland flow. In central Europe, infiltration excess overland flow is normally restricted to bare soil, compacted soil and paved or sealed surfaces (Bronstert and Katzenmaier, 2001). Redistribution of infiltrated water is also dependent on soil characteristics such as its hydraulic conductivity and water retention characteristics, which can be highly variable through a profile. Vertical flow is common among deep and coarse textured soils, whereas lateral shallow subsurface flow is found in fine textured soils (Beckedahl, 1996). Lateral flow is also common in shallow soils where the bedrock or impermeable surface force water to flow laterally above it (Wallach and Zaslavsky, 1991).

In the literature, soil characteristics (e.g. soil texture) and surface conditions (e.g. surface crusting) play an important role in determining streamflow rates and volumes from catchments. Such factors influence the redistribution of infiltrated water, and hence the soil moisture conditions across a landscape which result in different SGMs.

2.3.6 Geological parameters

Parameters describing geological conditions in a catchment are difficult to establish and to quantify. The difficulty is not only related to a lack of large-scale geological and hydrogeological maps from which parameters may be obtained, but more fundamentally revolves around the problem of developing an index which adequately describes the impact of geological parameters on streamflow. Past research has generally confirmed the important role of catchment geology on low flow estimation

and baseflow recession curves, although most studies have not attempted to include geological parameters as catchment characteristics in regression models. Another generalisation arising from past research is that soil profile characteristics and fractured rock play a major role in defining baseflow recession characteristics (Lacey and Grayson, 1998).

The influence of geological factors on streamflow is most apparent during baseflow periods when streamflow is fed almost exclusively by groundwater (Hughes, 1997). Hughes (1997) stated, "it is apparent that the analysis of streamflow records may provide significant information concerning the groundwater geology of an area". However, his study of a wide selection of South African catchments could only demonstrate weak relationships between baseflow master recession curves and catchment geology.

Demuth and Hagemann (1994) considered the necessity of a numerical system of describing the hydrogeological characteristics of each geological formation to assess the influence of geology on river flows. A geological index was developed based on a classification scheme which included both basin geology and hydrogeological data. Based on a set of 57 catchments within the province of Baden-Württemberg in Germany, this geological index, together with other basin characteristics, was tested successfully in a multiple regression model to estimate baseflow at ungaged sites.

Ogunkoya et al. (1984) reported that catchments underlain by highly faulted and fissured quartzites promoted rapid infiltration and effective storage of rainfall. Steep topography ensured rapid movement of water to channels, minimising losses to evapotranspiration and promoting a high annual runoff. By contrast, other rocks such as granite gneisses, amphibolites and schists are poorly jointed and are often associated with clayey saprolite. When combined with low relief, such catchments are characterised by a small groundwater contribution to total streamflow and low dry-season runoff. All geological variables used in their study accounted for an average of 66% of the variance of the runoff variables, indicating that runoff responses in the catchments were significantly influenced by the underlying soil and geology.

Farvolden (1963) cautions that baseflow may be limited by a single adverse geological control of subsurface flow. The presence of features such as impermeable dykes and sills may limit the rate of subsurface flow to the channel. Onda (1994) reported that the spatial variation of specific discharge in the Usetu mountains was larger in Palaeozoic sedimentary rocks than from granites. This spatial variation in streamflow generation suggests that fissures and cracks control spring location and discharge in the area. Such findings strongly suggest the importance of bedrock in controlling outflow from this catchment.

In catchments where baseflow constitutes an important component of the total streamflow, unconsolidated geological materials may be of major importance in the storage and transmission of water. These materials include river sediment and various forms of glacially deposited sediments. Highly variable streamflow discharges may indicate that rapid runoff and little deep percolation occurs within a catchment, while more uniform flows are produced when rainfall percolates to the groundwater store as it moves towards the stream (Hughes, 1997).

Even though past research has confirmed the important role of catchment geology on streamflow generation, it has proved to be a difficult task for researchers to establish and quantify parameters describing geological conditions in a catchment. However, literature does suggest that underlying geological material may have a significant influence on low flows and baseflow recessions.

* * * * * * * * * * * * * * * * * *

Preceding sections of Chapter 2 have focussed on an intensive review of SGMs and processes, and important physiograhic and climatic characteristics which have been shown to critically influence the hydrological responses of catchments. It is evident from this literature review that many researchers have used differing terminology to represent common elements of the streamflow generation process. It was therefore imperative that these components were identified and discussed in further detail to prevent confusion. These processes included direct stormflows, subsurface and lateral flows and groundwater flows. The next section of the literature review highlighted the climatic and physiographic attributes of a catchment which have been

identified as important factors which affect streamflow generation. Therefore the preceeding literature reviews formed the basis for understanding SGMs and processes, and provided the foundation for selecting parameters which should be included in the investigation of possible relationships between hydrological responses parameters and catchment climatic and physiographic attributes.

Chapter 3 which follows will outline the methodologies adhered to in this research in order to achieve the objectives outlined in Chapter 1. It provides background information on the concepts and structure of the *ACRU* model, and describes the overall research strategy and procedures followed in selecting an appropriate list of catchments for this study. Chapter 3 also describes the input data collected for setting up each catchment for simulation using the *ACRU* model.

3. METHODOLOGY

A number of studies using the *ACRU* model have highlighted the problem of correctly simulating flows from small catchments (Dunsmore, 1985; Angus, 1987; Topping 1992). The goal of this research was to seek links between catchment physical descriptors, patterns of streamflow and *ACRU* input parameter values required to simulate these flows. This chapter will provide some relevant background information on the *ACRU* model, describe the overall strategy of this research, and the criteria adopted in selecting appropriate catchments for this study.

3.1 Concepts and Structure of the *ACRU* Model

The *ACRU* agrohydrological model (Schulze, 1995) is a multi-purpose, daily time step, conceptual-physical model. It operates on multi-layer daily soil water budgeting, with outputs that include daily stormflow and baseflow contributions, sediment yield, reservoir yield as well as irrigation supply and demand. The *ACRU* model was originally developed in the early 1980s for studies of land use change impacts on water resource assessment, and has subsequently undergone continuous development and enhancement. It is well suited for use in southern Africa, with links to appropriate local land use, soil and climate databases.

ACRU can operate in lumped mode for smaller catchments, or as a distributed cell-type model for areas with more complex land uses or soils. Individually requested outputs for each subcatchment (which may be different to those of other subcatchments), or with different levels of information, may be generated. A schematic of the manner in which multi-layer soil water budgeting is accounted for in *ACRU* is depicted in Figure 10 (Schulze, 1995).

The model also includes a dynamic input option to facilitate modelling of hydrological responses to climate or land use changes over time. These may be long term / gradual changes (e.g. forest growth, urbanisation, climate trends) or abrupt changes (e.g. clear felling, fire impacts or construction of a dam).
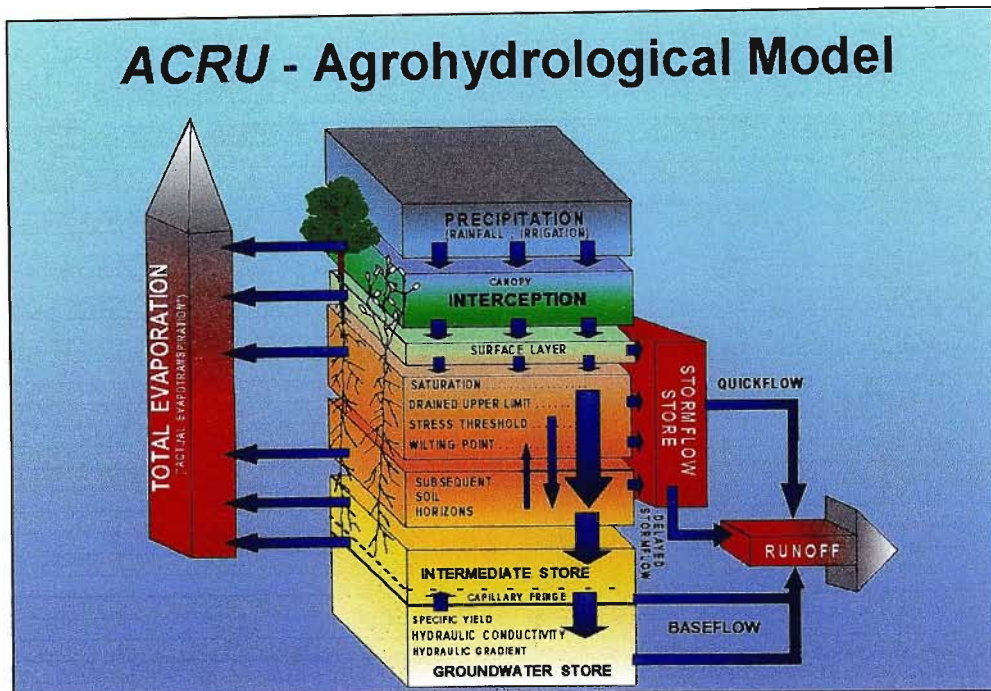
Figure 10: Structure of the *ACRU* agrohydrological modelling system (after Schulze, 1995).

ACRU also operates in conjunction with interactive *ACRU* Utilities (Smithers and Schulze, 1995). These comprise a suite of software tools to aid in the preparation of input and output information, e.g. a Menubuilder to compile catchment menus for *ACRU* application, the program CALC_PPTCOR to facilitate selection of appropriate rainfall stations, the decision support system AUTOSOILS (Pike and Schulze, 1995) to extract relevant soil characteristics and the Outputbuilder to select the appropriate output variables for graphical or statistical analysis. The components of the *ACRU* system are displayed in Figure 11 (Schulze, 1995). The version of the model used in this study was *ACRU* 331.
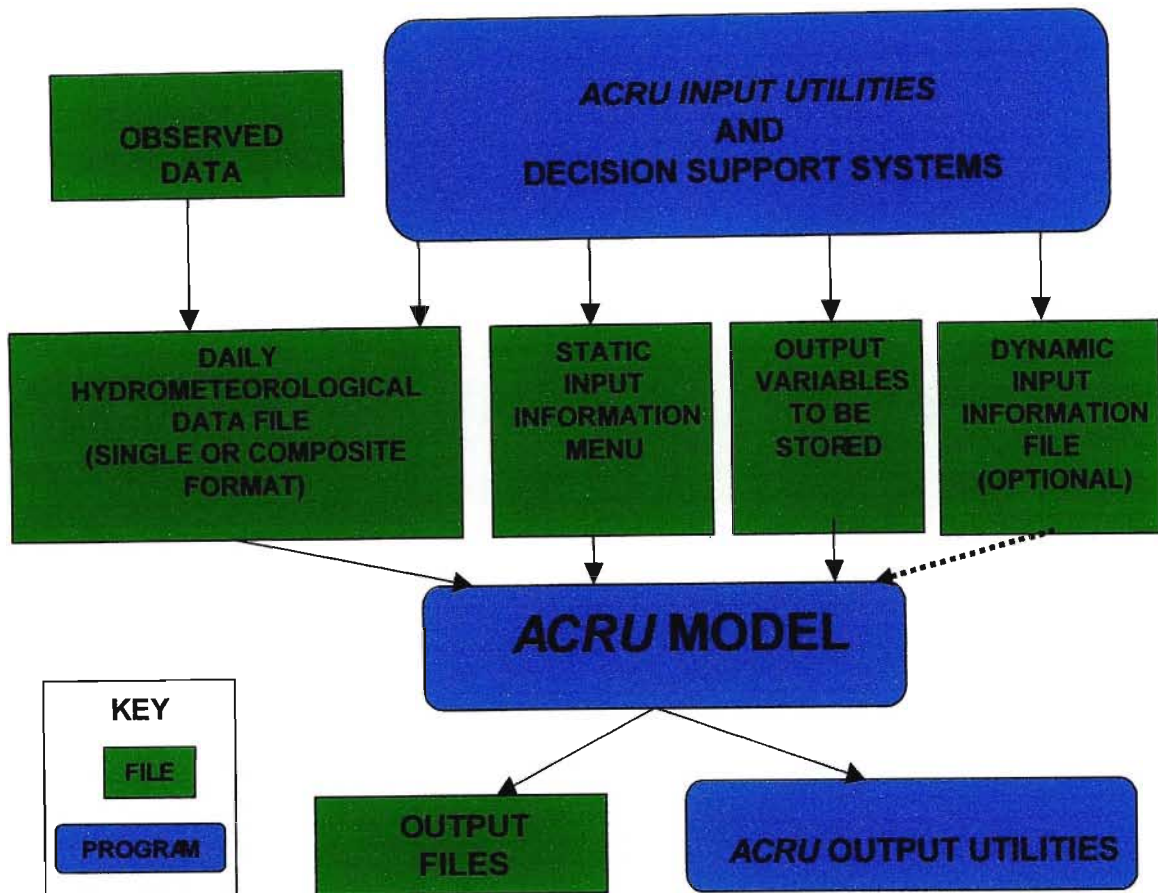
Figure 11: Components and structure of the *ACRU* modelling system (after Schulze, 1995).

3.2 Streamflow Simulation by *ACRU*

Streamflow components generated by the *ACRU* model comprise of baseflow and stormflow, the latter from both pervious and impervious areas. Stormflow from pervious areas consists of a quickflow response that is released into the stream on the same day as the rainfall event, and a delayed stormflow response which represents a surrogate for post-storm interflow. Baseflow is derived from the groundwater store that is recharged by drainage out of the lower active soil horizon when its water content exceeds the drained upper limit (Schulze, 2000b).

The estimation of stormflow depth is based on modifications to the equation derived by the Soil Conservation Services (United States Department of Agriculture, 1985) and Schmidt and Schulze (1987):

$$Q = \frac{(P_g - I_a)^2}{P_g - I_a + S} \quad \text{for } P_g > I_a$$

where,

Q	=	stormflow depth (mm)
P_g	=	gross daily precipitation amount (mm)
I_a	=	initial abstractions (mm) before stormflow commences
S	=	potential maximum retention (mm).

There are several conceptual differences between the original SCS stormflow equation and the form in which it is used in the *ACRU* model (Schulze, 1995):

- Interception is abstracted separately and before the commencement of potential runoff-producing rainfall, and is not part of the initial abstractions as in the SCS model.

- The coefficient of initial abstraction (COIAM) is not a one-off input parameter, but may be varied monthly. It is dependent on regional and seasonal rainfall intensity patterns, vegetation, as well as site and management characteristics (e.g. tillage).

- The potential maximum retention, S, is calculated as a soil water deficit by the multi-layer daily soil water budgeting routines of *ACRU* as the difference between soil water retention at porosity and the actual soil water content just prior to the rainfall event, assumed to occur at the end of a day after evapotranspiration losses have been accounted for.

- A coefficient of quickflow response (QFRESP) has been included in the model to account for any lagged response caused, for example, by catchment size, soils with high or low interflow potential, steep or urbanised catchments, and different vegetation types. This parameter therefore acts as an exponential decay function controlling the timing and distribution of stormflow over one or several days, but does not control the total amount of stormflow.

- The critical soil depth (SMDDEP), for which the soil moisture deficit is calculated for stormflow generation attempts to account for different dominant streamflow-producing mechanisms caused by different climates, vegetation

and soil conditions. For short vegetation, a default value equal to the depth of the topsoil horizon may be used. However, for a catchment with a dense canopy cover such as forest plantations, which dissipates the rainfall's energy, or has a deep litter or an organic layer, or contains highly leached soils resulting in relatively high infiltrability, the critical depth for calculating the soil water deficit may be deeper than the topsoil horizon because stormflow on such catchments may be perceived as being produced more by a "push through" / translatory mechanism. For purposes of this research SMDEPP was defaulted to the depth of the topsoil horizon, except under forested areas exceeding 50% of the catchment area. For these conditions an area weighted value of 0.35 m for 100 % afforested conditions was calculated (Schulze, 2000a).

With regard to baseflow generation, a number of response coefficients have been incorporated into the model. The first two relate to the drainage rate of water out of a soil horizon, when its soil water content exceeds the drained upper limit. ABRESP determines the rate at which excess water drains from the A- to B-horizon, while BFRESP controls the rate of saturated drainage from the B-horizon to the intermediate groundwater store. These response coefficients are slower for heavy than for light textured soils. Suggested values for ABRESP and BFRESP for different soil texture classes are given in Schulze (1995).

The third coefficient is that of baseflow response, COFRU, which controls the release of water as baseflow from the intermediate / groundwater store into the stream per day. Factors influencing baseflow release include geology, catchment area and slope. The assumption is made that the groundwater store is "connected" to, i.e. intersects the channel. A starting value of 0.009 is recommended by the model developers (Schulze, 2000a). COFRU, by definition, may be considered a baseflow recession constant. However, experience has shown that baseflow is not constant, but rather a function of the magnitude of the previous day's groundwater store. An empirical relationship used in *ACRU* and developed from intensive studies on the Mgeni catchment (Kienzle *et al.*, 1997) is given by the following equation:

$$F_{bff} = F_{bfi} \left[\left[(S_{gwp})^2 - S_{gwp} \right] / 1000 + 1.3 \right] / 1.1 \right]$$

where

F_{bff}	=	final baseflow release coefficient
F_{bfi}	=	input baseflow release coefficient
S_{gwp}	=	magnitude of previous day's groundwater store (mm).

Evaporation takes place from previously intercepted water, as well as simultaneously from the various soil horizons. It is either split into separate components of soil water evaporation (from the topsoil only) and plant transpiration (from all horizons in the root zone), or else combined as total evaporation (formerly termed "actual evapotranspiration"). Soil water evaporation for a day can either occur at maximum rate (if a minimum threshold of soil water content is exceeded), or below the maximum rate once soil water has dropped below this threshold. In the latter case, soil water evaporation declines very rapidly over time. Evaporation from a vegetation cover is estimated according to an atmospheric demand, calculated from a reference potential evaporation, and a water use coefficient which reflects, *inter alia*, the growth stage of the vegetation. Plant roots absorb soil water in proportion to the distributions of root mass density in the respective horizons, except when conditions of low soil water content prevail. In such cases the relatively wetter soil horizons provide higher proportions of soil water to the plant in order to obviate plant stress for as long as possible.

3.3   Overall Research Strategy

The research strategy adopted was to select a range of small catchments displaying a wide variety of physical features. Each one was configured for simulation with the *ACRU* model, and parameterised to provide a best fit to observed flows. The assumption was made that stormflow and baseflow are simulated accurately by the *ACRU* model. These were then summed on a daily basis to yield the total simulated streamflow leaving a cell or the catchment. The reason for summing baseflow and stormflow components was that observed streamflow records are not separated into individual streamflow components.

Once acceptable simulations had been achieved for each catchment, in most cases through subjective parameter changes within upper and lower limits prescribed in the *ACRU* User Manual (Smithers and Schulze, 1995), the range of values for those model parameters controlling flow was assessed. The criteria used to select model parameters for the study were as follows:

- Parameters governing the time distribution of streamflow generated were selected, and not variables (as distinct from parameters) which influence the amount of streamflow generated *per se*.

- These parameters were not explicitly physically based and, therefore, were in need of improved guidelines for initial parameter estimates.

The two parameters selected from the *ACRU* model for this study were the coefficient of baseflow response (COFRU) and the quickflow response fraction of the catchment (QFRESP). Relationships with the physical characteristics of the catchments and these parameters were sought as a guide for effective parameterisation of these parameters in future *ACRU* studies.

3.4   Catchment Selection

3.4.1 Selection criteria

Available hydrological data from small catchments were sourced from the Department of Water Affairs and Forestry (DWAF), Council of Scientific and Industrial Research (CSIR), School of Bioresources Engineering and Environmental Hydrology (BEEH), the University of Zululand, Rhodes University and the United States Department of Agriculture (USDA). Catchments were selected according to the following criteria:

- They were to be representative of the broad variations in climate, topography, vegetation and geology occurring throughout RSA. Small catchments in RSA are monitored mainly in the higher rainfall regions of the country, where runoff is significant and any land use changes may lead to marked changes in evapotranspiration and streamflow. A catchment from an arid zone in the USA

was therefore, included to capture flow characteristics that are typical of such areas.

- For this study small catchments were defined here as being < 100 km^2 in area.

- They were to cover a wide range of catchment areas, baseflow indices and recession constants, in order to assist in identifying relationships between required flow parameter values and physical characteristics of the catchments. Smakhtin and Watkins (1997) undertook a low flow analysis of data recorded at 252 streamflow recording stations in RSA, and calculated a Baseflow Recession Constant (RCONST) and Baseflow Index (BFI) for each catchment. The BFI concept was developed by the Institute of Hydrology in the UK (now Centre for Ecology and Hydrology) in 1980, to describe the effect of geology on low flows. It is a dimensionless ratio that is defined as the volume of baseflow divided by the volume of total streamflow. In catchments with a high groundwater contribution to streamflow, BFI may be close to unity. In the case of ephemeral streams, it may approach zero. The recession constant is a measure of the characteristic recession rate of each flow component of a storm hydrograph. In terms of low flow, the most important component is RCONST, which is a measure of the rate at which a groundwater store discharges in the absence of recharge, which then determines the rate at which baseflow recedes in the absence of rain (Smakhtin and Watkins, 1997).

- Catchments with significant impoundments were excluded from this study to ensure natural flow regimes. A useful list of "natural flow" catchments with a minimum record length of 20 years was provided in a report by King and Tharme (1994). In that report, Joubert and Hurly (1994) performed homogeneity tests to ensure that these catchments exhibit consistent and natural patterns of flow. From these catchments, Hughes (1997) compiled a list of 201 streamflow recording stations assumed to have a homogenous streamflow record. This list formed the basis for selection of catchments for this study.

- Raingauge density was to be sufficiently high to provide a reasonable estimate of rainfall falling over the catchment. Raingauge density was estimated by demarcating approximate catchment boundaries using a 200 m Digital Elevation Model (DEM) to determine the positions of raingauges in relation to catchment boundaries.

- There needed to be concurrent rainfall and streamflow data of an acceptable quality, and for a minimum period of 5 years. This minimum period was adjusted for specific catchments which had good quality rainfall and streamflow data available. Where possible the selected simulation period consisted of both wet and dry rainfall sequences to ensure that the subsequent analyses were representative of each catchment. The low flow analyses completed by Smakhtin and Watkins (1997) also proved very useful in the selection process by identifying those gauging stations with poor quality streamflow data.

- No significant change of land use was to have occurred over the simulation period. Aerial photographs were used to assess land use patterns within candidate catchments. Those catchments with significant land use changes, were then excluded from the selection process.

The selection process proved to be extensive. Some of the major hurdles encountered included the following:

- Incorrect co-ordinates were recorded for many gauging stations, leading to incorrect catchment areas. The correct locations of these gauging sites were checked against 1:50 000 scale maps.

- Data were often of poor quality; obvious errors and gaps were apparent in many data sets and were therefore excluded from the study.

- Data have been lost for key research catchments in the Eastern Cape (Bedford and Ecca catchments).

- A poor raingauge network was evident in many instances.

- A number of different formats have been used for storing hydrological data. Problems were experienced with data obtained from research catchments at Bethlehem, Zululand and Safford (USA) catchments, and much time was lost in reformatting data.

- A scarcity of data exists in RSA for arid catchments. The Safford research catchment in Arizona, USA, was eventually selected to evaluate hydrological responses from arid catchments.

In view of the paramount importance of high quality data in this research project, more reliance than was originally intended had to be placed on research catchments and less on operational catchments.

ACRU had to be configured for each of the selected catchments. The following data and information were required as model input, or for verifying model output:

- Reliable, concurrent time series data sets of streamflow and rainfall. These data sets were checked graphically for missing values, measurement and accuracy errors and possible phasing problems (e.g. events recorded a day early or late). An appropriate record length of 5 years or longer was selected for each catchment. Graphs of cumulative rainfall against cumulative streamflow were plotted for the selected simulated periods, to check for any marked non-homogeneity. Rainfall data needed to be representative of the entire catchment. For some catchments, there was the need to adjust recorded rainfall values for topographical variations using a computer program CALC-PPTCOR (Pike, 2001; pers com).

- Catchment boundaries which were delineated and digitised from 1:50 000 topographical maps. These coverages were then used to extract information from spatial data sets obtained from the School of BEEH. This involved running the *ACRU* Grid Extractor Arcview extension (Lynch, 2001; pers com).

Information extracted for each subcatchment / catchment included the following, with the source of information also given:

- Gridded mean monthly A-pan equivalent values reference potential evaporation at 1' x 1' latitude by longitude resolution (Schulze, 1997);
- Gridded MAP and altitude (Dent *et al.*, 1989);
- *ACRU* soils variables, calculated from the Institute of Soil, Climate and Water database (ISCW, 1993) on soil land types by the program AUTOSOILS (Pike and Schulze, 1995);

- Land cover, extracted from the National Land Cover Database produced by the CSIR (1996), with aerial photographs used to verify the land cover of operational catchments for the period of simulation; and

- Gridded monthly means of daily maximum and minimum temperatures (Schulze, 1997).

3.4.2 Descriptions of selected catchments

Fourteen catchments were eventually selected for this study. Table 4 lists information on the catchments while Figure 12 illustrates their geographic location. Figures 13 and 14 illustrate the range of catchment area, MAP, RCONST and BFI covered by these catchments.

Table 4: Catchments selected for use in this research study (with DWAF gauging station numbers in parentheses), together with their area, MAP, dominant vegetation, BFI and RCONST.

No.	Catchment	Area (km²)	Estimated MAP (mm)	Dominant Vegetation	BFI	RCONST
1	Westfalia B (B8H022)	0.33	1253	Indigenous Forest	0.25*	
2	Cathedral Peak IV (V1H005)	0.95	1400	Grass	0.30*	
3	Witklip V (X2H028)	1.08	1100	Forest	0.35*	
4	Lambrechtsbos B (G2H010)	0.66	1472	Forest and Fynbos	0.30*	
5	Zululand (W1H016)	3.32	1314	Thicket and Bushland	0.25*	
6	Watervalsrivier (G1H012)	36	664	Shrubland and Low Fynbos	0.30	0.985
7	Treurrivier (B6H003)	92	792	Unimproved Grassland and Forest Plantation	0.41	0.998
8	Groot-Nylrivier (A6H011)	73	654	Thicket and Bushland	0.44	0.971
9	Beestekraalspruit (X2H026)	14	977	North East Mountain Sourveld	0.51	0.991
10	Kruisrivier (H9H004)	50	645	Shrubland and Low Fynbos	0.35	0.990
11	Bloukransrivier (K7H001)	57	1003	Thicket and Bushland	0.26	0.990
12	Dieprivier (K4H003)	72	711	Pine Plantations	0.31	0.987
13	DeHoek (V1H015)	1.01	800	Grassland	0.30	
14	Safford (USA)	2.10	225	Shrubs		

* BFI estimated from spatial distribution of BFI mapped by Smakthin and Watkins (1997).
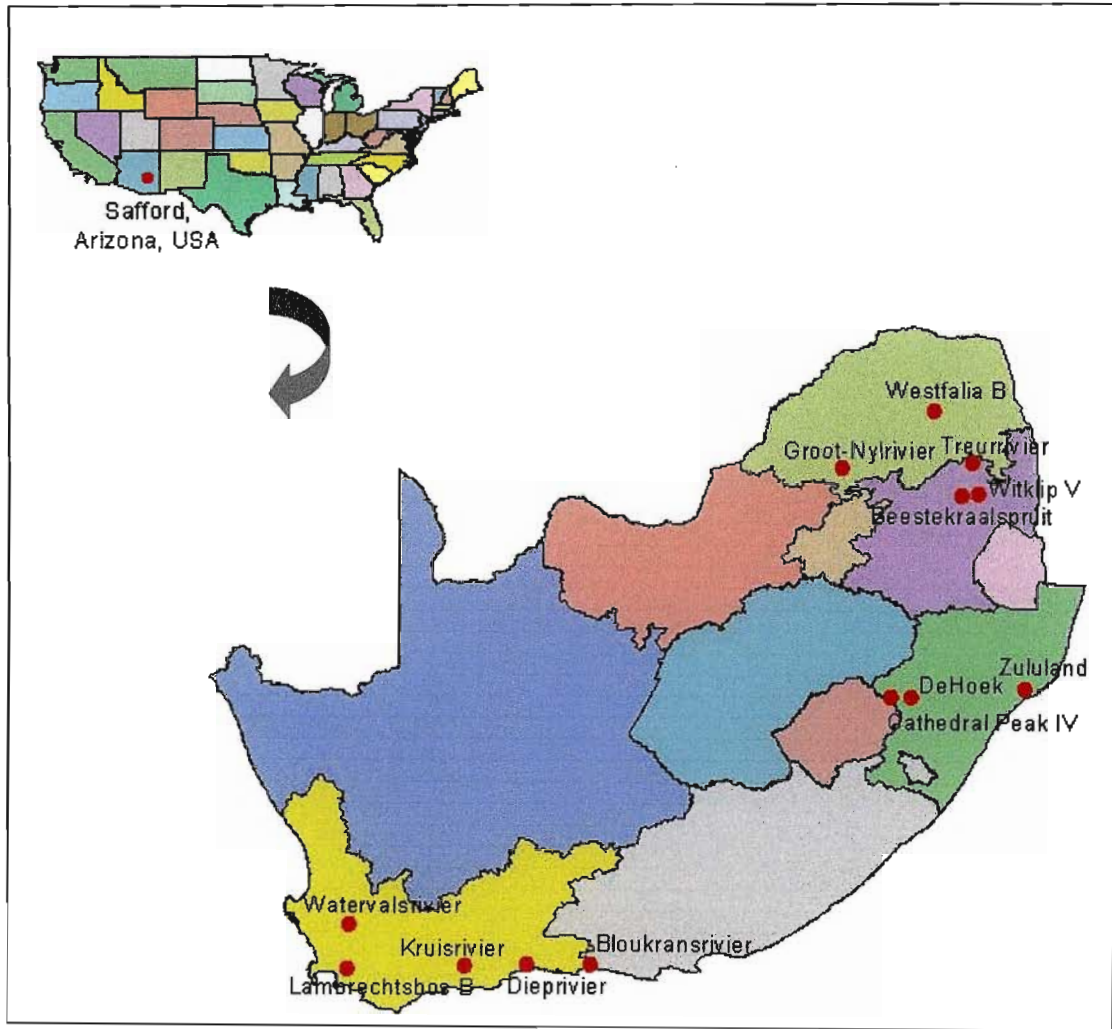
Figure 12: Location of catchments selected for this study.
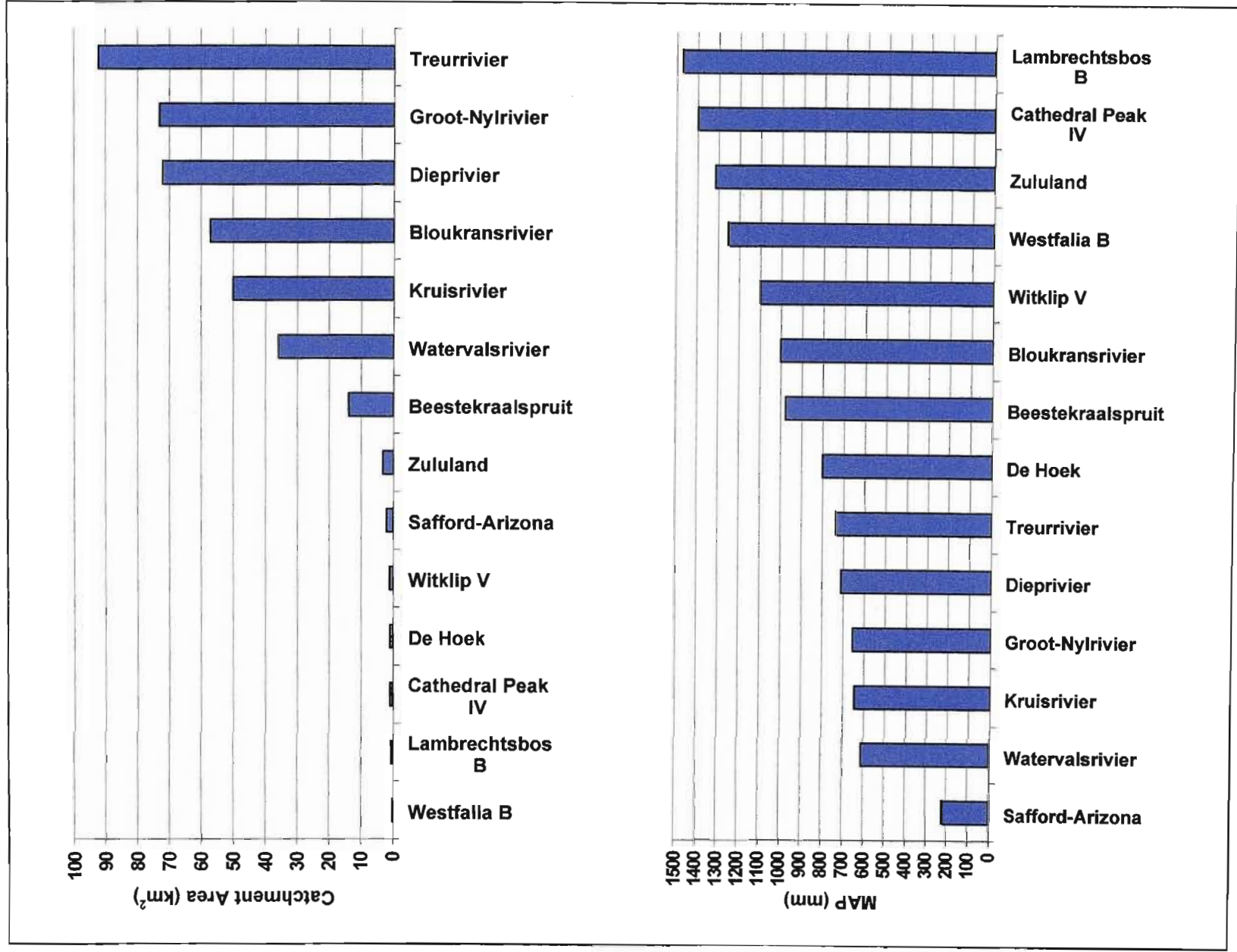
Figure 13: The range of catchment areas and MAPs exhibited by the selected catchments.
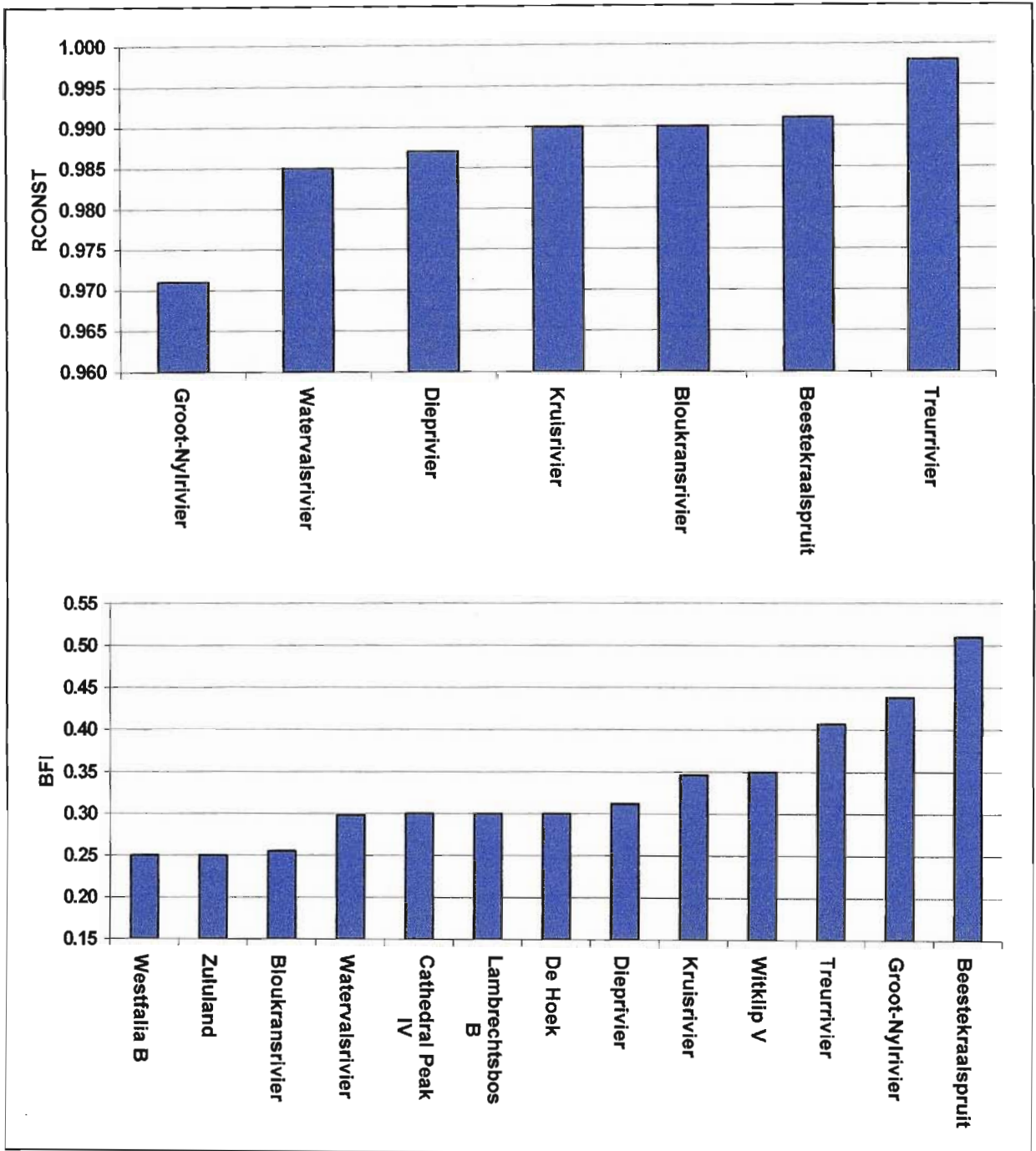
Figure 14: The range of RCONST and BFI exhibited by the selected catchments.

3.4.2.1 Safford research catchment, Arizona, USA

The Safford research catchment ARS No. 4501 located at 32° 55' N and 109° 48' W, is maintained by the Agricultural Research Service (ARS) of the United States Department of Agriculture (USDA). The catchment has an area of 2.10 km² with an altitude ranging from 990 to 1052 m.a.s.l (Figure 15). It is situated on a relatively flat

plain (Dunsmore, 1985). The catchment experiences an arid climate; MAP is 225 mm and mean annual runoff (MAR) is only 9.1 mm. Three rainfall gauges were situated within the catchment. Dunsmore (1985) cited temperature values for the Safford research catchments obtained from isotherms mapped by Baker (1936) for the region, as in Table 5.

Table 5: Monthly means of daily maximum and minimum temperatures (^{o}C) for Safford (after Baker, 1936).

	Jan	Feb	Mar	Apr	May	Jun	Jul	Aug	Sep	Oct	Nov	Dec
Max	13.9	15.6	16.7	22.8	27.8	33.3	33.9	33.3	28.3	23.9	17.2	12.8
Min.	-3.9	-1.1	1.1	3.3	6.7	11.1	17.2	16.7	11.7	5.6	1.1	-3.9
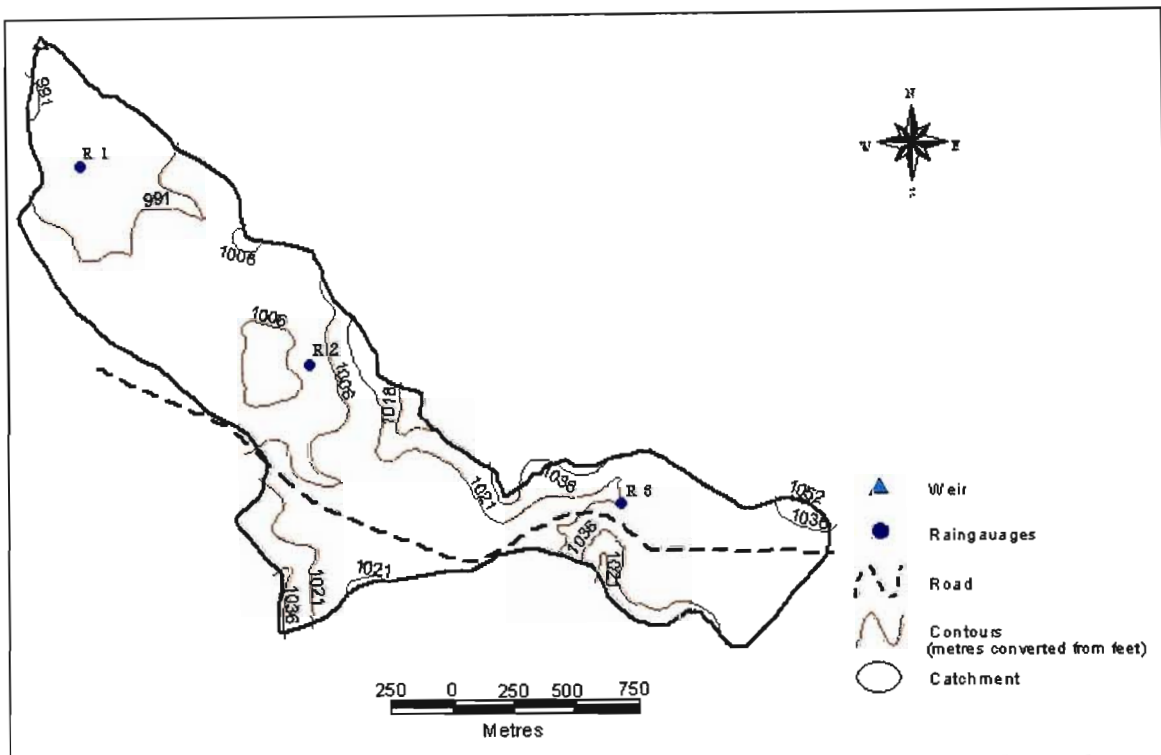
Figure 15: Safford research catchment ARS No. 4501 in Arizona, USA.

The topsoils are described as well-drained, granular stony loams and sandy loams, with an average thickness of only 0.14 m. The subsoil has an average thickness of 0.36 m and consists of stony, gravelly silty loam (USDA-ARS, 1957; cited in Dunsmore, 1985), having a high interflow potential with an impervious hard pan at a depth of 0.58 m (USDA-ARS, 1957; cited in Topping, 1992). This impervious layer does not play a significant hydrological role, since the low MAP precludes significant

wetting up of the catchment. Rainfall occurs mostly as short, high intensity events, which result in most of the runoff comprising stormflow rather than baseflow (Topping, 1992). Vegetation is very sparse, with approximately 10 to 20% of the soil having any form of cover. The predominant plants are small succulent shrubs, which have 90% of their roots in the topsoil (Schulze, 1985b). A concurrent rainfall and streamflow data set from 1939 to 1969 was used in this study.

3.4.2.2   Catchments in the Western Cape Province

3.4.2.2.1 Lambrechtsbos B (G2H010)

This 0.66 km^2 research catchment (33° 57'S; 18° 57'E) is situated in the long, narrow Jonkershoek valley (Figure 16), between the Stellenbosch and the Jonkershoek Mountains. It is enclosed by the transverse Dwarsberg block fault in the south east. Streams from the catchment form tributaries of the Eerste River, which flows through Stellenbosch. The catchment has a minimum elevation of 300 m and a maximum elevation of 1067 m (Scott et al., 2000).

The climate is of the humid mesothermal Mediterranean type with warm dry summers and cool wet winters. It has an MAP of 1145 mm and an MAR of 517.8 mm. Studies have revealed a steep, orographic rainfall gradient (Scott et al., 2000). Daily rainfall was recorded at gauge 15 situated at low altitude near the catchment outlet. These daily totals were adjusted upwards according to the monthly catch recorded in gauge 10. This gauge is located approximately midway along the catchment and its readings are, therefore, considered more representative of the average rainfall over the catchment. The mean daily maximum temperature for February is 27.9 °C and the mean daily minimum temperature for July is 5.9 °C (Versfeld and Donald, 1991).

Sandstone and quartzite (Early to Late Ordovician group) with intermittent thin shale bands of the Table Mountain Group (Lower Paleozoic Cape Supergroup) are found mostly in the upper slopes of the catchment. These are underlain by Cambrian Cape Granite, which is found mostly on the lower slopes and the valley floor.
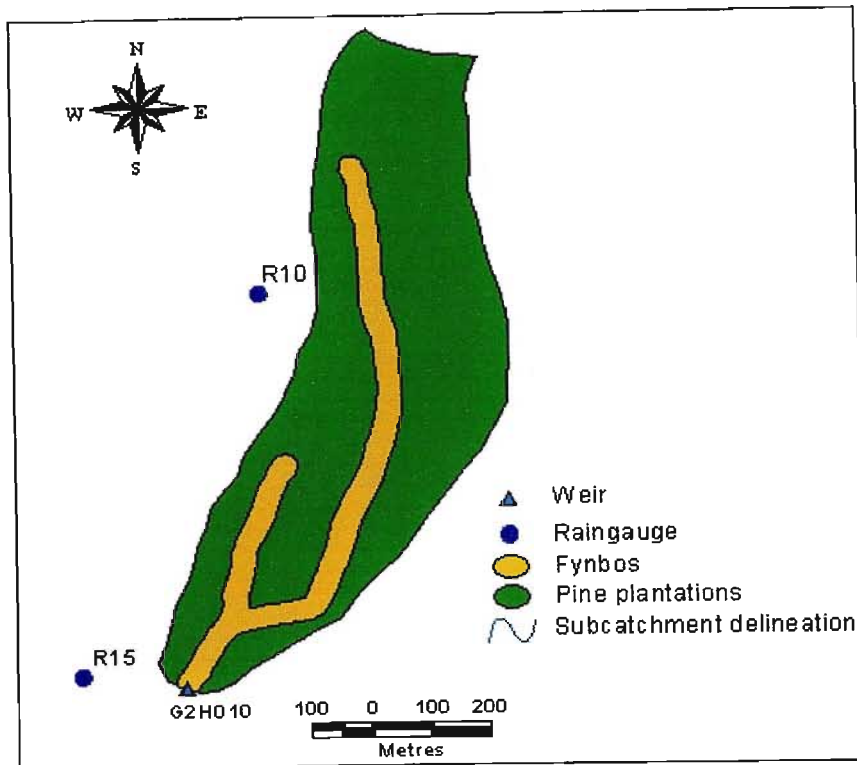
Figure 16: Lambrechtsbos B showing the location of rainfall stations 10 and 15.
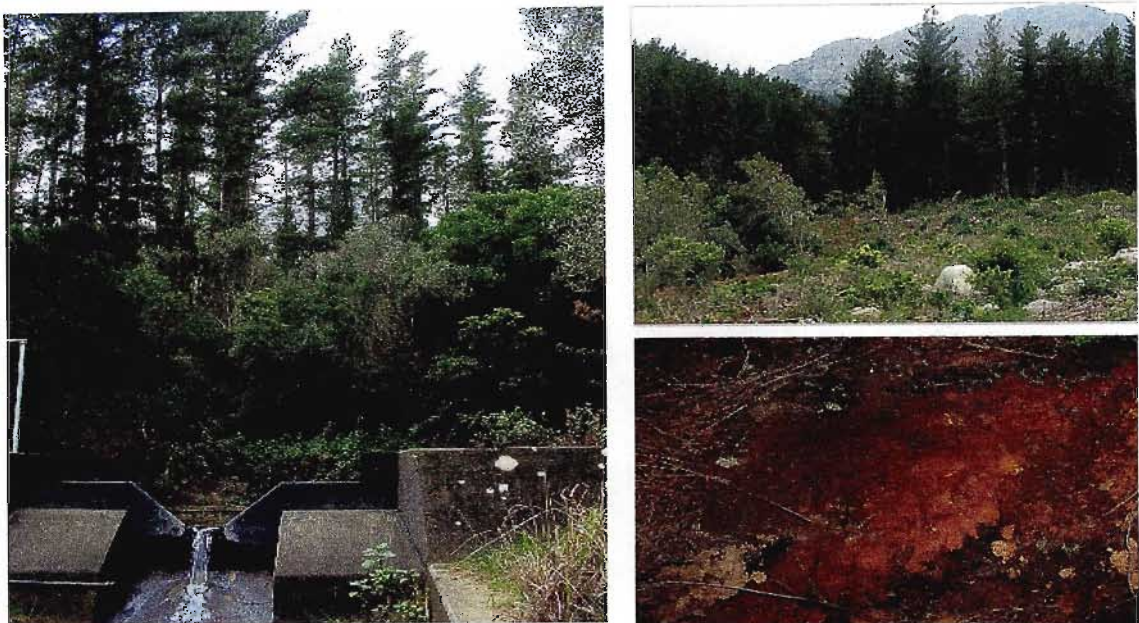
Figure 17: Views of the gauging structure, vegetation and a soil profile at Lambrechtsbos B.

Soils are complex, with depths of 1 to 2 m, with major forms being Hutton, Magwa and Nomanci (MacVicar *et al.*, 1977). The soils are characterised as acidic, sandy loams having a low organic matter content (Scott *et al.*, 2000). Subsoils consist of

either unconsolidated or decomposed material that allow free drainage of water. Soils have a high infiltrability and are well drained. By 1964 the catchment had been afforested to 82% with *Pinus radiata*, with 20 m strips left unplanted on either side of the stream banks. Small pockets of indigenous forest found along the stream banks were allowed to develop and have been protected from fire. The rocky cliffs and steeper slopes that form the upper parts of the catchment were also left unplanted (Scott *et al.*, 2000). The simulation period was from 1969 to 1974.

3.4.2.2.2 Watervalsrivier (G1H012)

This catchment (Figure 18) is situated around 33° 21'S and 19° 06'E, and is bordered by the Elandskloof and Watervals Mountains. Flow from the Watervalsrivier is monitored at weir G1H012. It is 36 km^2 in extent, and has an altitudinal range from 120 to 1086 m.a.s.l. The estimated MAP of the catchment, based on raingauge 0042201 W situated approximately 1 km from the weir at the Waterval Forest Station, is 664 mm. The mean annual temperature (MAT) is 18.1 °C (Schulze, 1997).
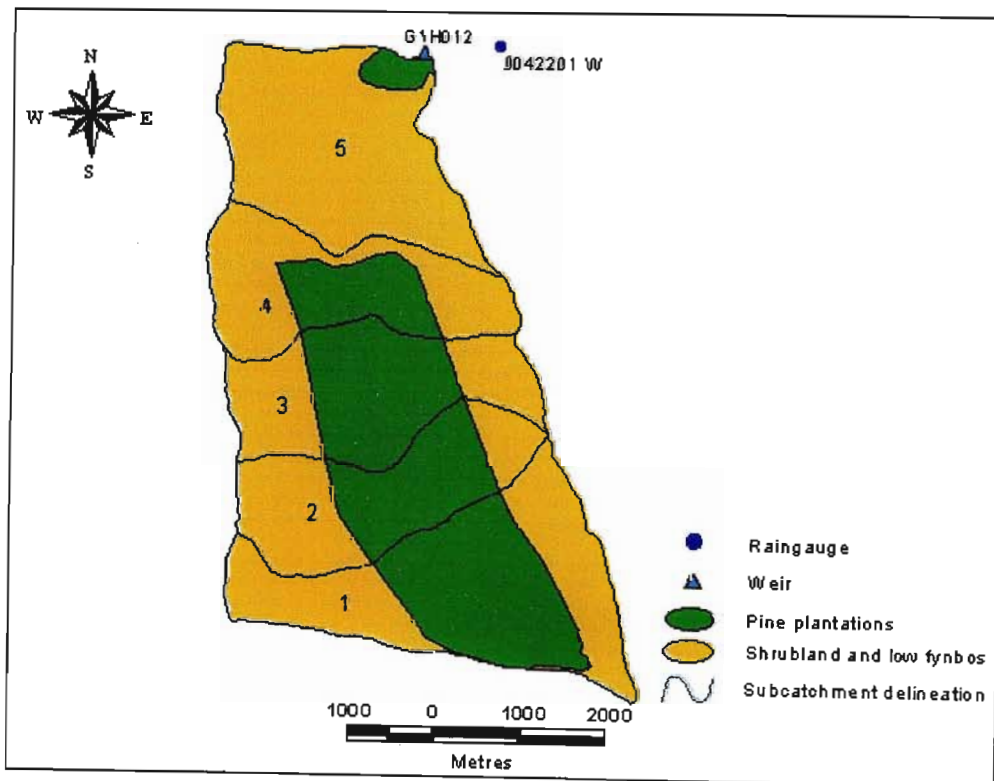
Figure 18: Watervalsrivier catchment showing subcatchment delineations, land cover and the location of the rainfall station used.
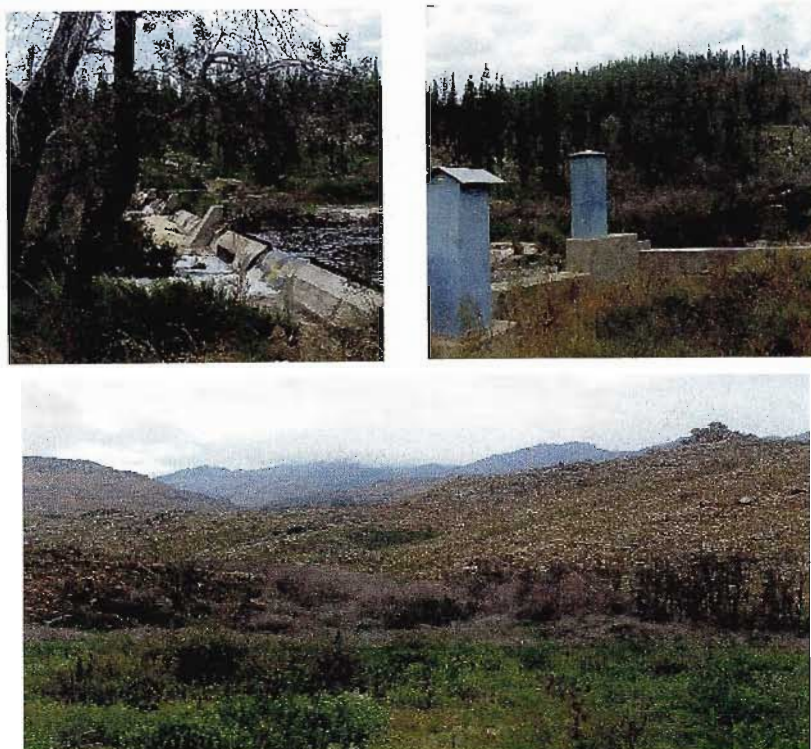
Figure 19: Views of the Watervalsrivier gauging structure and the surrounding vegetation.

The geological groups underlying the catchment are predominantly Malmesbury, Kango and Gariep, with a variety of phyllite, greywacke, conglomerate, sandstone, limestone, shale and dolomite. 81.3% of the catchment is covered with shrubland and low fynbos, 17.4% forest plantations and 1.3% unimproved grassland (CSIR, 1996). The period of simulation was from 1968 to 1974.

3.4.2.2.3 *Dieprivier (K4H003)*

The Dieprivier catchment (Figure 20) is situated around 33° 54'S and 22° 42'E, with the Outeniequa Mountains to the west. It is 72 km² in area, and flow is monitored at weir K4H003. It has an average altitude of 335 m near the outlet, with an average slope of 8.2°. The drainage density of the catchment is 0.081 km/km². The catchment falls within the all-year rainfall region, with a MAP of 711 mm and a MAT of 17.2°C (Hughes, 1997). Rainfall data from raingauges 0029291W, 0029294W and 0029297W were used for this study.
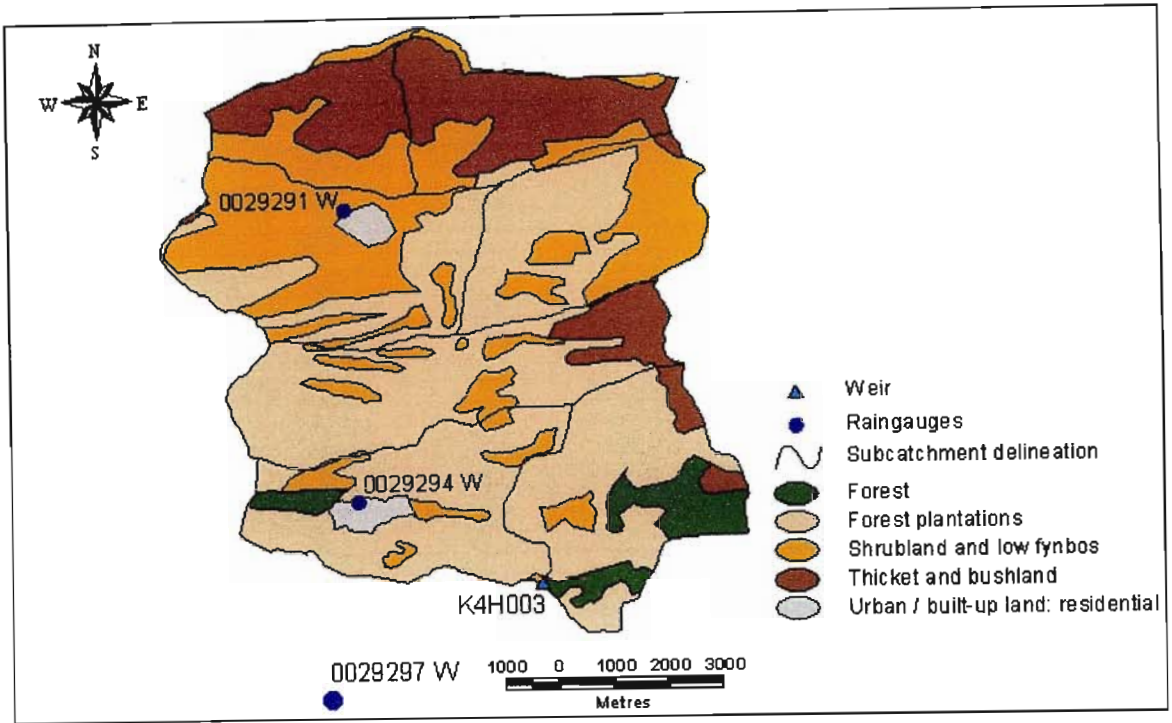
Figure 20: Dieprivier catchment showing land cover and the positions of rainfall stations.

Figure 21: Views of the Dieprivier catchment, including the residential establishments surrounded by pine plantations and the gauging structure.

The geology of this catchment consists primarily of an assemblage of compact arenaceous strata, including rocks from the Table Mountain Group, and a variety of quartzitic sandstone and subordinate shale and tillite (Vegter, 1995). The soils are highly variable and a large spectrum of soil types is found, owing to the many different geological formations and this being a highly dissected mountain basin with long geomorphological history (Pretorius, 2001). Soils range from deep, wet duplex clays formed from shale materials or from extensive weathering of sandstone parent material over a long period of time on subdued relief; to shallow, wet lithosols and lithocutanic podzols formed at higher altitude; while deep stony, colluvial soils consisting of soft, moist apedal loams or dry stony sandy loams occur in the central subcatchments. A large percentage of the catchment is covered by pines, which form part of the Bergplaas Plantation, with shrubland and low fynbos occurring in the higher altitude of the catchment. A small settlement, comprising approximately 52 families, occurs in the catchment. The simulation period was from 1968 to 1975.

3.4.2.2.4   Kruisrivier (H9H004)

This catchment (Figure 22) is 50 km^2 in area, and is situated at 34° 00'S and 21° 16'E, near the town of Riversdale. The Kruisrivier's flow is monitored at gauging structure H9H004.
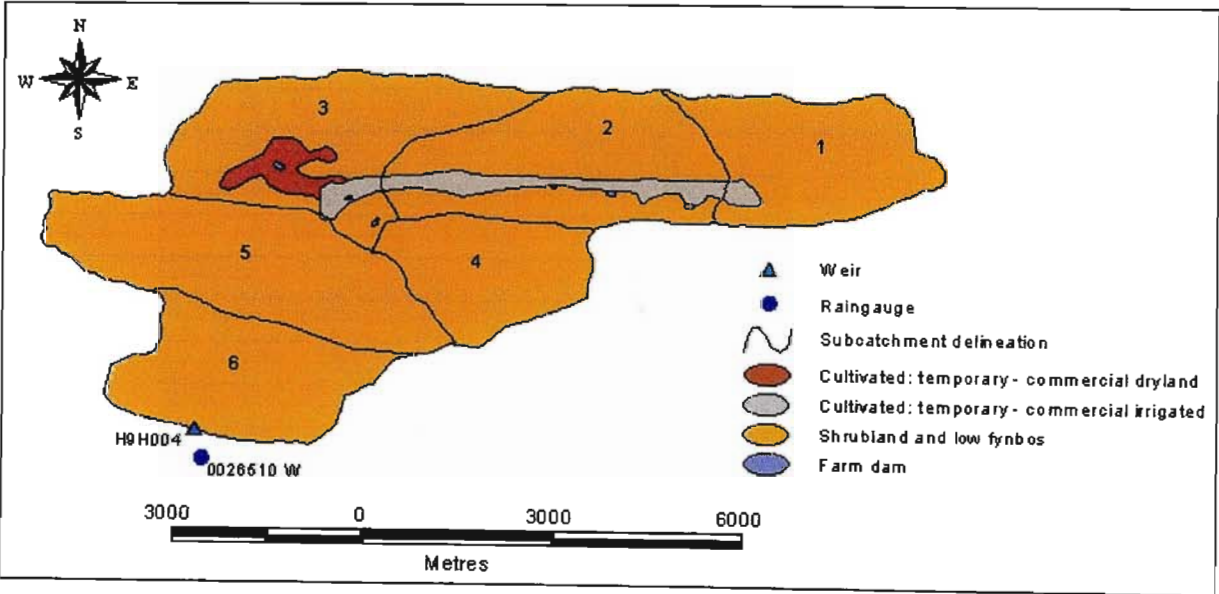
Figure 22:   Kruisrivier catchment illustrating land use and the location of the rainfall station used.

Figure 23: Views of the shrubland and low fynbos in the Kruisriver catchment. Photographs of the orchard and the soil profile are from the Langkloof area.

The drainage density of the catchment is 0.387 km/km^2, with an average catchment slope of 13.4° (Hughes, 1997). Rainfall is concentrated in the winter months from June to September, with a MAP of 645 mm estimated from raingauge 0026510 W located near the outlet of the catchment and used in the modelling exercise.

The geology of the catchment is primarily an assemblage of compact arenaceous strata, mainly those from the Table Mountain Group, and a variety of quartzitic sandstone, subordinate shale and tillite (Hughes, 1997). The dominant vegetation is shrubland and low fynbos, with a small percentage of cultivated commercial dryland and irrigated farmlands in the Langkloof area. The irrigated lands consist of orchards (Figure 23) which are irrigated from October to March from the six small farm dams located in the catchment. The simulation period was from 1981 to 1990.

3.4.2.2.5   Bloukransrivier (K7H001)

This catchment (Figure 24), which makes up the source area of the Bloukransrivier around (33° 57'S; 23° 37'E), is situated near Nature's Valley Reserve in the Western Cape Province. It is 57 km^2 in extent, and flow is monitored at weir K7H001. The drainage density of the catchment is 0.514 km/km^2, while the average catchment slope is 11.3° (Hughes, 1997). It has a MAP range from 686 to 1350 mm and is in the all year rainfall region.

Figure 24: Bloukransrivier catchment, illustrating land uses and location of the rainfall station used.

The geology of the catchment is primarily an assemblage of compact arenaceous strata, including those of the Table Mountain Group, and a variety of quartzitic sandstone, subordinate shale and tillite (Hughes, 1997). A large percentage of the catchment is shrubland and low fynbos, with scattered plots of indigenous forest and pine plantations near the outlet and some of the upper parts of the catchment. Indigenous forest found on the steep slopes near the catchment outlet is dense and has a thick understorey. The predominantly sandy soils are approximately 0.4 - 0.5 m deep. The simulation period was from 1989 to 1995.

Figure 25: Views of the dominant vegetation, a soil profile and the gauging weir of the Bloukransrivier catchment.

3.4.2.3　Catchments in KwaZulu-Natal

3.4.2.3.1 Zululand research catchment (W1H016)

The Zululand research catchment W1H016 (Figure 26) is situated around 28° 50' S and 31° 46' E, inland of the town of Mtunzini on the coastal belt of KwaZulu-Natal. Catchment W1H016 includes catchment W1H017 nested within it. It is 3.32 km² in area with an altitudinal range from 205 to 323 m.a.s.l. The Hydrological Research Unit of the University of Zululand has monitored the catchment since the late 1970s. The catchment is situated on a coastal plain with gently undulating terrain, but does slope upwards towards the Ngoye mountain range to the north of the catchment (Topping, 1992). The catchment is also characterised by a large number of rocky outcrops and is underlain by extremely resistant biotite granite gneiss, which forms part of the Ngoye range (Hope and Mulder, 1979).

This research catchment is one of the few small, sub-tropical research catchments in RSA and experiences significantly higher temperatures and humidities than the other catchments studied. Heavy orographic rainfall is sometimes induced when moisture-laden air is forced to rise some 300 m over the Ngoye range (Hope and Mulder, 1979).
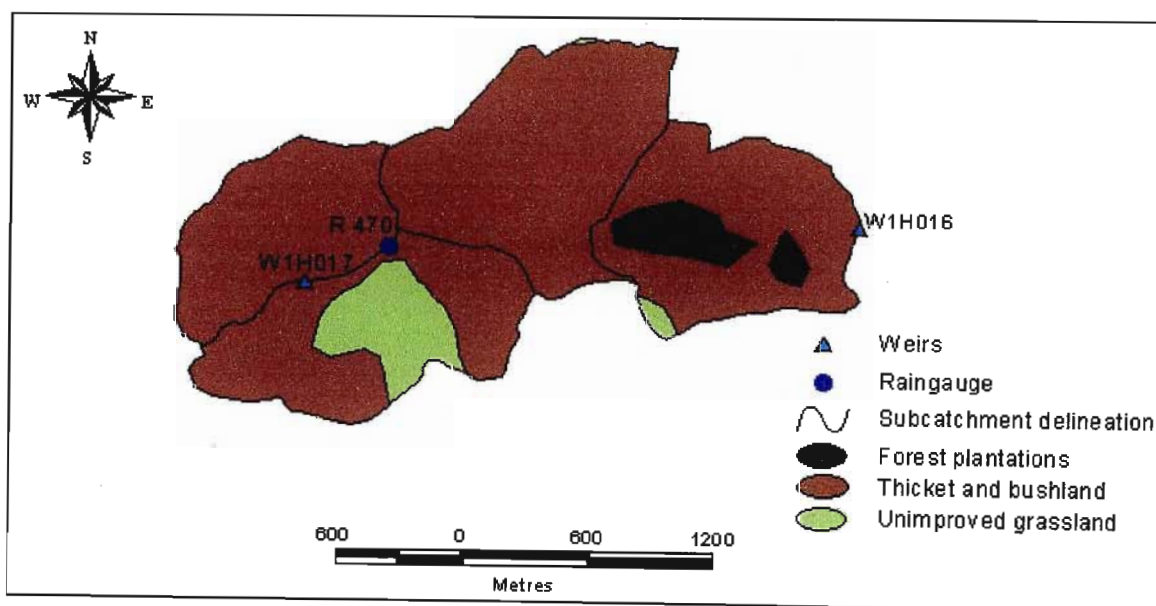
Figure 26: Zululand research catchment W1H016 with nested catchment W1H017 and location of rainfall station 470.

Raingauge 470, which was situated in the upper third of the catchment (MAP of 1314 mm, 291 m.a.s.l) was used for these simulations, as it was considered to be the most representative recording raingauge in the catchment (Mulder, 2000). Temperature data were obtained from the University of Zululand's meteorological station. Monthly means of daily maximum and minimum temperatures are displayed in Table 6 (Topping, 1992).

Table 6: Monthly means of daily maximum and minimum temperatures ($^{\circ}$C) for catchment W1H016 (from Topping, 1992).

	Jan	Feb	Mar	Apr	May	Jun	Jul	Aug	Sep	Oct	Nov	Dec
Max.	29.9	29.7	29.2	28.2	25.6	23.6	23.7	24.2	24.5	26.2	27.3	29.3
Min.	20.8	21.1	19.2	17.0	13.7	10.3	10.8	13.2	14.2	15.8	18.1	19.5

Ngongoni grassland in fair to good hydrological condition is the dominant land cover. Indigenous trees and shrubs are found bordering the main streams, with agricultural crops scattered throughout the catchment in small plots rarely exceeding 1 ha in size. It is difficult to perform accurate surveys of these subsistence plots, which are cultivated on a haphazard rotation system, depending on the needs of the farmer and the availability of labour (Hope and Mulder, 1979). The soils are predominantly sandy clay loams derived from granitic gneiss, having an average soil depth of 1400 mm with a moderate to high interflow potential (Angus, 1987). The simulation period was from 1977 to 1981.

3.4.2.3.2 Cathedral Peak catchment IV (V1H005)

There were at one stage fifteen gauged small research catchments at the Cathedral Peak Forest Station, located on the Little Berg plateau of the Drakensberg of KwaZulu-Natal. Cathedral Peak catchment IV (C IV) is situated around 29° 00'S and 29° 25'E (Figure 27). It has a catchment area of 0.99 km^2, with a minimum and maximum elevation of 1845 and 2226 m respectively.

It has a MAP of 1420 mm, with approximately 49 % (695 mm) converting to streamflow (Bosch, 1979). Cathedral Peak falls within the summer rainfall region and 84% of the rainfall occurs between October and March, while approximately half of all

rainfall events are thunderstorms (Schulze, 1975). Two thirds of the total annual streamflow is yielded during the four months from January to April. Winters are cold and dry (occasional snowfalls occur at high altitude) while summers are hot and wet.
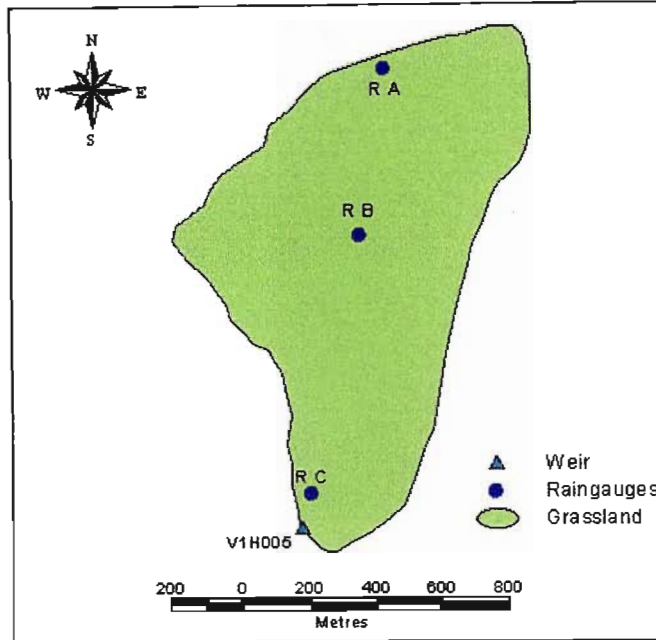
Figure 27: Cathedral Peak IV research catchment, with the positions of the rainfall stations and gauging weir shown.

This grassland catchment is dominated by the species *Themeda triandra*, which is burnt biennially in the spring. C IV is underlain by basaltic lavas, which overlie Clarens Sandstone. Three post-Karoo dolerite dykes, each ~3 m wide, cut across the Cathedral Peak research area, two of which cut across C IV (Bosch, 1979). Streams are perennial and rise above the apparently solid basalt. The soil profile is at least 1.5 m thick. Hutton and Griffin forms are most frequently encountered in the catchment and are associated with the gentler slopes of the catchments (Scott *et al.*, 2000). The simulation period was from 1971 to 1979.

3.4.2.3.3 DeHoek (V1H015)

The DeHoek grassland research catchment is located approximately 20 km from Estcourt, in the foothills of the Drakensberg mountain range. It is positioned around 29° 58' S and 30° 20' E, almost equidistant of Champagne Castle and Giant's Castle. It is 1.03 km² in area, with an altitudinal range from 1450 to 1630 m.a.s.l. It has

relatively steep slopes with an average slope of 12°. The catchment's south facing slopes are cooler and display higher soil moisture values throughout the year than slopes with other aspects (Topping, 1992). Nested within this catchment are subcatchments V1H010, V1H011 and V1H012, data from which were not, however, used in this study.

The Klein Bloukransrivier, which originates in this catchment, was monitored at weir V1H015. Rainfall has measured with two autographic gauges (raingauges 9 and 11) located at either end of the catchment (Figure 28). The MAP is 1115 mm. A majority of the summer rainfall events are convective, although low intensity events, occurring as a result of a passage of cold frontal systems over the catchment occur in Autumn and Spring (Topping, 1992). Schmidt and Schulze (1989) report average maximum temperatures of 24.5°C and 19.2°C and average minimum temperatures of 12.9°C and 0.3°C, for January and July respectively. Annual reference potential evaporation, measured with an A-pan, amounts to 1658 mm, with the highest monthly pan evaporation occurring from October to December (each ~160 mm) and the lowest (79 mm) in June (Schmidt and Schulze, 1989).
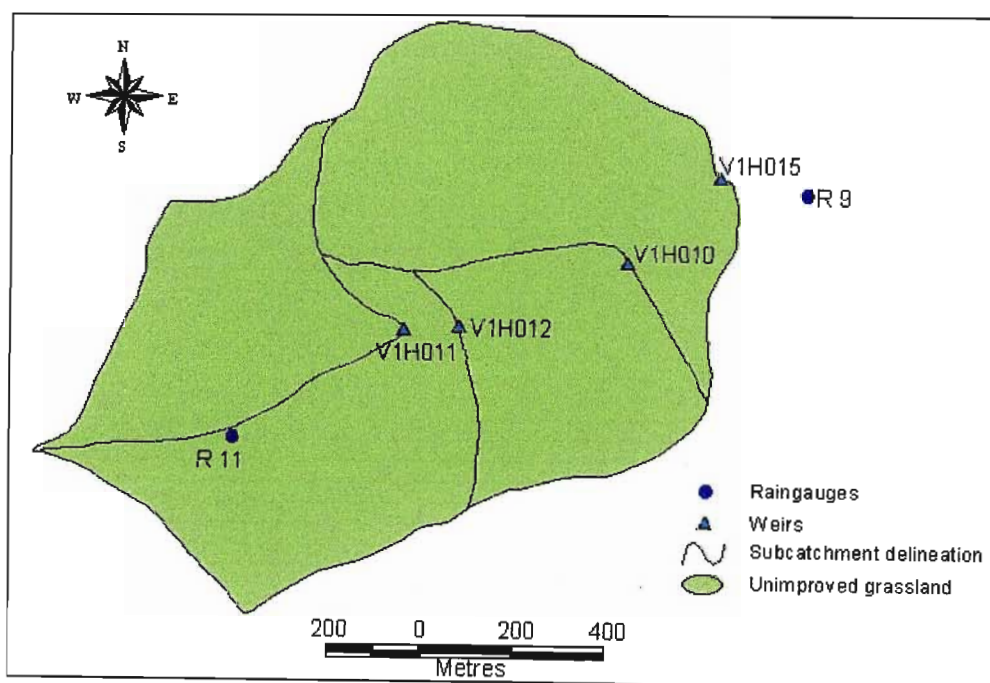
Figure 28: DeHoek research catchment V1H015, showing nested catchments V1H011, V1H012 and V1H010. The positions of rainfall stations 9 and 11 are also shown.

The soils of the DeHoek research catchment are dystrophic with low pH values, apedal structure and low erosion potential (Schulze, 1985a). Soil piping occurs in places in the catchment, predominantly on the south facing slopes. The vegetation is natural grassland that has been consistently well managed since the 1960s. The catchment is burnt annually in September to stimulate the next season's growth by removing moribund material (Topping, 1992). The simulation period was from 1985 to 1988.

3.4.2.4   Catchments in Mpumalanga

3.4.2.4.1 Witklip V (X2H038)

The Witklip research catchment V (Figure 29) is located around 25° 14'S and 30° 53'E, close to the town of White River. This catchment forms part of the Eastern Drakensberg escarpment and streamflow cascades into the Witklip River, which ultimately flows into the Crocodile River. The catchment is 1.08 km^2 in area, has a northwesterly aspect and an elevation range from 1000 to 1340 m.
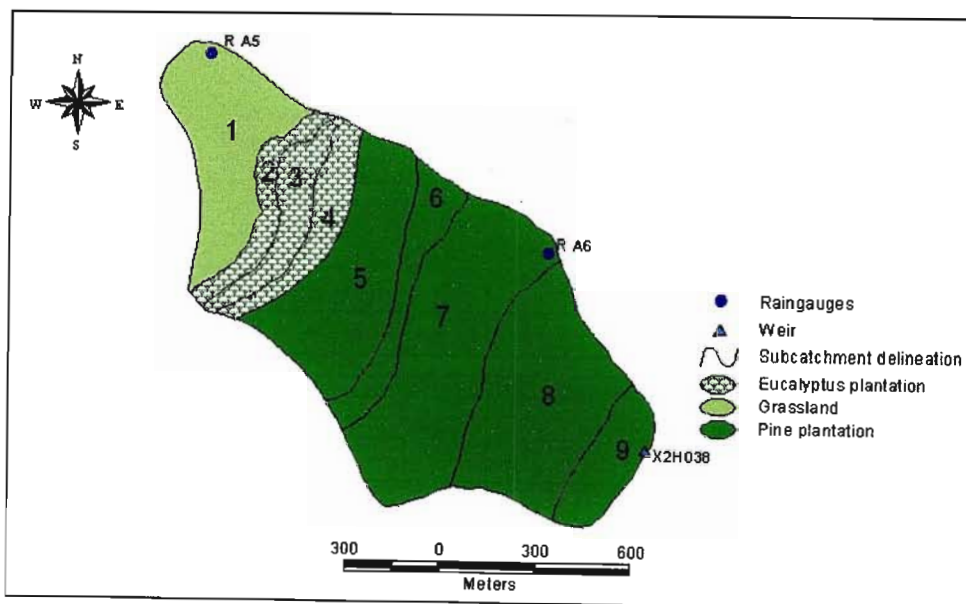
Figure 29:   Witklip research catchment V, illustrating land uses and the location of rainfall stations A5 and A6.

The Witklip research catchments were established in 1975. Witklip V has a MAP of 1100 mm and a MAR of 362.2 mm. It experiences a humid sub-tropical climate, with predominantly summer rainfall. The mean daily temperature in the hottest month (January) is 21.3°C and in the coldest month (July) is 13.4°C (Scott et al., 2000).

Figure 30: Views of pine plantations and the gauging weir in Witklip V.

In the 1955/56 season, 52% of the catchment was planted to *Pinus patula* and *P. roxburghii*, while *Eucalyptus saligna* and *E. paniculata* were planted as firebreaks. The remaining 48% of the catchment remained under indigenous vegetation with grasslands on the slopes and indigenous shrubs in the riparian zones. The plantations were felled in 1980 and 1983 and were progressively replanted (Scott *et al.*, 2000). Soils are formed mainly from deeply weathered granites. They are highly leached and well drained. Hutton and Clovelly soil forms dominate. Deep drilling at the nearby Frankfort State Forest, which has similar geology and soils, revealed a permeable, stone-free and uniform profile extending down to 38 m below the surface (Dye, 1996). Young eucalyptus trees growing at this specific site were exploiting water in these profiles to a depth of at least 8 m below the surface (Dye, 1996). The simulation period was from 1975 to 1983.

3.4.2.4.2 Treurrivier (B6H003)

This 92 km^2 catchment, streamflow from which is monitored at weir B6H003, is located around 24° 41'S and 30° 48'E (Figure 31). It is the source of the Treurrivier, which ultimately flows into the Blyde River. The drainage density of the catchment is 1.349 km/km^2 (Hughes, 1997). Three rainfall gauges (0594494 W, 0594590 W and 0594764 W), located outside the catchment boundaries but providing good quality data, were used in the study. Rainfall is concentrated in the summer months from November to April. Estimated MAP near the outlet of the catchment is 792 mm, but rises to approximately 1595 mm in the upper parts of the catchment. Altitude ranges between 1200 and 1835 m, with the average slope being 7.6°.

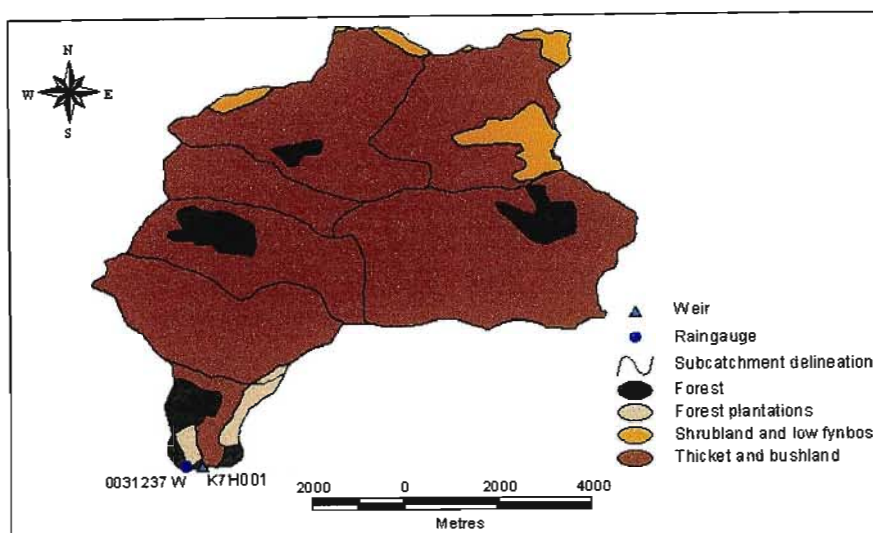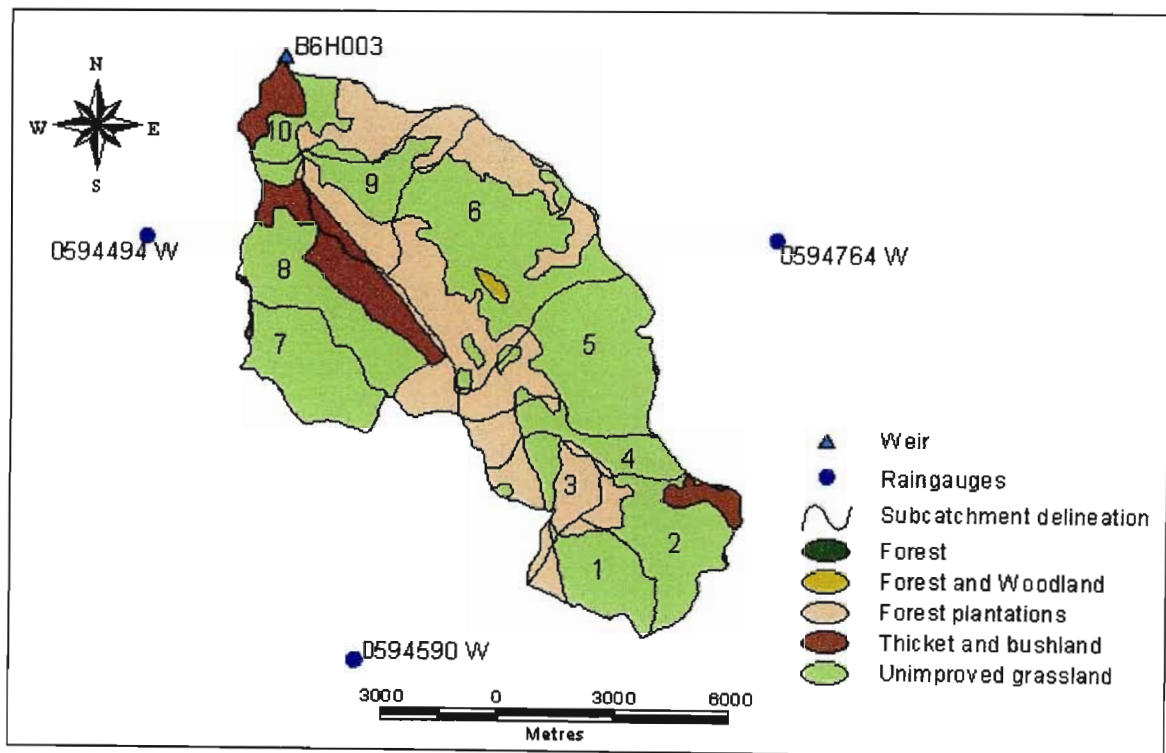**Figure 31:** Treurrivier catchment, illustrating land uses and the locations of rainfall stations.

The geology of the catchment is primarily an assemblage of compact sedimentary and extrusive rocks belonging to the Wolkberg Group and Godwan and Black Reef Formations. The vegetation comprises 62.3% indigenous grassland, 29.1% forest and 8.6% thicket and bushland (CSIR, 1996). The simulation period was from 1981 to 1986.

3.4.2.4.3 Beestekraalspruit (X2H026)

Beestekraalspruit (Figure 32) is located around 25° 17'S and 30° 34'E. It ultimately flows into the Crocodile River. Flows from this catchment are monitored at weir X2H026. It has a catchment area of 14 km^2, a MAP of 977 mm and an altitude range from 981 to 2190 m. The Mokobulaan research catchments are situated towards the west of Beestekraalspruit and data from their raingauges have been used to represent the higher rainfall regions of the catchment. Raingauge 0555137 W, located within the catchment and approximately 750 m from the outlet, was used to represent the remaining catchment area.
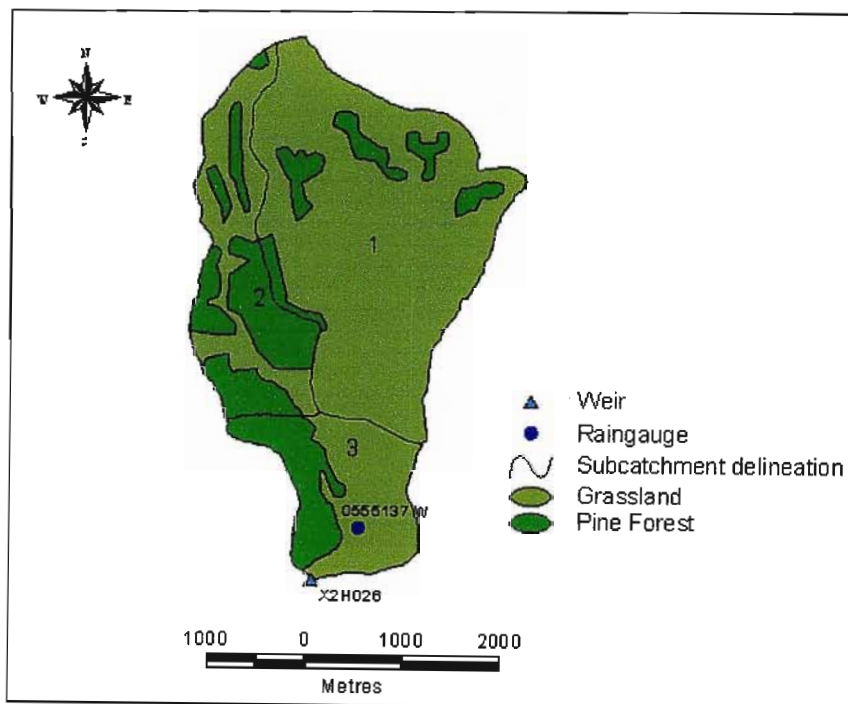
Figure 32: Beestekraalspruit catchment, illustrating land uses and the location of the rainfall station.

The geological groups underlying the catchment are predominantly the Rooihoogte Formation of the Pretoria diabase group, and the Chuniespoort Group of the Transvaal sequence which includes a variety of shale, quartzite, conglomerate, siltstone, andesite and dolomitic chert (Vegter, 1995). The natural vegetation is classified as Northeast Mountain sourveld, but approximately 24% of the catchment consists of forest plantations of the Uitsoek Plantation. The simulation period was from 1971 to 1975.

3.4.2.5 Catchments in Limpopo Province

3.4.2.5.1 Westfalia B (B8H022)

Westfalia research catchment B (23° 43'S and 30° 04'E) forms part of a paired catchment experiment situated on the Westfalia Estate. It lies 13 km southwest of Duiwelskloof and is northwest of Tzaneen. It is 0.33 km^2 in area (Figure 33), with a southeasterly aspect. Altitude ranges from 1140 to 1420 m. The streams in the area are tributaries of the Madikeleni stream, which in turn flows into the Great Letaba River. This paired catchment experiment was initiated to test the effect of removal of indigenous riparian vegetation on streamflow and the replacement of indigenous vegetation by exotic timber species.
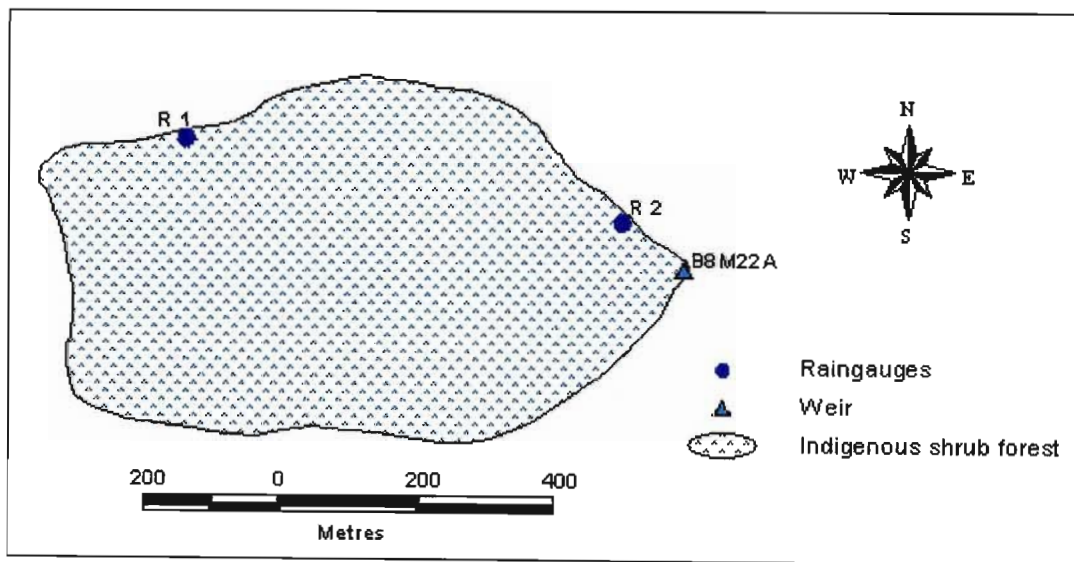
Figure 33: Westfalia B research catchment, illustrating the land use and the locations of rainfall stations.

The area experiences a subtropical climate. The MAP is 1253 mm, with almost 84% of rain falling in the summer months. Rainfall is mainly orographic, but convective thunderstorms are common, particularly early in the rainy season. Monthly means of daily maximum temperatures vary between 21 and 30°C. Monthly means of daily minimum temperatures vary between 2°C and 10 °C.

Figure 34: A close up view of the gauging weir and indigenous vegetation at Westfalia B.

Indigenous shrub forest comprised mainly of evergreen forest and deciduous woodland comprise the natural vegetation of the catchment. The dominant species present consist of *Syzygium cordatum* (Myrtaceae), *Nuxia floribunda* (Loganiaceae), *Rapanea melanophloeos* (Myrsinaceae) and *Trimeria grandiflora* (Flacourtiaceae). This indigenous closed canopy forest has a mean tree height of 10 m and mean trunk diameter at breast height of 100 mm (Bosch and Versfeld, 1984). The bedrock underlying the catchment is Archean granite gneiss with diabase dykes and sills criss-crossing the area, with some intrusions of Turfloop granite. This is underlain by the Pietersburg Group, comprising ultramafic and mafic metavolcanic rocks, and including serpentinite and schist. The soils are well drained, deep red series of the Hutton form. These dominant soils have a 20 to 60 % clay content and display high permeability and low erodibility characteristics (Scott *et al.*, 2000). The simulation period was from 1985 to 1990.

3.4.2.5.2 Groot-Nylrivier (A6H011)

This catchment is the source of the Groot-Nylrivier which ultimately flows into the Limpopo River. Flow is monitored at gauging structure A6H011 (Figure 35). The catchment is 74.75 km^2 in area, and is situated around 24° 45'S and 28° 44'E, midway between the towns of Warmbaths and Nylstroom. The drainage density of the catchment is 0.307 km/km^2 (Hughes, 1997). Four very small dams found in the catchment have very little influence on flows recorded at the weir.

The catchment has a MAP of 654 mm, an altitude range from 1213 m to 1508 m, and an average slope of 3.5°. Raingauges 0589586 W and 0589670 W were selected for this modelling exercise. Rainfall is concentrated in the summer months from November to April and occurs predominantly in the form of thunderstorms. Mean annual temperature averages 20°C, but ranges from 14.1 to 23.8 °C within the catchment (Schulze, 1997).
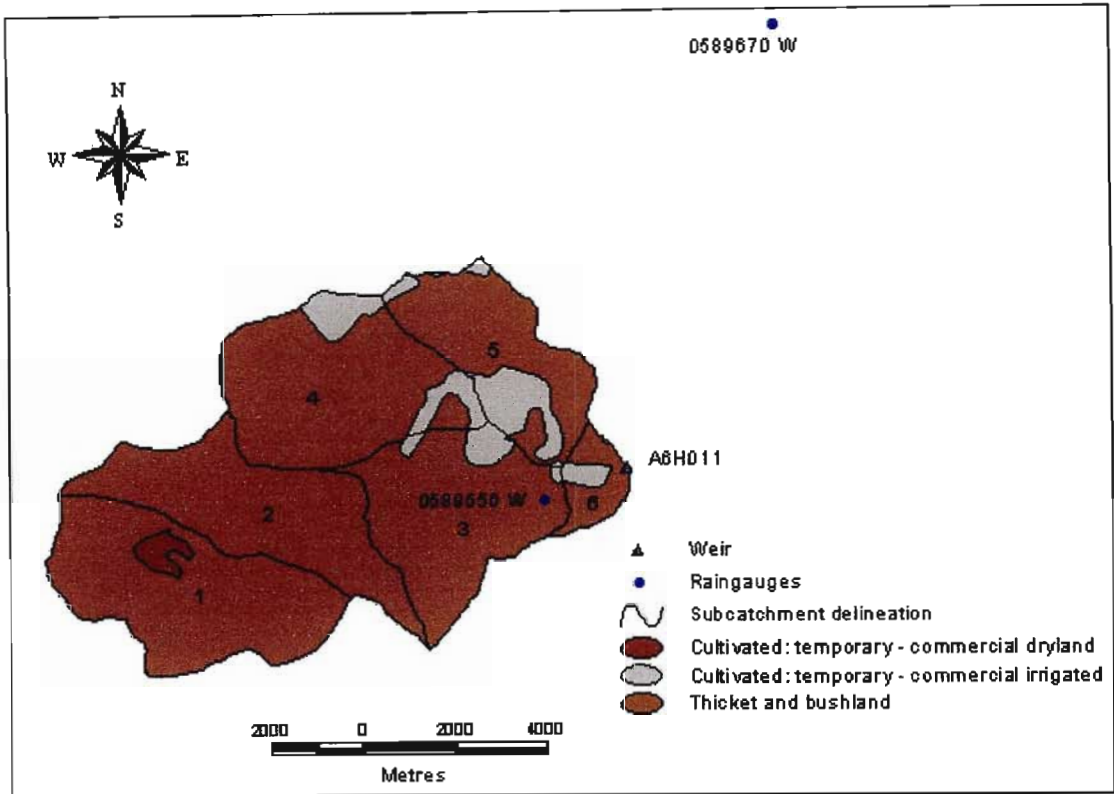
Figure 35: Groot-Nylrivier catchment, illustrating land uses and the locations of rainfall stations.

Sedimentary rocks of the Waterberg and Rooiberg Groups and a wide variety of sandstone, greywacke, grit, mudstone, siltstone, shale and conglomerate underlie the catchment. Soils are highly variable, but are predominantly acidic sands, loams or gravels with a maximum depth of 1.2 m. Low and Rebelo (1998) classified the area's natural vegetation, given as "Thicket and bushland" in Figure 35, as savanna, with Waterberg moist mountain bushveld covering 90% of the catchment. The remaining 10% consists of cultivated croplands, both dryland and irrigated. The simulation period was from 1968 to 1978.

3.4.3 Setting up *ACRU* input menus for catchment simulations

The *ACRU* Menubuilder was used to set up model runs with *ACRU* for each catchment, starting with best estimates of variables and parameters from the *ACRU* User Manual (Smithers and Schulze, 1995) and then analsying the fit between simulated and observed streamflow. The statistical functions and procedures used to evaluate the model results were:

- the comparison of the sums of total observed and simulated values,
- a comparison of cumulative plots of observed and simulated flow for the entire simulation period,
- the Nash-Sutcliffe coefficient (R^2),
- the slope and intercept of the regression line of modelled versus observed flows,
- the coefficient of efficiency, used for measuring the degree of association between observed and simulated values, and
- the coefficient of agreement, reflects the degree to which the regression model predicts the simulated values.

Manual adjustments were then made to selected parameter values (especially QFRESP and COFRU) according to guidelines provided in the *ACRU* manuals.

Because of the problem of equifinality of 'best' parameter estimates when applying manual calibration, use was made of the PEST **P**arameter **EST**imation computer program, details of which may be found at following internet address http://www.ozemail.com.au/~wcomp/. PEST is a model-independent non-linear parameter estimator which has proved useful in the calibration of environmental models of many types, including complex groundwater models (Doherty, 2001). PEST is now being applied increasingly to problems of surface water modelling (Qingyun *et al.*, 1992; Bosuk *et al.*, 2001). The methodology of non-linear parameter estimation disposes of the arduous, labour-intensive and often frustrating task of manual parameter model calibration. PEST has been effectively used to determine parameter values that may not be amenable to direct measurement (Doherty, 2001).

The PEST Parameter ESTimator software has the 'Gauss-Marquart-Levenburg' algorithm at the core of the optimisation routine. This algorithm provides unbiased and weighted parameter estimates for non-linear relationships such as rainfall:runoff relations. The weighted sum of squared differences between modelled and observed values is the objective function used in PEST. For most models, parameter estimation is an iterative process. By comparing parameter changes and objective function improvement achieved through the current iteration with those achieved in previous iterations, PEST can indicate whether it is worth undertaking a further optimisation iteration; if so, the whole process is repeated.

PEST was applied to all selected catchments, with constraints set to the upper and lower bounds of QFRESP and COFRU according to the *ACRU* User Manual. Improvements in model fit were obtained for some catchments, but not in all. The catchments in which PEST did improve the model fit were:

- Watervalsrivier
- Dieprivier
- Bloukransrivier
- Cathedral Peak IV
- DeHoek V1H015
- Treurrivier
- Beestekraalspruit and
- Groot-Nylrivier.

The results for these catchments using PEST are presented in the next chapter, together with the results of those catchments which were optimised manually.

The problems experienced when applying PEST to the *ACRU* model included the following:

- It is difficult to optimise parameters from a distributed catchment menu, partly because of inter-correlation between parameters. Therefore, parameter

constraints were set for one subcatchment and the resulting optimised parameters were then applied to the entire catchment.

- In striving towards the optimal objective function, minimum permissible values of QFRESP and COFRU were derived by PEST for some catchments. These deviated significantly from values obtained from the best-fit manual calibration runs.

The non-improvement in streamflow simulations for 6 of the 14 catchments selected may indicate that there are other parameters, together with QFRESP and COFRU, which need to be optimised in the model in order to improve streamflow generation patterns.

<div align="center">* * * * * * * * * * * * * * * * * * *</div>

Chapter 3 has provided the relevant background information on the procedures followed in selecting the fourteen catchments which were simulated using the *ACRU* model. Detailed descriptions of climate, vegetation and soils characteristics where available, including illustrations of the each catchment are also given in this Chapter. Section 3.4.3 summarises the set up of the *ACRU* input menus for catchment simulations, and the statistical functions and procedures which were used to evaluate the model results. These results of catchment simulations are presented in Chapter 4, which includes those catchments in which the PEST parameter estimation computer programme did improve model fit. However, the application of PEST to surface water modelling in general, and *ACRU* in particular, warrants further investigation.

4.   RESULTS AND DISCUSSION

This chapter provides a summary of the *ACRU* model simulation results for each of the 14 catchments that were selected for this study. Each summary consists of a description of the catchment, a monthly and daily comparison of simulated and observed streamflows, a scatter plot of simulated and observed flows, a statistical analysis of monthly totals of daily observed and simulated streamflows and the total daily simulated evaporation for the simulation period. The simulation results of the 13 South African catchments are summarised in Table 33 (p 122) at the end of this section. Table 33 also highlights those catchments in which the simulated flows mimicked the observed streamflows well enough to be included in the investigation of the relationships between catchment physical and climatic attributes and streamflow parameters. The results of the regression analysis are described in the last section of this chapter. Appendix 1 (pages 149-163), provides the *ACRU* menu inputs for each of the 14 catchments, to facilitate further analysis by future *ACRU* modellers. Detailed explanations for each of the *ACRU* menu input variables are found in Smithers and Schulze (1995).

4.1 Safford Research Catchment, Arizona, USA

The *ACRU* model input parameters for Safford are tabulated in Appendix 1, pages 160 to 163. Figure 36 illustrates the time series of observed and simulated monthly totals of daily streamflows from this arid catchment, as well as accumulated flows. Patterns of flow observed are typical of those from arid and semi-arid catchments, with markedly discontinuous flows, transient baseflows, and occasional very high quickflows. The pattern of accumulated observed and simulated flows illustrates that large discrepancies may occur around the time of high rainfall events. Variations in rainfall intensity and streamflow transmission losses into banks and the channel bed are believed to be causes of inconsistent responses to rainfall in this catchment. Hourly rainfall data for this catchment were examined to test the first of these two hypotheses. Figures 37 and 38 illustrate that under-simulation of quickflow correlates with high intensity rainfalls, whereas over-simulation of quickflow occurs in association with low intensity rainfall events. A plot of observed versus simulated

monthly totals of daily flows (Figure 39) reveals a relatively poor fit (R^2 = 0.56), and this is borne out by the statistics of fit in Table 7. Clearly, the present version of *ACRU*, as a daily time step model, is not structured conceptually to predicting flows in arid catchments where low soil infiltration rates, short rainfall events of highly variable rainfall intensity and significant transmission losses occur.

Figure 40 illustrates the episodic pattern of daily total evaporation (i.e. "actual evapotranspiration"). High rates, exceeding 7 mm per day, are possible during times of high soil moisture after rainfall, but they quickly reduce to much lower values as the soil dries out.
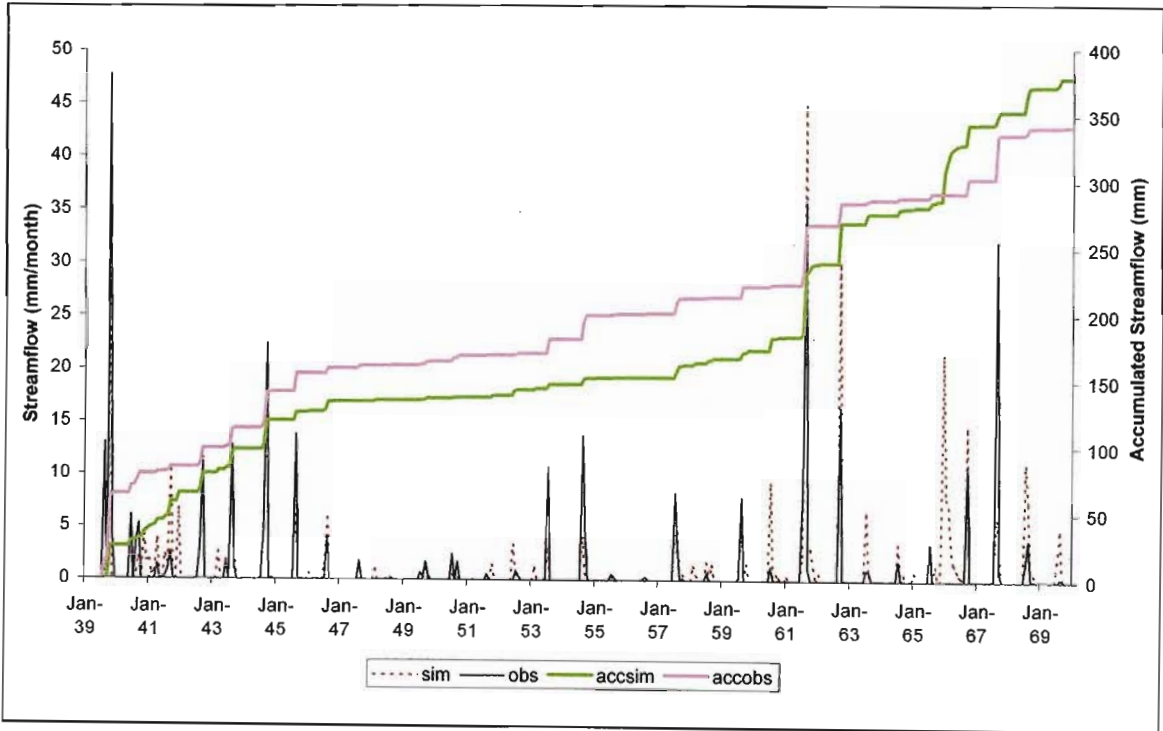
Figure 36: Time series of observed (obs) and simulated (sim) monthly totals of daily streamflows for the Safford research catchment. Accumulated flows (accsim; accobs) are also shown.
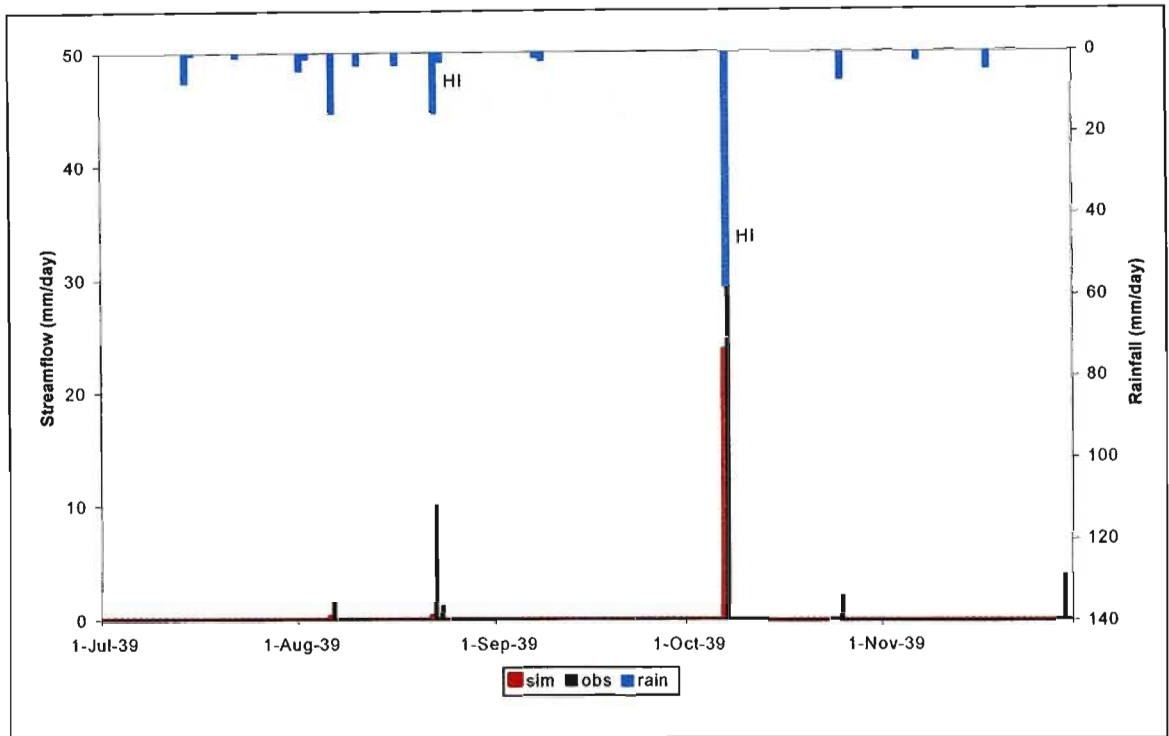
Figure 37: Comparison of daily observed (obs) and simulated (sim) streamflows from Safford for the period July 1939 to November 1939. HI indicates high intensity rainfall events.
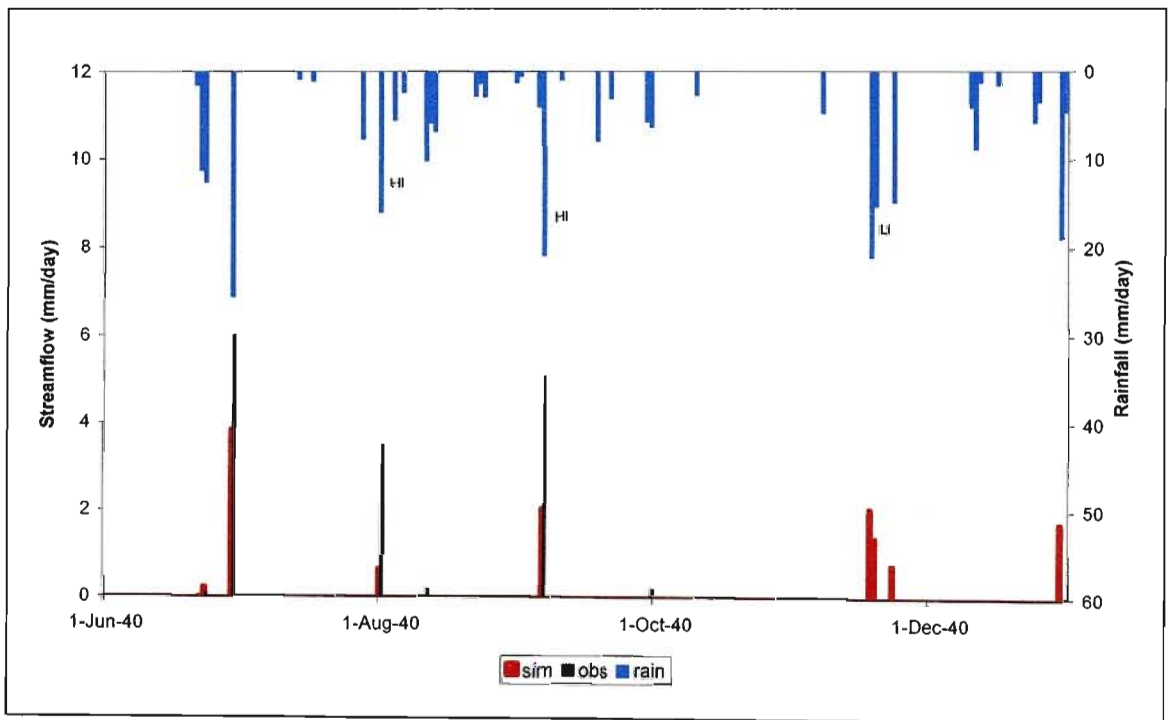
Figure 38: Comparison of daily observed (obs) and simulated (sim) streamflows from Safford for June 1940 to December 1940. HI and LI designate, respectively, high and low intensity rainfall events.
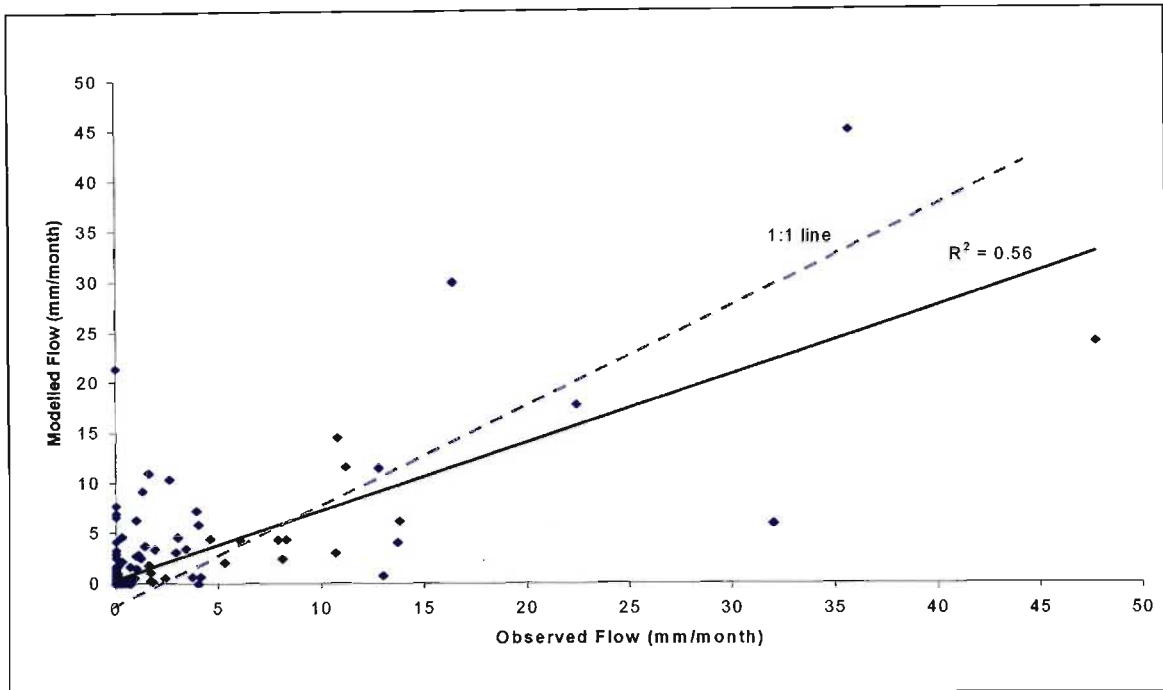
Figure 39: Scatter plot of monthly totals of daily simulated and observed streamflows for Safford from 1939 to 1969.

Table 7: Statistical analysis of monthly totals of daily observed and simulated streamflows for Safford from 1939 to 1969.

CONSERVATION STATISTICS	
Sum of observed values	341.90
Sum of simulated values	378.63
Mean of observed values	0.92
Mean of simulated values	1.02
% difference between means	-10.74
% difference between standard deviations	9.69
% difference between coefficients of variation	18.45
% difference between skewness coefficients	3.70
REGRESSION STATISTICS	
Coefficient of determination (r)	0.56
Slope of the regression line	0.68
Y intercept of the regression line	0.40
Coefficient of efficiency	0.43
Coefficient of agreement	0.84
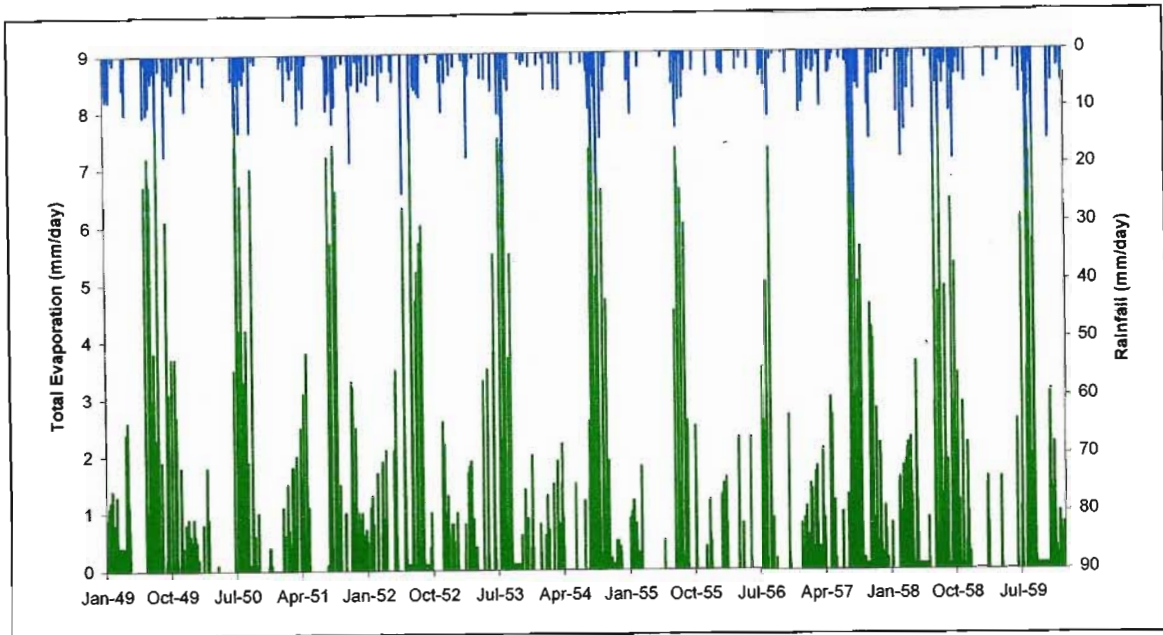
Figure 40: Time series of simulated daily total evaporation (i.e. "actual evapotranspiration") from the *ACRU* model for Safford from 1949 to 1959.

4.2 South African Catchments

4.2.1 Lambrechtsbos B

The *ACRU* model input parameters for Lambrechtsbos B are tabulated in Appendix 1, pages 149 to 153. Salient features of the catchment and model parameter values for QFRESP and COFRU are shown in Table 8.

Table 8: Summary table of catchment descriptors for Lambrechtsbos B.

Latitude (degrees minutes)	33 57
Longitude (degrees minutes)	18 57
Rainfall Seasonality	Winter
MAP (mm)	1472
Area (km^2)	0.66
Altitude Range (m)	300 – 1067
Dominant Land Use(s)	Forest and Fynbos
Operational or Research Catchment	Research
Average Depth of Soil Profile (m)	1.496
QFRESP (optimised manually)	0.210
COFRU (optimised manually)	0.006

79

Streamflows for Lambrechtsbos B are over-simulated, as shown in Figures 41 and 43. This may be due to the rainfall values which were used not representing the entire catchment, bearing in mind that this catchment extends upwards altitudinally into the Jonkershoek Mountains. Correlations between observed and simulated streamflows along the 1:1 line are poor, as shown in Figure 42.
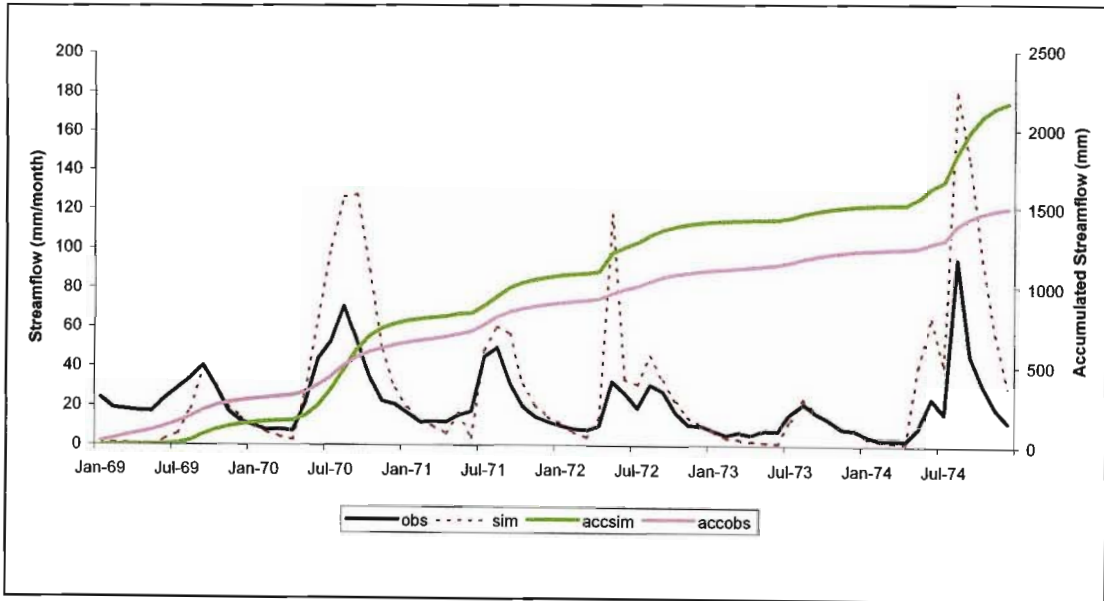
Figure 41: Time series of observed (obs) and simulated (sim) monthly totals of daily streamflows from 1969 to 1974 for Lambrechtsbos B. Accumulated flows (accsim, accobs) are also shown.
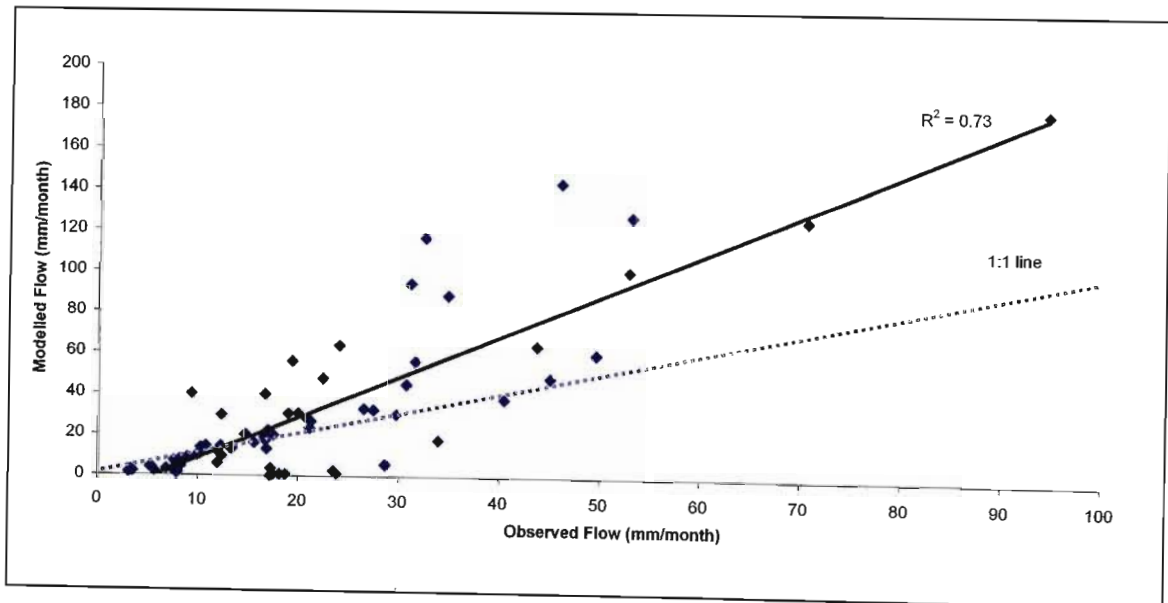
Figure 42: Scatter plot of simulated and observed monthly totals of daily streamflows for Lambrechtsbos B from 1969 to 1974.

Baseflow recessions are generally over-simulated, with the simulated baseflows receding slower that the observed flows, as shown in Figure 43. These differences between observed and simulated streamflows are illustrated by the large difference in standard deviations of 132.35% shown in Table 9. High rates of total daily evaporation exceeding 6 mm/day are simulated by the model, as shown in Figure 44.

Figure 43: Time series of observed (obs) and simulated (sim) daily streamflows from October 1970 to September 1974 for Lambrechtsbos B. Summary statistics of model fit to observed data for this period are also shown.

Table 9: Statistical analysis of monthly totals of daily observed and simulated streamflows for Lambrechtsbos B from 1969 to 1974.

CONSERVATION STATISTICS	
Sum of observed values	1496.81
Sum of simulated values	2168.89
Mean of observed values	20.79
Mean of simulated values	30.12
% difference between means	-44.90
% difference between standard deviations	-132.35
% difference between coefficients of variation	-60.35
% difference between skewness coefficients	1.52
REGRESSION STATISTICS	
Coefficient of determination (r)	0.73
Slope of the regression line	1.99
Y intercept of the regression line	-11.23
Coefficient of efficiency	0.49
Coefficient of agreement	0.92
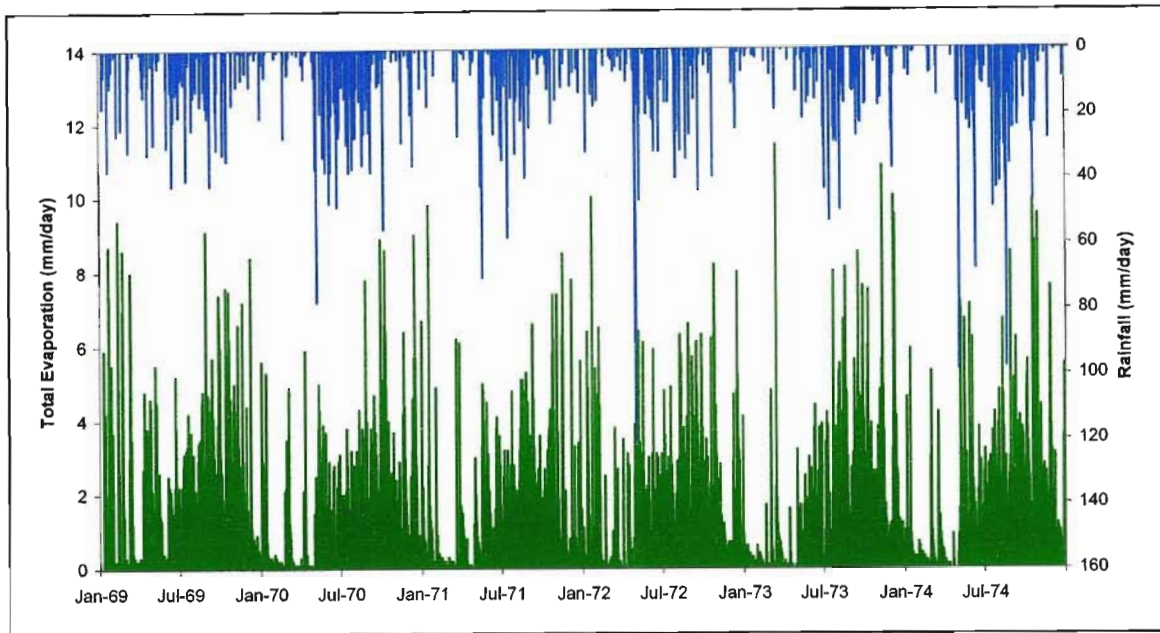
Figure 44: Time series of simulated daily total evaporation (i.e. "actual evapotranspiration") from the *ACRU* model for Lambrechtsbos B from 1969 to 1974.

4.2.2 Watervalsrivier

The *ACRU* model input parameters for Watervalsrivier are tabulated in Appendix 1, pages 149 to 153. Salient features of the catchment and model parameter values for QFRESP and COFRU are shown in Table 10, which were optimised using PEST.

Table 10: Summary table of catchment descriptors for Watervalsrivier.

Latitude (degrees minutes)	33 21
Longitude (degrees minutes)	19 06
Rainfall Seasonality	Winter
MAP (mm)	664
Area (km²)	36
Altitude Range (m)	120 - 1086
Dominant Land Use(s)	Shrubland and low fynbos
Operational or Research Catchment	Operational
Average Depth of Soil Profile	0.482
QFRESP (optimised with PEST)	0.20
COFRU (optimised with PEST)	0.035

Streamflows in the Watervalsrivier catchment are simulated well, as shown in Figures 45 and 47. These results indicate a good correlation between observed and

simulated streamflows using the *ACRU* model (Figure 46). Comparisons of the total observed and simulated streamflows in Table 10, indicate an over-simulation of streamflows, which may be attributed to rainfall values used being too high. Typically *ACRU* over-simulates early rainfall season streamflows, as shown in Figure 47, and this is usually associated with low intensity frontal rainfall.

Figure 45: Time series of observed (obs) and simulated (sim) monthly totals of daily streamflows from 1968 to 1974 for Watervalsrivier. Accumulated flows (accsim; accobs) are also shown.
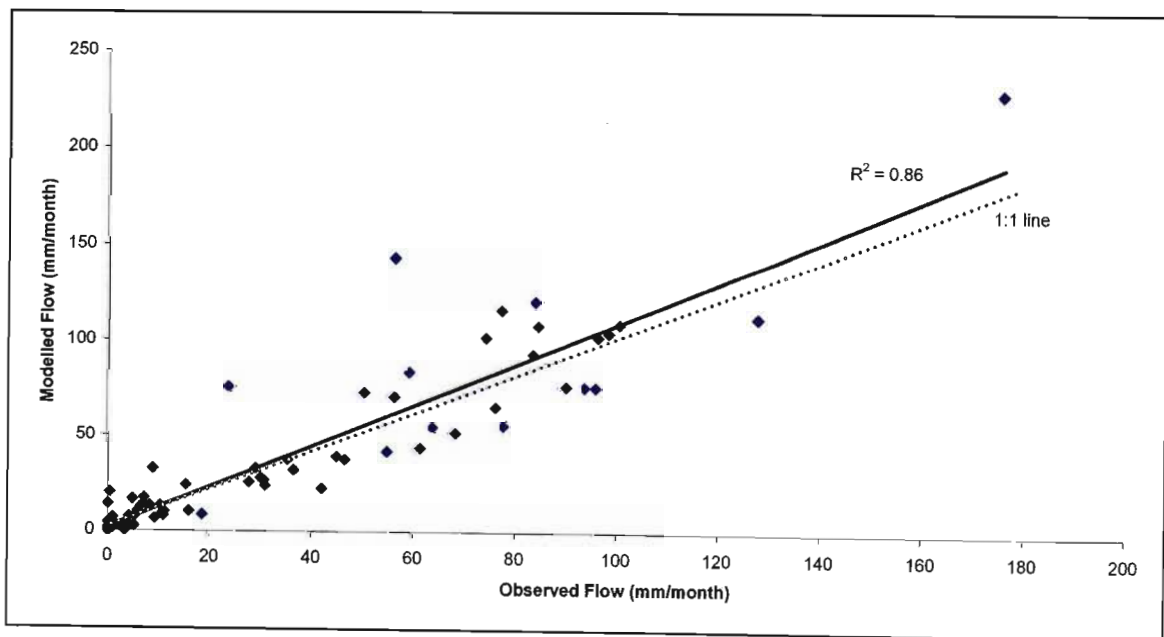
Figure 46: Scatter plot of simulated and observed monthly totals of daily streamflows for Watervalsrivier from 1968 to 1974.
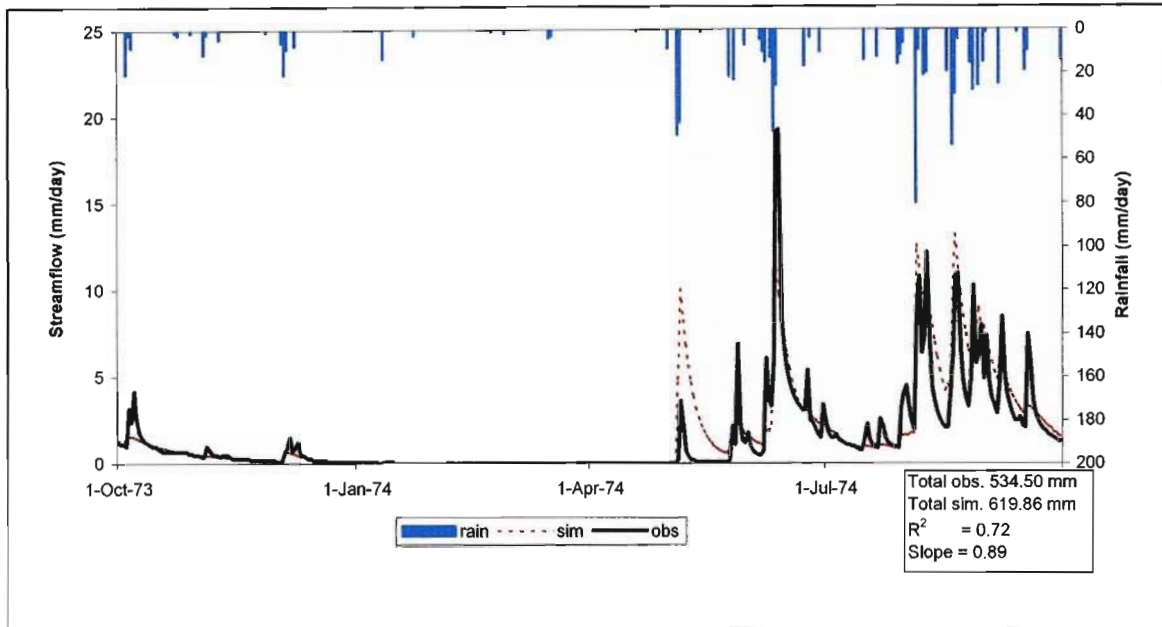
Figure 47: Time series of observed (obs) and simulated (sim) daily streamflows from October 1973 to September 1974 for Watervalsrivier. Summary statistics of model fit to observed data for this period are also shown.

Table 11: Statistical analysis of monthly totals of daily observed and simulated streamflows for Watervalsrivier from 1968 to 1974.

CONSERVATION STATISTICS	
Sum of observed values	2476.30
Sum of simulated values	2799.85
Mean of observed values	29.48
Mean of simulated values	33.33
% difference between means	-13.07
% difference between standard deviations	-15.21
% difference between coefficients of variation	-1.89
% difference between skewness coefficients	-29.53
REGRESSION STATISTICS	
Coefficient of determination (r)	0.86
Slope of the regression line	1.07
Y intercept of the regression line	1.86
Coefficient of efficiency	0.85
Coefficient of agreement	0.96
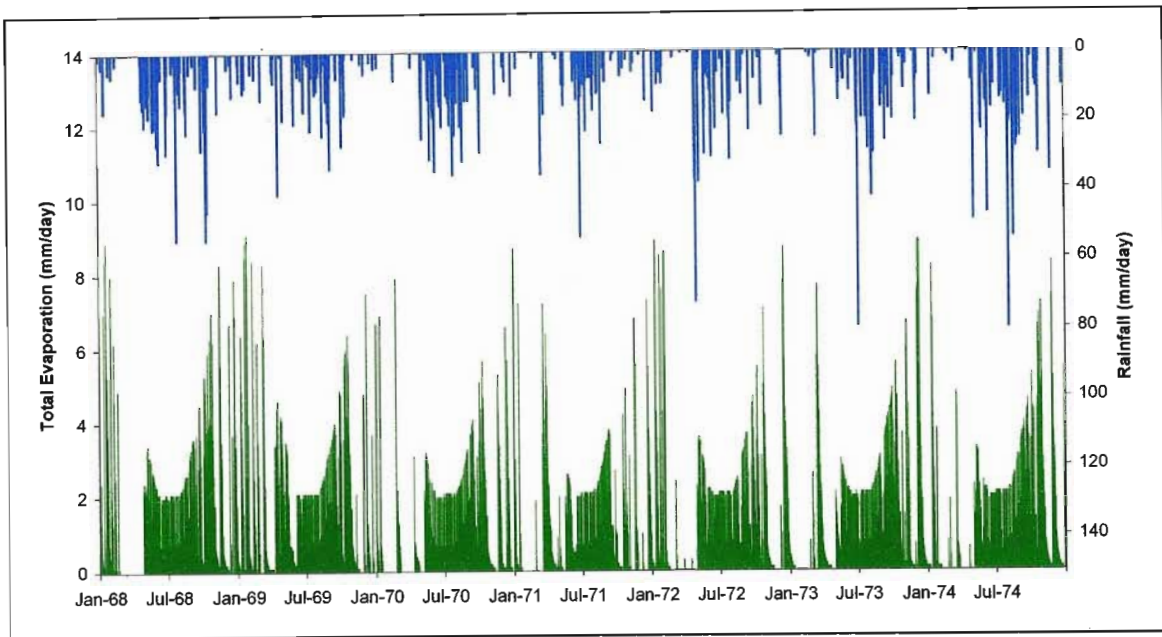
Figure 48: Time series of simulated daily total evaporation (i.e. "actual evapotranspiration") from the *ACRU* model for Watervalsrivier from 1968 to 1974.

4.2.3 Dieprivier

The *ACRU* model input parameters for Dieprivier are tabulated in Appendix 1, pages 149 to 153. Salient features of the catchment and model parameter values for QFRESP and COFRU are shown in Table 12. QFRESP and COFRU model parameters were optimised using PEST.

Table 12: Summary table of catchment descriptors for Dieprivier.

Latitude (degrees minutes)	33 54
Longitude (degrees minutes)	22 42
Rainfall Seasonality	All Year
MAP (mm)	711
Area (km²)	72
Altitude Range (m)	330 - 1034
Dominant Land Use(s)	Pine plantations
Operational or Research	Operational
Average Depth of Soil Profile	0.662
QFRESP (optimised with PEST)	0.750
COFRU (optimised with PEST)	0.026

Trends between observed and simulated streamflows for Dieprivier are poor, with large deviations between accumulated flows, as shown in Figure 49. Streamflows from the Dieprivier catchment are very flashy as shown in Figure 51.

Figure 49: Time series of observed (obs) and simulated (sim) monthly totals of daily streamflows from 1968 to 1975 for Dieprivier. Accumulated flows (accsim; accobs) are also shown.
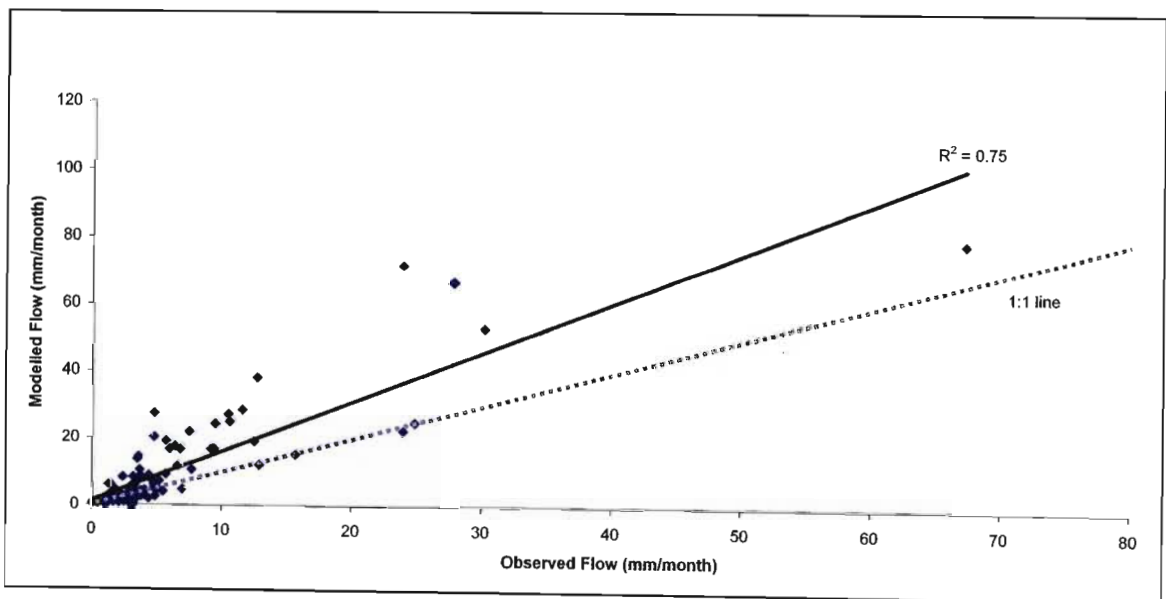
Figure 50: Scatter plot of simulated and observed monthly totals of daily streamflows for Dieprivier from 1968 to 1975.

Baseflow recessions are very rapid approaching near zero flows. It is hypothesised that the soils of this catchment may be much deeper than used in simulations; and that the two rainfall stations used were not representative enough of the entire catchment rainfall, accounting for the over-simulations.
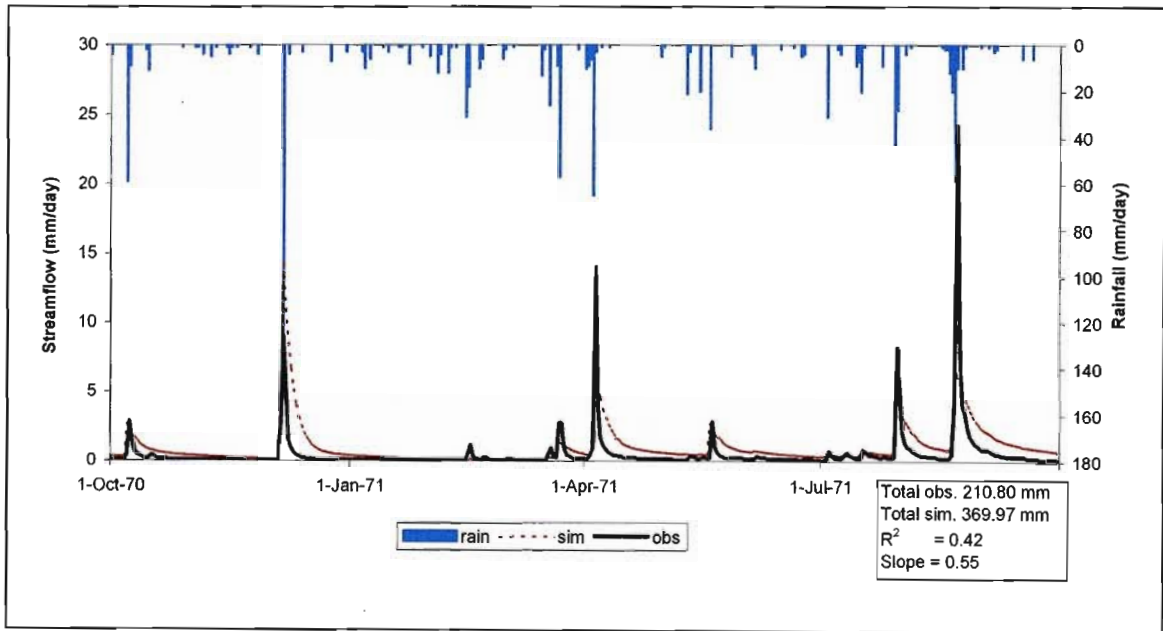
Figure 51: Time series of observed (obs) and simulated (sim) daily streamflows from October 1970 to September 1971 for Dieprivier. Summary statistics of model fit to observed data for this period are also shown.

Table 13: Statistical analysis of monthly totals of daily observed and simulated streamflows for Dieprivier from 1968 to 1975.

CONSERVATION STATISTICS	
Sum of observed values	577.70
Sum of simulated values	979.66
Mean of observed values	6.02
Mean of simulated values	10.21
% difference between means	-69.58
% difference between standard deviations	-70.84
% difference between coefficients of variation	-0.74
% difference between skewness coefficients	37.95
REGRESSION STATISTICS	
Coefficient of determination (r)	0.75
Slope of the regression line	1.48
Y intercept of the regression line	1.33
Coefficient of efficiency	0.59
Coefficient of agreement	0.92
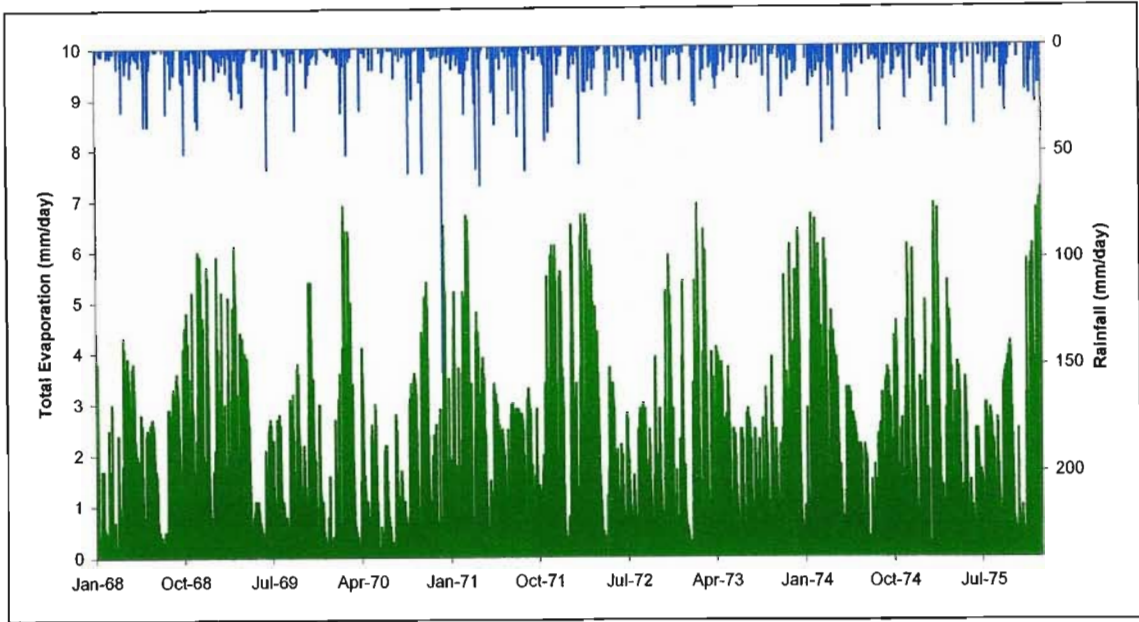
Figure 52: Time series of simulated daily total evaporation (i.e. "actual evapotranspiration") from the *ACRU* model for the Dieprivier catchment from 1968 to 1975.

4.2.4 Kruisrivier

The *ACRU* model input parameters for Kruisrivier are tabulated in Appendix 1, pages 149 to 153. Salient features of the catchment and model parameter values for QFRESP and COFRU are shown in Table 14.

Table 14: Summary table of catchment descriptors for Kruisrivier.

Latitude (degrees minutes)	34 00
Longitude (degrees minutes)	21 16
Rainfall Seasonality	All Year
MAP (mm)	645
Area (km²)	50
Altitude Range (m)	400 – 1325
Dominant Land Use(s)	Shrubland and low fynbos
Operational or Research	Operational
Average Depth of Soil Profile	0.253
QFRESP (optimised manually)	0.35
COFRU (optimised manually)	0.038

As a result of irrigation in the catchment during the summer months from October to February, it was decided to focus the simulations of this catchment on the winter months from June to September, during which time there were no abstractions. Simulated streamflows are represented fairly well, as shown in Figure 53, and if the first season (1981) were to be omitted, the accumulated flows over the entire simulation period would be nearly identical.
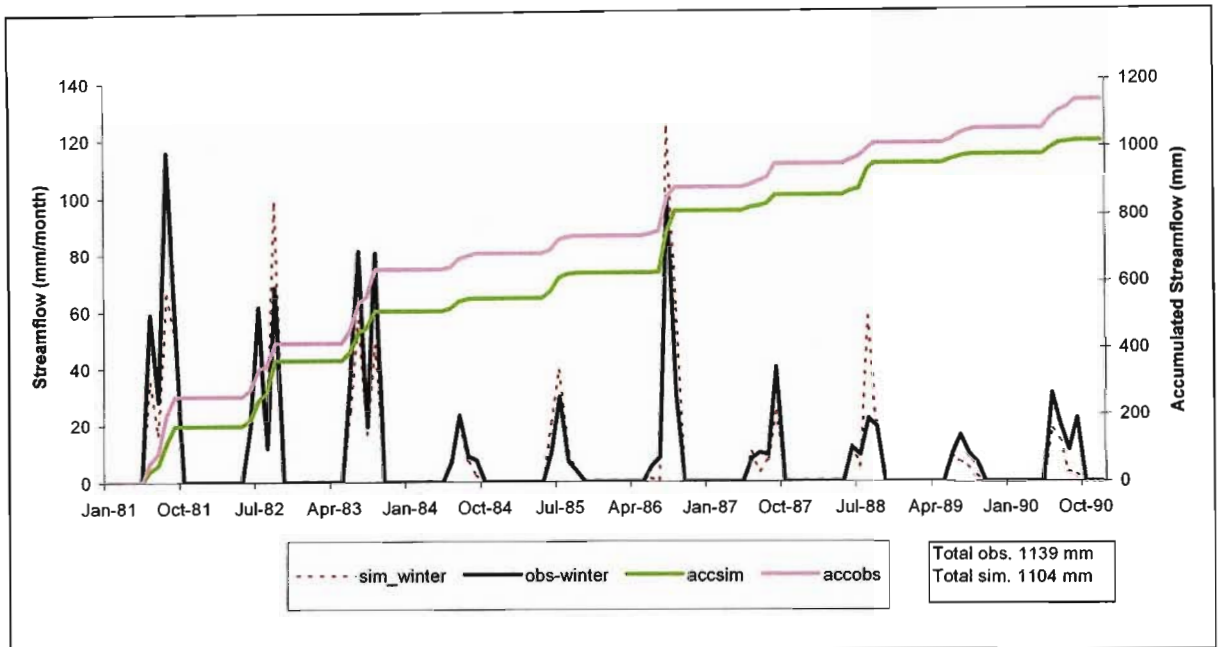
Figure 53: Time series of observed (obs_winter) and simulated (sim_winter) monthly totals of daily winter flows (June to September) from 1981 to 1990 for Kruisrivier. Accumulated winter flows (accsim; accobs) are also shown.

Figure 54 illustrates a relatively good trend between modelled and observed streamflows, with a slight under-simulation of flows as shown by the regression line. An acceptable model fit between observed and simulated daily streamflows is shown in Figure 55. Simulated daily total evaporation from the *ACRU* model for the Kruisrivier catchment are shown in Figure 56, illustrating lower daily evaporation totals during the winter months through June and July, as compared to higher evaporation totals as summer approaches.
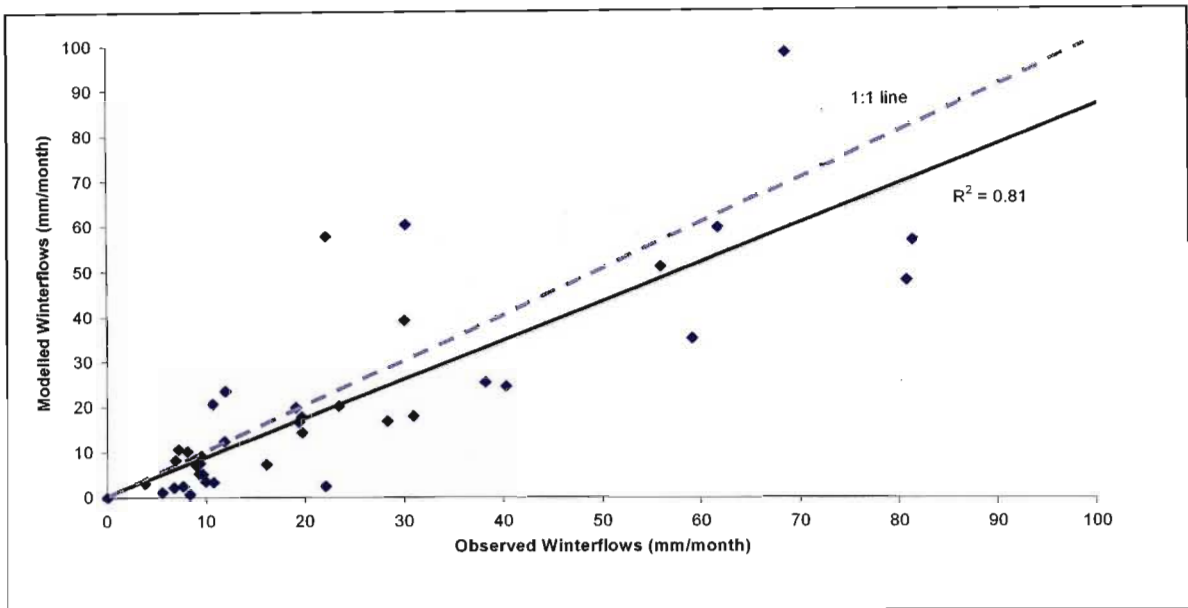
Figure 54: Scatter plot of simulated and observed monthly totals of daily winter flows for Kruisrivier from 1981 to 1990.
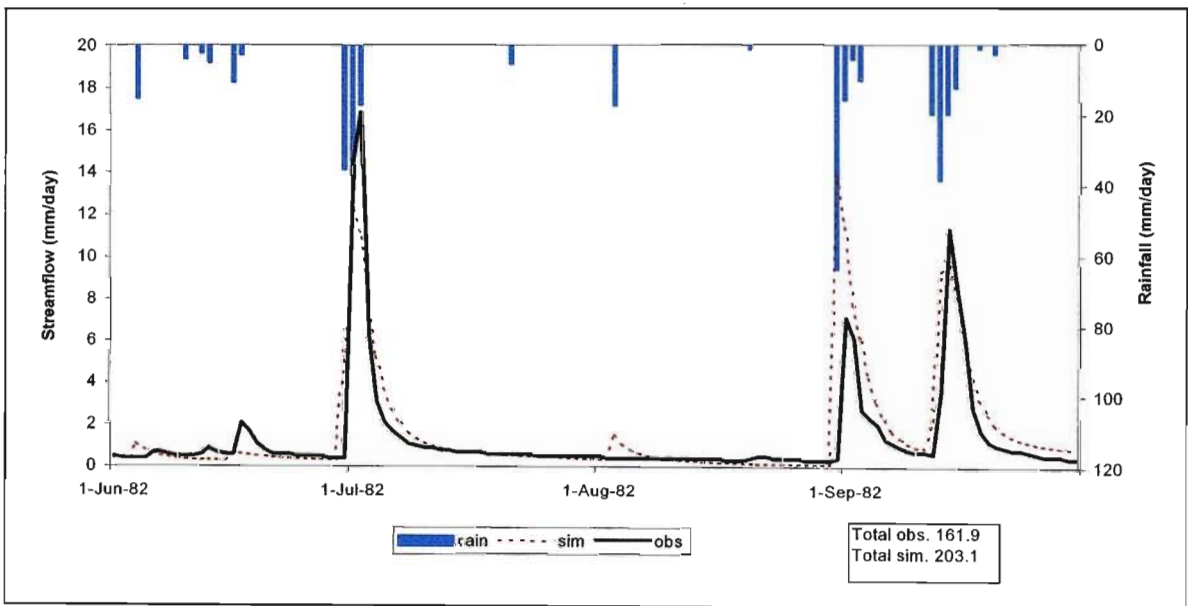
**Figure 55:** Time series of observed (obs) and simulated (sim) daily streamflows from June 1982 to September 1982 for Kruisrivier.
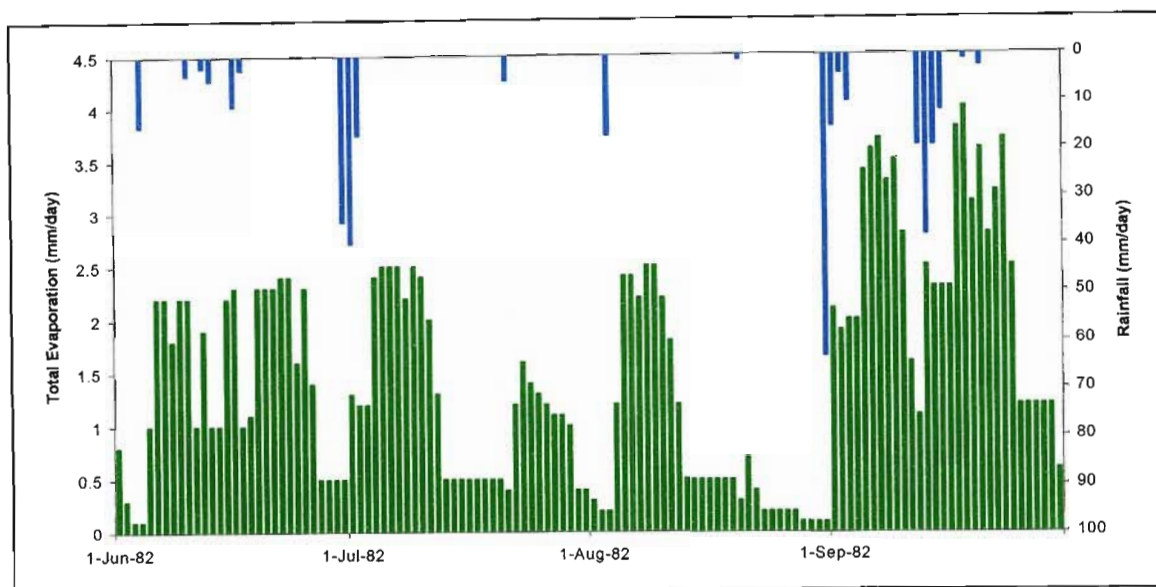
Figure 56: Time series of simulated daily total evaporation (i.e. "actual evapotranspiration") from the *ACRU* model for the Kruisrivier catchment from June 1982 to September 1982.

4.2.5 Bloukransrivier

The *ACRU* model input parameters for Bloukransrivier are tabulated in Appendix 1, pages 149 to 153. Salient features of the catchment and model parameter values for QFRESP and COFRU are shown in Table 15. QFRESP and COFRU model parameters were optimised using PEST.

Table 15: Summary table of catchment descriptors for Bloukransrivier.

Latitude (degrees minutes)	33 57
Longitude (degrees minutes)	23 37
Rainfall Seasonality	All Year
MAP (mm)	1003
Area (km²)	57
Altitude Range (m)	240 – 1676
Dominant Land Use(s)	Thicket and Bushland
Operational or Research	Operational
Average Depth of Soil Profile	0.534
QFRESP (optimised with PEST)	0.30
COFRU (optimised with PEST)	0.018

Good relationship between observed and simulated streamflows are illustrated in Figure 57 for the Bloukransrivier catchment, with general over-simulation in months with high flows. The results illustrate very good associations between observed and simulated streamflows, along the 1:1 line, as shown in Figure 58. Baseflow recessions are rapid reaching to near zero flows (Figure 59). The low percentage differences between standard deviations (7.43%) and coefficients of variation (8.96%) shown in Table 16 confirms the good relationships between observed and simulated streamflows.
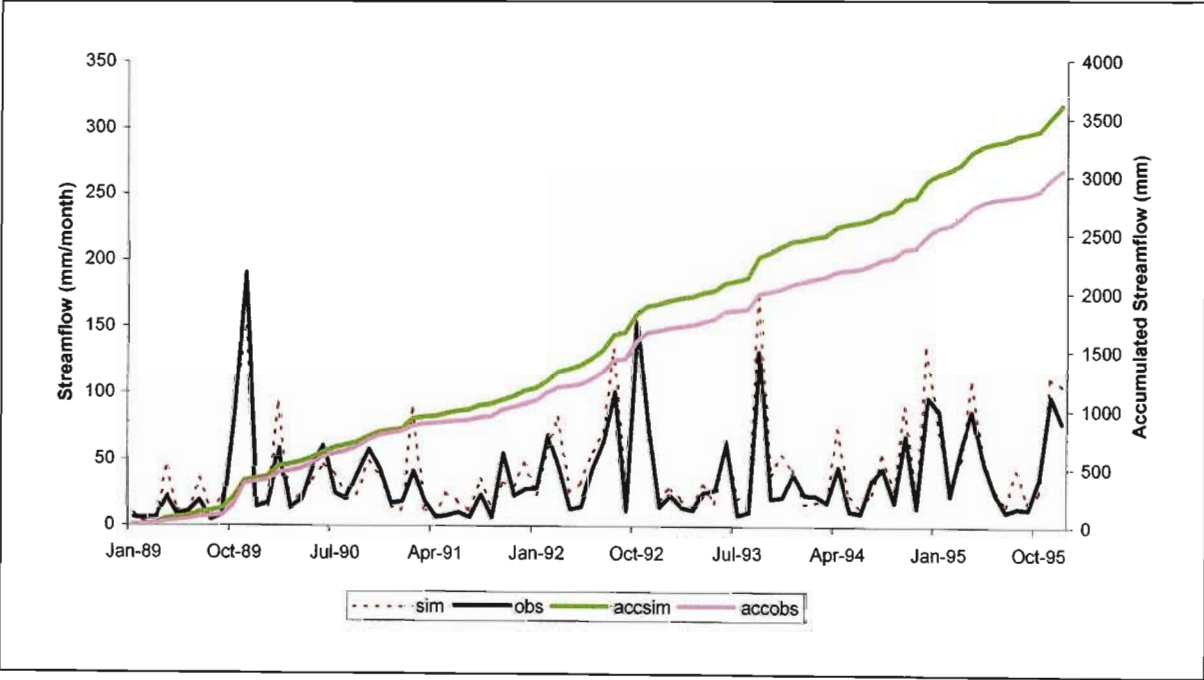
Figure 57: Time series of observed (obs) and simulated (sim) monthly totals of daily streamflows from 1989 to 1995 for Bloukransrivier. Accumulated flows (accsim; accobs) are also shown.
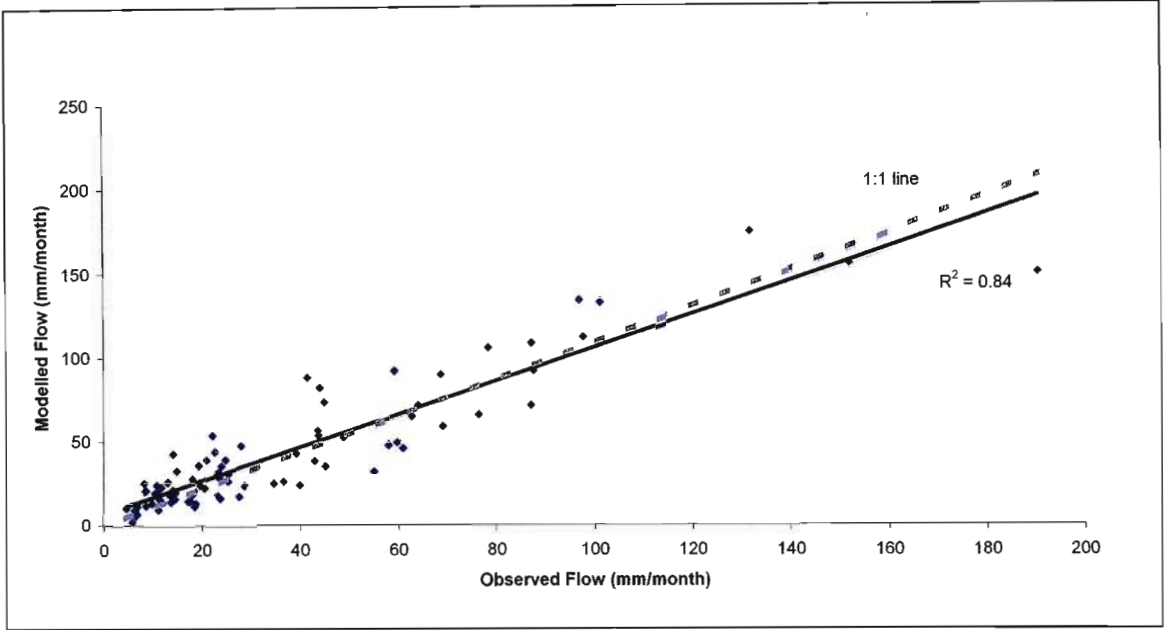
Figure 58: Scatter plot of simulated and observed monthly totals of daily streamflows for Bloukransrivier from 1989 to 1995.
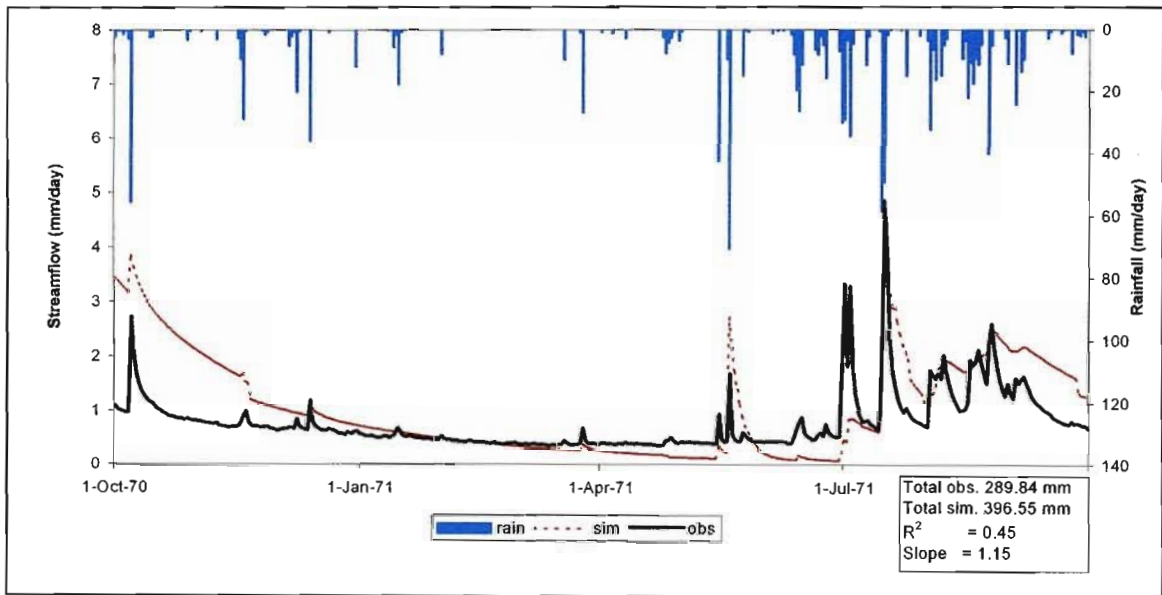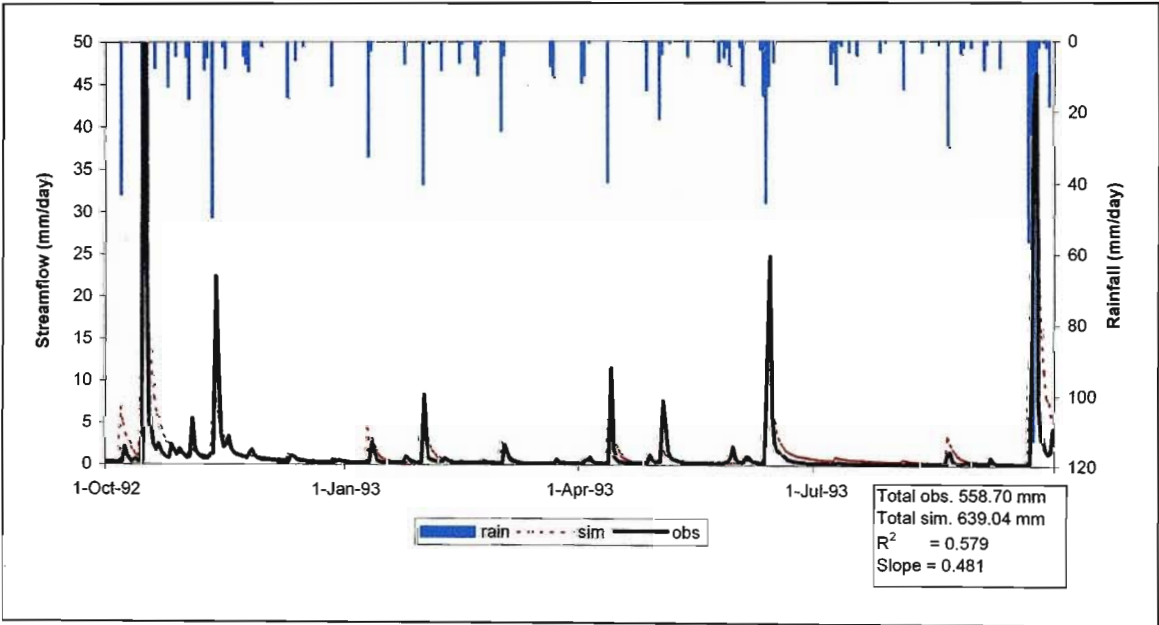

Figure 59: Time series of observed (obs) and simulated (sim) daily streamflows from October 1992 to September 1993 for Bloukransrivier. Summary statistics of model fit to observed data for this period are also shown.

Table 16: Statistical analysis of monthly totals of daily observed and simulated streamflows for Bloukransrivier from 1989 to 1995.

| CONSERVATION STATISTICS	
Sum of observed values	3074.40
Sum of simulated values	3627.98
Mean of observed values	36.60
Mean of simulated values	43.19
% difference between means	-18.01
% difference between standard deviations	-7.43
% difference between coefficients of variation	8.96
% difference between skewness coefficients	17.45
REGRESSION STATISTICS	
Coefficient of determination (r)	0.84
Slope of the regression line	0.99
Y intercept of the regression line	7.11
Coefficient of efficiency	0.84
Coefficient of agreement	0.81

Figure 60 illustrates the trend in simulated total daily evaporation total using the *ACRU* model. An average of 5 mm/day are simulated during the summer months, compared 2.5 mm/day estimated during the winter months.
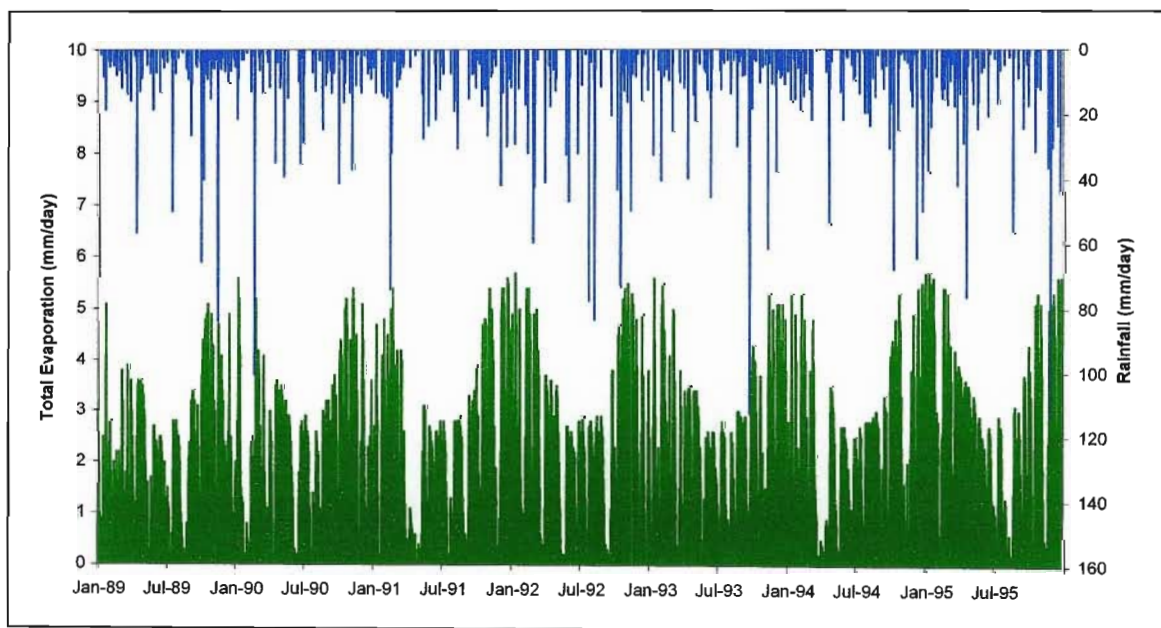
Figure 60: Time series of simulated daily total evaporation (i.e. "actual evapotranspiration") from the *ACRU* model for the Bloukransrivier catchment from 1989 to 1995.

4.2.6 Zululand Research Catchment W1H016

The *ACRU* model input parameters for the Zululand research catchment are tabulated in Appendix 1, pages 154 to 159. Salient features of the catchment and model parameter values for QFRESP and COFRU are shown in Table 17.

Table 17: Summary table of catchment descriptors for the Zululand research catchment W1H016.

Latitude (degrees minutes)	28 50
Longitude (degrees minutes)	31 46
Rainfall Seasonality	Early Summer
MAP (mm)	1314
Area (km^2)	3.32
Altitude Range (m)	205 - 323
Dominant Land Use(s)	Thicket and Bushland
Operational or Research	Research
Averaged Depth of Soil Profile (m)	0.35
QFRESP (optimised manually)	0.40
COFRU (optimised manually)	0.022

The results from this catchment also illustrate very good relationships between observed and simulated streamflows, as shown in Figure 61, with a very high correlation coefficient of 0.98. Deviations between observed and simulated streamflows are minimal and result mainly from differences between isolated events. It is also important to note that many of the data sets used in this study, in which the streamflow simulation results are highly acceptable, arise from the data collection in early 1970s and 1980s. This suggests that data collected during the above mentioned decade is of a more superior quality compared to current data sets. Figure 62 illustrates the good association between observed and simulated streamflows, along the 1:1 line, with a high correlation coefficient of 0.99. Daily streamflows from the Zululand research catchment W1H016 are very "flashy", as shown in Figure 63, with baseflow recessions receding very rapidly, approaching near zero flows. The excellent statistics shown in Table 18 confirm that simulated streamflows are highly correlated to observed streamflows from the Zululand research catchment W1H016, having a low percentage difference between standard deviations of 2.37%, and a high coefficient of agreement of 0.98. The average daily evaporation simulated using

the *ACRU* model is approximately 5 mm/day and 2 mm/day during the summer and winter months respectively, as shown in Figure 64.
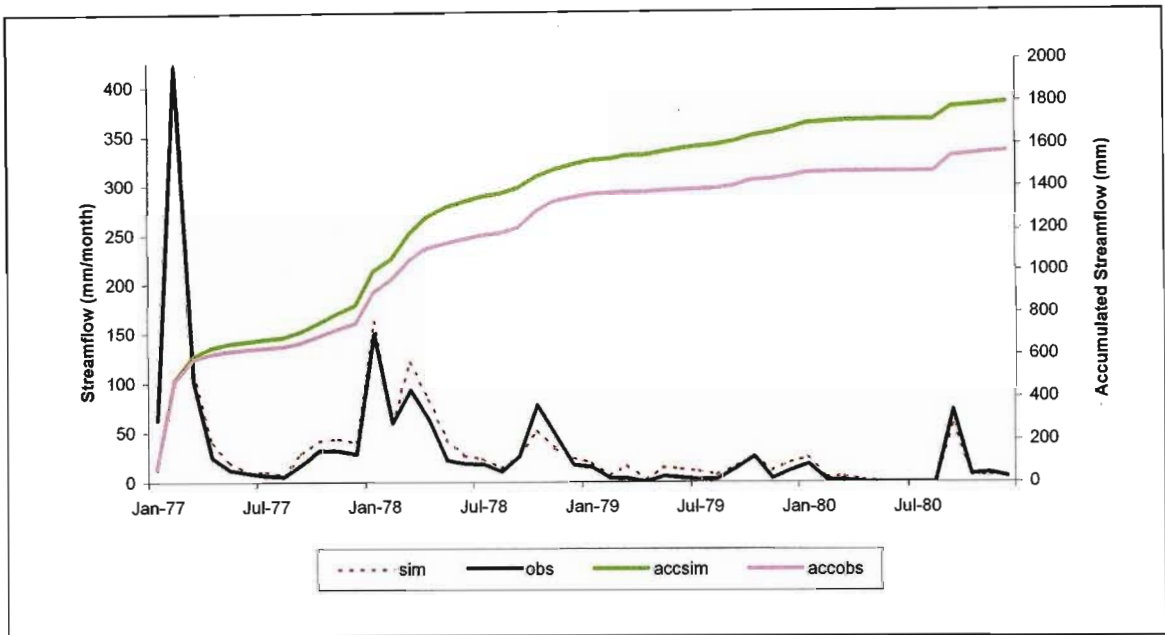
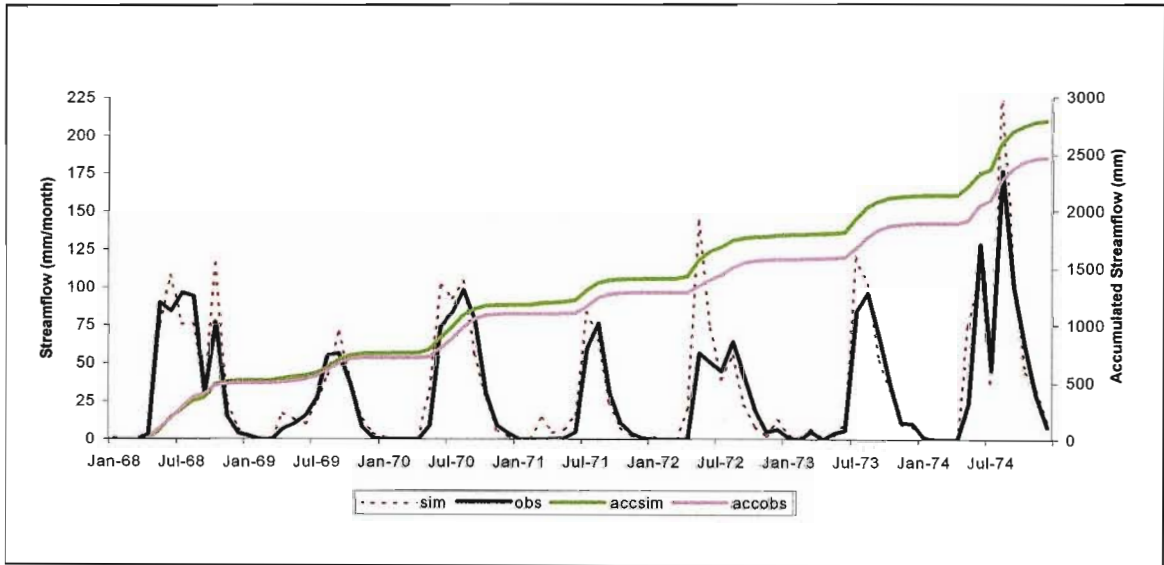**Figure 61:** Time series of observed (obs) and simulated (sim) monthly totals of daily streamflows from 1977 to 1980 for the Zululand research catchment W1H016. Accumulated flows (accsim; accobs) are also shown.
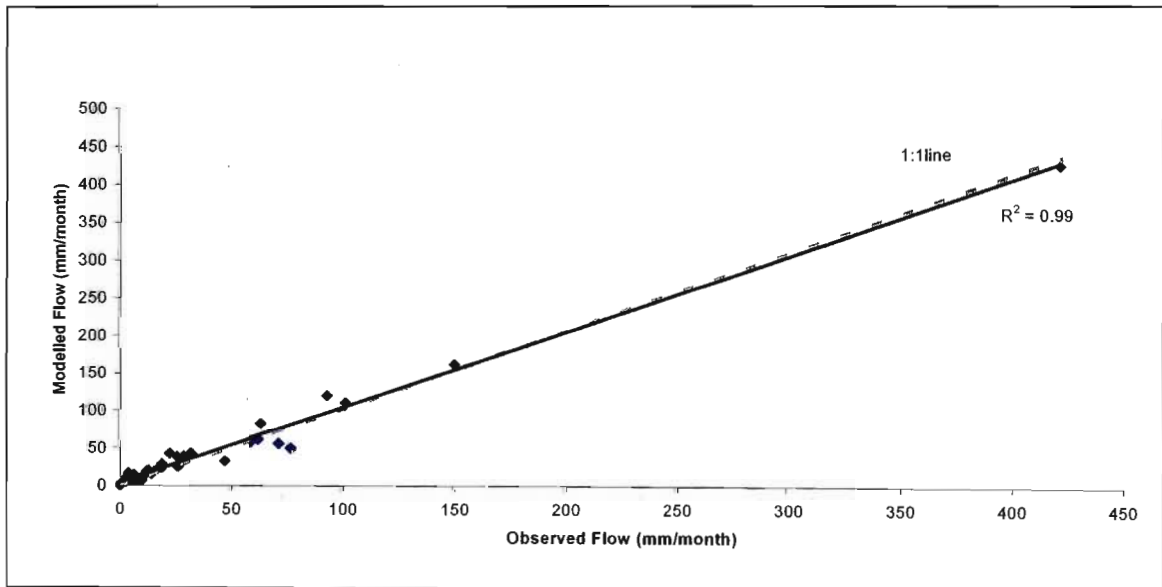
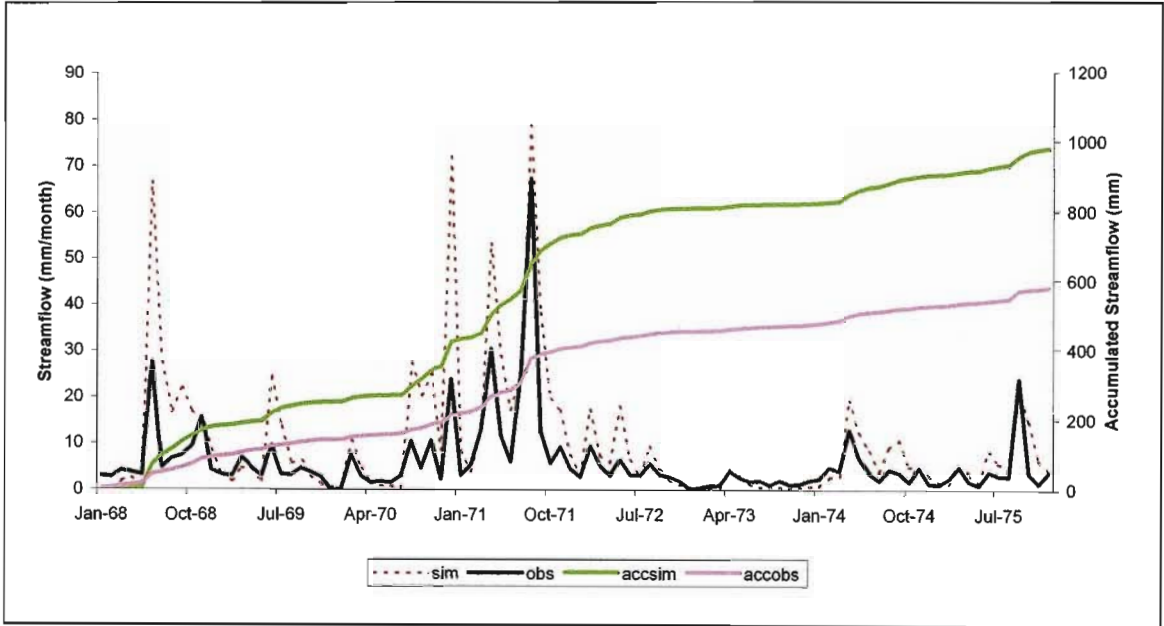**Figure 62:** Scatter plot of simulated and observed monthly totals of daily streamflows for the Zululand research catchment W1H016 from 1977 to 1980.
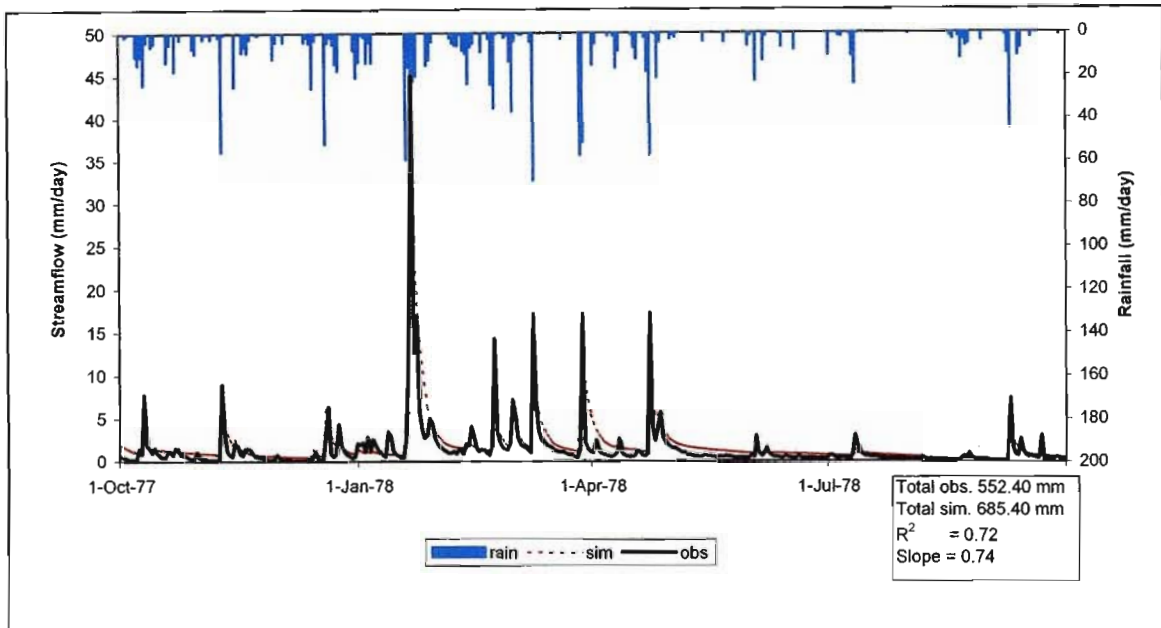
Figure 63: Time series of observed (obs) and simulated (sim) daily streamflows from October 1977 to September 1978 for the Zululand research catchment W1H016. Summary statistics of model fit to observed data for this period are also shown.

Table 18: Statistical analysis of monthly totals of daily observed and simulated streamflows for the Zululand research catchment W1H016 from 1977 to 1981.

CONSERVATION STATISTICS	
Sum of observed values	2165.60
Sum of simulated values	2289.50
Mean of observed values	36.09
Mean of simulated values	38.16
% difference between means	-5.72
% difference between standard deviations	2.37
% difference between coefficients of variation	7.65
% difference between skewness coefficients	-8.45
REGRESSION STATISTICS	
Coefficient of determination (r)	0.93
Slope of the regression line	0.94
Y intercept of the regression line	4.11
Coefficient of efficiency	0.93
Coefficient of agreement	0.98
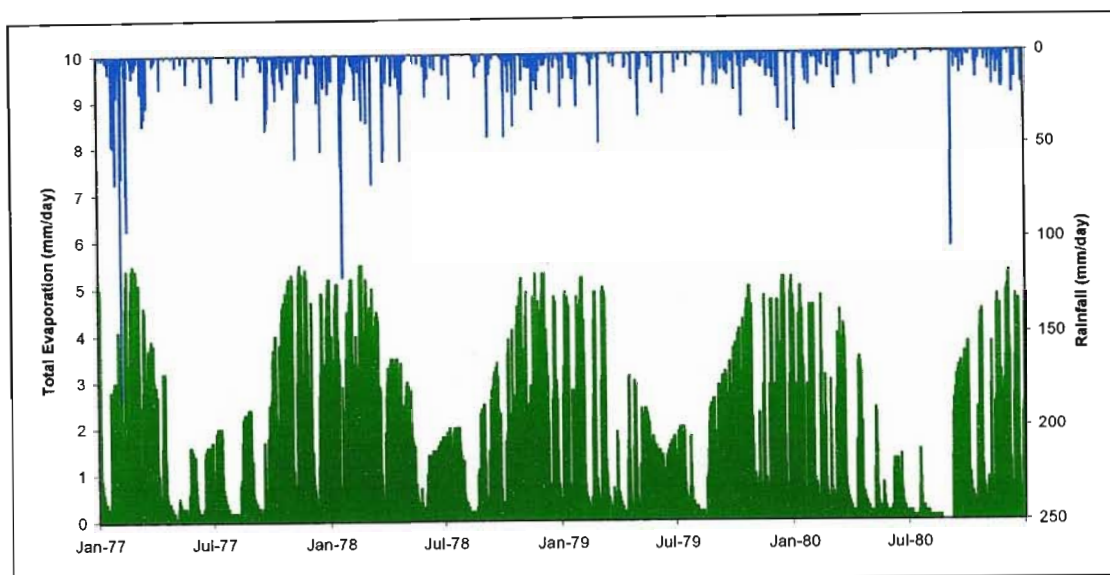
Figure 64: Time series of simulated daily total evaporation (i.e. "actual evapotranspiration") from the *ACRU* model for the Zululand research catchment W1H016 from 1977 to 1980.

4.2.7 Cathedral Peak Research Catchment IV

The *ACRU* model input parameters for the Cathedral Peak research catchment IV are tabulated in Appendix 1, pages 154 to 159. Salient features of the catchment and model parameter values for QFRESP and COFRU are shown in Table 19. QFRESP and COFRU model parameters were optimised using PEST.

Table 19: Summary table of catchment descriptors for the Cathedral Peak research catchment IV.

Latitude (degrees minutes)	29 00
Longitude (degrees minutes)	29 25
Rainfall Seasonality	Mid Summer
MAP (mm)	1400
Area (km²)	0.95
Altitude Range (m)	1845 – 2226
Dominant Land Use(s)	Grass
Operational or Research	Research
Averaged Depth of Soil Profile (m)	0.80
QFRESP (optimised with PEST)	0.06
COFRU (optimised with PEST)	0.018

Excellent relationships exist between observed and simulated streamflows for the Cathedral Peak research catchment, as shown in Figures 65 and 67. However, the "break" in the baseflow recession (Figure 67), which does occur in other simulations as well, arises from adjustments being made within *ACRU* to the baseflow release fraction, since experience has shown that the baseflow release "decay" is not constant, but rather a function of the magnitude of the previous day's groundwater store (Schulze, 1995). This resulting in changes to the baseflow release fraction and consequently to the baseflow recession. Excellent statistics are calculated between observed and simulated montly streamflows which are given in Table 20. These statistics indicate very high coefficients of correlation and agreement between simulated and observed flows of 0.94 and 0.98 respectively. Simulated daily evaporation totals shown in Figure 68, are estimated to be an average of 5 mm/day during the summer months, while declining to an average of 0.5 mm/day during the winter months.
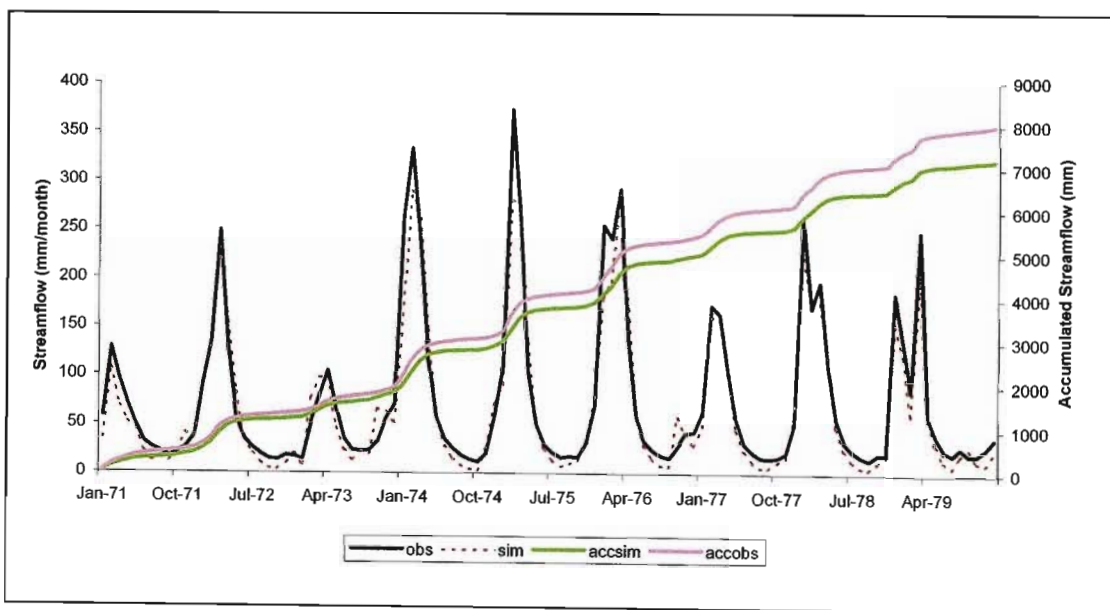
Figure 65:   Time series of observed (obs) and simulated (sim) monthly totals of daily streamflows from 1971 to 1979 for Cathedral Peak research catchment IV. Accumulated flows (accsim; accobs) are also shown.
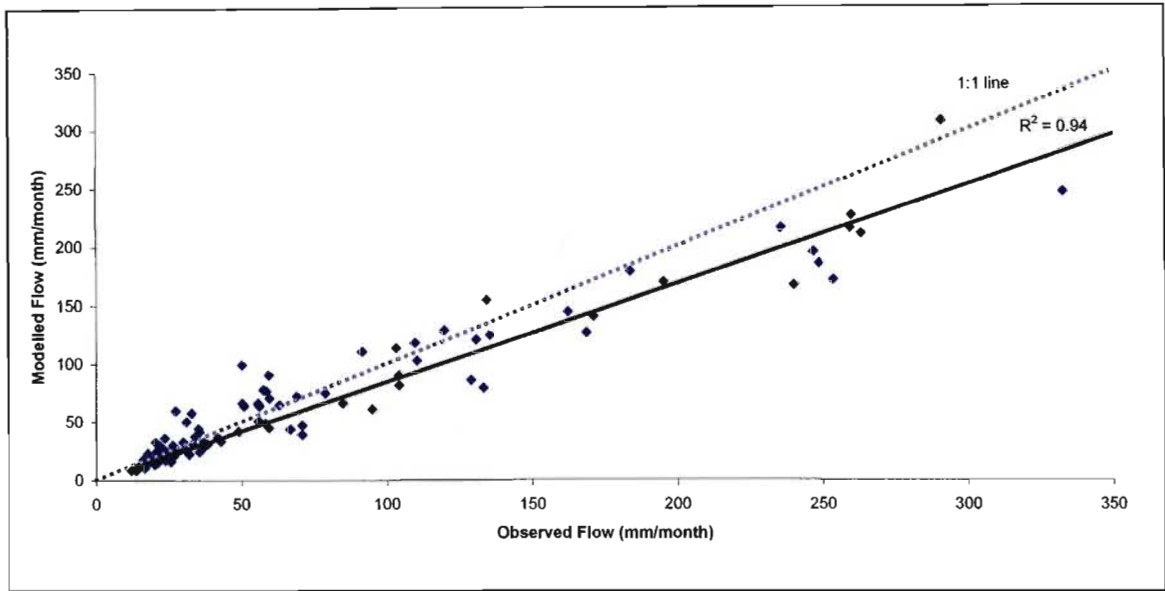
Figure 66: Scatter plot of simulated and observed monthly totals of daily streamflows for Cathedral peak research catchment IV for the period 1971 to 1979.
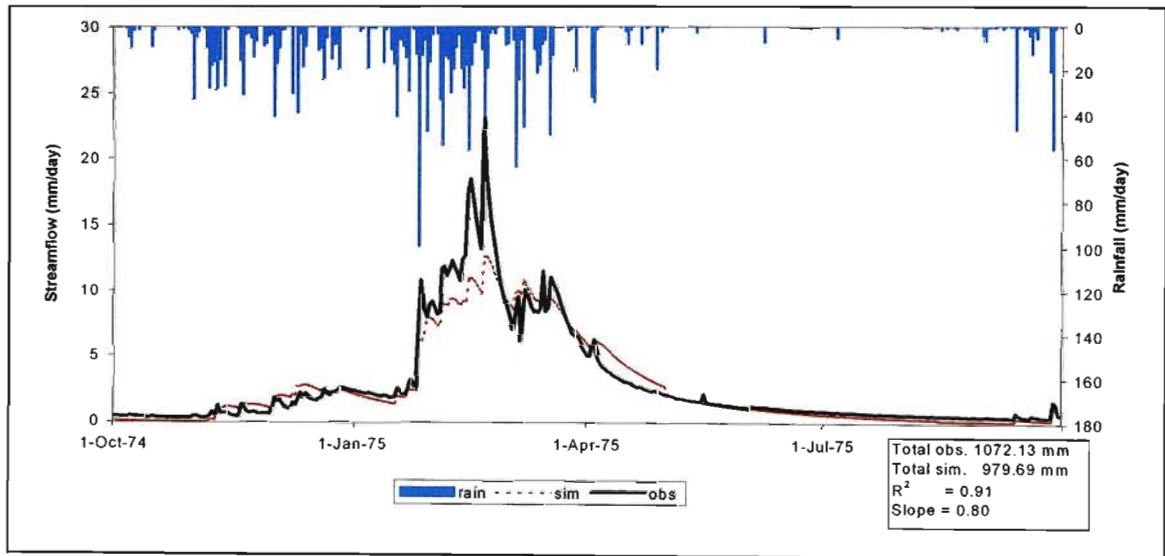
Figure 67: Time series of observed (obs) and simulated (sim) daily streamflows from October 1974 to September 1975 for Cathedral Peak research catchment IV. Summary statistics of model fit to observed data for this period are also shown.

Table 20: Statistical analysis of monthly totals of daily observed and simulated streamflows for Cathedral Peak research catchment IV from 1971 to 1979.

CONSERVATION STATISTICS	
Sum of observed values	8014.07
Sum of simulated values	7211.15
Mean of observed values	74.20
Mean of simulated values	66.77
% difference between means	10.02
% difference between standard deviations	8.88
% difference between coefficients of variation	-1.26
% difference between skewness coefficients	15.01
REGRESSION STATISTICS	
Coefficient of determination (r)	0.94
Slope of the regression line	0.88
Y intercept of the regression line	1.28
Coefficient of efficiency	0.91
Coefficient of agreement	0.98
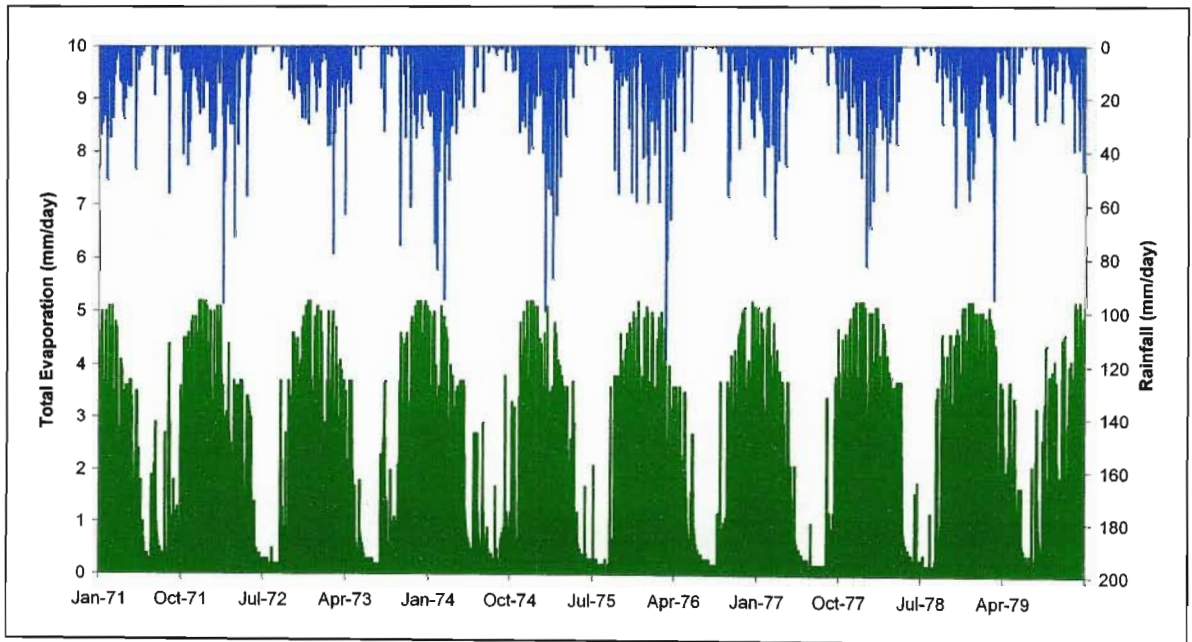
Figure 68: Time series of simulated daily total evaporation (i.e. "actual evapotranspiration") from the *ACRU* model for Cathedral Peak research catchment IV from 1971 to 1979.

4.2.8 DeHoek Research Catchment V1H015

The *ACRU* model input parameters for the DeHoek research catchment V1H015 are tabulated in Appendix 1, pages 154 to 159. Salient features of the catchment and model parameter values for QFRESP and COFRU are shown in Table 21. QFRESP and COFRU model parameters were optimised using PEST.

Table 21: Summary table of catchment descriptors for the DeHoek research catchment V1H015.

Latitude (degrees minutes)	29 58
Longitude (degrees minutes)	30 20
Rainfall Seasonality	Mid Summer
MAP (mm)	800
Area (km^2)	1.01
Altitude Range (m)	1450 – 1630
Dominant Land Use(s)	Grassland
Operational or Research	Research
Averaged Depth of Soil Profile (m)	0.824
QFRESP (optimised with PEST)	0.750
COFRU (optimised with PEST)	0.063

Results from this catchment indicate that the very high flows are simulated well by the model. Figure 69 indicates that there may be a data problem, with the streamflows records being out of phase during the months of January 1985 and 1986. However a good relationship exists between accumulative observed and simulated flows over the entire simulation period. An acceptable correlation coefficient of 0.78 is calculated from the scatter plot of simulated and observed monthly totals of daily streamflows in Figure 70. Figure 71 shows the typical over-simulation by the model of the first relatively high rainfall event of the rainy season. Topping (1992) showed that this catchment is highly responsive to rainfall intensity. Statistics shown in Table 22 also indicate good relationships between simulated and observed streamflows, with a difference between the means of only 0.22%. Daily evaporation trends simulated using the *ACRU* model (Figure 72) are in accordance with the expected high daily evaporation totals during the summer months from November to February, and declining as winter approaches.

Figure 69: Time series of observed (obs) and simulated (sim) monthly totals of daily streamflows from 1985 to 1988 for the DeHoek research catchment V1H015. Accumulated flows (accsim; accobs) are also shown.
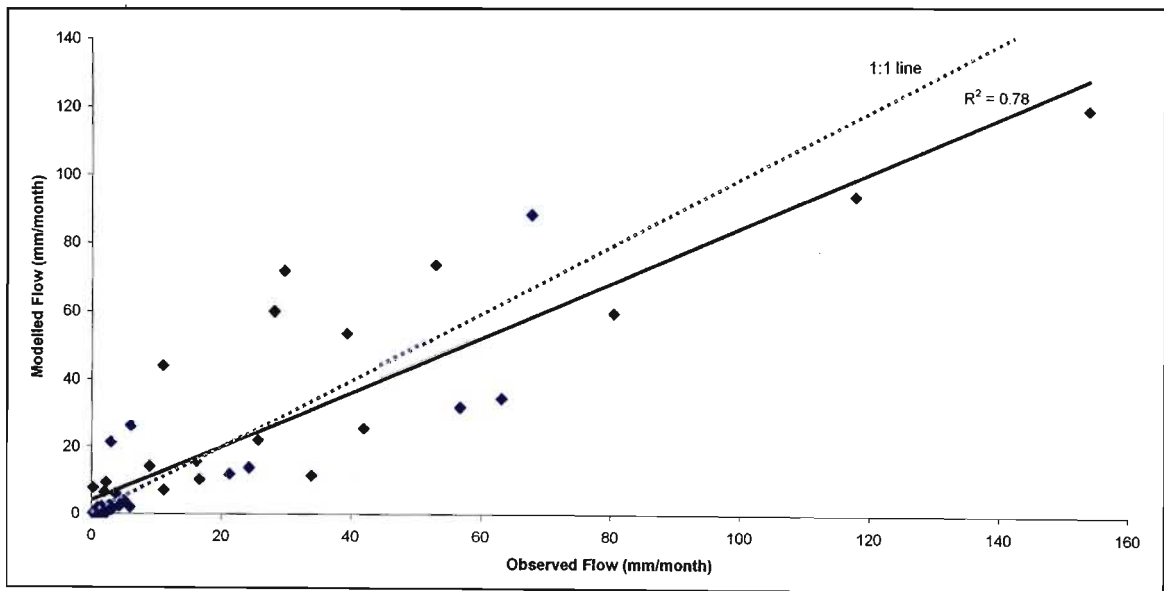
Figure 70: Scatter plot of simulated and observed monthly totals of daily streamflows for the DeHoek research catchment V1H015 from 1985 to 1988.

103
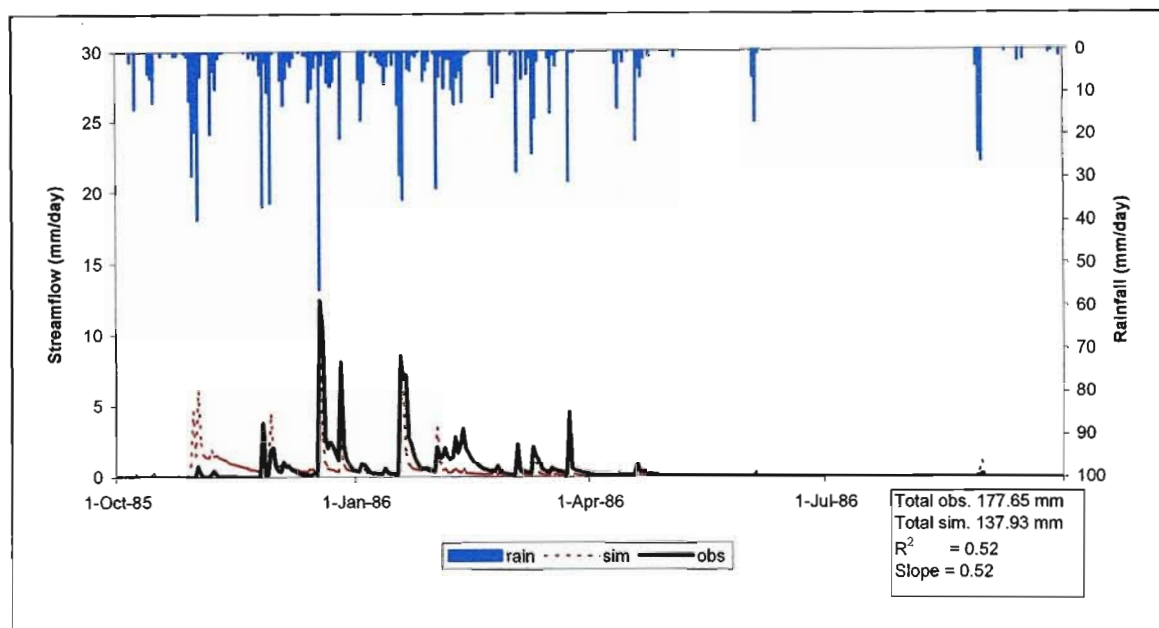
Figure 71: Time series of observed (obs) and simulated (sim) daily streamflows from October 1985 to September 1986 for the DeHoek research catchment V1H015. Summary statistics of model fit to observed data for this period are also shown.

Table 22: Statistical analysis of monthly totals of daily observed and simulated streamflows for the DeHoek research catchment V1H015 for the period 1985 to 1988.

| CONSERVATION STATISTICS	
Sum of observed values	963.60
Sum of simulated values	965.67
Mean of observed values	20.08
Mean of simulated values	20.12
% difference between means	-0.22
% difference between standard deviations	9.39
% difference between coefficients of variation	9.59
% difference between skewness coefficients	27.83
REGRESSION STATISTICS	
Coefficient of determination (r)	0.78
Slope of the regression line	0.80
Y intercept of the regression line	4.05
Coefficient of efficiency	0.73
Coefficient of agreement	0.94
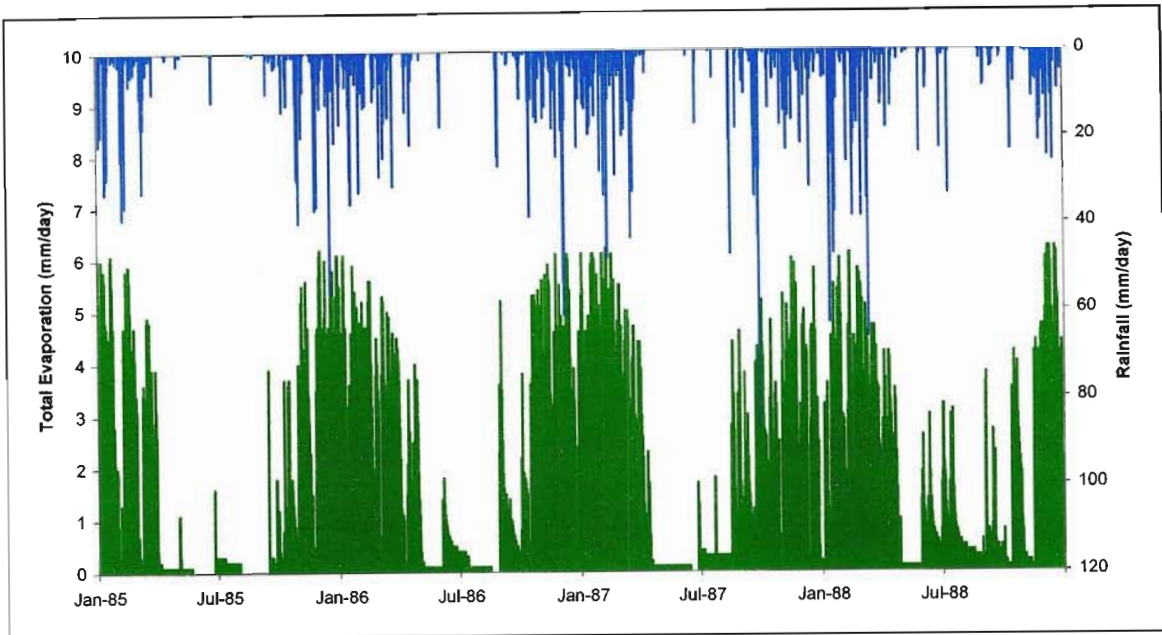
Figure 72: Time series of simulated daily total evaporation (i.e. "actual evapotranspiration) from the *ACRU* model for the DeHoek research catchment V1H015 from 1985 to 1988.

4.2.9 Witklip V

The *ACRU* model input parameters for Witklip V are tabulated in Appendix 1, pages 154 to 159. Salient features of the catchment and model parameter values for QFRESP and COFRU are shown in Table 23.

Table 23: Summary table of catchment descriptors for Witklip V.

Latitude (degrees minutes)	25 14
Longitude (degrees minutes)	30 53
Rainfall Seasonality	Early Summer
MAP (mm)	1100
Area (km²)	1.08
Altitude Range (m)	1000 – 1340
Dominant Land Use(s)	Forest
Operational or Research	Research
Averaged Depth of Soil Profile (m)	0.99
QFRESP (optimised manually)	0.11
COFRU (optimised manually)	0.012

Results show highly acceptable trends between observed and simulated streamflows for Witkip V. Differences in accumulated flows over the entire simulation, resulted

from a single event (cf. Figure 73), in January 1978. High correlation exists between simulated and observed streamflows, with a correlation coefficient of 0.9. Daily streamflows are over-simulated (Figure 75), possibly from the soil profile not being defined deep enough.

Figure 73: Time series of observed (obs) and simulated (sim) monthly totals of daily streamflows from 1981 to 1986 for Witklip V. Accumulated flows (accsim; accobs) are also shown.

Figure 74: Scatter plot of simulated and observed monthly totals of daily streamflows for Witklip V from 1975 to 1983.
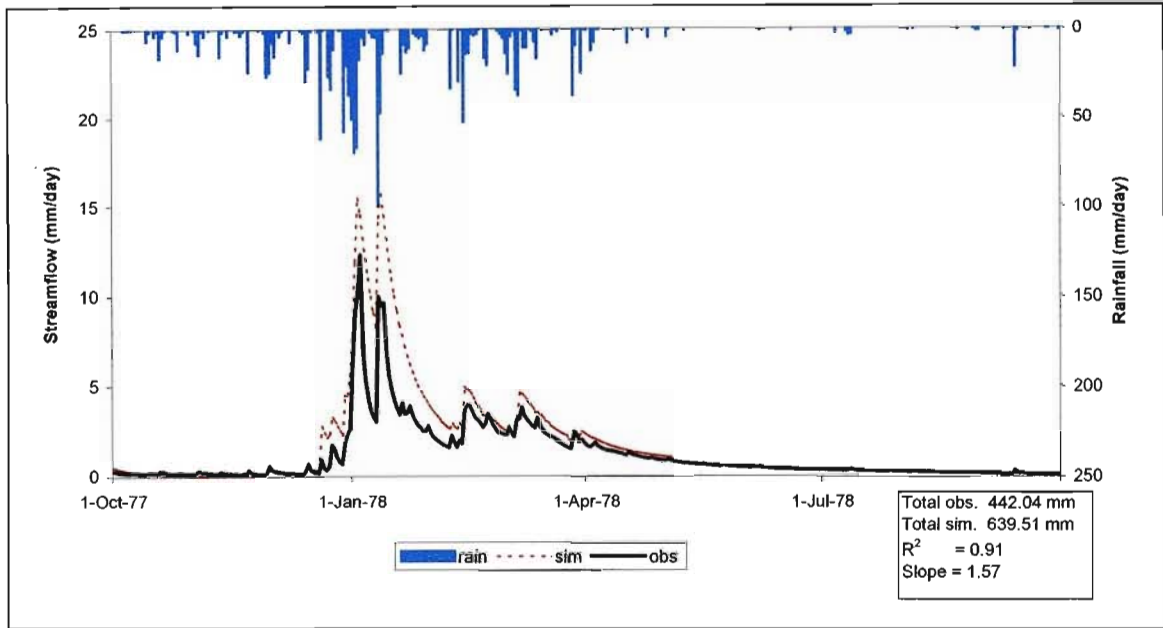
Figure 75: Time series of observed (obs) and simulated (sim) daily streamflows from October 1977 to September 1978 for Witklip V. Summary statistics of model fit to observed data for this period are also shown.

Regression statistics of monthly totals of daily observed and simulated streamflows are excellent (cf. Table 24), having a high coefficient of agreement of 0.98. Average daily evaporation totals of 6 mm/day are simulated by the model during the summer months, which is expected from a predominantly forested catchment (Figure 76).

Table 24: Statistical analysis of monthly totals of daily observed and simulated streamflows for Witklip V from 1975 to 1981.

CONSERVATION STATISTICS	
Sum of observed values	2284.93
Sum of simulated values	2560.01
Mean of observed values	21.16
Mean of simulated values	23.70
% difference between means	-12.04
% difference between standard deviations	-50.07
% difference between coefficients of variation	-33.94
% difference between skewness coefficients	-33.22
REGRESSION STATISTICS	
Coefficient of determination (r)	0.91
Slope of the regression line	1.43
Y intercept of the regression line	-6.64
Coefficient of efficiency	0.83
Coefficient of agreement	0.98
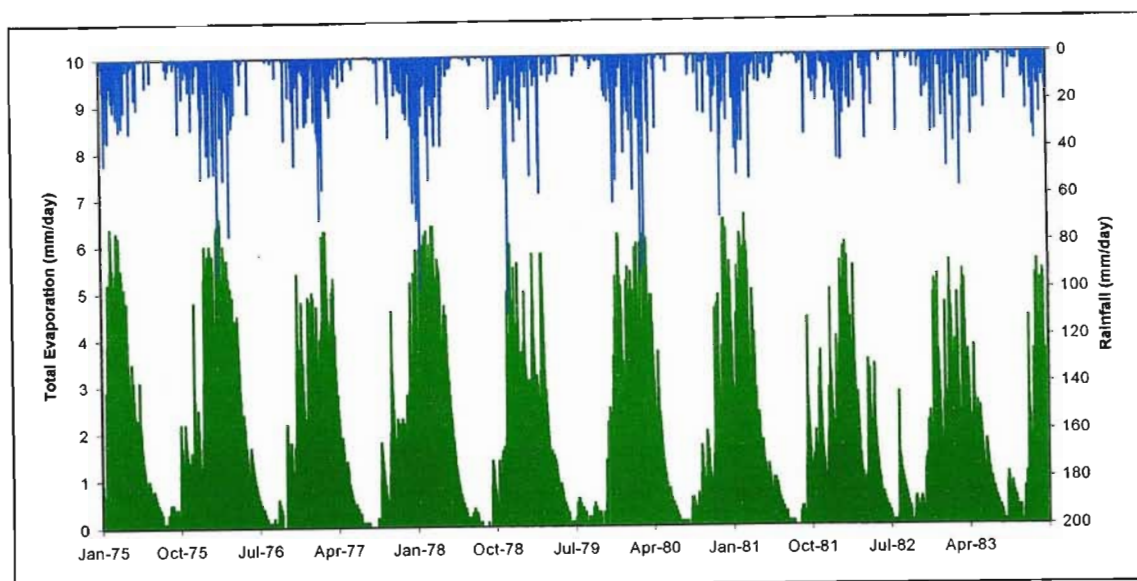
Figure 76: Time series of simulated daily total evaporation (i.e. "actual evapotranspiration") from the *ACRU* model for the Witklip V catchment from 1975 to 1983.

4.2.10 Treurrivier

The *ACRU* model input parameters for Treurrivier are tabulated in Appendix 1, pages 154 to 159. Salient features of the catchment and model parameter values for QFRESP and COFRU are shown in Table 25. QFRESP and COFRU model parameters were optimised using PEST.

Table 25: Summary table of catchment descriptors for Treurrivier.

Latitude (degrees minutes)	24 41
Longitude (degrees minutes)	30 48
Rainfall Seasonality	Mid Summer
MAP (mm)	792
Area (km²)	92
Altitude Range (m)	1200 – 1835
Dominant Land Use(s)	Unimproved grassland and forest plantation
Operational or Research	Operational
Averaged Depth of Soil Profile (m)	0.667
QFRESP (optimised with PEST)	0.19
COFRU (optimised with PEST)	0.014

The results for the Treurrivier catchment illustrate excellent relationships between observed and simulated streamflows (Figure 77), with a good correlation trends

shown in Figure 78. Figure 79 shows the typical over-simulation by the model of the first relatively high rainfall event of the rainy season, however baseflow recessions are simulated well by the model. The results for theTreurrivier catchment are borne out by the excellent statistics of fit (R^2 = 0.95), shown in in Table 26.
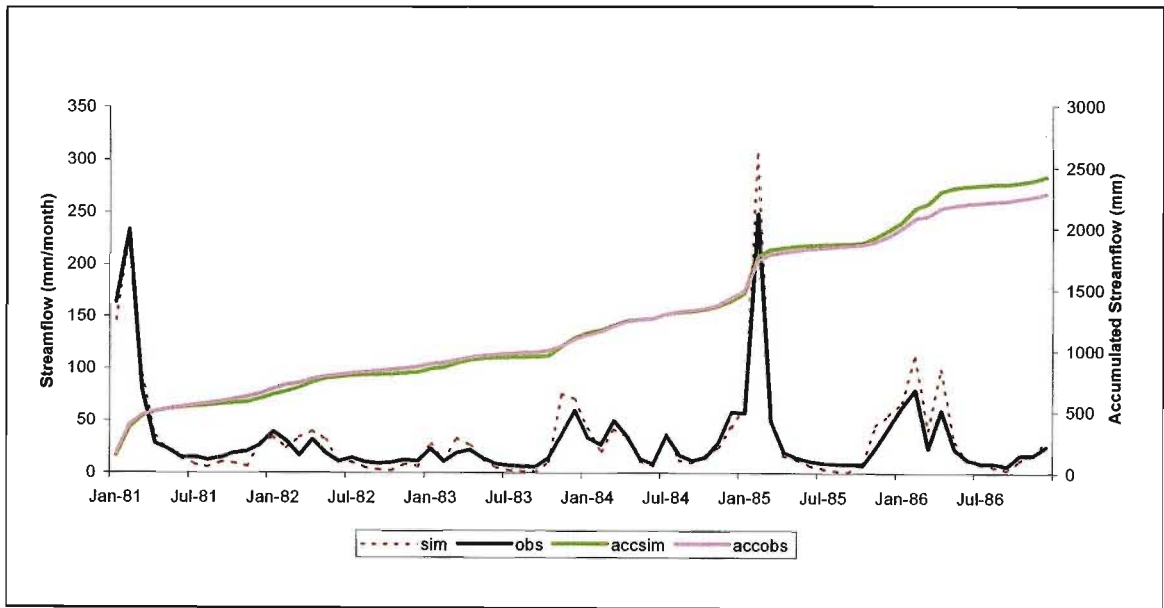
Figure 77: Time series of observed (obs) and simulated (sim) monthly totals of daily streamflows from 1981 to 1986 for Treurrivier. Accumulated flows (accsim; accobs) are also shown.
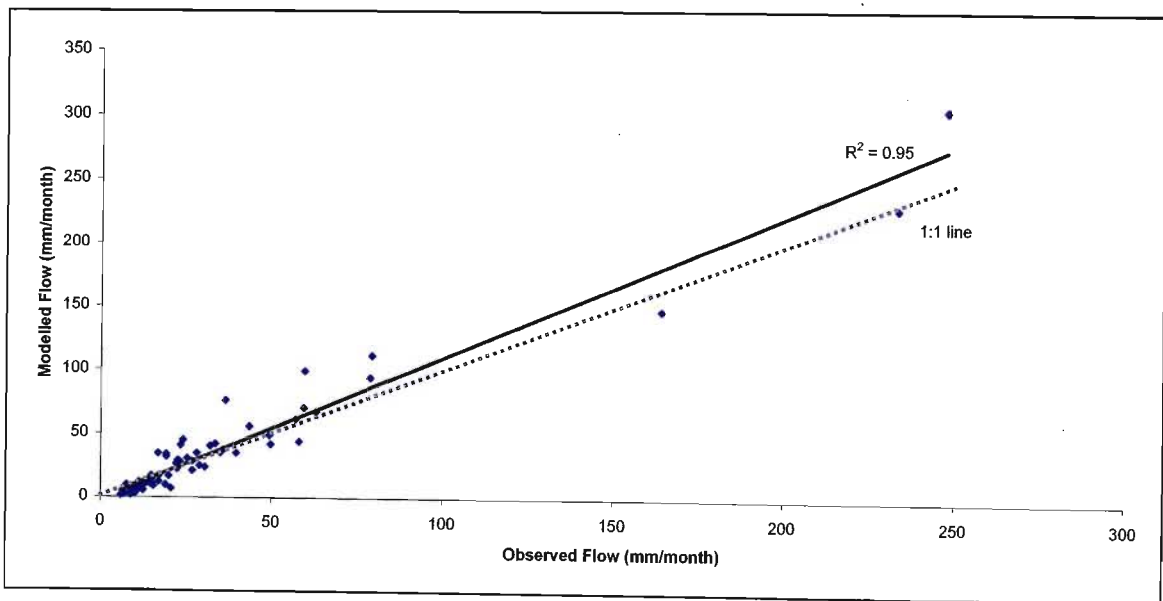
Figure 78: Scatter plot of simulated and observed monthly totals of daily streamflows for Treurrivier from 1981 to 1986.
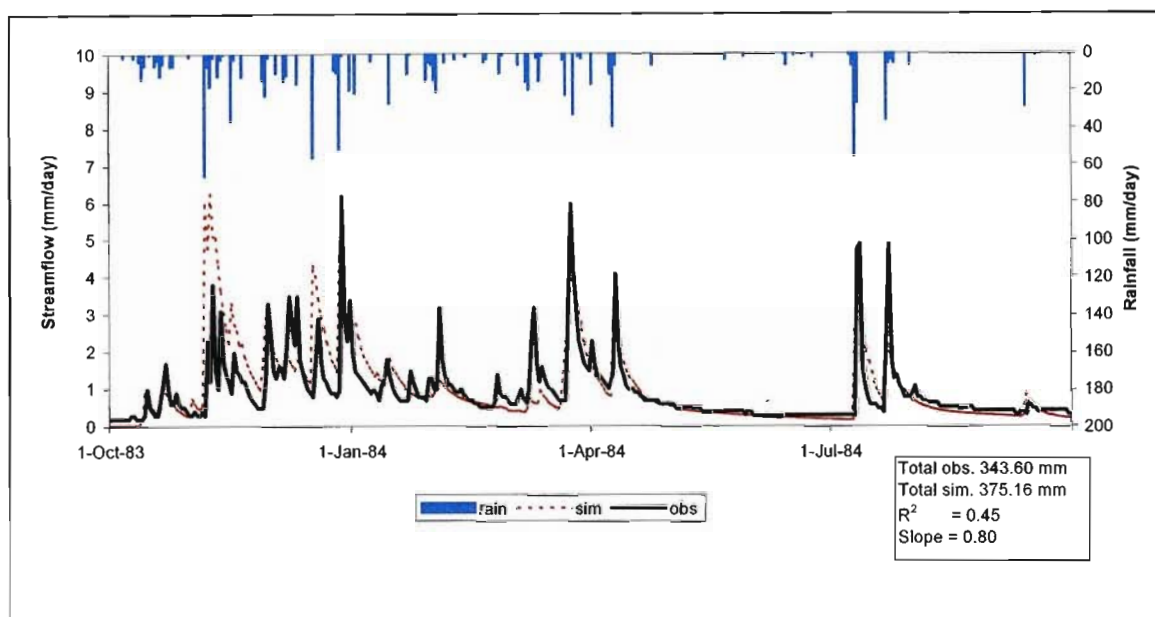
Figure 79: Time series of observed (obs) and simulated (sim) daily streamflows from October 1983 to September 1984 for Treurrivier. Summary statistics of model fit to observed data for this period are also shown.

Table 26: Statistical analysis of monthly totals of daily observed and simulated streamflows for Treurrivier from 1981 to 1986.

CONSERVATION STATISTICS	
Sum of observed values	2284.90
Sum of simulated values	2422.37
Mean of observed values	31.74
Mean of simulated values	33.64
% difference between means	-6.04
% difference between standard deviations	-14.11
% difference between coefficients of variation	-7.63
% difference between skewness coefficients	4.65
REGRESSION STATISTICS	
Coefficient of determination (r)	0.95
Slope of the regression line	1.11
Y intercept of the regression line	-1.56
Coefficient of efficiency	0.93
Coefficient of agreement	0.99

Daily evaporation totals simulated by the model indicate an average 6 mm/day during the summer months, which is expected from a catchment which is predominantly covered with unimproved grassland and forest plantations.
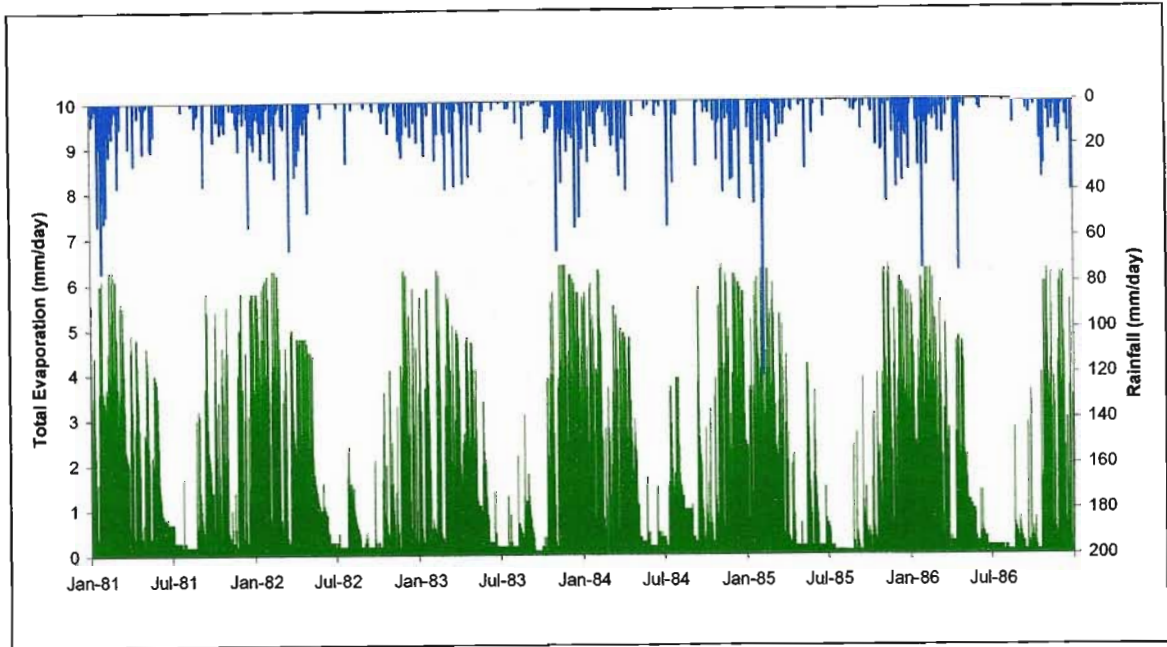
Figure 80: Time series of simulated daily total evaporation (i.e. "actual evapotranspiration") from the *ACRU* model for the Treurrivier catchment from 1981 to 1986.

4.2.11 Beestekraalspruit

The *ACRU* model input parameters for Beestekraalspruit are tabulated in Appendix 1, pages 160 to 163. Salient features of the catchment and model parameter values for QFRESP and COFRU are shown in Table 27. QFRESP and COFRU model parameters were optimised using PEST.

Table 27: Summary table of catchment descriptors for Beestekraalspruit.

Latitude (degrees minutes)	25 17
Longitude (degrees minutes)	30 34
Rainfall Seasonality	Early Summer
MAP (mm)	977
Area (km^2)	14
Altitude Range (m)	981 – 2190
Dominant Land Use(s)	Grassland
Operational or Research	Operational
Averaged Depth of Soil Profile (m)	0.3
QFRESP (optimised with PEST)	0.010
COFRU (optimised with PEST)	0.247

Trends between observed and simulated streamflows for Beestekraalspruit are satisfactory, with large deviations between accumulated flows, shown in Figure 81, arising from large differences between observed and simulated flows in the first year of the simulation, possibly due to a large baseflow store from the previous season. Streamflows on this catchment are predominantly under-simulated, which may have been caused by rainfall values not being representative of the entire catchment. However, baseflow recessions are simulated well through the 1973 and 1974 hydrological years. An acceptable correlation coefficient of 0.76 was calculated from the regression of simulated streamflows against observed monthly streamflows, shown in Figure 82 and and associated statistics in Table 28. Figure 83 shows that the model does not mimic the flashy responses of daily observed streamflows from the Beestekraalspruit catchment satisfactorily. However, the "steps" in the observed baseflow recessions indicate measurement errors or poor digitizing of flow recorder charts. Daily evaporation totals simulated by the model are in accordance with the rainfall patterns over the simulation period, and an average of 5 mm/day is expected during the summer months (Figure 84).
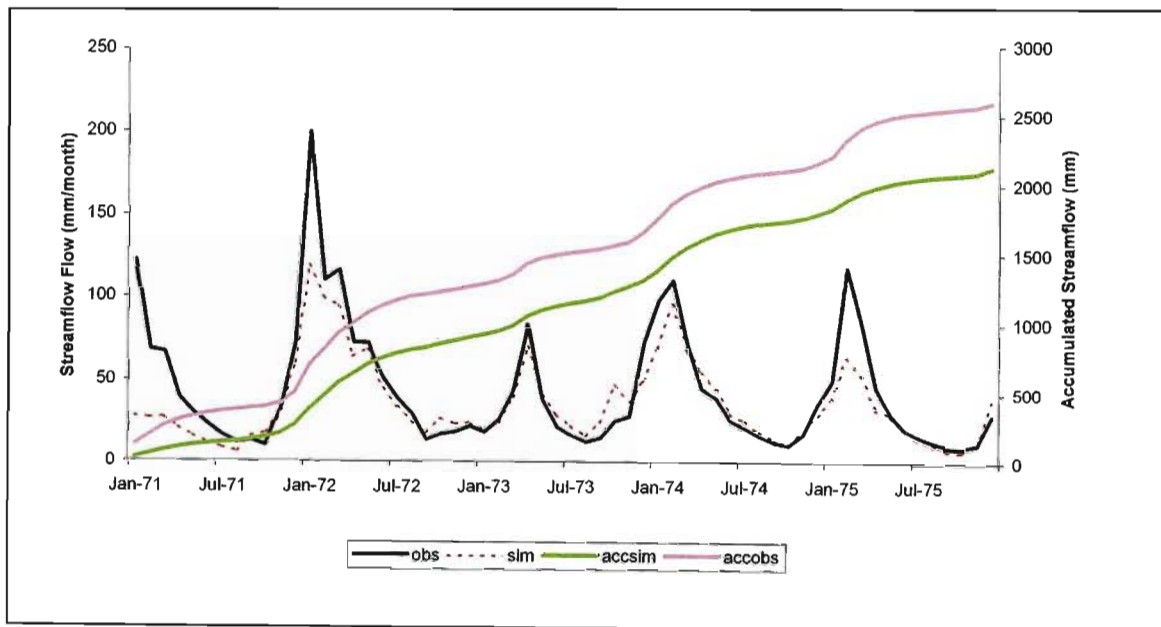
Figure 81: Time series of observed (obs) and simulated (sim) monthly totals of daily streamflows from 1971 to 1975 for Beestekraalspruit. Accumulated flows (accsim; accobs) are also shown.
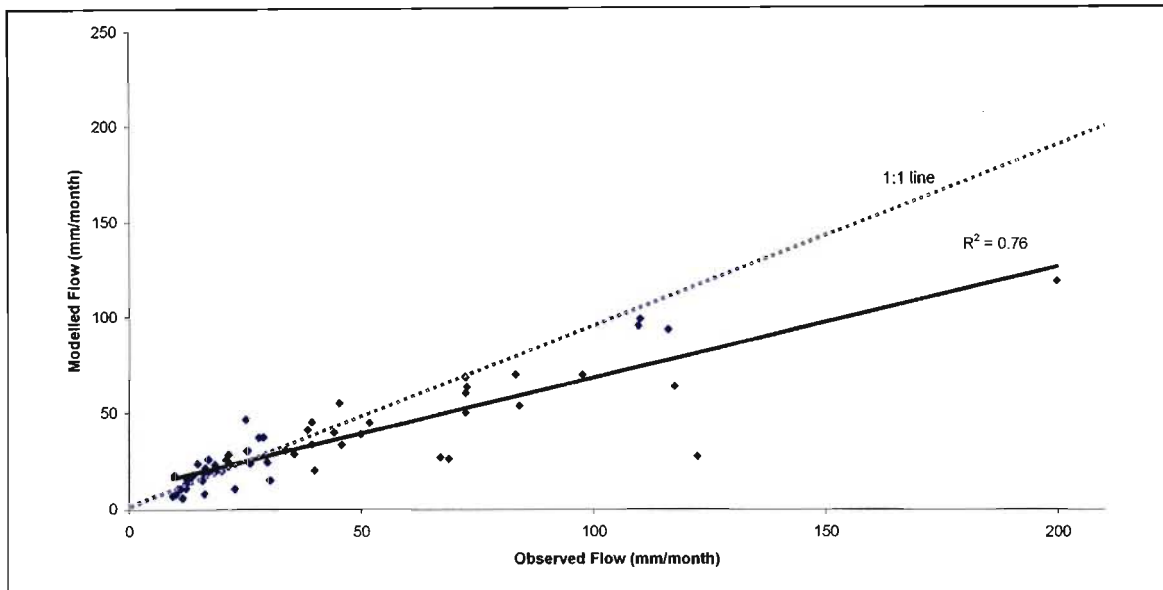
**Figure 82:** Scatter plot of simulated and observed monthly totals of daily streamflows for Beestekraalspruit from 1971 to 1975.
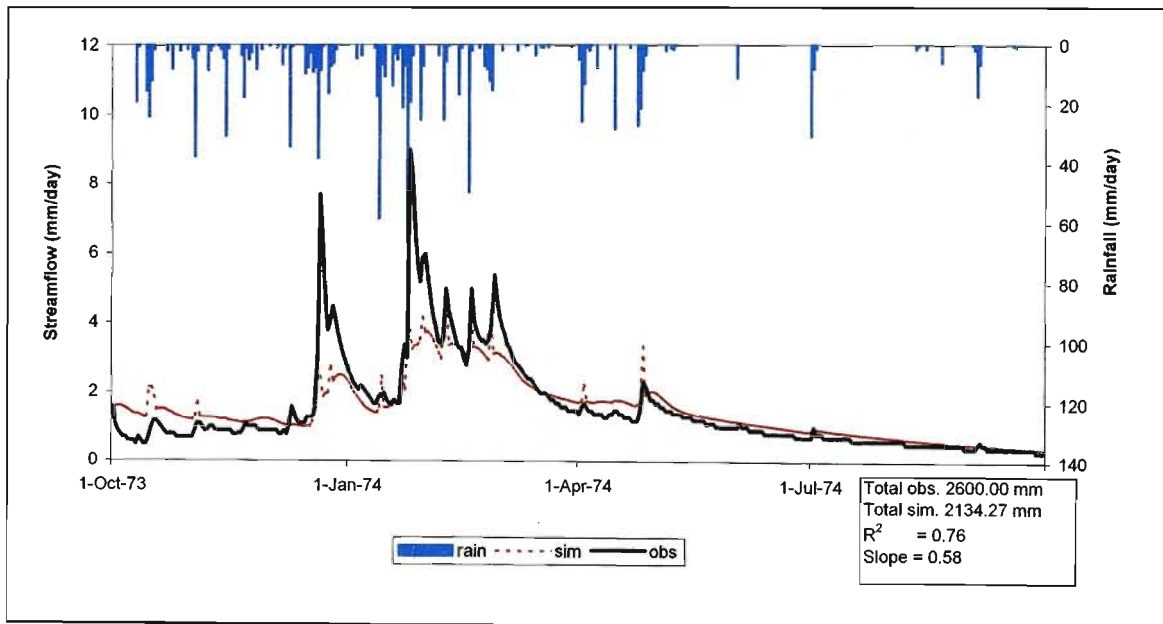
Figure 83: Time series of observed (obs) and simulated (sim) daily streamflows from October 1973 to September 1974 for Beestekraalspruit. Summary statistics of model fit to observed data for this period are also shown.

113

Table 28: Statistical analysis of monthly totals of daily observed and simulated streamflows for Beestekraalspruit from 1971 to 1975.

CONSERVATION STATISTICS	
Sum of observed values	2600.00
Sum of simulated values	2134.27
Mean of observed values	43.33
Mean of simulated values	35.57
% difference between means	17.91
% difference between standard deviations	33.58
% difference between coefficients of variation	19.08
% difference between skewness coefficients	22.87
	REGRESSION STATISTICS
Coefficient of determination (r)	0.76
Slope of the regression line	0.58
Y intercept of the regression line	10.52
Coefficient of efficiency	0.26
Coefficient of agreement	0.93
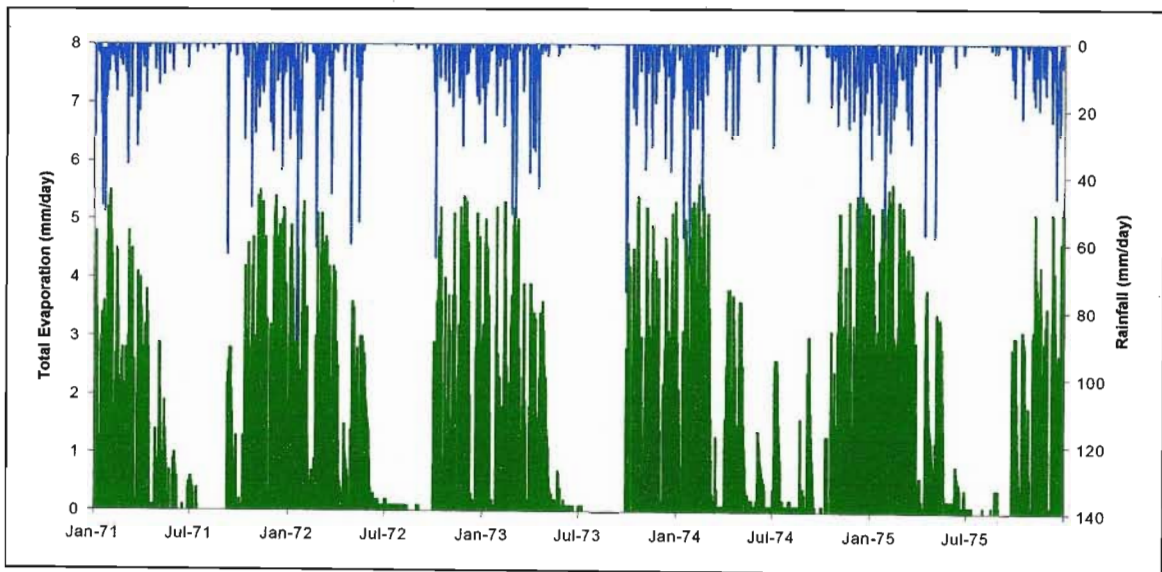
Figure 84: Time series of daily total evaporation (i.e. "actual evapotranspiration") from the *ACRU* model for Beestekraalspruit from 1971 to 1975.

4.2.12 Westfalia B

The *ACRU* model input parameters for Westfalia B are tabulated in Appendix 1, pages 160 to 163. Salient features of the catchment and model parameter values for QFRESP and COFRU are shown in Table 29.

114

Table 29:   Summary table of catchment descriptors for Westfalia B.

Latitude (degrees minutes)	23 43
Longitude (degrees minutes)	30 04
Rainfall Seasonality	Mid Summer
MAP (mm)	1253
Area (km^2)	0.33
Altitude Range (m)	1140 – 1420
Dominant Land Use(s)	Indigenous Forest
Operational or Research	Research
Averaged Depth of Soil Profile (m)	1.10
QFRESP (optimised manually)	0.28
COFRU (optimised manually)	0.007
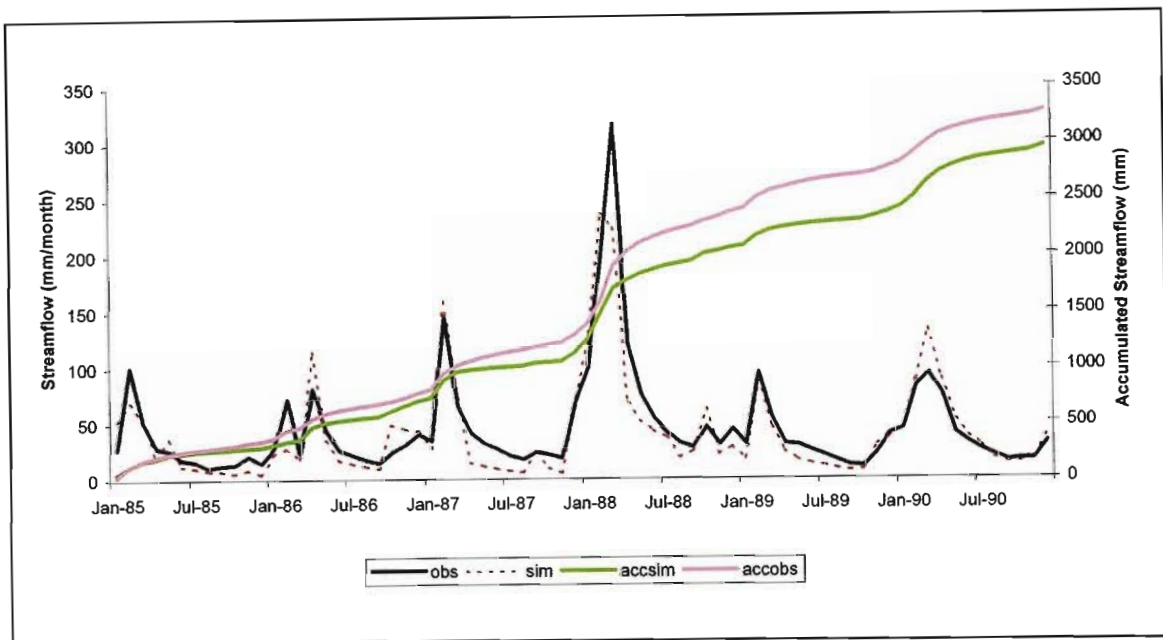
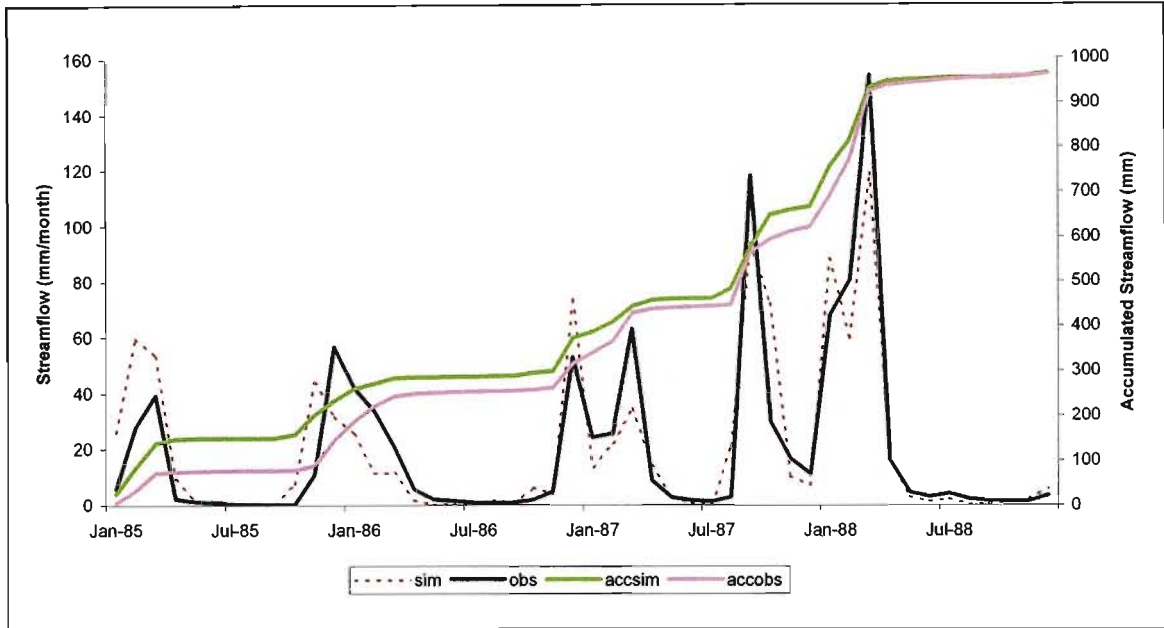**Figure 85:**   Time series of observed (obs) and simulated (sim) monthly totals of daily streamflows from 1985 to 1990 for Westfalia B. Accumulated flows (accsim; accobs) are also shown.

Streamflows for Westfalia B are under-simulated by the model, as shown by the accumulated flows in Figure 85. A distinct under-simulation of low flows occurs in June 1987, which suggests that there may be problems with the rainfall records for this period. The possibility of leaks across the catchment boundary of Westfalia B has long been suspected (Dye, 2001 pers com), potentially affecting the streamflow records from this catchment. However, bearing in mind the small catchment area (0.33 km^2) of Westfalia B, streamflows are simulated within acceptable limits for the period 1985 to 1990, and is substantiated by the high correlation shown in Figure 86

(R^2 = 0.84), and the statistics in Table 30. Excellent model fit between observed and simulated daily streamflows from October 1985 to September 1986 are illustrated in Figure 87. An average daily evaporation total of 4.5 mm/day is from from the grassland catchment during the higher rainfall periods (Figure 88).
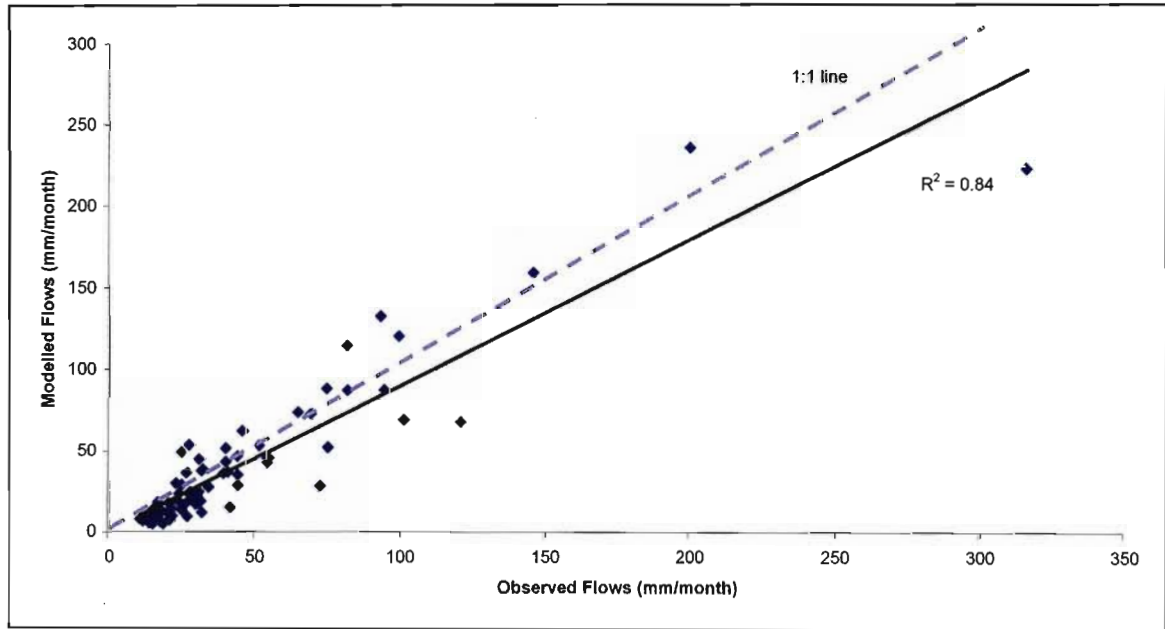
Figure 86: Scatter plot of simulated and observed monthly totals of daily streamflows for Westfalia B from 1985 to 1990.
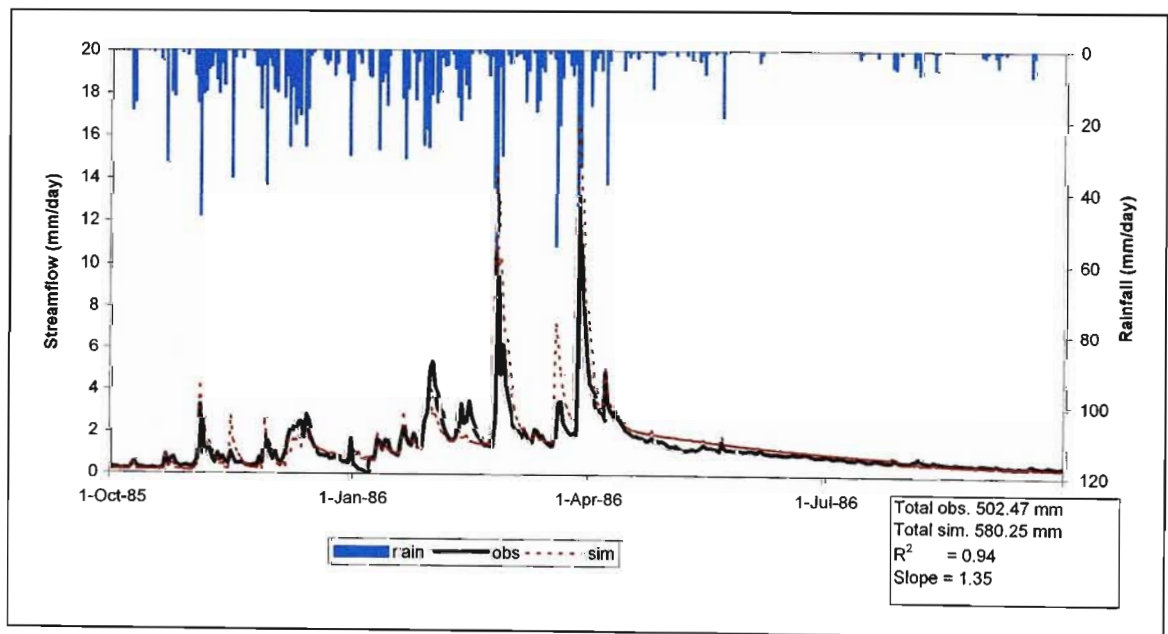
Figure 87: Time series of observed (obs) and simulated (sim) daily streamflows from October 1985 to September 1986 for Westfalia B. Summary statistics of model fit to observed data for this period are also shown.

Table 30: Statistical analysis of monthly totals of daily observed and simulated streamflows for Westfalia B from 1985 to 1990.

| CONSERVATION STATISTICS	
Sum of observed values	3265.68
Sum of simulated values	2953.20
Mean of observed values	45.36
Mean of simulated values	41.02
% difference between means	9.57
% difference between standard deviations	2.57
% difference between coefficients of variation	-7.74
% difference between skewness coefficients	28.87
REGRESSION STATISTICS	
Coefficient of determination (r)	0.84
Slope of the regression line	0.90
Y intercept of the regression line	0.42
Coefficient of efficiency	0.82
Coefficient of agreement	0.96
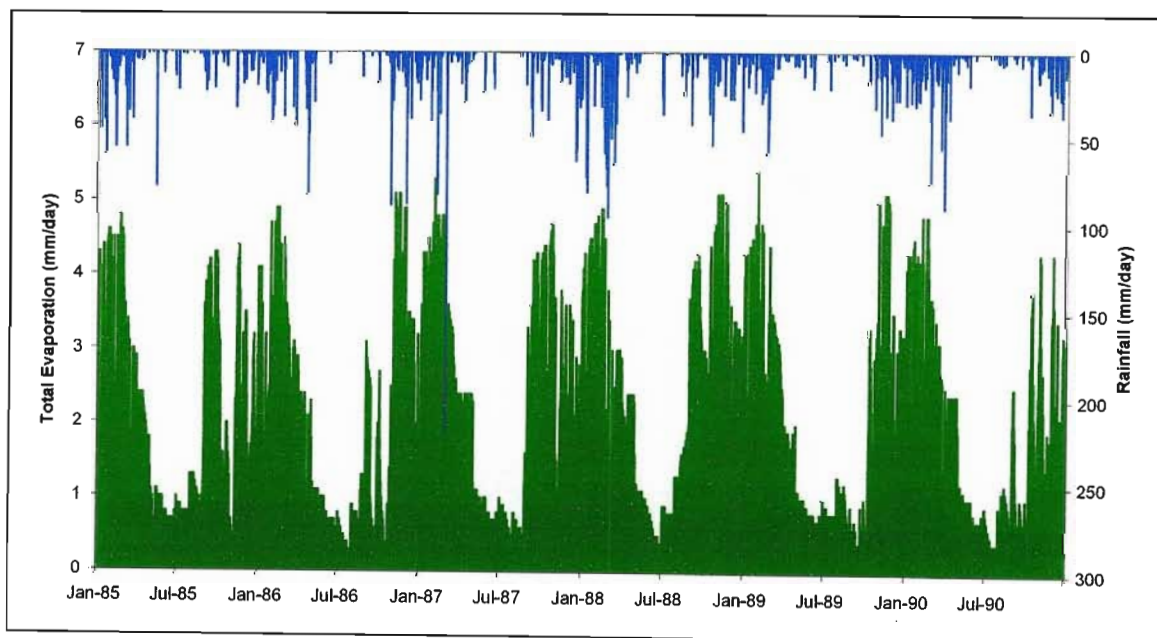
Figure 88: Time series of simulated daily total evaporation (i.e. "actual evapotranspiration") from the *ACRU* model for Westfalia B from 1985 to 1990.

4.2.13 Groot-Nylrivier

The *ACRU* model input parameters for Groot-Nylrivier are tabulated in Appendix 1, pages 160 to 163. Salient features of the catchment and model parameter values for

117

QFRESP and COFRU are shown in Table 31. QFRESP and COFRU model parameters were optimised using PEST.

Table 31: Summary table of catchment descriptors for Groot-Nylrivier.

Latitude (degrees minutes)	24 45
Longitude (degrees minutes)	28 44
Rainfall Seasonality	Mid Summer
MAP (mm)	654
Area (km^2)	73
Altitude Range (m)	1213 – 1508
Dominant Land Use(s)	Thicket and Bushland
Operational or Research	Operational
Averaged Depth of Soil Profile (m)	0.526
QFRESP (optimised with PEST)	0.050
COFRU (optimised with PEST)	0.004

Observed streamflows are over-simulated for the Groot-Nylrivier catchment (Figure 89), probably owing to the rainfall values used from two gauges located in this area being unrepresentative of the entire catchment rainfall. The poorly simulated streamflows events during 1972 and 1977 are also possibly a result of problems with the rainfall data sets used. Figure 90 shows an acceptable correlation along the 1:1 line, with a correlation coefficient of 0.76.
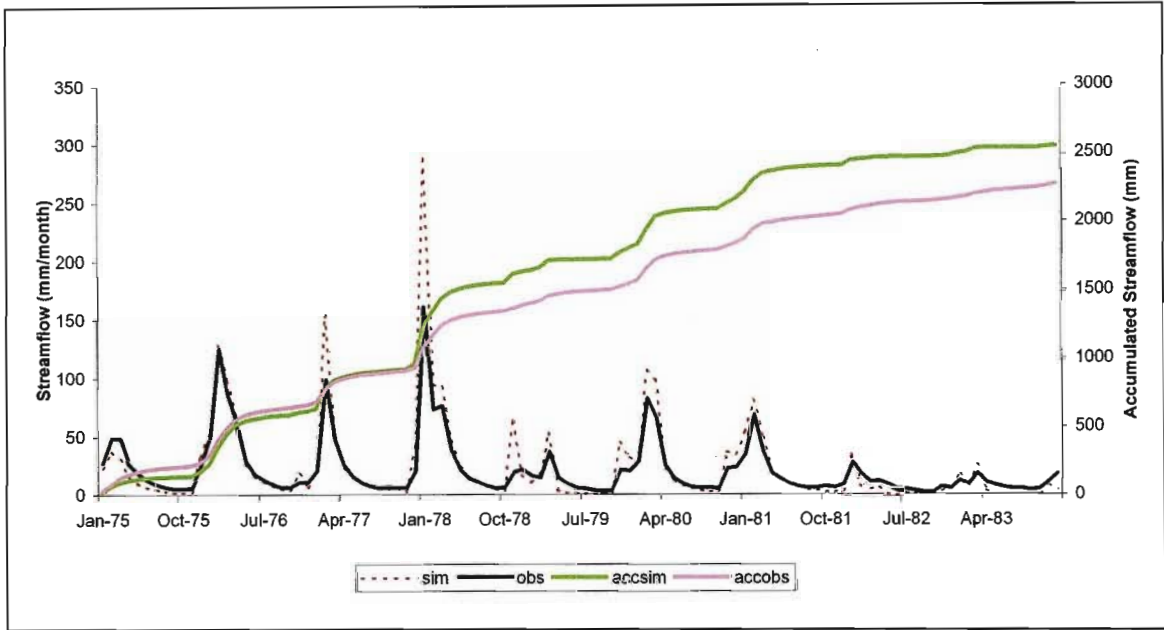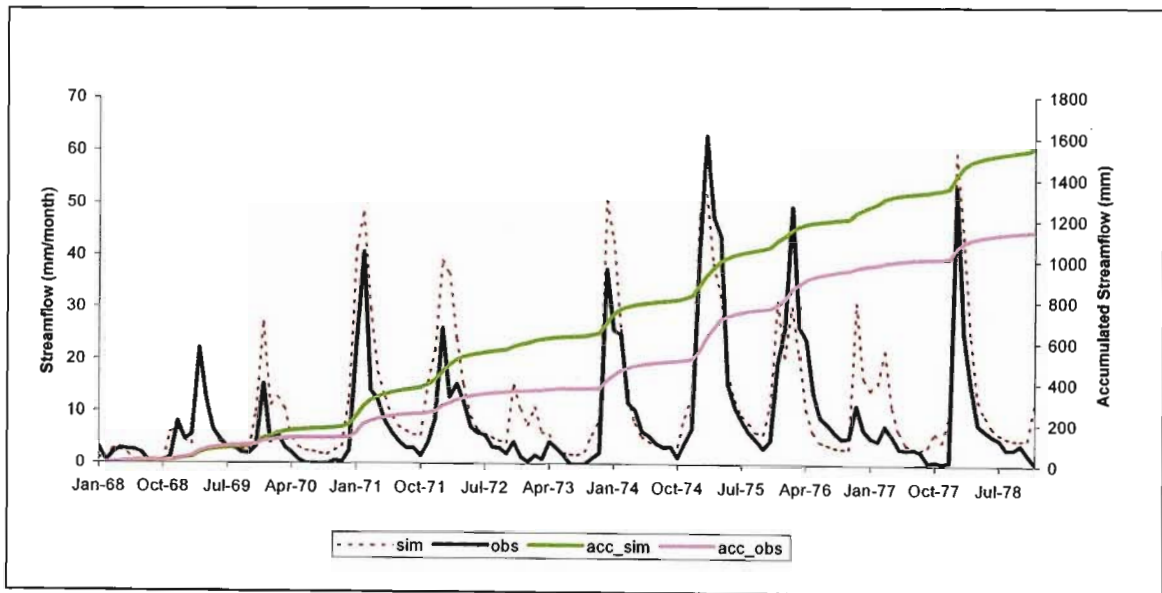

Figure 89: Time series of observed (obs) and simulated (sim) monthly totals of daily streamflows from 1968 to 1978 for Groot-Nylrivier. Accumulated flows (accsim; accobs) are also shown.
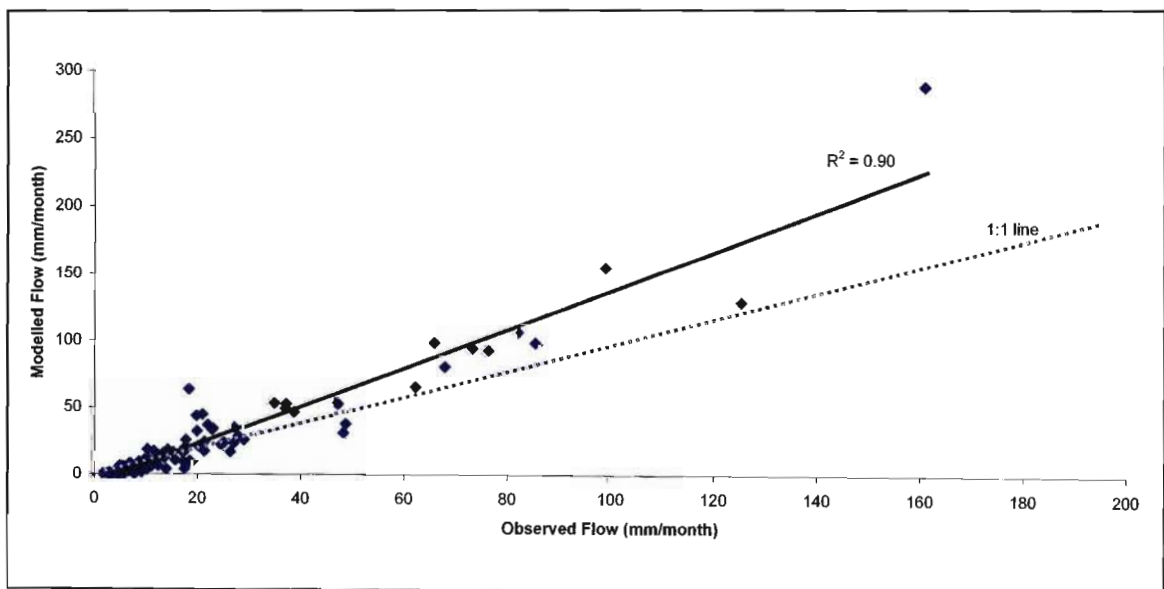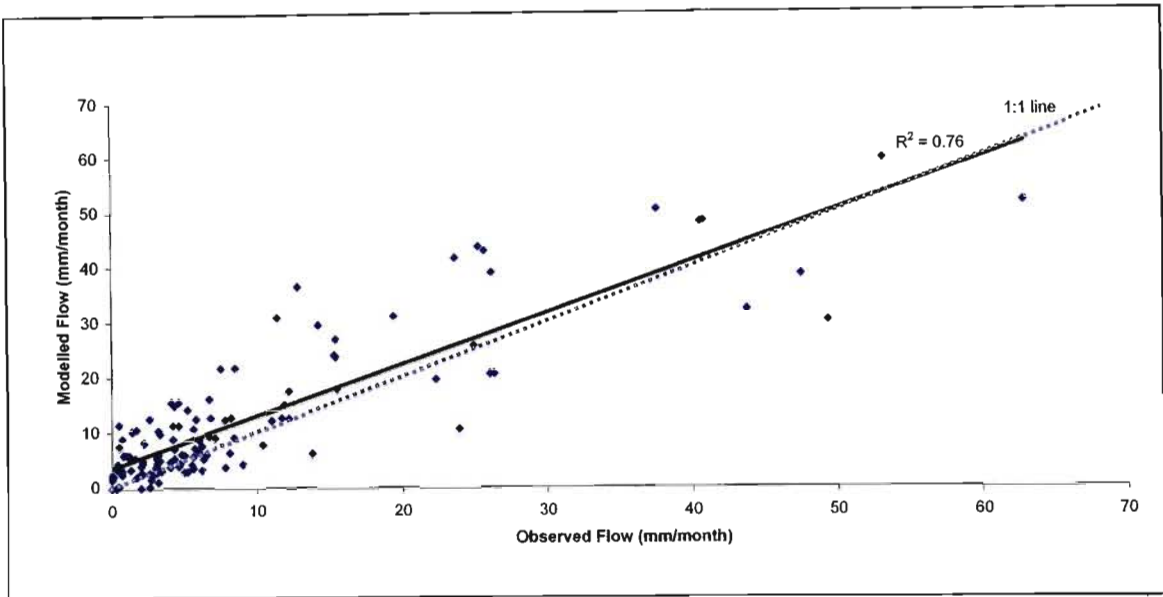
**Figure 90:** Scatter plot of simulated and observed monthly totals of daily streamflows for Groot-Nylrivier from 1968 to 1978.

Daily streamflows shown in Figure 91, indicate that observed stormflow peaks are not simulated well, however the "steppy" responses in the observed data set towards the end of the season is evidence of measurement errors or poor digitizng. Statistics calculated on monthly totals of daily observed and simulated streamflows (Table 32) show a reasonable difference between standard deviations of 6.84%, and a high coefficient of agreement of 0.93. Daily evaporation totals simulated by the model are very seasonal and rainfall dependent, as shown in Figure 92. Approximately 7.5 mm/day is estimated to evaporate during the rainfall periods from the predominantly thicket and bushland covered catchment.
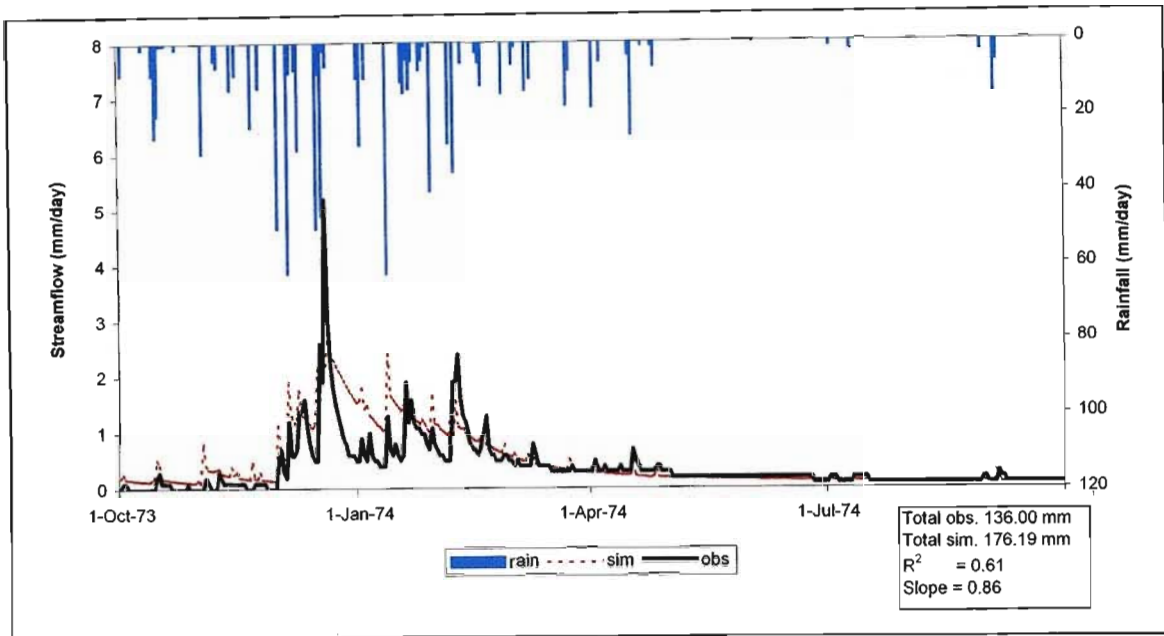
Figure 91: Time series of observed (obs) and simulated (sim) daily streamflows from October 1973 to September 1974 for Groot-Nylrivier. Summary statistics of model fit to observed data for this period are also shown.

Table 32: Statistical analysis of monthly totals of daily observed and simulated streamflows for Groot-Nylrivier from 1968 to 1978.

CONSERVATION STATISTICS	
Sum of observed values	1146.90
Sum of simulated values	1553.53
Mean of observed values	8.70
Mean of simulated values	11.77
% difference between means	-35.46
% difference between standard deviations	-6.84
% difference between coefficients of variation	21.13
% difference between skewness coefficients	25.22
REGRESSION STATISTICS	
Coefficient of determination (r)	0.76
Slope of the regression line	0.93
Y intercept of the regression line	3.67
Coefficient of efficiency	0.70
Coefficient of agreement	0.93
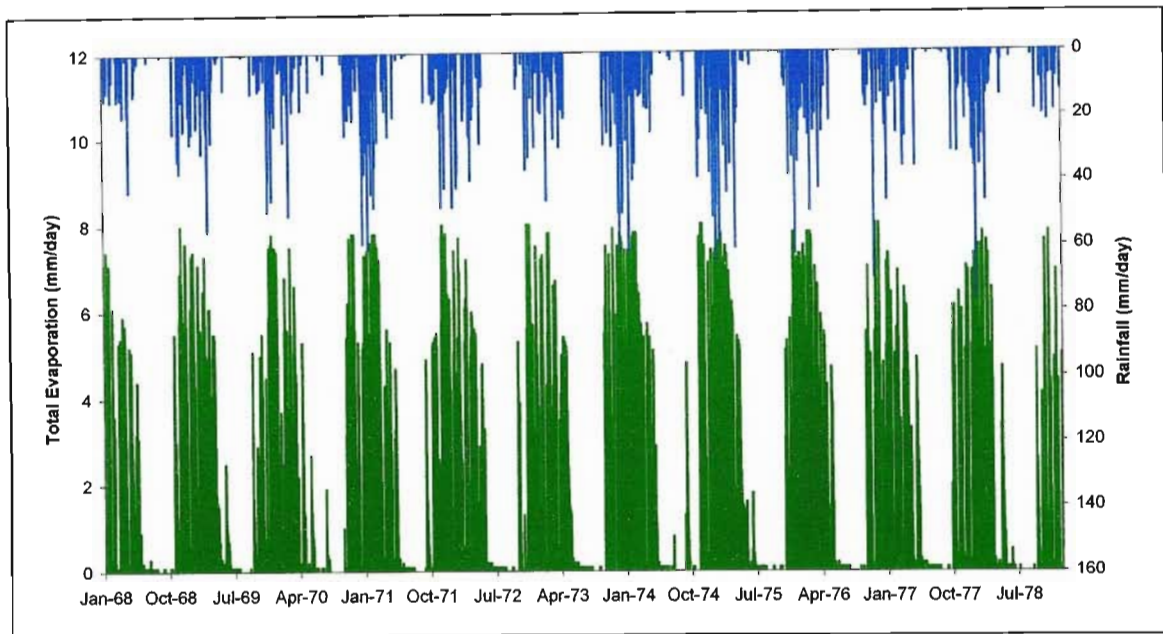
Figure 92: Time series of simulated daily total evaporation (i.e. "actual evapotranspiration") from the *ACRU* model for the Groot-Nylrivier catchment from 1968 to 1978.

The simulation results of the South African catchments are best summarised and compared by referring to Table 33. A list of relevant page and figure numbers are also found in Table 33. This enables quick reference to specific *ACRU* input menus and South African catchments simulation results. The results of catchments which were found acceptable, and the *ACRU* flow parameters considered representative of the hydrological responses of catchments are also highlighted. Selected catchments were then used in the next phase of this research study described in section 4.3, which involved an investigation of relationships between catchment physical and climatic attributes and specific *ACRU* model streamflow parameters.

Table 33: Summary of the simulation results for all South African catchments used.

Catchment	DWAF Weir No.	Figure Numbers	Page reference	Appendix Page reference	Lat (dm)	Long (dm)	MAP (mm)	R^2	Slope	Intercept	Accumulated flows as % of observed flows	Comments	Flow Parameters Acceptable
Lambrechtsbos B	G2H010	41–44	80-82	149-153	33 57	18 57	1472	0.73	1.99	-11.23	69.01		
Watervalsrivier	G1H012	45-48	83-85	149-153	33 21	19 06	664	0.86	1.07	1.86	88.44		√
Dieprivier	K4H003	49-52	86-88	149-153	33 54	22 42	711	0.75	1.48	1.33	58.97		
Kruisrivier	H9H004	53-56	89-91	149-153	34 00	21 16	645					Irrigation, simulated only June to Sept each year	√
Bloukransrivier	K7H001	57-60	92-94	149-153	33 57	23 37	1003	0.84	0.99	7.11	84.74		√
Zululand	W1H016	61-64	96-98	154-159	28 50	31 46	1314	0.93	0.94	4.11	94.59		√
Cathedral Peak IV	V1H005	65-68	99-101	154-159	29 00	29 25	1400	0.94	0.88	1.28	111.13		√
DeHoek	V1H015	69-72	103-105	154-159	29 58	30 20	800	0.78	0.80	4.05	99.79		
Witklip V	X2H038	73-76	106-108	154-159	25 14	30 53	1100	0.91	1.43	-6.64	89.25		√
Treurrivier	B6H003	77-80	109-111	154-159	24 41	30 48	792	0.95	1.11	-1.56	94.32		√
Beestekraalspruit	X2H026	81-84	112-114	160-163	25 17	30 34	977	0.76	0.58	10.52	121.82		
Westfalia B	B8H022	85-88	115-117	160-163	23 43	30 04	1253	0.84	0.90	0.42	110.58		√
Groot-Nylrivier	A6H011	89-92	118-121	160-163	24 45	28 44	654	0.76	0.93	3.67	73.83		

Lat = latitude, °S

Long = longitude, °E

dm = degrees and minutes

4.3 Relationships between Streamflow Parameters and Catchment Physical and Climatic Attributes

4.3.1 Final selection of catchments

Out of the 14 catchments used in this study, streamflows from six were relatively poorly simulated, and the *ACRU* flow parameters considered too uncertain to include in the investigation of relationships between catchment attributes and streamflow parameters. The reasons for the poorer simulations are unknown, and vary from catchment to catchment, but potentially include the following:

- Errors might be present in streamflow or, especially, rainfall records.
- Rainfall values used were not representative of the entire catchment, especially in the case of larger catchments with a single raingauge.
- Catchment leakage may have occurred, especially from small catchments.
- *ACRU* does not yet simulate water extraction by deep-rooted forests from beyond the agriculturally defined subsoil horizon depth when simulating afforested catchments.
- Furthermore, *ACRU*, as a daily timestep model, is unable to adequately take into account rainfall intensity.
- High transmission losses that are hydrologically important in arid catchments are also not yet simulated with *ACRU*.
- In steep terrain catchments, rapid subsurface processes become more prominent, and therefore important to simulate accurately from a catchment. However, such processes, e.g. macropore flow, are not yet simulated by the model.
- Because different combinations of parameter values can give similar statistics of goodness-of-fit, it is difficult to arrive at an optimum set of parameter values to simulate the observed flow characteristics.

The final list of catchments used in attempting to relate key *ACRU* streamflow generating parameters to physiographic characteristics are shown in Table 34. The values QFRESP and COFRU from the simulations described in the previous section

are matched to the relevant catchment MAP, catchment area, average altitude (AVALT), drainage density (DD), mean slope (MSLOPE), profile plant available water (PPAW), maximum basin relief (MBR), the geomorphological indices representing an elongation ratio (ER) and shape factor (SF), and the average depth of the soil profile of the A and B horizons (ADSP) applicable to each catchment. The elongation ratio was calculated as a ratio of the main channel length to the catchment area. The shape factor used is a function of the length of the main channel and the distance along the main channel from the catchment outlet to a point on the main channel in the approximate centre of the catchment. The physical and climatic characteristics selected above were highlited from the comprehensive review of past research studies. The following sections of this chapter included two phases, namely scatter plots, and the regression analysis of *ACRU* model parameters and catchment physical and climatic attributes. Only the strongest trends identified from the scatter plots of *ACRU* model parameters QFRESP and COFRU and catchment physical and climatic attributes will be discussed in the next sections.

Table 34: Summary of catchment physical and climatic attributes used in the association exercise. The *ACRU* streamflow parameters tested are also shown.

No.	Name	QFRESP	COFRU	MAP (mm)	Area (km²)	Altitude Range (m)	Drainage Density (km/km²)	Mean Catchment Slope	Average Altitude (m)	Maximum Basin Relief (m)	Elongation Ratio	Shape Factor	Profile Plant Available Water (mm)	Average Depth of Soil Profile (m)
1	Cathedral Peak IV (V1H005)	0.06	0.018	1400	0.95	1845-2226	2.50	20.30	2000	381	0.93	0.75	102.60	0.80
2	Witklip V (X2H038)	0.11	0.012	1100	1.08	1000-1340	2.20	24.70	1179	340	2.55	1.53	106.67	0.99
3	Zululand (W1H016)	0.40	0.022	1314	3.32	205-323	3.37	2.93	242	118	0.96	1.62	33.45	0.35
4	Watervalsrivier (G1H012)	0.20	0.035	608	36.00	120-1086	1.47	16.88	243	966	0.34	3.33	31.08	0.48
5	Treurrivier (B6H003)	0.19	0.014	736	92.00	1200-1835	1.07	11.18	1455	635	0.27	5.15	51.84	0.67
6	Kruisrivier (H9H004)	0.35	0.038	645	50.00	400-1325	1.06	20.53	741	925	0.32	3.93	21.30	0.25
7	Westfalia B (B8H022)	0.28	0.007	1253	0.33	1140-1420	3.03	15.75	1250	280	4.55	1.06	130.84	1.10
8	Bloukransrivier (K7H001)	0.30	0.018	1003	57.00	240-1676	1.24	23.46	554	1436	0.33	4.56	35.34	0.53

4.3.2 Relationships between QFRESP and catchment physical and climatic variables

In the *ACRU* model the parameter QFRESP determines the fraction of the total stormflow that will run off from the catchment/subcatchment on the same day as the rainfall event. In small catchments of the size range selected in this study, a high QFRESP (tending towards unity) is typical of steep catchments, where the rapid arrival of surface and near surface water is the dominant hydrological process. This parameter is hypothesised to reduce as catchment size increases, or soils become sandier and the time for quickflow to exit the catchment lengthens.

Figure 93 shows no clear relationship between QFRESP and catchment area, but this may be attributed to the relatively small sample size of the catchments also chosen for this study. There is a high degree of variation in QFRESP in the very smaller catchments with areas < 4km^2.
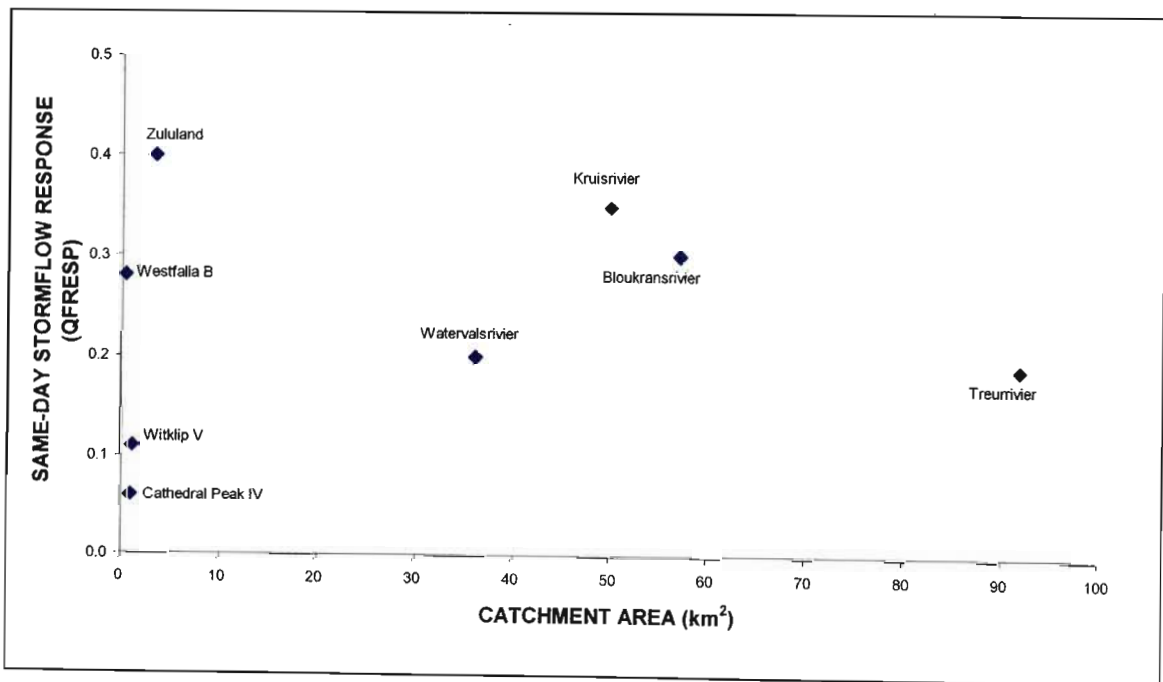
Figure 93: The association between the same day stormflow response fraction, QFRESP, and catchment area.

The highest value is associated with the Zululand catchment, where coarse-textured soils and steep slopes permit very rapid movement of subsoil water towards the

stream channel. Hydrographs from this region typically show very quick, "flashy" response to rainfall, i.e. stormflow peaks are high and recede very rapidly. Hope and Mulder (1979) report very rapid stormflow push-through mechanisms, based on experiments conducted in this catchment. The lowest optimised QFRESP is associated with Cathedral Peak IV. Catchments in this area are characterised by very deep subsoils that permit high water storage capacity (Everson et al., 1998). Streamflow responses to the first spring rains at Cathedral Peak are typically delayed until January, as infiltrating rainwater enters storage and is only released slowly towards the channel (Everson et al., 1998). Witklip V is similarly, associated with a low QFRESP, which may reflect the very deep granite-derived soils of that area. In a similar area on Frankfort State Forest, bedrock was estimated to be approximately 40 m beneath the surface (Dye et al., 1997). The relatively high QFRESP estimated for Westfalia B is unexpected, since it is likewise associated with deep, granite-derived soils. The possibility of leaks across the catchment boundary has long been suspected (Dye, 2001 pers com), and may be responsible for the high QFRESP.

Figure 94 illustrates the relationship between average soil depth and QFRESP. There is a convincing association, with only Westfalia B not conforming to an overall trend. This trend suggests that the same-day stormflow response fraction from a catchment decreases as the average depth of the soil profile increases. Such a relationship is expected, since deeper soils would absorb more water, and therefore resulting in less stormflow leaving the catchment and contributing to streamflow.

Figure 95 indicates a relationship between same day stormflow response and the maximum relief of the catchment. The overall trend indicates an increase in QFRESP as the maximum relief of the catchment increases, except for the Zululand and Westfalia B research catchments. The high QFRESP for Zululand is expected due to the flashy response to rainfall, as explained earlier. Again, Westfalia B does not conform to the trend, which could be associated with the possibility of leaks across the catchment.
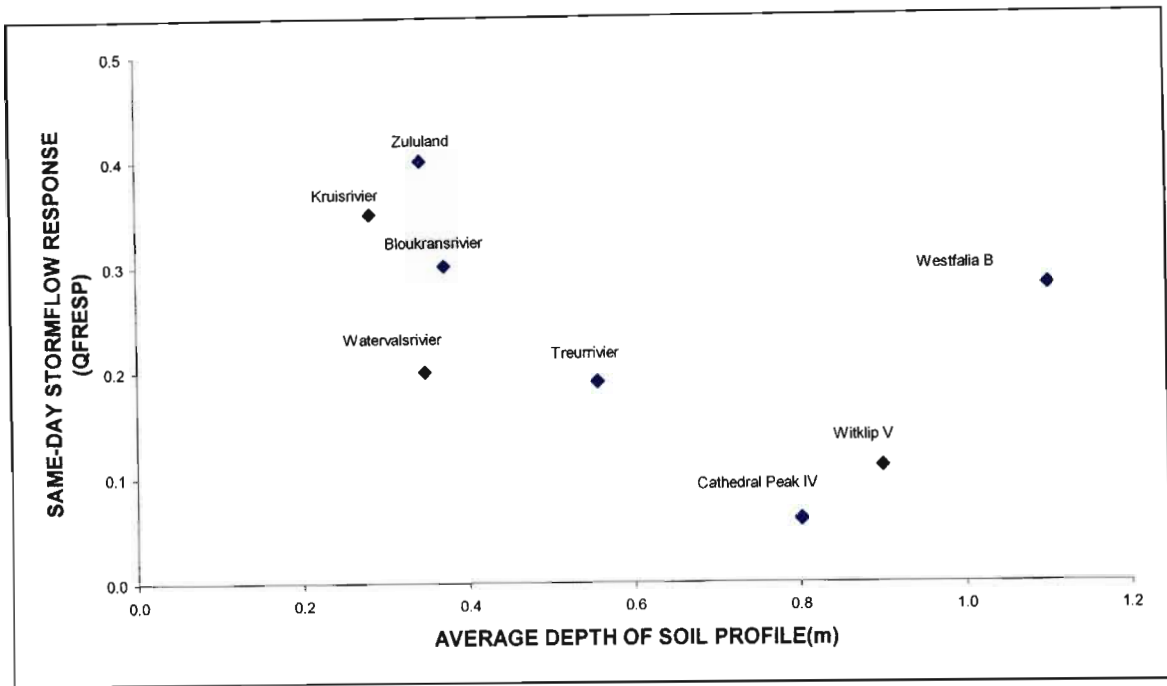
Figure 94: The association between the same day stormflow response fraction, QFRESP, and the average depth of the soil profile for a catchment.
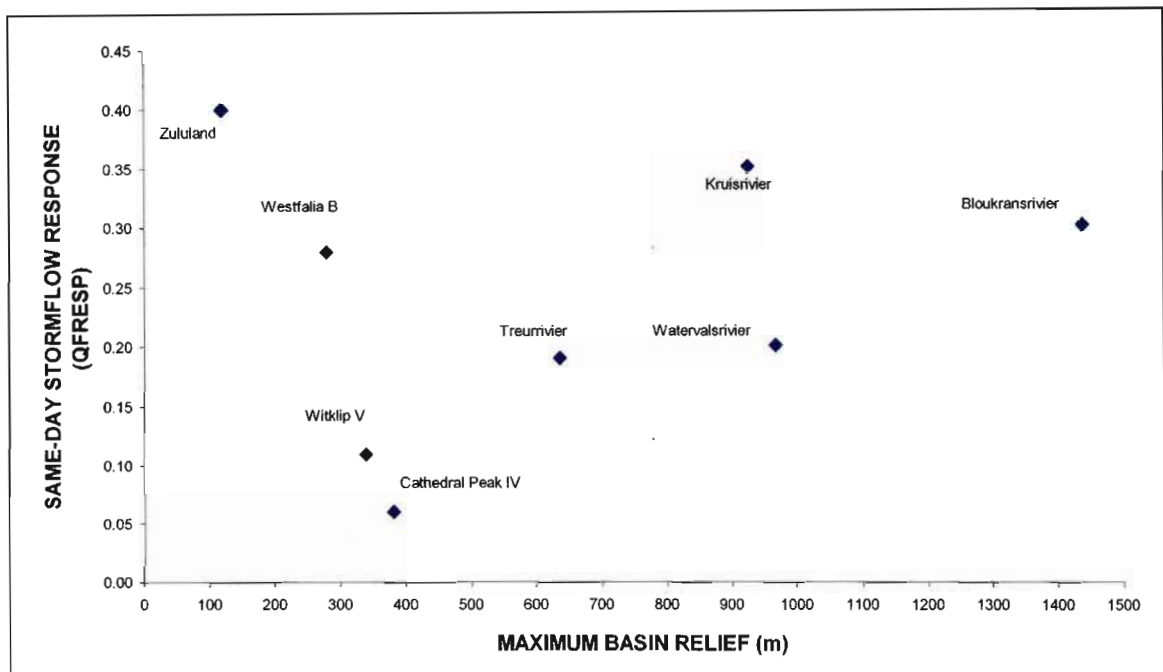
Figure 95: The association between the same day stormflow response fraction, QFRESP, and the maximum catchment relief.

4.3.3 Relationships between COFRU and catchment physical and climatic variables

The coefficient of baseflow response, COFRU, is the fraction of water from the intermediate/groundwater store that is released as the baseflow component of streamflow on a particular day. Figure 96 shows a tendency for this coefficient to be higher in lower rainfall catchments that are associated with shallow soil depths, than in higher rainfall areas.
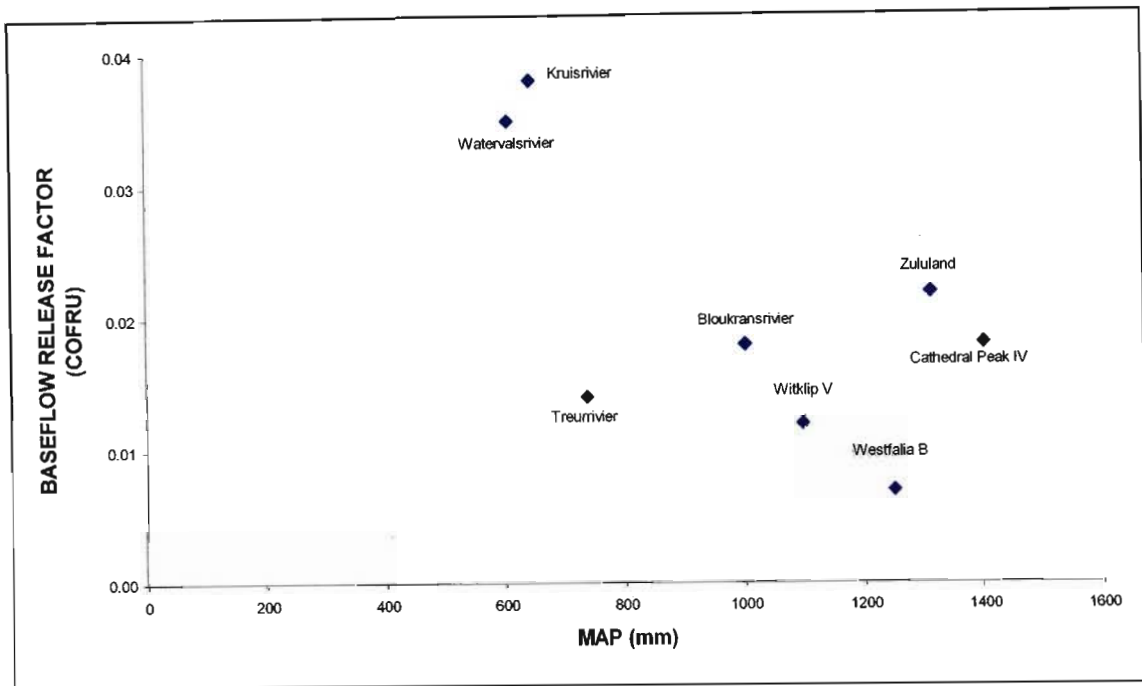
Figure 96: The association between the baseflow release fraction, COFRU, from catchments and their MAP.

Figure 97 illustrates a strong negative association between COFRU and profile plant available water. Profile plant available water is largely dependent on the depth of the soil profile and includes the effects of texture in the soil profile. A hypothesis is that deeper soils, with enhanced soil water storage, provide greater opportunity for vegetation to take up soil water and release it to the atmosphere through transpiration, with correspondingly less reaching the groundwater store. A second hypothesis which could explain the trends in Figure 97, is that the *ACRU* model at this stage includes rapid and delayed forms of subsurface stormflow as a component of baseflow. Therefore, deep soils which exhibit more delayed subsurface stormflow,

have lower baseflow release fractions, compared to shallower soils which exhibit rapid subsurface stormflows, and have higher baseflow release fractions.
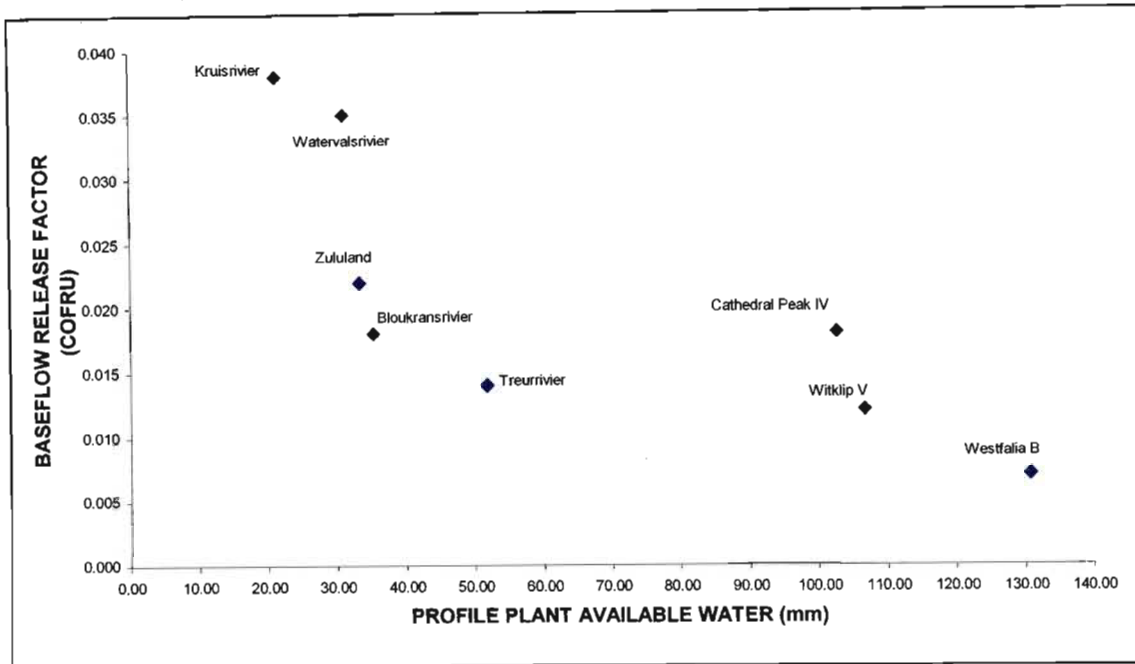
Figure 97: The association between the baseflow release fraction, COFRU, from catchments and their profile plant available water.

However, some of the anomalies shown in the above figures could be explained by certain mechanisms and processes discussed in earlier chapters. For example, Bonell (1993) stated that subsurface stormflow may be the dominant quickflow mechanism observed from undisturbed forested catchments. This statement could explain the high stormflow response attributed to Westfalia B. Similar catchments which display a high stormflow reponse may result from the presence of macropores or pipes in the catchments which contribute to higher subsurface and lateral stormflows. Another process commonly referred to as the "thatched roof effect" is also an example of rapid subsurface flows which may occur through the litter layer of upland forested catchments and therefore contribute to increased streamflows.

4.3.4 Regression analysis

The second phase of this study included a regression analysis of the streamflow model parameters QFRESP and COFRU against catchment attributes listed in Table 34. The catchment attributes selected were based on the literature review of

streamflow generation mechansims, and the physiographic and climatic characteristics which have in past research studies, shown to influence the hydrological responses of catchments. The regression analysis included three steps, namely:

- Simple linear regressions between the streamflow parameters QFRESP and COFRU, and all catchment predictor variables;
- A correlation matrix of all catchment predictor variables as a check of independency between attributes; and
- Multiple regression analyses of selected catchment predictor variables for QFRESP and COFRU.

Linear regressions equations between QFRESP, COFRU and catchment predictor variables are found in Tables 35 and 36. Linear regressions between QFRESP and the catchment attributes were not significant, except for average catchment altitude. However, this result may be spurious, since there is no logical hydrological explanation for this trend. Linear regressions between COFRU and catchment attributes highlight two significant relationships that are shown in Table 36. These are the Average Depth of the Soil Profile ($p < 0.019$; $R^2 = 0.626$), and the Profile Plant Available Water ($p < 0.026$; $R^2 = 0.522$), which had already been identified from the scatter plots.

Table 35: Linear regression of same-day stormflow response fraction QFRESP and catchment predictor variables.

Predictor Variables (x)	QFRESP (y)		
	Equation	Probablity (p)	R^2
Elongation Ratio	0.244 - 0.006 x	0.856	0.006
Shape Factor	0.187 + 0.018 x	0.534	0.068
Profile Plant Available Water	0.334 – 0.002x	0.156	0.019
Mean Annual Precipitation	0.287 - 0.0001 x	0.751	0.018
Drainage Density	0.215 + 0.012 x	0.844	0.007
Mean Slope	0.370 - 0.008 x	0.227	0.232
Area	0.221 + 0.0004 x	0.737	0.020
Average Altitude	0.365 - 0.0001 x	0.047	0.509
Maximum Basin Relief	0.211 + 0.00004 x	0.727	0.022
Average Depth of the Soil Profile	0.354 - 0.200 x	0.181	0.276

Table 36: Linear regression of baseflow release fraction COFRU and catchment predictor variables.

Predictor Variables (x)	COFRU (y)		
	Equation	Probability (p)	R^2
Elongation Ratio	0.026 - 0.005 x	0.078	0.429
Shape Factor	0.014 + 0.002 x	0.395	0.122
Profile Plant Available Water	0.033 – 0.0002x	0.026	0.522
Mean Annual Precipitation	0.043 - 0.00002 x	0.094	0.398
Drainage Density	0.031 – 0.005 x	0.268	0.199
Mean Slope	0.020 + 0.00001 x	0.987	0.00005
Area	0.018 + 0.00008 x	0.556	0.061
Average Altitude	0.030 – 0.00001 x	0.160	0.299
Maximum Basin Relief	0.013 + 0.00001 x	0.270	0.198
Average Depth of the Soil Profile	0.037 – 0.028 x	0.019	0.626

A correlation matrix of all predictor variables used in the regression analysis was then drawn up to check for interdependency between the catchment attributes, as shown in Table 37. The correlation matrix indicates that the geomorphological indices Elongation Ratio and Catchment Shape Factor are strongly correlated to other catchment attributes such as area, drainage density, MAP and maximum basin relief.

Table 37: Correlation matrix of all predictor variables used in the multiple regression analysis. These have been abbreviated to MAP, area, average altitude (AVALT), drainage density (DD), mean slope (MSLOPE), profile plant available water (PPAW), maximum basin relief (MBR), elongation ratio (ER), shape factor (SF) and the average depth of the soil profile of the A and B horizons (ADSP).

	ADSP	AVALT	AREA	DD	ER	MAP	MBR	MSLOPE	PPAW	SF
ADSP	1									
AVALT	0.690	1								
AREA	-0.530	-0.100	1							
DD	0.493	0.078	-0.853	1						
ER	0.862	0.280	-0.622	0.624	1					
MAP	0.564	0.378	-0.747	0.851	0.507	1				
MBR	-0.567	-0.355	0.651	-0.815	-0.557	-0.633	1			
MSLOPE	0.236	0.279	-0.013	-0.440	0.071	-0.147	0.485	1		
PPAW	0.993	0.702	-0.593	0.537	0.841	0.628	-0.581	0.255	1	
SF	-0.643	-0.302	0.970	-0.877	-0.651	-0.799	0.761	0.046	-0.707	1

A multiple regression analysis was then undertaken for each streamflow model parameter, excluding those variables which were not independent, as identified by the correlation matrix in Table 37. No significant multiple regressions models were

obtained for the same-day stormflow release fraction QFRESP and catchment attributes. However, a significant multiple regression model was obtained for the baseflow release fraction COFRU (F probability 0.04), using MAP, catchment area and profile plant available water:

$$COFRU = 0.0645 - 0.0000242 \text{ MAP (mm)} - 0.0002316 \text{ Area (km}^2) - 0.0001976$$
$$\text{Profile Plant Available Water (mm)}$$

The above regression model will be useful to future *ACRU* model users in estimating an initial value of COFRU, provided the physiographic and climatic information is available. The results from the regression analysis were limited by the sample sizee f catchments used. Therefore, trends between the *ACRU* model parameters QFRESP and COFRU, and catchment physical and climatic attributes such as catchment area, average depth of the soil profile and maximum basin relief, MAP and profile plant available water, warrant further investigation with a larger number of catchments.

* * * * * * * * * * * * * * * * * * * *

Chapter 4 illustrates the results obtained from simulating catchment streamflows using the *ACRU* model, for all 14 catchments selected for this research study. Each catchment was summarised using a catchment descriptor table, a monthly and daily comparison of simulated and observed streamflows, a scatter plot of simulated and observed flows, a statistical analysis of monthly totals of daily observed and simulated streamflows, and simulated daily evaporation totals over each simulation period. Analysis of the model results, revealed that six catchments were relatively poorerly simulated, and the *ACRU* flow parameters considered too uncertain to include in the investigation of relationships between catchment attributes and streamflow parameters. From the regression analysis trends were identified between *ACRU* model parameters QFRESP and COFRU, and catchment physical and climatic attributes. However, only a single significant multiple regression model was obtained for the baseflow release fraction COFRU from a catchment using MAP, catchment area and profile plant available water. Chapter 5 which follows includes further discussion on the results obtained from this research study, together with recommendations for future research.

5. CONCLUSIONS AND RECOMMENDATIONS FOR FURTHER RESEARCH

The principal goal of this study was to establish whether the stormflow parameter QFRESP and the baseflow parameter COFRU could be determined from catchment attributes, in order to offer guidance to *ACRU* users on appropriate values of these two parameters for use in simulations of catchment streamflow, and to also verify process descriptions in the model. A general weakness in many catchment hydrological models is that the below-ground movement of water towards the stream channel is poorly understood. Streamflow generation processes are varied, and not necessarily amenable to simulation even by the most sophisticated models. An appropriate approach in modelling streamflows, bearing in mind limitations of time available for most such studies, is to link streamflow characteristics to the physical attributes of the catchment. This study was designed to search for such relationships.

The initial task was to configure the *ACRU* model for each of the 14 selected catchments, building up the model menus in the conventional manner of first using the *ACRU* User Manual as a guide. Some trial-and-error fitting of selected parameters was undertaken to obtain an acceptable fit of simulated to observed flows. Streamflows from eight out of the original 14 catchments were simulated sufficiently well to provide confidence in their use to realistically predict streamflow regulating parameter values. Possible reasons for poor model performance in the remaining six catchments are varied. In the case of the arid Safford catchment, variation in rainfall intensity and transmission losses are the probable main causes of poor predictions of quickflows. The causes of poor model predictions in the remaining five catchments are unknown. Possible causes include, amongst others, errors in streamflow and rainfall records; rainfall values used not representing the entire catchment; leakages, especially from small catchments and the *ACRU* model not being able yet to simulate soil water extraction from beyond the agriculturally defined subsoil horizon depth, also not yet being able to simulate certain subsurface processes such as macropore flow. Menu inputs are included in Appendix 1, so that further analysis of these catchments by future *ACRU* modellers is possible.

A critical issue to evaluate in such simulation studies is whether model performance, when poor on certain catchments, is due to low quality hydrological data inputs, or whether the problem also lies in the incomplete conceptualisation of processes in the model itself. A useful approach is to use statistical models to explore the degree of variance that can be accounted for in model simulations. If variance is high, then it shows a likelihood that a consistency exists in the data and that the model structure, or its parameterisation, is likely to be at the core of the problem. Parameter optimising software such as PEST is potentially useful for such evaluations. Conversely, if variation accounted for in the simulation is low, then the input data may be at fault. One such statistical model (IHACRES; Jakeman *et al.*, 1990) has been applied to the Lambrechtsbos A (not used in this study) and Groot-Nylrivier (used in this study) catchments (Dye and Croke, 2001). The Lambrechtsbos A simulation by IHACRES was useful in revealing a very predictable response of runoff to rainfall (R^2 = 0.88), with the exception of one intense rainfall event when the normal response processes broke down.

This is the first *ACRU* study on the parameters QFRESP and COFRU to compare results from such a wide range of small catchments with such diverse physical characteristics. Streamflow parameter values determined in the eight successfully simulated catchments indicate the overriding importance of soil depth and profile water storage capacity in determining quickflow response. The strong associations between soil depth and profile plant available water, and QFRESP and COFRU is particularly welcome, as it demonstrates that the soil characteristics derived from the national soils database by the *ACRU* decision support system AUTOSOILS (Pike and Schulze, 1995), are hydrologically appropriate for *ACRU* simulations.

A note of caution should be sounded, however. Geological and soil properties in a catchment may be spatially highly variable and complex. The presence of dolerite dykes, macropores, and leakage across catchment boundaries are just three common features in South African catchments that may override broadly applicable relationships between flow characteristics and the readily apparent physical attributes of a catchment. Research needs to be strengthened and supplemented by the application of new measuring techniques such as ground penetrating radar for the non-invasive characterisation of soil characteristics and topography of the soil-

bedrock interface. Particular emphasis should be placed on investigating the combined effects of macropore flows and less permeable soil layers on the spatial pattern and temporal variation of streamflow generation i.e. characterising typical hillslope responses.

There has been considerable effort in using environmental isotopes and other natural tracers in interpreting flow mechanisms by end member mixing models. However, there is some doubt as to their reliability, given the many variabilities in source signal and mixing flowpaths. Therefore, these techniques need to be integrated with hydrometric methods in order to define flow pathways, residence times and fluxes (Buttle, 1994).

Greater insights (and therefore further research) into streamflow generation processes are required from a broader range of catchments to improve confidence in *ACRU* simulations for ungauged catchments in areas not represented by past and present research catchments. An improved understanding of streamflow generation mechanisms and more rapid estimate of flow volumes will also aid in understanding the transport of solutes to streams or in relating the hydrological environment to the biogeochemical environment using topographic indices and hydrological response units.

6. REFERENCES

Acreman, M.C. and Sinclair, C.D. 1986. Classification of drainage basins according to their physical characteristics, an application for flood frequency analysis in Scotland. Journal of Hydrology, 84, 365-380.

Anderson, M. and Burt, T. 1990. Process studies in hillslope hydrology: An overview. In: Process Studies in Hillslope Hydrology. Anderson, M. and Burt, T. (eds). John Wiley and Sons, Chichester, UK. 1-8.

Angus, G.R. 1987. A distributed version of the ACRU model. Unpublished MSc dissertation. Department of Agricultural Engineering, University of Natal, Pietermaritzburg. pp 137.

Ayers, H.D. and Ding, J.Y.H. 1967. Effects of surficial geology on streamflow distribution in southern Ontario. Canadian Journal of Earth Sciences, 4, 187-197.

Baker, O.E. 1936. Atlas of American Agriculture. United States Department of Agriculture, Washington DC, USA.

Beckedahl, H. 1996. Subsurface soil erosion phenomena in Transkei and Southern KwaZulu-Natal, South Africa. Unpublished PhD thesis, Department of Geography, University of Natal, Pietermaritzburg. pp 224.

Becker, A., Bonell, M., Feddes, R., Krysanova, V., McDonnell, J.J., Schulze, R.E. and Valentin, C. 2002. Chapter D2 Responses of hydrological processes to environmental change at small catchment scales. IGBP-BAHC Synthesis. Springer Verlag, Heidelberg, Germany. In press.

Becker, A. and McDonnell, J.J. 1998. Topographical and ecological controls of runoff generation and lateral flows in mountain catchments. In: Hydrology, Water Resources and Ecology in Headwaters. IAHS publ. No. 248, 199-206.

Berger, K.P. and Entekhabi, D. 2001. Basin hydrologic response relations to distributed physiographic descriptors and climate. Journal of Hydrology, 247, 169-182.

Beven, K.J., Wood, E.F. and Sivapalan, M. 1988. On hydrological heterogeneity: Catchment morphology and catchment response. Journal of Hydrology, 100, 353-375.

Birkhead, A.L., James, C.S. and Olbrich, B.W. 1996. Developing an Integrated Approach to Predicting the Water Use of Riparian Vegetation. WRC Report 474/1/97, Water Research Commission, Pretoria, RSA.

Bonell, M., Hendriks, M.R., Ineson, A.C. and Hazelhoff, L. 1984. The generation of storm runoff in a forested clayey drainage basin in Luxembourg. Journal of Hydrology, 71, 53-77.

Bonell, M. 1993. Progress in the understanding of runoff generation dynamics of forests. Journal of Hydrology, 150, 217-275.

Bonell, M. 1998. Selected challenges in runoff generation research in forests from the hillslope to headwater drainage basin scale. Journal of American Water Resources Association, 34, 765-785.

Bosch, J.M. 1979. Treatment effects on annual and dry period streamflow at Cathedral Peak. South African Forestry Journal, 108, 29-38.

Bosch, J.M. and Versfeld, D.B. 1984. A vegetation survey of catchment D, Westfalia Estate. South African Forestry Research Institute Centre Report, JFRC 84/20. pp 10.

Bosch, J.M. and von Gadow, K. 1990. Regulating afforestation for water conservation in South Africa. South African Forestry Journal, 153, 41-54.

Bosuk, M.E., Higdon, D., Stow, C.A. and Reckhow, K.H. 2001. A Bayesian hierarchal model to predict benthic oxygen demand from organic matter loading in estuaries and coastal zones. Ecological Modelling, 143, 165-181.

Bronstert, A. and Katzenmaier, D. 2001. The role of infiltration conditions on storm runoff generation at the hillslope and lower meso-scale. *In: Runoff Generation and Implications for River Basin Modelling. Proceedings of the International Workshop on Runoff Generation and Implications for River Basin Modelling.* Leibundgut, C., Uhlenbrook, S. and McDonnell, J.J. (eds). University of Freiburg i. Br., Germany. 60-67.

Brown, V.A., McDonnell, J.J., Burns, D.A. and Kendall, C. 1999. The role of event water, rapid shallow flowpaths and catchment size in summer stormflow. Journal of Hydrology, 217, 171-190.

Burt, T. 1989. Storm runoff generation in small catchments in relation to the flood response of large basins. *In: Floods.* Beven, K. and Carling, P. (eds). John Wiley, Chichester, UK. 11-35.

Buttle, J.M. 1994. Isotope hydrograph separations and rapid delivery of pre-event water from drainage basins. Progress In Physical Geography, 18, 16-41.

Buttle, J.M. and Turcotte, D. 1999. Runoff processes on a forested slope on the Canadian shield. Nordic Hydrology, 30, 1-20.

Calder, I.R. 1999. *The Blue Revolution: Land Use and Integrated Water Resources Management.* Earthscan, London, UK. pp 192.

Chorley, R. 1978. The hillslope hydrological cycle. *In: Hillslope Hydrology.* Kirkby, M. (ed). John Wiley and Sons, Chichester, UK. 1-42.

Chow, V.T. 1964. *Handbook of Applied Hydrology.* Chapter 14. Mc-Graw-Hill Book, New York.

Cook, R. and Doornkamp, J. 1990. *Geomorphology in Environmental Management.* Oxford University Press, 2nd Edition, UK.

CSIR. 1996. South African National Land Cover Database Project, CSIR (Environmentek), Pretoria, RSA.

Demuth, S. and Hageman, I. 1994. Estimation of flow parameters applying hydrgeological area information. *In: FRIEND Flow Regimes from International Experimental and Network Data.* IAHS publ. No. 221, 151-157.

Dent, M.C., Lynch, S.D. and Schulze, R.E. 1989. Mapping Mean Annual and Other Rainfall Statistics over Southern Africa. WRC Report 109/1/89, Water Research Commission, Pretoria, RSA.

Dingman, S.L. *Physical Hydrology.* MacMillan Publishing Company, New York. 361-430.

Doherty, J. 2001. Model Calibration and Predictive Analysis Using PEST. PEST Course Theory and Practical Manual. Unpublished.

Donkin, A.D., Smithers, J.C., Lorentz, S.A. and Schulze, R.E. 1995. Direct estimation of total evaporation from a Southern African wetland. *In: Versatility of Wetlands in the Agricultural Landscape.* Campbell, K.L. (ed). American Society of Agricultural Engineers, St Joseph MI, USA. 501-513.

Dunne, T. 1978. Field studies of hillslope processes. *In: Hillslope Hydrology.* Kirkby, M.J. (ed). John Wiley and Sons Ltd, 227-293.

Dunne, T. and Leopold, L.B. 1978. *Water in Environmental Planning.* W.H. Freeman and Company, San Francisco, USA. pp 818.

Dunsmore, S.J. 1985. Antecedent soil moisture in design stormflow estimation. Unpublished MSc Eng dissertation. Department of Agricultural Engineering, University of Natal, Pietermaritzburg. pp 114.

Dye, P.J. 1996. Response to Eucalyptus grandis trees to soil water deficits. Tree Physiology, 16, 233-238.

Dye, P.J. 2001. Personal Communication. CSIR, Pietermaritzburg, RSA.

Dye, P. J. and Bosch, J.M. 2000. Sustained water yield in afforested catchments – the South African experience. *In: Sustainable Forest Management*. Von Gadow, K., Putkala, T. and Tomé, M. (eds). Kluwer, Dordrecht, Netherlands. 99-120.

Dye, P.J. and Croke, B.F.W. 2001. Evaluation of streamflow predictions by the IHACRES rainfall-runoff model in two South African catchments. Proceedings of the MODSIM 2001 Congress, 10-13 December 2001, Canberra.

Dye, P.J., Poulter, A.G., Soko, S. and Maphanga, D. 1997. The determination of the relationship between transpiration rate and declining available water for *Eucalyptus grandis*. WRC Report 441/1/97, Water Research Commission, Pretoria, RSA.

Edwards, W.M., Norton, L.D. and Redmond, C.E. 1988. Characterizing macropores that affect infiltration into nontilled soil. Soil Science Society of America Journal, 52, 483-487.

Esprey, L. 1997. Hillslope experiments in the North Eastern Cape to measure and model subsurface flow processes. Unpublished MSc dissertation. Department of Agricultural Engineering, University of Natal, Pietermaritzburg, RSA. pp 180.

Everson, C.S., Molefe, G.L. and Everson, T.M. 1998. Monitoring and modelling components of the water balance in a grassland catchment in the summer rainfall area of South Africa. WRC Report 493/1/98, Water Research Commission, Pretoria, RSA.

Farvolden, R.N. 1963. Geologic controls on groundwater storage and baseflow. Journal of Hydrology, 1, 219-249.

Federer, C.A. 1973. Forest transpiration greatly speeds streamflow recession. Water Resources Research, 9, 1599-1604.

Freeze, R.A. 1972. The role of subsurface flow in generating surface runoff. 2. Upstream source areas. Water Resources Research, 8, 1271-1283.

Freeze, R.A. 1974. Streamflow generation. Reviews of Geophysics and Space Physics, 12, 627-647.

Gerits, J., Lima, J. and van der Broek, T. 1990. Overland flow and erosion. *In: Process Studies in Hillslope Hydrology*. Anderson, M. and Burt, T. (eds). John Wiley and Sons, Chichester, UK. 173-214.

Germann, P. 1990. Macropores and hydrologic hillslope processes. *In: Process Studies in Hillslope Hydrology*. Anderson, M. and Burt, T. (eds). John Wiley and Sons, Chichester, UK. 327-363.

Hawkins, R.H. 1978. Runoff curve numbers with varying site moisture. Journal of Irrigation and Drainage Division, 106, 257-258.

Heerdegen, R.G. and Reich, B.M. 1974. Unit hydrographs of catchments of different sizes and dissimilar regions. Journal of Hydrology, 22, 143-153.

Hewlett, J.D. and Hibbert, A.R. 1967. Factors affecting the response of small watersheds to precipitation in humid areas. *In: Forest Hydrology*. Sopper W.E., Lull H.W. (eds). Pergamon, New York, USA. 275-290.

Hickson, R. 2000. Defining small catchment runoff responses using hillslope hydrological process observations. Unpublished MSc dissertation. School of Bioresources Engineering and Environmental Hydrology, University of Natal, Pietermaritzburg, RSA. pp117.

Hills, R.C. 1971. The influence of land management and soil characteristics on infiltration and the occurrence of overland flow. Journal of Hydrology, 13, 163-181.

Hope, A.S. and Mulder, G.J. 1979. Hydrological investigations of small catchments in the Natal coastal belt and the role of physiography and land use in the rainfall runoff process. Hydrolology Research Unit, Report 1, Department of Geography, University of Zululand, KwaDlangezwa, RSA, pp 283.

Horton, R.E. 1933. The role of infiltration in the hydrological cycle. EOS, American Geophysical Union Transactions, 14, 446-460.

Howe, B.J. 1999. Development of new techniques for variable source area sediment yield modelling. Unpublished MSc dissertation. School of Bioresources Engineering and Environmental Hydrology, University of Natal, Pietermaritzburg, RSA. pp 159.

Hughes, G.O. 1997. An analysis of baseflow recession in the Republic of South Africa. Unpublished MSc dissertation. Department of Agricultural Engineering. University of Natal, Pietermaritzburg, RSA. pp 205.

Ineson, J. and Downing, R.A. 1964. The groundwater components of river discharge and its relation to hydrogeology. Journal of the Institute of Water Engineers, 18, 519-541.

ISCW. 1993. Land Type series. Department of Agriculture and Water Supply, Pretoria, Institute for Soil Climate and Water. *Memoirs on the Agricultural Natural Resources of South Africa.*

Jakeman, A.J., Littlewood, I.G. and Whitehead, P.G. 1990. Computation of the instantaneous unit hydrograph and identifiable component flows with application to two small upland catchments. Journal of Hydrology, 117, 275-300.

Joubert, A. and Hurly, P.R. 1994. The use of daily flow data to classify South African rivers. *In: Assessment of the Instream Flow Incremental Methodology and Initial Development of Alternative Instream Flow Methodologies for South Africa.* King, J.M. and Tharme, R.E. (eds). WRC Report 295/1/94, Chapter 11. Water Research Commission, Pretoria, RSA.

Kendall, K., Shanley, J. and McDonnell, J.J. 1999. A hydrometric and geochemical approach to testing the transmissivity feedback hypothesis during snowmelt. Journal of Hydrology, 219, 188-205.

Kienzle, S.W., Lorentz, S.A. and Schulze, R.E. 1997. Hydrology and Water Quality of the Mgeni Catchment. WRC Report TT87/97, Water Research Commission, Pretoria, RSA, pp 105.

King, J.M. and Tharme, R.E. 1994. Assessment of the instream flow incremental methodology and initial development of alternative instream flow methodologies for South Africa. WRC Report 295/1/94, Chapter 11. Water Research Commission, Pretoria, RSA.

Kirkby, M. 1988. Hillslope runoff processes and models. Journal of Hydrology, 100, 315-339.

Lacey, G.C. and Grayson, R.B. 1998. Relating baseflow to catchment properties in south-eastern Australia. Journal of Hydrology, 204, 231-250.

Linsley, R.K., Kohler, M.A. and Paulhus, J.L.P. 1958. *Hydrology for Engineers.* McGraw-Hill, New York, USA.

Lorentz, S. and Esprey, L. 1998. Baseline hillslope study prior to afforestation in the Umzimvubu headwaters of the North Eastern Cape Province, South Africa. *In: Hydrology, Water Resources and Ecology in Headwaters*. IAHS publ. No. 248, 267-273.

Low, A.B. and Rebello, A.G. 1998. Vegetation of South Africa, Lesotho and Swaziland, Department of Environmental Affairs and Tourism, Pretoria, RSA.

L'vovich, M.I. 1979. *World Water Resources and the Future*. AGU, Washington DC, USA (English translation edited by R.L. Nace).

Lynch, S.D. 2001. Personal Communication. School of Bioresources Engineering and Environmental Hydrology. University of Natal, Pietermaritzburg, RSA.

MacVicar, C.N., de Villiers, J.M., Loxton, R.F., Verster, E., Lambrechts, J.J.W., Merryweather, F.R., le Roux, J., van Rooyen, T.H. and Harmses, H.J. 1977. Soil classification – A binomial system for South Africa. Department of Agricultural Technical Services, Pretoria, RSA. pp 150.

Malherbe, H.L. 1968. Afforestation and water supplies in South Africa. Department of Forestry Report of the Interdepartmental Committee of Investigation into Afforestation and Water Supplies in South Africa, Cape Town, RSA. pp 115.

McDonnell, J.J. 1990. A rationale for old water discharge through macropores in a steep, humid catchment. Water Resources Research, 26, 2821-2832.

McDonnell, J.J., Owens, I.F. and Stewart, M.K., 1991. A case study of shallow flow paths in a steep zero-order basin. Water Resources Bulletin, 27, 679-685.

McDonnell, J.J., Rowe, L. and Stewart, M. 1999. A combined tracer-hydrometric approach to assessing the effects of catchment scale on water flowpaths, source and age. *In: Integrated Methods in Catchment Hydrology – Tracer, Remote Sensing and New Hydrometric Techniques*. IAHS publ No. 258, 265-274.

McGlynn, B., McDonnell, J.J. and Brammer, D. 2002. A review of the evolving perceptual model of hillslope flowpaths at the Maimai catchments, New Zealand. Journal of Hydrology, 257, 1-26.

Meier, K.B., Brodie, J.R., Schulze, R.E., Smithers, J.C. and Mnguni, D. 1997. Modelling the impacts of riparian zone alien vegetation on catchment water resources using the *ACRU* model. Eighth South African National Hydrology Symposium Proceedings (Available on CD), Water Research Commission, Pretoria.

Meyles, E., Williams, A., Dowd, J. and Ternan, L. 2001. Soil moisture patterns and runoff generation in a small Dartmoor catchment, south-west England. *In: Runoff Generation and Implications for River Basin Modelling. Proceedings of the International Workshop on Runoff Generation and Implications for River Basin Modelling.* Leibundgut, C., Uhlenbrook, S. and McDonnell, J. (eds). University of Freiburg i. Br., Germany. 28-36.

Moore, E.C.S. 1989. Sanitary Engineering: A practical treatise on the collection, removal and final disposal of sewage and the design and construction of works of drainage and sewage. Batsford, London.

Mosley, M.P. 1979. Streamflow generation in a forested watershed, New Zealand. Water Resources Research, 15, 795-806.

Mulder, G.J. 2000. Personal Communication, Hydrology Department, University of Zululand, South Africa.

Musto, J.W. 1994. Changes in soil physical properties and related hydraulic characteristics caused by *Eucalyptus* plantations. Unpublished MSc dissertation. Department of Agronomy. University of Natal, Pietermaritzburg, RSA. pp 185.

Ogunkoya, O.O., Adejuwon, J.O. and Jeje, L.K. 1984. Runoff response to basin parameters in southwestern Nigeria. Journal of Hydrology, 72, 67-84.

Onda, Y. 1994. Contrasting hydrological characteristics, slope processes and topography underlain by Paleozoic sedimentary rocks and granite. Transactions, Japanese Geomorphological Union, 15A, 49-65.

Pearce, A.J. 1990. Streamflow generation processes: An Austral View. Water Resources Research, 26, 3037-3047.

Pearce, A.J. and Mckerchar, A.I. 1979. Upstream generation of storm runoff. *In: Physical Hydrology-New Zealand Experience.* Murray, D.L. and Ackroyd, P. (eds) New Zealand Hydrological Society, Wellington, 165-192.

Philip, J.R. 1957. The theory of infiltration. 5. The influence of initial soil moisture content. Soil Science, 84, 329-339.

Pike, A. 2001. Personal Communication. School of Bioresources Engineering and Environmental Hydrology. University of Natal, Pietermaritzburg, RSA.

Pike, A. and Schulze, R.E. 1995. AUTOSOILS Version 3: A Soils Decision Support System for South African Soils. School of Bioresources Engineering and Environmental Hydrology, University of Natal, Pietermaritzburg, South Africa.

Pilgrim, D.H., Chapman, T.G. and Doran, D.G. 1988. Problems of rainfall runoff modelling in arid and semi-arid regions. Hydrological Sciences Journal, 33, 379-400.

Pretorius, J. 2001. Personal Communication. Bergplaas Forest Station. Western Cape, RSA.

Quigyun, D., Sorooshian, S. and Gupta, V. 1992. Effective and efficient global optimisation for conceptual and rainfall-runoff models. Water Resources Research, 28, 1015-1031.

Rassmussen, T., Baldwin, R., Dowd, J. and Williams, A. 2000. Tracer versus pressure wave velocities through unsaturated saprolite. Soil Sciences Society of America Journal, 64, 75-85.

Rice, K. and Hornberger, G. 1998. Comparison of hydrochemical tracers to estimate source contributions to peak flows in a small, forested, headwater catchment. Water Resources Research, 34, 1755-1766.

Rodhe, A. 1987. The origin of streamwater traced by oxygen-18. PhD thesis. Department of Physical Geography, Uppsala University, Sweden. pp 260.

Scherrer, S. and Naef, F. 2001. A decision scheme to identify dominant flow processes at the plot-scale for the evaluation of contributing areas at the catchment -scale. *In: Runoff Generation and Implications for River Basin Modelling. Proceedings of the International Workshop on Runoff Generation and Implications for River Basin Modelling.* Leibundgut, C., Uhlenbrook, S. and McDonnell, J.J. (eds). University of Freiburg i. Br., Germany. 11-16.

Schmidt, E.J. and Schulze, R.E. 1987. Flood volume and peak discharge from small catchments in southern Africa, based on the SCS technique. Technology Transfer Report TT/3/87. Water Research Commission, Pretoria, RSA. pp 164.

Schmidt, E.J. and Schulze, R.E. 1989. The DeHoek and Ntabamhlope hydrological research catchments. *ACRU* Report No. 34, Department of Agricultural Engineering, University of Natal, Pietermaritzburg, RSA.

Schultz, G. 1999. A call for hydrological models based on remote sensing, tracers and other modern hydrometric techniques. *In: Integrated Methods in Catchment Hydrology – Tracer, Remote Sensing and New Hydrometric Techniques.* IAHS Publ. No. 258, 3-9.

Schulze, R.E. 1975. Mapping potential evapotranspiration in hilly terrain. South African Geographical Journal, 57, 26-35.

Schulze, R.E. 1984. Hydrological Models for Application to Small Rural Catchments in Southern Africa: Refinements and Development. WRC Report 63/2/84. Water Research Commission, Pretoria, RSA. pp 248.

Schulze, R.E. 1985a. The DeHoek and Ntabamhlope hydrological research catchments – Excursion Guide. *ACRU* Report No. 21, Department. of Agricultural Engineering, University of Natal, Pietermaritzburg, RSA.

Schulze, R.E. 1985b. Personal Communication. Department. of Agricultural Engineering, University of Natal, Pietermaritzburg, RSA. Communicated to Dunsmore in 1985.

Schulze, R.E. 1995. Hydrology and Agrohydrology. Report TT69/95. Water Research Commission, Pretoria, RSA, pp 552.

Schulze, R.E. 1997. South African Atlas of Agrohydrology and –Climatology. WRC Report TT82/96, Water Research Commission, Pretoria, RSA. pp 274.

Schulze, R.E. 1998. Hydrological Modelling : Concepts and Practice. School of Bioresources Engineering and Environmental Hydrology, University of Natal, Pietermaritzburg, RSA. pp 134.

Schulze, R.E. 2000a. Personal Communication. School of Bioresources Engineering and Environmental Hydrology. University of Natal, Pietermaritzburg, RSA.

Schulze, R.E. 2000b. Transcending scales of space and time in impact studies of climate and climate change on agrohydrological responses. Agriculture, Ecosystems and Environment, 82, 185-212.

Schulze, R.E. 2001. Hydrological Responses at River Basin Scales. *ACRU*cons Report 35. School of Bioresources Engineering and Environmental Hydrology, University of Natal, Pietermaritzburg, RSA. pp 102.

Schulze, R.E. and Arnold, H. 1979. Estimation of volume and rate of runoff from small catchments in South Africa, based on the SCS Technique. *ACRU* Report No. 8. Department of Agricultural Engineering, University of Natal, Pietermaritzburg, RSA. pp 79.

Schulze, R.E., Schmidt, E.J. and Smithers, J.C. 1992. SCS-SA User Manual. ACRU Report No. 40, Department of Agricultural Engineering, University of Natal, Pietermaritzburg, RSA. pp 78.

Scott, D.F. 1993. The hydrological effects of fire in South African catchments. Journal of Hydrology, 150, 409-432.

Scott, D.F., Le Maitre, D.C. and Fairbanks, D.H.K. 1998. Forestry and streamflow reductions in South Africa. A reference system for assessing extent and distribution. Water SA, 24, 187-199.

Scott, D.F., Prinsloo, F.W., Moses, G., Mehlomakulu, M. and Simmers A.D.A. 2000. A re-analysis of the South African catchment afforestation experimental data. WRC Report 810/1/00, Water Research Commission, Pretoria, RSA.

Sefton, C.E.M. and Howarth, S.M. 1998. Relationships between dynamic response characteristics and physical descriptors of catchments in England and Wales. Journal of Hydrology, 221, 1-16.

Seyhan, E. 1976. Calculation of runoff from basin physiography (GRBP). Geography Institute, University of Utrecht, Netherlands.

Smakhtin, V.Y. and Watkins, D.A. 1997. Low flow estimation in South Africa. WRC Report 494/1/97, Water Research Commission, Pretoria, RSA, pp 596.

Smith, R.E. and Hebbert, R.H.B. 1983. Mathematical simulation of interdependent surface and subsurface hydrological processes. Water Resources Research, 19, 987-1001.

Smithers, J.C. and Schulze, R.E. 1995. *ACRU Agrohydrological Modelling System : User Manual Version 3.00*. Report TT70/95, Water Research Commission, Pretoria, RSA. pp 368.

Strahler, A.N. 1964. Quantitative geomorphology of drainage basins and channel networks, SEC. 4-11 In: *Handbook of applied hydrology*, Chow, V.T. (ed). McGraw-Hill, New York.

Topping, C.C. 1992. Improving stormflow simulation using rainfall intensity related initial abstractions. Unpublished MSc dissertation, Department of Agricultural Engineering, University of Natal, Pietermaritzburg, RSA. pp 175.

Tsukamoto, Y. and Ohta, T. 1988. Runoff processes on a steep forested slope. Journal of Hydrology, 102, 165-178.

Uhlenbrook, S. and Leibundgut, C. 1999. Integration of tracer information into the development of a rainfall-runoff model. *In: Integrated Methods in Catchment Hydrology – Tracer, Remote Sensing and New Hydrometric Techniques*. IAHS publ. No. 258, 93-100.

Uhlenbrook, S., McDonnell, J.J. and Leibundgut, C. 2001. Foreword. *In: Runoff Generation and Implications for River Basin Modelling. Proceedings of the International Workshop on Runoff Generation and Implications for River Basin Modelling.* Leibundgut, C., Uhlenbrook, S. and McDonnell, J.J. (eds). University of Freiburg i. Br., Germany.

United States Department of Agriculture. Agricultural Research Service. 1957. Monthly precipitation and runoff for small agricultural watersheds in the United States. Washington DC, USA.

United States Department of Agriculture. 1985. National Engineering Handbook, Section 4, Hydrology. USDA Soil Conservation Service, Washington DC, USA.

Vegter, J.R. 1995. An explanation of a set of national groundwater maps. WRC Report TT74/95, Water Research Commission, Pretoria, RSA.

Versfeld, D.B. and Donald, D.G.M. 1991. Litterfall and nutrient release in mature *Pinus radiata* in the South-western Cape. South African Forestry Journal, 156, 61-69.

Wallach, R. and Zaslavsky, D. 1991. Lateral flow in a layered profile of an infinite uniform slope. Water Resources Research, 27, 1809-1818.

Ward, R.C. and Robinson, M. 1999. *Principles of Hydrology.* McGraw-Hill, London, UK. pp 450.

Weiler, M., Naef, F. and Leibundgut, C. 1998. Study of runoff generation on hillslopes using tracer experiments and a physically-based numerical hillslope model. *In: Hydrology, Water Resources and Ecology in Headwaters.* IAHS publ. No. 248, 353-360.

Wright, C.E. 1970. Catchment characteristics influencing low flow. Waste and Water Engineering, 468-471.

Zecharias, Y.B. and Brutsaert, W. 1988. The influence of basin morphology on groundwater outflow. Water Resources Research, 24, 1645-1650.

7. APPENDIX 1: *ACRU* input menus for catchment simulations

Group Description	Variable	LAMBRECHTSBOS B	WATERVALSRIVIER	DIEPRIVIER	KRUISRIVIER	BLOUKRANSRIVIER
Mode of simulation	ICELL	1 (distributed)	1 (distributed)	1 (distributed)	1 (distributed)	1 (distributed)
Distributed mode options	ISUBNO MINSUB MAXSUB LOOPBK	2 1 2 0	5 1 5 0	7 1 7 0	6 1 6 0	7 1 7 0
Flow routing options	IROUTE DELT	N N/A	N N/A	N N/A	N N/A	N N/A
Subcatchment configuration	ICELLN IDSTRM	1, 2 2, 3	1, 2, 3, 4, 5 2, 3, 4, 5, 5	1, 2, 3, 4, 5, 6, 7 3, 3, 5, 5, 6, 7, 7	1, 2, 3, 4, 5, 6 2, 3, 5, 5, 6, 6	1, 2, 3, 4, 5, 6, 7 2, 3, 5, 5, 6, 7, 7
Rainfall file	IRAINF	CMPB6991	0042201.sin	(1-3,5): 0029291P.sin (4): 0029297.sin (6,7): 029294P.sin	0026510.sin	0031237.sin
Rainfall information	FORMAT PPTCOR MAP	1 Y 1384	2, 2, 2, 2, 2 N 732, 708, 682, 696, 608	2 (1-7) N 688, 667, 638, 757, 695, 749, 760	2 (1-6) Y (1-6) 527, 799, 799, 553, 517, 663	2 (1-7) Y (1-3), N (4-6), Y (7) 967, 934, 989, 1094, 1004, 1078, 990
Monthly rainfall adjustment factors	CORPPT	1.29, 1.29, 1.16, 1.29, 1.17, 1.28, 1.29, 1.21, 1.29, 1.22, 1.29, 1.29	N/A	N/A	1:090, 0.90, 0.90, 1.02, 1.21, 1.12, 1.02, 1.25, 0.93, 0.90, 0.90, 0.90 2:0.90, 0.90, 0.90, 0.94, 1.22, 1.01, 0.84, 1.10, 0.90, 0.90, 0.90, 0.90 3:0.90, 0.90, 0.90, 0.90, 1.02, 0.90, 0.90, 0.93, 0.90, 0.90,0 .90, 0.90 4:0.70, 0.70, 0.70, 0.88, 1.14, 0.96, 0.88, 1.03, 0.79, 0.77, 0.70, 0.70 5:0.70, 0.70, 0.70, 0.82, 0.99, 0.87, 0.82, 0.90, 0.75, 0.73, 0.70, 0.70 6:0.90, 0.92, 0.94, 1.05, 1.18, 1.09, 1.04, 1.11, 0.99, 0.97 0.93, 0 .88	1:0.70, 0.82, 0.86, 0.90, 0.90, 0.90, 0.90, 0.90, 0.86, 0.83, 0.87, 0.79 2:0.70, 0.80, 0.85, 0.88, 0.90, 0.90, 0.90, 0.90, 0.92, 0.90, 0.84, 0.77 3:0.77, 0.87, 0.82, 0.84, 0.90, 0.90, 0.90, 0.90, 0.87, 0.86, 0.80, 0.84 4-6: N/A 7:0.82, 0.85, 0.87, 0.87, 0.90, 0.90, 0.90, 0.90, 0.88, 0.87, 0.87, 0.8
Availability of observed streamflow data	IOBSTQ IOBSPK IOBOVR	0, 1 0, 0 0, 0	0, 0, 0, 0, 1 0, 0, 0, 0, 0 0, 0, 0, 0, 0	0, 0, 0, 0, 0, 0, 1 0, 0, 0, 0, 0, 0, 0 0, 0, 0, 0, 0, 0, 0	0, 0, 0, 0, 0, 1 0, 0, 0, 0, 0, 0 0, 0, 0, 0, 0, 0	0, 0, 0, 0, 0, 0, 1 0, 0, 0, 0, 0, 0, 0 0, 0, 0, 0, 0, 0, 0
Streamflow file	ISTRMF	N/A	G1H012.SIN	K4H003P.SIN	H9H004.SIN	K7H001.SIN
Dynamic file name	DNAMIC IDYNFL	Y, N LAMBD.FIL	N -	N -	N -	N -
Catchment information	CLAREA ELEV ALAT ALONG IHEMI IQUAD	0.49, 0.17 700, 700 33.97, 33.97 18.95, 18.95 2, 2 1, 1	9.69, 5.87, 6.31, 5.98, 8.10 301.6, 240.4, 227.8, 336.5, 119.3 33.42, 33.40, 33.38, 33.37, 33.35 19.10, 19.10, 19.10, 19.10, 19.10 2, 2, 2, 2, 2 1, 1, 1, 1, 1	8.16, 6.57, 13.36, 9.75, 12.71, 11.09, 11.23 740.0, 722.0, 494.0, 525.0, 499.8, 381.8, 405.8 33.82, 33.82, 33.85, 33.85, 33.87, 33.88, 33.88 22.70, 22.65, 22.43, 22.70, 22.68, 22.67, 22.72 2 (1-7) 1 (1-7)	6.82, 9.73, 9.48, 5.31, 10.06, 7.03 959.4, 827.6, 636.2, 853.8, 683.1, 550.0 33.95, 33.95, 33.95, 33.97, 33.97, 33.98 21.37, 21.33, 21.30, 21.32, 21.28, 21.28 (1-6) 1 (1-6)	9.21, 9.87, 3.52, 14.34, 6.76, 7.70, 3.05 796.1, 610.8, 497.6, 556.5, 450.7, 429.2, 243.1 33.87, 33.87, 33.88, 33.90, 33.90, 33.92, 33.93 23.68, 23.65, 23.63, 23.68, 23.63, 23.63, 23.63 2 (1-7) 1 (1-7)
Period of record for simulation	IYSTRT IYREND	1969 1974	1968 1974	1968 1975	1981 1990	1987 1996

Group Description	Variable	LAMBRECHTSBOS B	WATERVALSRIVIER	DIEPRIVIER	KRUISRIVIER	BLOUKRANSRIVIER
Monthly means of daily maximum temperature	TMAX	23.0, 21.0, 19.0, 17.0, 15.0, 13.0, 13.0, 15.0, 16.0, 17.0, 19.0, 20.0	1:28.7, 29.1, 27.1, 23.9, 20.1, 17.1, 16.3, 17.3, 19.3, 22.7, 25.9, 27.1 2:29.3, 29.5, 27.5, 24.5, 20.5, 17.5, 16.6, 17.6, 19.6, 22.9, 26.3, 27.6 3:29.4, 29.5, 27.5, 24.5, 20.5, 17.5, 16.6, 17.6, 19.6, 23.4, 26.4, 27.8 4:28.4, 28.8, 26.8, 23.8, 19.8, 16.8, 16.1, 17.1, 19.1, 22.4, 25.4, 27.1 5:30.0, 30.7, 28.7, 25.0, 21.0, 18.2, 17.5, 18.2, 20.5, 24.0, 27.2, 28.8	1:28.7, 28.7, 26.3, 23.3, 19.7, 17.0, 16.0, 18.0, 20.0, 22.3, 25.3, 27.3 2:28.7, 28.3, 26.3, 23.3, 19.3, 16.7, 16.3, 18.3, 20.3, 22.3, 25.3, 27.3 3:28.6, 28.6, 26.6, 23.8, 20.6, 18.2, 17.6, 18.8, 20.6, 22.8, 25.2, 27.2 4:28.0, 28.0, 26.3, 23.5, 20.5, 17.8, 17.8, 18.8, 20.3, 22.3, 24.5, 27.0 5:27.6, 27.6, 25.8, 23.6, 20.6, 17.6, 17.6, 18.6, 19.8, 21.8, 24.6, 26.6 5:28.0, 28.0, 26.0, 23.8, 21.0, 18.5, 18.0, 19.0, 20.5, 22.0, 24.5, 26.5 6:27.8, 27.8, 26.0, 23.6, 20.6, 18.2, 18.0, 18.8, 20.4, 22.2, 24.6, 26.6	1:26.2, 24.9, 23.2, 21.4, 18.4, 15.5, 15.5, 15.9, 17.9, 20.2, 22.4, 24.9 2:26.8, 25.2, 23.8, 22.0, 19.0, 16.9, 16.3, 16.4, 18.7, 21.0, 23.4, 25.7 3:27.7, 26.0, 24.5, 23.4, 20.2, 17.9, 17.4, 17.5, 19.7, 21.9, 24.5, 26.7 4:26.1, 24.1, 22.8, 21.8, 18.8, 16.7, 16.4, 15.8, 18.3, 20.4, 22.8, 25.1 5:27.2, 25.4, 23.9, 23.1, 19.7, 17.6, 17.2, 17.2, 19.2, 21.2, 23.9, 26.1 6:27.6, 26.7, 24.8, 23.3, 20.3, 18.1, 17.6, 18.0, 19.6, 22.0, 24.3, 26.3	1:25.4, 25.5, 23.9, 21.6, 18.7, 16.1, 16.1, 16.7, 18.5, 20.0, 21.9, 23.9 2:25.6, 25.8, 24.5, 22.6, 19.8, 17.4, 17.0, 18.0, 18.8, 20.6, 22.6, 24.2 3:25.8, 26.0, 24.7, 22.8, 20.4, 17.8, 17.6, 18.4, 19.4, 20.8, 22.8, 24.4 4:24.9, 25.3, 23.9, 22.4, 19.9, 17.6, 17.0, 17.8, 18.7, 20.5, 22.1, 23.8 5:25.9, 26.1, 24.9, 22.9, 20.3, 18.0, 17.9, 18.3, 19.6, 21.1, 22.9, 24.6 6:25.8, 26.3, 24.8, 22.8, 20.4, 18.4, 17.6, 18.4, 19.8, 21.4, 22.8, 24.8 7:26.0, 26.4, 25.0, 23.4, 21.0, 19.0, 18.4, 19.0, 20.0, 22.0, 23.4, 25.0
Monthly means of daily minimum temperature	TMIN	9.0, 11.0, 11.0, 10.0, 7.0, 7.0, 5.0, 5.0, 7.0, 8.0, 9.0, 10.0	1:14.1, 14.5, 13.4, 10.5, 8.4, 5.8, 4.8, 5.7, 7.4, 9.5, 11.4, 13.1 2:14.6, 14.7, 13.7, 10.7, 8.8, 5.9, 4.9, 5.8, 7.8, 9.7, 11.7, 13.6 3:14.6, 14.6, 13.6, 10.7, 8.7, 5.8, 4.9, 5.9, 7.7, 9.7, 11.6, 13.6 4:14.1, 14.1, 13.1, 10.4, 8.4, 5.7, 4.7, 5.7, 7.4, 9.4, 11.0, 13.1 5:14.9, 15.6, 14.0, 11.6, 9.0, 6.6, 5.2, 6.0, 8.0, 10.0, 12.6, 13.9	1:12.3, 13.3, 12.0, 9.0, 6.3, 4.3, 3.3, 4.0, 5.3, 7.3, 10.0, 11.3 2:12.7, 13.3, 12.3, 9.3, 6.3, 4.3, 3.3, 4.3, 5.3, 7.3, 10.0, 11.3 3:13.8, 14.2, 13.0, 10.2, 7.8, 5.8, 5.0, 5.4, 7.0, 8.8, 11.0, 12.8 4:13.8, 13.8, 12.8, 10.3, 7.8, 6.0, 5.0, 5.3, 6.8, 8.8, 10.8, 12.8 5:13.6, 13.6, 12.6, 10.6, 7.6, 6.2, 5.4, 5.6, 6.6, 8.6, 10.6, 12.6 6:14.0, 14.5, 13.3, 10.8, 8.5, 6.8, 5.8, 6.0, 7.5, 9.5, 11.5, 13.0 7:14.0, 14.4, 13.0, 10.6, 8.4, 6.6, 5.6, 6.0, 7.4, 9.2, 11.2, 13.0	1:10.9, 11.4, 10.4, 8.0, 6.2, 4.2, 3.3, 3.3, 4.5, 6.2, 8.2, 9.9 2:11.8, 12.0, 11.0, 8.9, 7.0, 5.0, 4.0, 4.2, 5.7, 7.0, 9.0, 10.9 3:12.5, 12.9, 11.9, 9.7, 7.5, 5.9, 4.5, 4.9, 6.0, 7.9, 9.9, 11.5 4:10.8, 11.8, 11.0, 9.0, 7.0, 5.0, 4.0, 4.4, 5.5, 6.8, 8.7, 10.4 5:12.2, 12.7, 11.7, 9.6, 7.6, 5.6, 4.6, 4.8, 6.1, 7.7, 9.7, 11.2 6:12.6, 13.3, 12.3, 9.6, 7.6, 6.0, 4.7, 5.0, 6.6, 8.3, 10.3, 11.8	1:11.5, 12.1, 11.4, 9.1, 7.1, 5.1, 4.2, 4.7, 5.7, 7.1, 8.8, 10.2 2:12.4, 13.1, 12.1, 10.1, 8.1, 6.6, 5.6, 5.6, 6.8, 8.4, 10.4, 11.6 3:13.4, 13.7, 12.7, 10.7, 8.7, 6.8, 5.8, 6.1, 7.4, 8.8, 10.8, 12.1 4:12.8, 13.4, 12.4, 10.4, 8.4, 6.9, 6.1, 6.1, 6.9, 8.8, 10.4, 11.7 5:13.6, 14.0, 13.0, 10.9, 8.9, 7.0, 6.1, 6.3, 7.3, 9.1, 11.0, 12.3 6:13.4, 14.4, 13.4, 11.1, 8.8, 7.1, 6.4, 6.4, 7.6, 9.4, 11.4, 12.4 7:14.4, 15.0, 14.0, 12.0, 9.4, 8.0, 7.0, 7.4, 8.4, 10.4, 12.0, 13.4
Reference potential evaporation option	EQPET	101	102	102	102	102
Evaporation input availability control flags	IEIF ILRF IWDF IRHF ISNF IRDF IPNF	0 0 0 0 0 0 0	1 0 0 0 0 0 0	1 0 0 0 0 0 0	1 0 0 0 0 0 0	1 0 0 0 0 0 0
Monthly totals of A-pan equivalent evaporation	E	N/A	1:308.8, 252.6, 218.1, 129.1, 84.8, 59.5, 63.4, 82.6, 113.7, 183.1, 239.7, 297.3 2:314.8, 259.7, 223.1, 132.9, 86.0, 59.7, 69.3, 83.3, 115.0, 187.6, 247.0, 303.0 3:317.2, 262.6, 227.0, 134.5, 87.1, 59.8, 63.5, 83.7, 116.5, 190.0, 250.7, 305.3 4:307.5, 253.4, 222.3, 129.5, 85.8, 59.1, 64.2, 83.1, 113.9, 183.4, 242.6, 297.0 5:330.9, 278.5, 240.0, 141.7, 91.0, 61.9, 64.2, 84.7, 121.1, 201.0, 267.3, 319.9	1:269.0, 213.6, 173.3, 124.0, 98.3, 80.7, 88.3, 105.0, 114.0, 187.3, 202.6, 266.3 2:271.3, 215.3, 174.6, 124.6, 99.0, 81.0, 89.0, 105.6, 115.3, 188.6, 203.3, 268.6 3:256.4, 205.0, 170.0, 126.0, 101.2, 83.0, 89.2, 106.2, 115.2, 187.2, 193.8, 252.2 4:236.0, 190.7, 161.2, 120.2, 96.8, 81.3, 87.8, 102.5, 110.0, 179.0, 181.5, 234.7 5:229.8, 185.6, 159.8, 119.8, 97.0, 81.0, 87.2, 101.4, 110.8, 179.2, 178.6, 229.8 6:219.2, 178.7, 154.7, 119.7, 98.0, 82.3, 87.5, 102.5, 109.5, 176.7, 172.0, 221.0 7:221.2, 180.2, 155.4, 119.2, 97.2, 82.0, 87.4, 101.6, 108.4, 176.8, 173.6, 222.2	1:254.1, 167.2, 153.6, 118.1, 85.1, 71.2, 80.1, 90.1, 116.3, 162.4, 188.4, 246.3 2:260.1, 169.1, 153.7, 122.2, 89.5, 72.0, 79.9, 91.9, 117.3, 168.4, 193.0, 251.2 3:273.9, 183.4, 162.9, 129.9, 90.6, 71.2, 76.6, 91.6, 120.5, 177.5, 202.5, 261.2 4:240.2, 147.3, 135.5, 115.9, 86.8, 70.2, 78.4, 89.3, 112.7, 155.9, 170.9, 232.4 5:255.6, 166.1, 146.1, 123.4, 88.8, 70.6, 76.5, 90.3, 116.5, 167.1, 183.8, 245.6 6:250.1, 165.0, 134.5, 122.6, 88.6, 70.6, 74.6, 90.1, 115.3, 165.7, 174.0, 241.7	1:195.5, 156.3, 151.1, 107.1, 84.2, 74.7, 81.6, 90.8, 102.4, 155.9, 161.3, 198.9 2:198.3, 157.6, 149.4, 109.9, 87.6, 77.2, 83.1, 93.8, 104.7, 161.7, 162.4, 198.0 3:191.2, 153.8, 144.8, 109.6, 89.1, 78.6, 83.9, 94.6, 104.0, 160.4, 158.3, 191.9 4:182.4, 147.7, 143.7, 107.1, 86.6, 77.0, 82.2, 92.2, 105.2, 154.1, 152.8, 186.2 5:188.0, 153.0, 143.1, 109.5, 89.8, 79.3, 84.3, 95.1, 102.1, 160.8, 157.1, 189.8 6:178.6, 149.3, 139.5, 108.1, 89.8, 79.9, 84.6, 95.1, 98.6, 157.1, 152.8, 183.9 7:176.5, 150.0, 138.3, 110.5, 93.4, 82.4, 85.9, 97.4, 99.6, 163.1, 153.3, 182.6
Temperature adjustment for altitude	TELEV LRREG	N N/A	N N/A	N N/A	N N/A	N N/A

Group Description	Variable	LAMBRECHTSBOS B	WATERVALSRIVIER	DIEPRIVIER	KRUISRIVIER	BLOUKRANSRIVIER
Mean lapse rates for min and max temperature	TMAXLR TMINLR	7.00 5.50	7.00 5.50	7.00 5.50	7.00 5.50	7.00 5.50
Mean daily wind speed (m/s)	WNDSPD	1.6	1.6	1.6	1.6	1.6
Penman equation option for S-tank or A-pan equivalent evaporation	SAPANC	N	N	N	N	N
Smoothed mean monthly A-pan/S-pan ratios	SARAT	N/A	N/A	N/A	N/A	N/A
Pan adjustment option	PANCOR CORPAN	1 1.15	0 -	0 -	0 -	0 -
Level of soils information	PEDINF	1	1	1	1	1
Soils texture information	ITEXT	5	7	7 (1-2), 10 (3-7)	5	7 (1-5), 3 (6-7)
Soil thickness information	PEDDEP	2	2	2	2	2
Soils information	DEPAHO DEPBHO WP1 WP2 FC1 FC2 PO1 PO2 ABRESP BFRESP	0.21, 0.21 1.35, 1.10 0.108, 0.108 0.105, 0.105 0.190, 0.190 0.202, 0.202 0.446, 0.446 0.440, 0.440 0.47, 0.47 0.47, 0.47	0.20 (1-5) 0.43, 0.28, 0.30, 0.23, 0.17 0.111 (1-5) 0.110 (1-5) 0.197 (1-5) 0.204 (1-5) 0.449 (1-5) 0.442 (1-5) 0.44 (1-5) 0.44 (1-5)	0.23 (1-7) 0.27, 0.24, 0.47 (3-4), 0.48 (5-7) 0.92, 0.82, 0.92 (3-5), 0.99, 0.92 0.88, 0.85, 0.88 (3-5), 0.91, 0.88 0.187, 0.77, 0.187 (3-5), 0.192, 0.187 0.188, 0.185, 0.188 (3-5), 0.193, 0.188 0.456, 0.455, 0.456 (3-5), 0.465, 0.456 0.454, 0.459, 0.454 (3-5), 0.455, 0.454 0.50, 0.48, 0.55 (3-5), 0.49, 0.55 0.50, 0.48, 0.55 (3-5), 0.49, 0.55	0.15 (1-6) 0.12 (1-2), 0.10, 0.04, 0.09, 0.15 0.78 (1-2), 0.86, 0.82, 0.97, 0.98 0.99 (1-2), 0.101, 0.75, 0.95, 0.106 0.152 (1-2), 0.161, 0.152, 0.174, 0.176 0.171 (1-2), 0.175, 0.151, 0.176, 0.186 0.366 (1-2), 0.375, 0.361, 0.399, 0.404 0.361 (1-2), 0.370, 0.357, 0.394, 0.402 0.65 (1-3), 0.35, 0.34, 0.38 0.65 (1-3), 0.35, 0.34, 0.38	0.19 (1-3), 0.20, 0.19 (5-6), 0.21 0.31 (1-2), 0.32, 0.30, 0.32, 0.31, 0.51 0.74 (1-3), 0.73, 0.74 (5-6), 0.99 0.96, 0.96, 0.95, 0.98, 0.95, 0.95, 0.140 0.170 (1-6), 0.190 0.191 (1-3), 0.192, 0.191 (5-6), 0.224 0.453, 0.453, 0.454, 0.452, 0.454, 0.454, 0.449 0.458, 0.458, 0.459, 0.456, 0.459, 0.459, 0.442 0.38 (1-6), 0.37 0.38 (1-6), 0.37
Initial soil water content	SMAINI SMBINI	0.80 0.80	0.00 0.00	0.00 0.00	0.80 (1-3), 0.00 (4-6) 0.80 (1-3), 0.00 (4-6)	0.00 0.00
Level of land cover information	LCOVER CROPNO	1, 0 0, 2020102	1 -	1 -	1 -	1 -
Determination of canopy interception loss	INTLOS	2, 1	1	1	1	1
Leaf area index information	LAIND	1, 0	0	0	0	0
Monthly means of crop coefficients	CAY	1:0.85; 2:0.40, 0.40, 0.40, 0.42, 0.44, 0.44, 0.42, 0.48, 0.50, 0.45, 0.40, 0.40	1:0.61, 0.61, 0.61, 0.62, 0.63, 0.63, 0.62, 0.65, 0.66, 0.64, 0.61, 0.61 2:0.61, 0.61, 0.61, 0.62, 0.63, 0.63, 0.62, 0.65, 0.66, 0.64, 0.61, 0.61 3:0.65, 0.65, 0.65, 0.66, 0.67, 0.67, 0.66, 0.68, 0.69, 0.67, 0.65, 0.65 4:0.54, 0.54, 0.54, 0.55, 0.57, 0.57, 0.55, 0.59, 0.61, 0.57, 0.54, 0.54 5:0.42, 0.42, 0.42, 0.44, 0.46, 0.46, 0.44, 0.50, 0.52, 0.47, 0.42, 0.42	1:0.53, 0.53, 0.53, 0.53, 0.53, 0.50, 0.49, 0.55, 0.58, 0.57, 0.53, 0.53 2:0.49, 0.49, 0.49, 0.48, 0.47, 0.43, 0.41, 0.49, 0.54, 0.52, 0.49, 0.49 3:0.62, 0.62, 0.61, 0.59, 0.55, 0.52, 0.51, 0.56, 0.62, 0.60, 0.62, 0.62 4:0.64, 0.64, 0.64, 0.60, 0.55, 0.46, 0.46, 0.53, 0.62, 0.66, 0.64, 0.64 5:0.66, 0.66, 0.66, 0.67, 0.58, 0.57, 0.55, 0.51, 0.64, 0.60, 0.66, 0.66 6: 0.85, Jan-Dec 7: 0.85, Jan-Dec	1:0.30, 0.30, 0.40, 0.56, 0.57, 0.57, 0.56, 0.59, 0.65, 0.63, 0.35, 0.30 2:0.37, 0.37, 0.40, 0.51, 0.53, 0.53, 0.51, 0.55, 0.60, 0.57, 0.37, 0.33, 3:0.55, 0.54, 0.49, 0.52, 0.53, 0.53, 0.52, 0.54, 0.57, 0.55, 0.43, 0.49 4:0.40, 0.40, 0.40, 0.42, 0.44, 0.44, 0.42, 0.48, 0.50, 0.45, 0.40, 0.40 5:0.30, 0.30 0.40, 0.56, 0.57, 0.57, 0.57, 0.56, 0.59, 0.65, 0.63, 0.30 6:0.40, 0.40, 0.40, 0.42, 0.44, 0.44, 0.42, 0.48, 0.50, 0.45, 0.40, 0.40	1:0.48, 0.52, 0.53, 0.52, 0.52, 0.47, 0.47, 0.51, 0.56, 0.58, 0.52, 0.48 2:0.50, 0.53, 0.55, 0.54, 0.52, 0.52, 0.55, 0.57, 0.52, 0.59, 0.53, 0.50 3:0.75, 0.75, 0.75, 0.65, 0.55, 0.40, 0.40, 0.50, 0.65, 0.75, 0.75, 0.75 4:0.65, 0.67, 0.67, 0.65, 0.58, 0.53, 0.53, 0.57, 0.62, 0.68, 0.65, 0.65 5:0.80, 0.80, 0.80, 0.75, 0.63, 0.55, 0.55, 0.60, 0.68, 0.78, 0.78, 0.80 6:0.85, 0.85, 0.85, 0.80, 0.75, 0.68, 0.68, 0.73, 0.80, 0.85, 0.85, 0.85 7:0.87, 0.87, 0.87, 0.85, 0.77, 0.74, 0.74, 0.76, 0.79, 0.85, 0.85, 0.87

Group Description	Variable	LAMBRECHTSBOS B	WATERVALSRIVIER	DIEPRIVIER	KRUISRIVIER	BLOUKRANSRIVIER
Monthly means of leaf area index	ELAIM	1:4.90 2: N/A	N/A (1-5)	N/A (1-7)	N/A (1-6)	N/A (1-7)
Canopy interception loss (mm) per rainday	VEGINT	1:N/A 2:2.00, 2.00, 2.00, 1.60, 1.20, 1.20, 1.20, 1.20, 1.40, 1.80, 2.00, 2.00	1:2.71, 2.71, 2.71, 2.49, 2.28, 2.28, 2.28, 2.28, 2.39, 2.60, 2.71, 2.71 2:2.71, 2.71, 2.71, 2.49, 2.28, 2.28, 2.28, 2.28, 2.39, 2.60, 2.71, 2.71 3:2.83, 2.83, 2.83, 2.65, 2.47, 2.47, 2.47, 2.47, 2.56, 2.74, 2.83, 2.83 4:2.47, 2.47, 2.47, 2.19, 1.91, 1.91, 1.91, 1.91, 2.05, 2.33, 2.47, 2.47 5:2.08, 2.08, 2.08, 1.70, 1.32, 1.32, 1.32, 1.32, 1.51, 1.89, 2.08, 2.08	1:2.33, 2.33, 2.25, 1.98, 1.71, 1.71, 1.71, 1.71, 1.85, 2.20, 2.33, 2.33 2:2.12, 2.12, 2.00, 1.70, 1.40, 1.40, 1.40, 1.40, 1.55, 1.97, 2.12, 2.12 3:2.37, 2.37, 2.25, 2.06, 1.87, 1.86, 1.86, 1.86, 1.95, 2.27, 2.37, 2.37 4:2.44, 2.44, 2.16, 2.03, 1.90, 1.90, 1.90, 1.96, 2.55, 2.37, 2.44, 2.44 5:2.14, 2.14, 2.10, 1.76, 1.42, 1.42, 1.42, 1.42, 1.59, 1.97, 2.14, 2.14 6:2.46, 2.46, 2.45, 2.22, 2.00, 1.99, 1.99, 1.99, 2.10, 2.34, 2.46, 2.46 7:2.71, 2.71, 2.60, 2.46, 2.33, 2.33, 2.33, 2.33, 2.40, 2.64, 2.71, 2.71	1:1.25, 1.25, 1.00, 1.05, 0.95, 1.00, 1.10, 1.20, 1.30, 1.15, 1.25, 1.25 2:1.80, 1.80, 1.73, 1.45, 1.14, 1.15, 1.18, 1.20, 1.38, 1.63, 1.80, 1.80 3:1.06, 1.15, 1.05, 0.95, 0.69, 0.70, 0.74, 0.78, 0.86, 0.88, 0.96, 0.97 4:2.00, 2.00, 2.00, 1.60, 1.20, 1.20, 1.20, 1.20, 1.40, 1.80, 2.00, 2.00 5:1.25, 1.25, 1.00, 1.05, 0.95, 1.00, 1.10, 1.20, 1.30, 1.15, 1.25, 1.25 6:2.00, 2.00, 2.00, 1.60, 1.20, 1.20, 1.20, 1.20, 1.40, 1.80, 2.00, 2.00	1:1.90, 1.90, 1.73, 1.60, 1.40, 1.40, 1.40, 1.40, 1.60, 1.90, 1.90, 1.90 2:2.02, 2.02, 1.93, 1.80, 1.60, 1.60, 1.60, 1.80, 2.02, 2.02, 2.02 3:2.50, 2.50, 2.00, 2.00, 2.00, 2.00, 2.00, 2.00, 2.00, 2.50, 2.50, 2.50 4:2.43, 2.43, 2.27, 2.20, 2.10, 2.10, 2.10, 2.10, 2.20, 2.43, 2.43, 2.43 5:2.85, 2.85, 2.60, 2.60, 2.60, 2.60, 2.60, 2.60, 2.60, 2.85, 2.85, 2.85 6:2.50, 2.50, 2.25, 2.25, 2.25, 2.25, 2.25, 2.25, 2.25, 2.50, 2.50, 2.50 7:2.78, 2.78, 2.68, 2.68, 2.68, 2.68, 2.68, 2.68, 2.68, 2.78, 2.78, 2.78
Fraction of active root system in topsoil horizon specified month by month	ROOTA	Jan-Dec 1:0.40 Jan-Dec 2:0.60	Jan-Dec 1:0.63 Jan-Dec 2:0.63 Jan-Dec 3:0.63 Jan-Dec 4:0.62 Jan-Dec 5:0.60	Jan-Dec (1-7) 0.75	1:0.80, 0.80, 0.80, 0.76, 0.68, 0.63, 0.58, 0.80, 0.80, 0.80, 0.80, 0.80 2:0.65, 0.65, 0.65, 0.64, 0.62, 0.61, 0.59, 0.65, 0.65, 0.65, 0.65, 0.65 3:0.79, 0.79, 0.80, 0.81, 0.79, 0.77, 0.75, 0.84, 0.84, 0.84, 0.84, 0.81 4:0.60, 0.60, 0.60, 0.60, 0.60, 0.60, 0.60, 0.60, 0.60, 0.60, 0.60, 0.60 5:0.80, 0.80, 0.80, 0.76, 0.68, 0.63, 0.58, 0.80, 0.80, 0.80, 0.80, 0.80 6:0.60, 0.60, 0.60, 0.60, 0.60, 0.60, 0.60, 0.60, 0.60, 0.60, 0.60, 0.60	1:0.80, 0.80, 0.83, 0.83, 0.83, 0.83, 0.83, 0.83, 0.83, 0.80, 0.80, 0.80 2:0.78, 0.78, 0.80, 0.80, 0.80, 0.80, 0.80, 0.80, 0.80, 0.78, 0.78, 0.78 3:0.80, 0.80, 0.90, 0.90, 0.90, 0.90, 0.90, 0.90, 0.90, 0.80, 0.80, 0.80 4:0.77, 0.77, 0.80, 0.80, 0.80, 0.80, 0.80, 0.80, 0.80, 0.77, 0.77, 0.77 5:0.75, 0.75, 0.80, 0.80, 0.80, 0.80, 0.80, 0.80, 0.80, 0.75, 0.75, 0.75 6:0.73, 0.73, 0.78, 0.78, 0.78, 0.78, 0.78, 0.78, 0.78, 0.73, 0.73, 0.73 7:0.70, 0.70, 0.72, 0.72, 0.72, 0.72, 0.72, 0.72, 0.72, 0.70, 0.70, 0.70
Effective total rooting depth	EFRDEP	Defaulted to DEPAHO+DEPBHO	Defaulted to DEPAHO+DEPBHO	Defaulted to DEPAHO+DEPBHO	Defaulted to DEPAHO+DEPBHO	Defaulted to DEPAHO+DEPBHO
Total evaporation control variables	EVTR FPAW	2 0	2 0	2 0	2 0	2 0
Fraction of PAW at which plant stress sets in	CONST	1: 0.10 2: 0.40	1:0.90 2:0.90 3:0.50 4:0.40 5:0.40	1:0.65 2:0.40 3:0.60 4:0.48 5:0.65 6:0.90 7:0.90	0.40 (1-6)	0.40 (1-6), 0.90
Critical leaf water potential	CRLEPO	N/A	N/A	N/A	N/A	N/A
Option for enhanced wet canopy evaporation	FOREST	1, 0	1 (1-4) 0 (5)	0 (1-2) 1 (3-7)	0	0 (1-6), 1
Mean temperature threshold for active growth	TMPCUT	1.0	1.0	1.0	1.0	1.0
Unsaturated soil moisture redistribution	IUNSAT	Y	Y	Y	Y	Y
Streamflow simulation control variables	QFRESP COFRU SMDDEP IRUN ADJIMP DISIMP STOIMP	0.21, 0.21 0.006, 0.006 0.35, 0.00 Y, Y 0.00, 0.00 0.00, 0.00 1.00, 1.00	0.20 (1-5) 0.035 (1-5) 0.27, 0.27, 0.28, 0.25, 0.21 Y (1-5) 0.00 (1-5) 0.630 (1-5) 1.00 (1-5)	0.75 (1-7) 0.026 (1-7) 0.00 (1-2), 0.35 (3-7) Y (1-7) 0.00 (1-7) 0.454, 0.684, 0.454 (3-5), 0.250, 0.454 1.00 (1-7)	0.35 (1-6) 0.038 (1-6) 0.00 (1-6) Y (1-6) 0.00 (1-6) 0.508, 0.508, 0.583, 0.640, 0.652, 0.426 1.00 (1-6)	0.30 (1-7) 0.018 (1-7) 0.00 (1-6), 0.35 Y (1-7) 0.00 (1-6), 0.001 0.644, 0.644, 0.639, 0.652, 0.639, 0.639, 0.301 1.00 (1-7)

Group Description	Variable	LAMBRECHTSBOS B	WATERVALSRIVIER	DIEPRIVIER	KRUISRIVIER	BLOUKRANSRIVIER
Coefficient of initial abstraction	COIAM	1:0.35 Jan - Dec 2:0.15, 0.15,0.15, 0.20, 0.30, 0.30, 0.30, 0.30, 0.30, 0.35, 0.25, 0.25	Jan-Dec (1-5): 0.30	Jan-Dec 1: 0.30 Jan-Dec 2: 0.30 Jan-Dec 3: 0.32 Jan-Dec 4: 0.33 Jan-Dec 5: 0.34 Jan-Dec 6: 0.34 Jan-Dec 7: 0.34	1:0.15, 0.15, 0.35, 0.20, 0.30, 0.30, 0.30, 0.30, 0.30, 0.30, 0.20, 0.15 2:0.15, 0.15, 0.35, 0.20, 0.30, 0.30, 0.30, 0.30, 0.30, 0.30, 0.20, 0.15 3:0.18, 0.18, 0.27, 0.23, 0.30, 0.30, 0.30, 0.30, 0.30, 0.32, 0.20, 0.20 4:0.20, 0.20, 0.20, 0.20, 0.20, 0.20, 0.20, 0.20, 0.20, 0.20, 0.20, 0.20 5:0.15, 0.15, 0.35, 0.20, 0.30, 0.30, 0.30, 0.30, 0.30, 0.30, 0.20, 0.15 6:0.20, 0.20, 0.20, 0.20, 0.20, 0.20, 0.20, 0.20, 0.20, 0.20, 0.20, 0.20	1:0.20, 0.20, 0.20, 0.20, 0.30, 0.30, 0.30, 0.30, 0.30, 0.30, 0.20, 0.20 2:0.20, 0.20, 0.20, 0.20, 0.30, 0.30, 0.30, 0.30, 0.30, 0.30, 0.20, 0.20 3:0.20, 0.20, 0.20, 0.20, 0.30, 0.30, 0.30, 0.30, 0.30, 0.30, 0.20, 0.20 4:0.28, 0.28, 0.28, 0.28, 0.30, 0.30, 0.30, 0.30, 0.30, 0.30, 0.28, 0.28 5:0.28, 0.28, 0.28, 0.28, 0.30, 0.30, 0.30, 0.30, 0.30, 0.30, 0.28, 0.28 6:0.20, 0.20, 0.20, 0.20, 0.30, 0.30, 0.30, 0.30, 0.30, 0.30, 0.20, 0.20 7:0.32, 0.32, 0.32, 0.32, 0.34, 0.34, 0.34, 0.34, 0.34, 0.34, 0.32, 0.32
Abstraction option	IDOMR	0 (no abstraction)	0 (no abstraction)	0 (1-5,7), 1 (6)	0 (no abstraction)	0 (no abstraction)
Monthly averages of daily abstractions	DOMABS	N/A	N/A	(1-5): N/A 6: 0.1 Jan-Dec 7: N/A	N/A	N/A

Group Description	Variable	ZULULAND	CATHEDRAL PEAK	DEHOEK	WITKLIP	TREURRIVIER
Mode of simulation	ICELL	1 (distributed)	0 (lumped)	1 (distributed)	1 (distributed)	1 (distributed)
Distributed mode options	ISUBNO MINSUB MAXSUB LOOPBK	4 1 4 0	1 1 1 0	4 1 4 0	9 1 9 0	10 1 10 0
Flow routing options	IROUTE DELT	N N/A	N N/A	N N/A	N N/A	N N/A
Subcatchment configuration	ICELLN IDSTRM	1, 2, 3, 4 2, 3, 3, 4	1 1	1, 2, 3, 4 2, 3, 4, 4	1, 2, 3, 4, 5, 6, 7, 8, 9 2, 3, 4, 5, 6, 7, 8, 9, 9	1, 2, 3, 4, 5, 6, 7, 8, 9, 10 3, 3, 4, 5, 6, 9, 8, 9, 10, 10
Rainfall file	IRAINF	470.sin	Cmp7179	(1-2): n11b.sin, n11b.sin (3-4): n9.sin, n9.sin	CmpV7590	(1, 2, 4, 5): 0594764.sin (9): 0594494.sin (3, 6, 7, 8, 10): 0594590.sin
Rainfall information	FORMAT PPTCOR MAP	2 N 1314	1 Y 1664	2, 2, 2, 2 N 751, 751, 820, 820	1 N 1100	2 (1-9) Y (1-9) 1425, 1595, 1355, 1548, 1512, 1254, 1028, 953, 792, 1009
Monthly rainfall adjustment factors	CORPPT	N/A	Jan-Dec: 1.20	N/A	N/A	1:0.98, 0.95, 0.92, 0.85, 0.98, 10.02, 0.70, 0.70, 0.80, 0.98, 0.99, 0.89 2:1.08, 1.05, 1.03, .97, 1.08, 1.13, .78, .70, .92, 1.10, 1.10, 1.00 3:1.07, 1.03, 1.13, 1.25, 1.06, .70, .94, 1.18, 1.13, 1.14, 1.13, 1.21 4:1.05, 1.03, .99, .95, 1.06, 1.02, .71, .70, .85, 1.05, 1.07, .97 5:1.02, 1.00, .97, .95, 1.05, 1.02, .70, .70, .84, 1.02, 1.04, .96 6:0.97, 0.94, 1.03, 1.20, 1.02, 0.70, 0.78, 1.00, 0.98, 1.04, 1.03, 1.13 7:0.79, 0.77, 0.84, 0.97, 0.83, 0.70, 0.70, 0.70, 0.73, 0.86, 0.87, 0.91 8:0.73, 0.71, 0.78, 0.91, 0.77, 0.70, 0.70, 0.70, 0.70, 0.79, 0.80, 0.84 9:1.25, 1.26, 1.24, 1.16, 1.18, 1.30, 1.30, 1.30, 1.30, 1.19, 1.18, 1.21 10:0.76, 0.75, 0.81, 0.97, 0.83, 0.70, 0.70, 0.70, 0.70, 0.81, 0.83, 0.88
Availability of observed streamflow data	IOBSTQ IOBSPK IOBOVR	0, 0, 0, 1 0, 0, 0, 0 0, 0, 0, 0	1 0 0	0, 0, 0, 1 0, 0, 0, 0 0, 0, 0, 0	0, 0, 0, 0, 0, 0, 0, 0, 1 0, 0, 0, 0, 0, 0, 0, 0, 0 0, 0, 0, 0, 0, 0, 0, 0, 0	0, 0, 0, 0, 0, 0, 0, 0, 0, 1 0, 0, 0, 0, 0, 0, 0, 0, 0, 0 0, 0, 0, 0, 0, 0, 0, 0, 0, 0
Streamflow file	ISTRMF	W1h016f.sin	COMPOSITE FORMAT	V1h015.sin	COMPOSITE FORMAT	B6h003f.sin
Dynamic file name	DNAMIC IDYNFL	N -	N -	N -	N -	N -
Catchment information	CLAREA ELEV ALAT ALONG IHEMI IQUAD	0.71, 0.73, 1.08, 0.72 252.0, 252.0, 252.0, 202.0 28.83, 28.83, 28.82, 28.82 31.75, 31.77, 31.77, 31.78 2, 2, 2, 2 1, 1, 1, 1	0.99 2000.0 29.00 29.42 2 1	0.21, 0.27, 0.19, 0.34 1685, 1685, 1511, 1511 29.00, 29.02, 29.02, 29.00 29.62, 29.62, 29.63, 29.63 2, 2, 2, 2 1, 1, 1, 1	0.52, 0.02, 0.05, 0.02, 0.10, 0.02, 0.18, 0.14, 0.03 1250, 1180, 1180, 1180, 1100 (5-9) 25.23 (1-9) 30.88 (1-9) 2 (1-9) 1 (1-9)	5.30, 8.42, 4.67, 4.83, 12.42, 21.84, 6.86, 14.22, 7.41, 7.48 1587.0, 1545.0, 1516.0, 1629.0, 1596.7, 1462.1, 1460.0, 1349.2, 1200.0, 1305.0 24.82, 24.80, 24.80, 24.78, 24.75, 24.73, 24.77, 24.73, 24.72, 24.70 30.88, 30.90, 30.88, 30.88, 30.87, 30.82, 30.83, 30.83, 30.83 2 (1-10) 1 (1-10)
Period of record for simulation	IYSTRT IYREND	1977 1981	1971 1979	1985 1988	1975 1983	1981 1986

154

Group Description	Variable	ZULULAND	CATHEDRAL PEAK	DEHOEK	WITKLIP	TREURRIVIER
Monthly means of daily maximum temperature	TMAX	Jan-Dec (1-4): 29.8, 30.5, 29.3, 28.1, 25.7, 23.5, 23.7, 24.3, 24.5, 26.4, 27.4, 29.3	Jan-Dec: 26.0, 25.6, 24.6, 22.3, 19.9, 17.3, 17.6, 19.7, 22.0, 23.1, 24.0, 25.6	1:26.5, 25.8, 25.0, 22.7, 20.3, 18.0, 18.2, 20.2, 22.8, 23.4, 24.3, 26.1 2:26.5, 25.8, 25.0, 22.7, 20.3, 18.0, 18.2, 20.2, 22.8, 23.4, 24.3, 26.1 3:26.7, 26.2, 25.2, 23.0, 20.7, 18.3, 18.6, 20.5, 23.0, 23.7, 24.6, 26.3 4:26.7, 26.2, 25.2, 23.0, 20.7, 18.3, 18.6, 20.5, 23.0, 23.7, 24.6, 26.3	Jan-Dec (1-9): 28.0, 27.9, 26.8, 25.5, 24.6, 22.6, 22.8, 24.7, 27.2, 27.0, 27.1, 27.8	1:23.0, 23.0, 22.0, 21.0, 19.5, 17.5, 17.5, 19.0, 21.0, 21.5, 22.0, 23.0 2:23.3, 23.3, 22.3, 21.7, 20.0, 18.0, 18.3, 20.0, 21.0, 21.7, 22.3, 23.0 3:23.5, 23.5, 22.5, 21.5, 19.5, 17.0, 17.5, 19.0, 21.0, 22.0, 22.5, 23.0 4:22.5, 22.5, 21.5, 21.0, 19.5, 17.5, 17.5, 19.0, 20.5, 21.5, 21.5, 22.5 5:23.3, 22.5, 22.5, 21.3, 20.3, 17.8, 18.0, 19.3, 20.8, 21.5, 22.0, 22.5 6:23.9, 23.8, 22.9, 21.6, 20.0, 17.8, 18.0, 19.8, 21.6, 22.4, 22.9, 23.5 7:24.0, 23.5, 23.0, 21.5, 20.0, 17.5, 17.5, 19.5, 21.5, 22.5, 23.0, 23.5 8:24.8, 24.4, 23.8, 22.4, 20.8, 18.2, 18.4, 20.4, 22.2, 23.0, 23.6, 24.2 9:26.0, 25.0, 25.0, 23.0, 21.5, 19.0, 19.0, 21.0, 23.0, 24.0, 24.0, 25.0 10:25.0, 25.0, 24.0, 22.7, 21.0, 18.3, 19.0, 20.7, 22.7, 23.7, 24.0, 24.7
Monthly means of daily minimum temperature	TMIN	Jan-Dec (1-4): 20.4, 21.1, 20.2, 17.0, 13.8, 10.3, 10.8, 13.1, 13.8, 16.0, 18.1, 21.0	Jan-Dec: 13.9, 13.7, 12.4, 9.0, 5.5, 2.6, 2.4, 4.5, 7.5, 9.7, 11.4, 13.0	1: 14.1, 14.1, 12.9, 10.1, 6.9, 3.9, 4.0, 5.7, 8.0, 9.9, 11.6, 13.2 2: 14.1, 14.1, 12.9, 10.1, 6.9, 3.9, 4.0, 5.7, 8.0, 9.9, 11.6, 13.2 3: 14.0, 13.9, 12.5, 9.2, 5.3, 2.1, 2.1, 4.4, 7.5, 9.7, 11.5, 13.1 4: 14.0, 13.9, 12.5, 9.2, 5.3, 2.1, 2.1, 4.4, 7.5, 9.7, 11.5, 13.1	Jan-Dec (1-9): 14.3, 14.4, 13.6, 10.6, 8.5, 5.5, 5.4, 6.5, 8.9, 11.3, 12.3, 13.7	1: 13.0, 13.0, 12.0, 10.0, 7.0, 4.5, 4.5, 6.0, 8.0, 10.0, 11.5, 12.5, 2: 13.0, 13.0, 12.3, 10.7, 8.3, 5.7, 5.3, 7.0, 8.7, 10.3, 11.3, 13.0, 3: 13.5, 13.0, 12.0, 10.0, 6.5, 4.0, 3.5, 5.5, 8.0, 10.0, 12.0, 13.0, 4: 12.5, 12.5, 12.0, 10.5, 8.0, 6.0, 5.0, 7.0, 8.5, 10.0, 11.5, 12.5, 5: 12.8, 12.5, 12.8, 10.5, 8.3, 6.0, 5.8, 7.3, 8.8, 10.0, 11.5, 12.5, 6: 13.6, 13.6, 12.9, 10.5, 7.6, 4.8, 4.6, 6.3, 8.5, 10.5, 11.9, 13.4, 7: 13.5, 13.5, 12.5, 11.0, 8.0, 5.5, 5.5, 7.0, 9.0, 10.5, 12.0, 13.5, 8: 14.2, 14.2, 13.4, 10.4, 7.2, 4.4, 4.2, 6.2, 8.6, 10.8, 12.6, 13.8, 9: 15.0, 15.0, 14.0, 11.0, 7.0, 4.0, 4.0, 6.0, 9.0, 12.0, 13.0, 15.0, 10: 14.7, 14.7, 13.7, 11.0, 8.3, 5.3, 5.3, 7.0, 9.3, 11.3, 13.0, 14.0,
Reference potential evaporation option	EQPET	102	102	102	102	102
Evaporation input availability control flags	IEIF ILRF IWDF IRHF ISNF IRDF IPNF	1 0 0 0 0 0 0	1 0 0 0 0 0 0	1 0 0 0 0 0 0	0, 1, 1, 1, 1, 1, 1, 1 0, 0, 0, 0, 0, 0, 0, 0, 0 0, 0, 0, 0, 0, 0, 0, 0, 0 0, 0, 0, 0, 0, 0, 0, 0, 0 0, 0, 0, 0, 0, 0, 0, 0, 0 0, 0, 0, 0, 0, 0, 0, 0, 0 0, 0, 0, 0, 0, 0, 0, 0, 0	1 0 0 0 (1-10) 0 0 0

Group Description	Variable	ZULULAND	CATHEDRAL PEAK	DEHOEK	WITKLIP	TREURRIVIER
Monthly totals of A-pan equivalent evaporation	E	1:190.0, 164.0, 163.0, 139.0, 108.0, 84.0, 104.0, 127.0, 140.0, 169.0, 165.0, 195.0 2:190.7, 164.9, 163.1, 139.3, 108.5, 84.0, 104.6, 127.1, 140.2, 169.4, 165.3, 195.3 3:190.0, 164.0, 163.0, 139.0, 108.0, 84.0, 104.0, 127.0, 140.0, 169.0, 165.0, 195.0 4:191.0, 165.0, 163.0, 138.0, 108.0, 84.0, 104.0, 126.0, 139.0, 169.0, 166.0, 196.0	156.3, 132.3, 122.8, 111.4, 96.9, 83.9, 96.9, 130.7, 143.8, 145.9, 144.9, 168.0	1:194.4, 161.4, 148.0, 121.8, 99.8, 92.1, 101.5, 138.1, 162.4, 163.5, 170.9, 196.6 2:194.4, 161.4, 148.0, 121.8, 99.8, 92.1, 101.5, 138.1, 162.4, 163.5, 170.9, 196.6 3:192.9, 163.7, 151.3, 122.7, 100.6, 91.3, 101.0, 136.6, 161.4, 167.1, 174.3, 197.8 4:192.9, 163.7, 151.3, 122.7, 100.6, 91.3, 101.0, 136.6, 161.4, 167.1, 174.3, 197.8	190.0, 170.0, 170.0, 135.0, 125.0, 105.0, 115.0, 145.0, 170.0, 190.0, 190.0, 200.0	1:169.5, 160.5, 160.0, 145.0, 134.0, 109.5, 117.0, 147.0, 166.5, 185.0, 175.5, 177.0, 2:168.0, 163.3, 161.3, 148.3, 135.6, 111.0, 118.6, 146.6, 167.6, 186.0, 173.0, 176.0, 3:173.5, 161.5, 161.5, 145.0, 132.5, 107.5, 115.5, 146.5, 168.0, 187.0, 177.5, 179.5, 4:167.0, 160.5, 159.5, 147.5, 136.5, 111.5, 118.5, 147.5, 166.5, 183.5, 173.0, 174.5, 5:168.7, 160.7, 160.0, 149.0, 137.0, 112.2, 120.0, 148.0, 168.0, 185.2, 174.2, 175.7, 6:177.2, 161.7, 162.0, 145.0, 132.7, 108.3, 116.6, 147.6, 169.6, 188.8, 180.8, 182.3, 7:182.0, 158.5, 162.5, 144.5, 132.0, 108.0, 116.0, 148.5, 171.5, 189.5, 185.0, 186.5, 8:186.2, 161.0, 164.2, 144.0, 131.0, 107.4, 116.0, 148.4, 172.4, 192.4, 187.4, 189.8, 9:193.0, 164.0, 167.0, 143.0, 130.0, 106.5, 116.0, 148.5, 174.5, 196.5, 192.5, 195.5, 10:186.3, 163.3, 164.6, 143.3, 130.3, 106.6, 116.0, 148.6, 172.3, 193.3, 187.6, 190.3,
Temperature adjustment for altitude	TELEV LRREG	N N/A	N N/A	N N/A	N N/A	N N/A
Mean lapse rates for min and max temperature	TMAXLR TMINLR	7.00 5.50	7.00 5.50	7.00 5.50	7.00 5.50	7.00 5.50
Mean daily wind speed (m/s)	WNDSPD	1.6	1.6	1.6	1.6	1.6
Penman equation option for S-tank or A-pan equivalent evaporation	SAPANC	N	N	N	N	N
Smoothed mean monthly A-pan/S-pan ratios	SARAT	N/A	N/A	N/A	N/A	N/A
Pan adjustment option	PANCOR CORPAN	0 -	0 -	0 -	0 -	0 -
Level of soils information	PEDINF	1	1	1	1	1
Soils texture information	ITEXT	7	11	9	5	7
Soil thickness information	PEDDEP	2	2	2	2	2

156

Group Description	Variable	ZULULAND	CATHEDRAL PEAK	DEHOEK	WITKLIP	TREURRIVIER
Soils information	DEPAHO DEPBHO WP1 WP2 FC1 FC2 PO1 PO2 ABRESP BFRESP	0.20 (1-4) 0.16, 0.14 (2-4) 0.118, 0.129 (2-4) 0.105, 0.108 (2-4) 0.209, 2.224 (2-4) 0.204, 0.210 (1-4) 0.465, 0.450 (2-4) 0.442, 0.427 (2-4) 0.36, 0.34 (2-4) 0.36, 0.34 (2-4)	0.20 0.60 0.250 0.245 0.370 0.376 0.476 0.491 0.50 0.50	0.31, 0.31, 0.28, 0.28 0.59, 0.59, 0.47, 0.47 0.137, 0.137, 0.139, 0.139 0.197, 0.197, 0.190, 0.190 0.223, 0.223, 0.225, 0.225 0.268, 0.268, 0.263, 0.263 0.433, 0.433, 0.432, 0.432 0.406 (1-4) 0.44 (1-2), 0.42 (3-4) 0.44 (1-2), 0.42 (3-4)	0.34 (1-9) 0.43, 0.68 (2-9) 0.174 (1-9) 0.219 (1-9) 0.282 (1-9) 0.344 (1-9) 0.400 (1-9) 0.429 (1-9) 0.65 (1-9) 0.65 (1-9)	0.25, 0.23, 0.25, 0.24, 0.22, 0.24, 0.23, 0.23, 0.25, 0.24 0.40, 0.29, 0.65, 0.38, 0.28, 0.58, 0.24, 0.30, 0.58, 0.59 0.142, 0.154, 0.142, 0.154, 0.157, 0.141, 0.146, 0.152, 0.147, 0.145 0.180, 0.184, 0.180, 0.186, 0.176, 0.163, 0.169, 0.179, 0.169, 0.168 0.233, 0.252, 0.233, 0.251, 0.256, 0.234, 0.234, 0.244, 0.238, 0.237 0.269, 0.284, 0.269, 0.286, 0.279, 0.254, 0.254, 0.271, 0.259, 0.259 0.433, 0.420, 0.433, 0.420, 0.419, 0.435, 0.432, 0.425, 0.431, 0.431 0.416, 0.419, 0.416, 0.419, 0.419, 0.414, 0.408, 0.412, 0.411, 0.411 0.43, 0.40, 0.43, 0.41, 0.39, 0.42, 0.35, 0.36, 0.38, 0.39 0.43, 0.40, 0.43, 0.41, 0.39, 0.42, 0.35, 0.36, 0.38, 0.39
Initial soil water content	SMAINI SMBINI	0.00 0.00	0.80 0.80	0.00 0.00	0.50 0.50	0.00 0.00
Level of land cover information	LCOVER	1	1	1	1	1
	CROPNO	-	-	-	-	-
Determination pf canopy interception loss	INTLOS	1	1	1	1, 2 (2-9)	1 (1-10)
Leaf area index information	LAIND	0	0	0	0, 1 (2-9)	0 (1-10)
Monthly means of crop coefficients	CAY	1: 0.75, 0.75, 0.75, 0.65, 0.55, 0.40, 0.40, 0.50, 0.65, 0.75, 0.75, 0.75 2:0.70, 0.70, 0.70, 0.60, 0.27, 0.20, 0.20, 0.25, 0.32, 0.87, 0.87, 0.87 3:0.70, 0.70, 0.70, 0.60, 0.27, 0.20, 0.20, 0.25, 0.32, 0.87, 0.87, 0.87 4:0.82, 0.82, 0.82, 0.77, 0.61, 0.57, 0.57, 0.60, 0.63, 0.91, 0.91, 0.91	0.70, 0.70, 0.60, 0.50, 0.30, 0.20, 0.20, 0.20, 0.35, 0.55, 0.70, 0.70	0.65, 0.65, 0.65, 0.55, 0.30, 0.20, 0.20, 0.20, 0.30, 0.50, 0.55, 0.65	1:0.65, 0.65, 0.65, 0.55, 0.30, 0.20, 0.20, 0.20, 0.30, 0.50, 0.55, 0.65 (2-9) N/A	1:0.78, 0.78, 0.78, 0.75, 0.67, 0.63, 0.63, 0.63, 0.67, 0.73, 0.75, 0.70 2:0.78, 0.78, 0.78, 0.74, 0.59, 0.54, 0.54, 0.55, 0.60, 0.71, 0.73, 0.70 3:0.75, 0.75, 0.75, 0.70, 0.58, 0.53, 0.53, 0.53, 0.58, 0.68, 0.70, 0.70, 4:0.80, 0.80, 0.80, 0.78, 0.71, 0.69, 0.69, 0.69, 0.71, 0.76, 0.78, 0.80, 5:0.71, 0.71, 0.71, 0.62, 0.45, 0.35, 0.35, 0.38, 0.48, 0.62, 0.65, 0.70, 6:0.73, 0.73, 0.73, 0.67, 0.52, 0.45, 0.45, 0.46, 0.53, 0.65, 0.68, 0.70, 7:0.70, 0.70, 0.70, 0.60, 0.43, 0.30, 0.30, 0.35, 0.48, 0.63, 0.65, 0.70, 8:0.74, 0.74, 0.74, 0.66, 0.53, 0.44, 0.44, 0.48, 0.57, 0.68, 0.70, 0.70, 9:0.75, 0.75, 0.75, 0.69, 0.57, 0.51, 0.51, 0.52, 0.59, 0.69, 0.71, 0.70 10:0.71, 0.71, 0.71, 0.63, 0.46, 0.37, 0.37, 0.39, 0.48, 0.62, 0.65, 0.71
Monthly means of leaf area index	ELAIM	N/A	N/A	N/A	N/A (1) 4.50 (2-4) 4.90 (5-9)	N/A

157

Group Description	Variable	ZULULAND	CATHEDRAL PEAK	DEHOEK	WITKLIP	TREURRIVIER
Canopy interception loss (mm) per rainday	VEGINT	1:2.50, 2.50, 2.00, 2.00, 2.00, 2.00, 2.00, 2.00, 2.00, 2.50, 2.50, 2.50 2:2.00, 2.00, 1.75, 1.75, 1.75, 1.75, 1.75, 1.75, 1.75, 2.00, 2.00, 2.00 3:2.00, 2.00, 1.75, 1.75, 1.75, 1.75, 1.75, 1.75, 1.75, 2.00, 2.00, 2.00 4:2.25, 2.25, 2.12, 2.12, 2.12, 2.12, 2.12, 2.12, 2.12, 2.25, 2.25, 2.25	1.40, 1.40, 1.40, 1.40, 1.20, 1.00, 1.00, 1.00, 1.10, 1.20, 1.40, 1.40	Jan-Dec (1-4): 1.50	Jan-Dec (1-9): 1.50	1:2.83, 2.83, 2.83, 2.83, 2.83, 2.83, 2.83, 2.83, 2.83, 2.83, 2.83, 2.83 2:2.66, 2.66, 2.59, 2.59, 2.59, 2.59, 2.59, 2.59, 2.59, 2.66, 2.66, 2.66 3:2.50, 2.50, 2.50, 2.50, 2.50, 2.50, 2.50, 2.50, 2.50, 2.50, 2.50, 2.50 4:3.00, 3.00, 3.00, 3.00, 3.00, 3.00, 3.00, 3.00, 3.00, 3.00, 3.00, 3.00 5:2.07, 2.07, 1.93, 1.93, 1.93, 1.93, 1.93, 1.93, 2.07, 2.07, 2.07, 2.07 6:2.27, 2.27, 2.27, 2.25, 2.24, 2.24, 2.24, 2.24, 2.24, 2.25, 2.26, 2.27 7:2.00, 2.00, 1.75, 1.75, 1.75, 1.75, 1.75, 1.75, 1.75, 2.00, 2.00, 2.00 8:2.38, 2.38, 2.19, 2.19, 2.19, 2.19, 2.19, 2.19, 2.19, 2.38, 2.38, 2.38 9:2.50, 2.50, 2.43, 2.43, 2.43, 2.43, 2.43, 2.43, 2.50, 2.50, 2.50 10:2.10, 2.10, 2.00, 2.00, 2.00, 2.00, 2.00, 2.00, 2.00, 2.10, 2.10, 2.10
Fraction of active root system in topsoil horizon specified month by month	ROOTA	1:0.80, 0.80, 0.90, 0.90, 0.90, 0.90, 0.90, 0.90, 0.90, 0.80, 0.80, 0.80 2:0.85, 0.85, 0.90, 0.92, 0.94, 0.95, 0.95, 0.95, 0.95, 0.88, 0.85, 0.85 3:0.85, 0.85, 0.90, 0.92, 0.94, 0.95, 0.95, 0.95, 0.95, 0.88, 0.85, 0.85 4:0.75, 0.75, 0.77, 0.79, 0.80, 0.80, 0.80, 0.80, 0.80, 0.76, 0.75, 0.75	0.90, 0.90, 0.90, 0.95,1.00,1.00, 1.00,1.00, 0.95, 0.90, 0.90, 0.90	0.90, 0.90, 0.90, 0.94, 0.98, 1.00, 1.00, 1.00, 1.00, 0.95, 0.90, 0.90	1: 0.90, 0.90, 0.90, 0.94, 0.98, 1.00, 1.00, 1.00,1.00, 0.95, 0.90, 0.90 2-4: 0.45 5-9: 0.40	1:0.74, 0.74, 0.74, 0.75, 0.77, 0.77, 0.77, 0.77, 0.77, 0.76, 0.74, 0.74 2:0.77, 0.77, 0.78, 0.79, 0.80, 0.81, 0.81, 0.81, 0.81, 0.78, 0.77, 0.77 3:0.78, 0.78, 0.78, 0.80, 0.82, 0.83, 0.83, 0.83, 0.83, 0.81, 0.78, 0.78 4:0.72, 0.72, 0.72, 0.72, 0.73, 0.74, 0.75, 0.75, 0.75, 0.73, 0.72, 0.72 5:0.84, 0.84, 0.87, 0.89, 0.91, 0.92, 0.92, 0.92, 0.92, 0.87, 0.84, 0.84 6:0.80, 0.80, 0.80, 0.83, 0.86, 0.87, 0.87, 0.87, 0.87, 0.84, 0.80, 0.80 7:0.85, 0.85, 0.90, 0.92, 0.94, 0.95, 0.95, 0.95, 0.95, 0.88, 0.85, 0.85 8:0.80, 0.80, 0.84, 0.86, 0.87, 0.88, 0.88, 0.88, 0.88, 0.82, 0.80, 0.80 9:0.78, 0.78, 0.79, 0.81, 0.83, 0.84, 0.84, 0.84, 0.84, 0.80, 0.78, 0.78 10:0.83, 0.83, 0.85, 0.88, 0.90, 0.91, 0.91, 0.91, 0.91, 0.86, 0.83, 0.83
Effective total rooting depth	EFRDEP	Defaulted to DEPAHO+DEPBHO	Defaulted to DEPAHO+DEPBHO	0.50	Defaulted to DEPAHO+DEPBHO	Defaulted to DEPAHO+DEPBHO
Total evaporation control variables	EVTR FPAW	1 0	2 0	2 0	2 0	2 0
Fraction of PAW at which plant stress sets in	CONST	0.4	0.40	0.40	0.40 (1), 0.10 (2-4), 0.90 (5-9)	0.73, 0.47, 0.65, 0.77, 0.47, 0.58, 0.40, 0.52, 0.61, 0.50
Critical leaf water potential	CRLEPO	N/A	N/A	N/A	N/A	N/A
Option for enhanced wet canopy evaporation	FOREST	0	0	0	0, 1 (2-9)	(1,2, 4-8): 0 (3,9,10): 1
Mean temperature threshold for active growth	TMPCUT	1.0	1.0	1.0	1.0	1.0
Unsaturated soil moisture redistribution	IUNSAT	Y	Y	Y	Y	Y

Group Description	Variable	ZULULAND	CATHEDRAL PEAK	DEHOEK	WITKLIP	TREURRIVIER
Streamflow simulation control variables	QFRESP COFRU SMDDEP IRUN ADJIMP DISIMP STOIMP	0.40 (1-4) 0.022 (1-4) 0.00 (1-3), 0.20 (4) Y (1-4) 0.10, 0.009 (2-4) 0.105, 0.100 (2-4) 1.00 (1-4)	0.06 0.018 0.40 Y 0.00 0.00 1.00	0.75 (1-4) 0.063 (1-4) 0.00 (1-4) Y (1-4) 0.023 (1-2), 0.019 (3-4) 0.047 (1-2), 0.125 (3-4) 1.00 (1-4)	0.11 (1-9) 0.012 (1-9) 0.00, 0.35 (2-9) Y (1-9) 0.001 (1-9) 0.075 (1-9) 1.00 (1-9)	0.19 (1-10) 0.014 (1-10) 0.00 (1, 2, 4, 5, 7, 8), 0.35 (3, 6, 9, 10) Y (1-10) 0.002, 0.003, 0.002, 0.001, 0.003, 0.003, 0.007, 0.003, 0.007, 0.003 0.358, 0.469, 0.358, 0.254, 0.427, 0.465, 0.302, 0.209, 0.320, 0.293 1.00 (1-10)
Coefficient of initial abstraction	COIAM	1:0.20, 0.20, 0.20, 0.20, 0.30, 0.30, 0.30, 0.30, 0.30, 0.30, 0.20, 0.20 2:0.17, 0.17, 0.17, 0.20, 0.30, 0.30, 0.30, 0.30, 0.30, 0.30, 0.20, 0.17 3:0.17, 0.17, 0.17, 0.20, 0.30, 0.30, 0.30, 0.30, 0.30, 0.30, 0.20, 0.17 4:0.26, 0.26, 0.26, 0.28, 0.32, 0.32, 0.32, 0.32, 0.32, 0.32, 0.28, 0.26	0.20, 0.20, 0.20, 0.25, 0.30, 0.30, 0.30, 0.30, 0.30, 0.30, 0.20, 0.20	0.15, 0.15, 0.15, 0.20, 0.30, 0.30, 0.30, 0.30, 0.30, 0.30, 0.20, 0.15 (1-4)	1: 0.15, 0.15, 0.15, 0.20, 0.30, 0.30, 0.30, 0.30, 0.30, 0.30, 0.20, 0.15 2-9: 0.35, 0.35, 0.35, 0.35, 0.35, 0.35, 0.35, 0.35, 0.35, 0.35, 0.35, 0.35	1:0.28, 0.28, 0.28, 0.30, 0.33, 0.33, 0.33, 0.33, 0.33, 0.33, 0.30, 0.28 2:0.27, 0.27, 0.27, 0.29, 0.33, 0.33, 0.33, 0.33, 0.33, 0.33, 0.29, 0.27 3:0.25, 0.25, 0.25, 0.28, 0.33, 0.33, 0.33, 0.33, 0.33, 0.33, 0.28, 0.25, 4:0.30, 0.30, 0.30, 0.31, 0.34, 0.34, 0.34, 0.34, 0.34, 0.34, 0.31, 0.30 5:0.19, 0.19, 0.19, 0.22, 0.31, 0.31, 0.31, 0.31, 0.31, 0.31, 0.22, 0.19 6:0.23, 0.23, 0.23, 0.25, 0.32, 0.32, 0.32, 0.32, 0.32, 0.32, 0.25, 0.23 7:0.18, 0.18, 0.18, 0.20, 0.30, 0.30, 0.30, 0.30, 0.30, 0.30, 0.20, 0.18 8:0.22, 0.22, 0.22, 0.24, 0.31, 0.31, 0.31, 0.31, 0.31, 0.31, 0.24, 0.22 9:0.24, 0.24, 0.24, 0.26, 0.32, 0.32, 0.32, 0.32, 0.32, 0.32, 0.26, 0.24 10:0.20, 0.20, 0.20, 0.23, 0.31, 0.31, 0.31, 0.31, 0.31, 0.31, 0.23, 0.20
Abstraction option	IDOMR	0 (no abstraction)	0 (no abstraction)	0 (no abstraction)	0 (no abstraction)	0 (no abstraction)
Monthly averages of daily abstractions	DOMABS	N/A	N/A	N/A	N/A	N/A

Group Description	Variable	BEESTEKRAALSPRUIT	WESTFALIA B	GROOT-NYLRIVIER	SAFFORD
Mode of simulation	ICELL	1 (distributed)	0 (lumped)	1 (distributed)	0 (lumped)
Distributed mode options	ISUBNO	3	1	6	1
	MINSUB	1	1	1	1
	MAXSUB	3	1	6	1
	LOOPBK	0	0	0	0
Flow routing options	IROUTE	N	N	N	N
	DELT	N/A	N/A	N/A	N/A
Subcatchment configuration	ICELLN	1, 2, 3	1	1, 2, 3, 4, 5, 6	1
	IDSTRM	3, 3, 3	1	2, 3, 6, 5, 6, 6	1
Rainfall file	IRAINF	moko.sin, moko.sin, x2h026.sin	CmpB8590	(1-3,5,6): 0589586.sin (4): 0589670.sin	RG00002.SIN
Rainfall information	FORMAT	2, 2, 2	1	2, 2, 2, 2, 2	2
	PPTCOR	N	N	Y (1-6)	N
	MAP	1087, 1004, 822	1404	625, 633, 649, 625, 649, 704	225
Monthly rainfall adjustment factors	CORPPT	N/A	N/A	1:0.98, 0.88, 0.96, 0.70, 0.79, 0.70, 0.70, 0.70, 1.01, 0.83, 0.92, 0.89 2:0.99, 0.89, 0.96, 0.70, 0.79, 0.70, 0.70, 0.70, 1.02, 0.84, 0.93, 0.90 3:0.99, 0.92, 0.97, 0.76, 0.79, 0.70, 0.70, 0.70, 1.03, 0.89, 0.95, 0.92 4:1.02, 0.97, 1.08, 1.01, 0.70, 0.70, 0.70, 0.70, 0.73, 0.85, 0.99, 1.00 5:1.00, 0.93, 0.95, 0.75, 0.79, 0.70, 0.70, 0.70, 1.05, 0.86, 0.94, 0.91 6:1.00, 0.99, 1.00, 0.98, 0.95, 0.70, 0.70, 0.70, 0.92, 0.99, 1.00, 1.00	N/A
Availability of observed streamflow data	IOBSTQ	0, 0, 1	1	0, 0, 0, 0, 0, 1	1
	IOBSPK	0, 0, 0	0	0, 0, 0, 0, 0, 0	0
	IOBOVR	0, 0, 0	0	0, 0, 0, 0, 0, 0	0
Streamflow file	ISTRMF	X2h026f.sin	COMPOSITE FORMAT	A6h011f.sin	4501.SIN
Dynamic file name	DNAMIC	N	N	N	N
	IDYNFL	-	-	-	-
Catchment information	CLAREA	7.80, 3.12, 2.44	0.33	16.54, 14.00, 13.96, 16.63, 11.06, 2.56	2.10
	ELEV	1373.6, 1359.0, 1128.0	1250.0	1416.6, 1390.0, 1324.0, 1405.0, 1266.0, 1220.0	1020.0
	ALAT	25.25, 25.23, 25.27	23.72	24.77, 24.77, 24.77, 24.73, 24.73, 24.75	32.92
	ALONG	30.58, 30.57, 30.57	30.07	28.25, 28.27, 28.30, 28.28, 28.32, 28.33	99.59
	IHEMI	2, 2, 2	2	2	1
	IQUAD	1, 1, 1	1	1	2
Period of record for simulation	IYSTRT	1971	1985	1968	1939
	IYREND	1975	1990	1978	1969
Monthly means of daily maximum temperature	TMAX	1:25.0, 24.7, 24.0, 22.3, 20.7, 18.3, 18.3, 20.7, 22.7, 23.3, 23.7, 24.7 2:25.0, 25.0, 24.0, 23.0, 21.0, 18.0, 19.0, 21.0, 23.0, 23.0, 24.0, 25.0 3:27.0, 26.0, 26.0, 24.0, 22.0, 20.0, 20.0, 22.0, 24.0, 25.0, 25.0, 26.0	28.0, 27.0, 27.0, 25.0, 23.0, 22.0, 21.0, 23.0, 25.0, 27.0, 28.0, 29.0	1: 27.5, 27.0, 25.8, 24.0, 21.5, 18.8, 18.8, 21.5, 24.5, 25.8, 26.5, 27.0 2: 28.0, 27.0, 26.0, 24.0, 22.0, 19.0, 19.0, 22.0, 25.0, 26.0, 27.0, 27.0 3: 28.2, 27.4, 26.4, 24.4, 22.4, 19.4, 19.4, 22.4, 25.4, 26.4, 27.4, 27.4 4: 27.7, 27.0, 25.8, 24.2, 21.7, 18.8, 18.8, 21.7, 24.7, 25.7, 26.7, 27.2 5: 28.3, 28.0, 26.7, 25.0, 22.3, 19.7, 19.7, 22.3, 25.3, 26.7, 27.3, 28.0 6: 29.0, 28.0, 27.0, 25.0, 23.0, 20.0, 20.0, 23.0, 26.0, 27.0, 28.0, 28.0	13.9, 15.6, 16.7, 22.8, 27.8, 33.3, 33.9, 33.3, 28.3, 23.9, 17.2, 12.8

Group Description	Variable	BEESTEKRAALSPRUIT	WESTFALIA B	GROOT-NYLRIVIER	SAFFORD
Monthly means of daily minimum temperature	TMIN	1:14.3, 14.0, 13.3, 10.7, 7.3, 5.0, 5.0, 6.3, 9.0, 10.7, 12.3, 13.7 2:14.0, 14.0, 13.0, 11.0, 7.0, 5.0, 5.0, 6.0, 9.0, 11.0, 12.0, 14.0 3:15.0, 15.0, 14.0, 11.0, 7.0, 4.0, 4.0, 6.0, 9.0, 12.0, 14.0, 15.0	19.0, 18.0, 17.0, 13.0, 9.0, 7.0, 7.0, 9.0, 11.0, 13.0, 15.0, 17.0	1:15.0, 14.5, 13.0, 10.0, 5.8, 2.5, 2.5, 4.7, 8.5, 11.8 13.2, 14.3 2:15.0, 15.0, 13.0, 10.0, 5.3, 2.3, 2.3, 4.3, 8.3, 11.8, 13.3, 14.3 3:15.4, 15.0, 13.6, 10.0, 5.8, 2.4, 2.2, 4.8, 8.8, 12.0, 13.6, 14.6 4:15.0, 14.7, 13.2, 10.0, 5.8, 2.5, 2.3, 4.7, 8.5, 11.7, 13.3, 14.3 5:16.0, 15.3, 14.0, 10.0, 6.0, 2.0, 2.0, 5.0, 9.0, 12.0, 14.0, 15.0 6:16.0, 16.0, 14.0, 10.0, 6.0, 2.0, 2.0, 5.0, 9.0, 12.0, 14.0, 15.0	-3.9, -1.1, 1.1, 3.3, 6.7, 11.1, 17.2, 16.7, 11.7, 5.6, 1.1, -3.9
Reference potential evaporation option	EQPET	102	102	102	110
Evaporation input availability control flags	IEIF ILRF IWDF IRHF ISNF IRDF IPNF	1 0 0 0 0 0 0	1 0 0 0 0 0 0	1 0 0 0 0 0 0	0 0 0 0 0 0 0
Monthly totals of A-pan equivalent evaporation	E	1:159.0, 138.3, 138.6, 115.3, 101.0, 76.6, 86.0, 118.0, 143.0, 164.3, 151.6, 162.0 2:161.0, 139.0, 139.0, 115.0, 101.0, 77.0, 86.0, 118.0, 144.0, 165.0, 154.0, 163.0 3:169.0, 144.0, 143.0, 114.0, 98.0, 75.0, 86.0, 118.0, 147.0, 171.0, 161.0, 172.0	191.0, 175.0, 171.0, 147.0, 134.0, 112.0, 120.0, 156.0, 182.0, 214.0, 207.0, 199.0	1:235.5, 191.0, 190.6, 155.0, 139.0, 115.6, 124.5, 168.0, 208.6, 237.6, 237.0, 235.6 2:235.5, 191.2, 190.7, 154.7, 138.5, 115.5, 124.2, 168.0, 208.7, 238.0, 237.0, 236.2 3:236.4, 193.4, 192.0, 154.0, 138.0, 114.8, 124.0, 167.4, 208.4, 239.0, 237.2, 237.2 4:235.1, 190.3, 190.3, 154.8, 139.0, 115.6, 124.8, 167.8, 208.5, 237.6, 237.0, 235.8 5:238.6, 195.3, 192.6, 154.6, 137.6, 114.6, 124.0, 167.0, 208.6, 240.6, 237.6, 238.6 6:239.0, 197.0, 193.0, 154.0, 137.0, 114.0, 124.0, 167.0, 209.0, 242.0, 237.0, 239.0	100.9, 154.0, 129.9, 131.0, 116.8, 99.5, 97.4, 109.2, 130.2, 139.5, 140.6, 140.2
Temperature adjustment for altitude	TELEV LRREG	N N/A	724.0 1	N N/A	N N/A
Mean lapse rates for min and max temperature	TMAXLR TMINLR	7.00 5.50	7.00 5.50	7.00 5.50	7.00 5.50
Mean daily wind speed (m/s)	WNDSPD	1.6	1.6	1.6	1.6
Penman equation option for S-tank or A-pan equivalent evaporation	SAPANC	N	N	N	N
Smoothed mean monthly A-pan/S-pan ratios	SARAT	N/A	N/A	N/A	N/A
Pan adjustment option	PANCOR CORPAN	0 -	0 -	0 -	0 -
Level of soils information	PEDINF	1	1	1	1
Soils texture information	ITEXT	10	7	4	5
Soil thickness information	PEDDEP	2	2	2	2
Soils Information	DEPAHO DEPBHO WP1 WP2 FC1 FC2 PO1 PO2 ABRESP BFRESP	0.15 (1-3) 0.15 (1-3) 0.175 (1-2), 0.172 0.186 (1-2), 0.206 0.282 (1-2), 0.279 0.303 (1-2), 0.327 0.399 (1-2), 0.397 0.424 (1-2), 0.425 0.20 (1-3) 0.20 (1-3)	0.37 0.73 0.164 0.210 0.271 0.335 0.403 0.430 0.40 0.40	0.23, 0.23, 0.26, 0.22, 0.25, 0.26 0.25, 0.25, 0.37, 0.23, 0.37, 0.37 0.132, 0.132, 0.118, 0.128, 0.114, 0.118 0.137, 0.137, 0.125, 0.127, 0.118, 0.125 0.220, 0.220, 0.208, 0.218, 0.206, 0.208 0.229, 0.229, 0.222, 0.223, 0.217, 0.222 0.447, 0.447, 0.455, 0.449, 0.457, 0.455 0.427, 0.427, 0.439, 0.429, 0.441, 0.439 0.53, 0.57, 0.54, 0.50, 0.56, 0.54 0.53, 0.57, 0.54, 0.50, 0.56, 0.54	0.14 0.36 0.070 0.100 0.133 0.209 0.412 0.412 0.50 0.50
Initial soil water content	SMAINI SMBINI	0.80 0.80	0.75 0.75	0.00 0.00	0 0

Group Description	Variable	BEESTEKRAALSPRUIT	WESTFALIA B	GROOT-NYLRIVIER	SAFFORD
Level of land cover information	LCOVER	1	1	1	1
	CROPNO	-	-	-	-
Determination pf canopy interception loss	INTLOS	1	1	1	1
Leaf area index information	LAIND	0	0	0	0
Monthly means of crop coefficients	CAY	1:0.71, 0.71, 0.67, 0.62, 0.53, 0.46, 0.44, 0.58, 0.62, 0.67, 0.71, 0.71 2:0.78, 0.78, 0.75, 0.73, 0.68, 0.64, 0.63, 0.71, 0.73, 0.75, 0.78, 0.78 3:0.75, 0.75, 0.72, 0.69, 0.63, 0.57, 0.56, 0.66, 0.69, 0.72, 0.75, 0.75	0.75, 0.75, 0.60, 0.50, 0.25, 0.25, 0.25, 0.50, 0.70, 0.70, 0.75, 0.56	1:0.91, 0.88, 0.65, 0.50, 0.45, 0.37, 0.38, 0.43, 0.50, 0.55, 0.56, 0.75 2:0.75, 0.75, 0.75, 0.65, 0.56, 0.40, 0.40, 0.50, 0.65, 0.75, 0.75, 0.75 3:0.69, 0.69, 0.69, 0.63, 0.56, 0.43, 0.43, 0.52, 0.67, 0.75, 0.70, 0.69 4:0.64, 0.64, 0.64, 0.60, 0.58, 0.46, 0.46, 0.54, 0.68, 0.76, 0.66, 0.64 5:0.53, 0.53, 0.53, 0.55, 0.61, 0.52, 0.52, 0.58, 0.71, 0.77, 0.57, 0.53 6:0.64, 0.64, 0.64, 0.60, 0.58, 0.46, 0.46, 0.54, 0.68, 0.76, 0.66, 0.64	0.45, 0.45, 0.45, 0.45, 0.45, 0.50, 0.50, 0.50, 0.50, 0.45, 0.45, 0.45
Monthly means of leaf area index	ELAIM	N/A	N/A	N/A	N/A
Canopy interception loss (mm) per rainday	VEGINT	Jan-Dec 1: 2.18 Jan-Dec 2: 3.10 Jan-Dec 3: 2.13	2.60, 2.60, 2.60, 2.40, 2.20, 2.00, 2.00, 2.00, 2.20, 2.60, 2.60, 2.37	1:1.66, 1.88, 1.62, 1.53, 1.16, 1.15, 1.15, 1.15, 1.15, 1.40, 1.40, 1.42 2:2.50, 2.50, 2.00, 2.00, 2.00, 2.00, 2.00, 2.00, 2.00, 2.50, 2.50, 2.50 3:2.30, 2.30, 1.80, 1.85, 1.87, 1.88, 1.90, 1.92, 1.92, 1.92, 2.30, 2.30 4:2.10, 2.10, 1.60, 1.70, 1.74, 1.76, 1.80, 1.84, 1.84, 2.10, 2.10, 2.10 5:1.70, 1.70, 1.20, 1.40, 1.48, 1.52, 1.60, 1.68, 1.68, 1.70, 1.70, 1.70 6:2.10, 2.10, 1.60, 1.70, 1.74, 1.76, 1.80, 1.84, 1.84, 2.10, 2.10, 2.10	0.30
Fraction of active root system in topsoil horizon specified month by month	ROOTA	1:0.81, 0.81, 0.81, 0.85, 0.85, 0.85, 0.85, 0.85, 0.83, 0.81, 0.81, 0.81 2:0.62, 0.62, 0.62, 0.64, 0.64, 0.64, 0.64, 0.64, 0.62, 0.62, 0.62, 0.62 3:0.69, 0.69, 0.69, 0.72, 0.72, 0.72, 0.72, 0.72, 0.70, 0.69, 0.69, 0.69	0.80, 0.80, 0.80, 0.85, 0.90, 1.00, 1.00, 1.00 0.87, 0.80, 0.85, 0.87	1:0.79, 0.77, 0.86, 0.92, 0.95, 0.95, 0.95, 0.95, 0.95, 0.90, 0.89, 0.83 2:0.80, 0.80, 0.90, 0.90, 0.90, 0.90, 0.90, 0.90, 0.90, 0.80, 0.80, 0.80 3:0.82, 0.82, 0.91, 0.90, 0.88, 0.88, 0.87, 0.91, 0.91, 0.82, 0.82, 0.82 4:0.84, 0.84, 0.92, 0.90, 0.87, 0.85, 0.83, 0.92, 0.92, 0.84, 0.84, 0.84 5:0.88, 0.88, 0.94, 0.91, 0.84, 0.80, 0.76, 0.94, 0.94, 0.88, 0.88, 0.88 6:0.84, 0.84, 0.92, 0.90, 0.87, 0.85, 0.83, 0.92, 0.92, 0.84, 0.84, 0.84	0.90
Effective total rooting depth	EFRDEP	Defaulted to DEPAHO+DEPBHO	Defaulted to DEPAHO+DEPBHO	Defaulted to DEPAHO+DEPBHO	Defaulted to DEPAHO+DEPBHO
Total evaporation control variables	EVTR FPAW	2 0	2 0	2 0	2 1
Fraction of PAW at which plant stress sets in	CONST	1: 0.45 2: 0.66 3: 0.58	0.40	0.40	N/A
Critical leaf water potential	CRLEPO	N/A	N/A	N/A	-800.0
Option for enhanced wet canopy evaporation	FOREST	0, 1, 0	0	0	0
Mean temperature threshold for active growth	TMPCUT	1.0	1.0	1.0	1.0
Unsaturated soil moisture redistribution	IUNSAT	Y	Y	Y	Y

Group Description	Variable	BEESTEKRAALSPRUIT	WESTFALIA B	GROOT-NYLRIVIER	SAFFORD
Streamflow simulation control variables	QFRESP COFRU SMDDEP IRUN ADJIMP DISIMP STOIMP	0.01 (1-3) 0.247 (1-3) 0.00, 0.31, 0.00 Y (1-3) 0.001, 0.001, 0.002 0.125, 0.125, 0.064 1.00 (1-3)	0.28 0.007 0.0 Y 0.018 0.062 1.00	0.05 (1-6) 0.004 (1-6) 0.0 (1-6) Y 0.014 (1-3), 0.016 (4-5), 0.014 0.316, 0.316, 0.196, 0.324, 0.184, 0.196 1.00 (1-6)	1.00 0.007 0.14 Y 0.00 0.00 1.00
Coefficient of initial abstraction	COIAM	1: 0.21 2: 0.28 3: 0.25	0.20, 0.20, 0.25, 0.30, 0.30, 0.30, 0.30, 0.30, 0.30, 0.25, 0.20, 0.27	1:0.22, 0.25, 0.30, 0.30, 0.30, 0.30, 0.30, 0.30, 0.30, 0.32, 0.25, 0.22 2:0.20, 0.20, 0.30, 0.30, 0.30, 0.30, 0.30, 0.30, 0.30, 0.30, 0.20, 0.17 3:0.29, 0.20, 0.30, 0.30, 0.30, 0.30, 0.30, 0.30, 0.30, 0.30, 0.20, 0.17 4:0.27, 0.22, 0.30, 0.30, 0.30, 0.30, 0.30, 0.30, 0.30, 0.31, 0.22, 0.19 5:0.32, 0.20, 0.30, 0.30, 0.30, 0.30, 0.30, 0.30, 0.30, 0.20, 0.20, 0.16 6:0.30, 0.20, 0.30, 0.30, 0.30, 0.30, 0.30, 0.30, 0.30, 0.30, 0.20, 0.17	0.20
Abstraction option	IDOMR	0 (no abstraction)	0 (no abstraction)	0 (no abstraction)	0 (no abstraction)
Monthly averages of daily abstractions	DOMABS	N/A	N/A	N/A	N